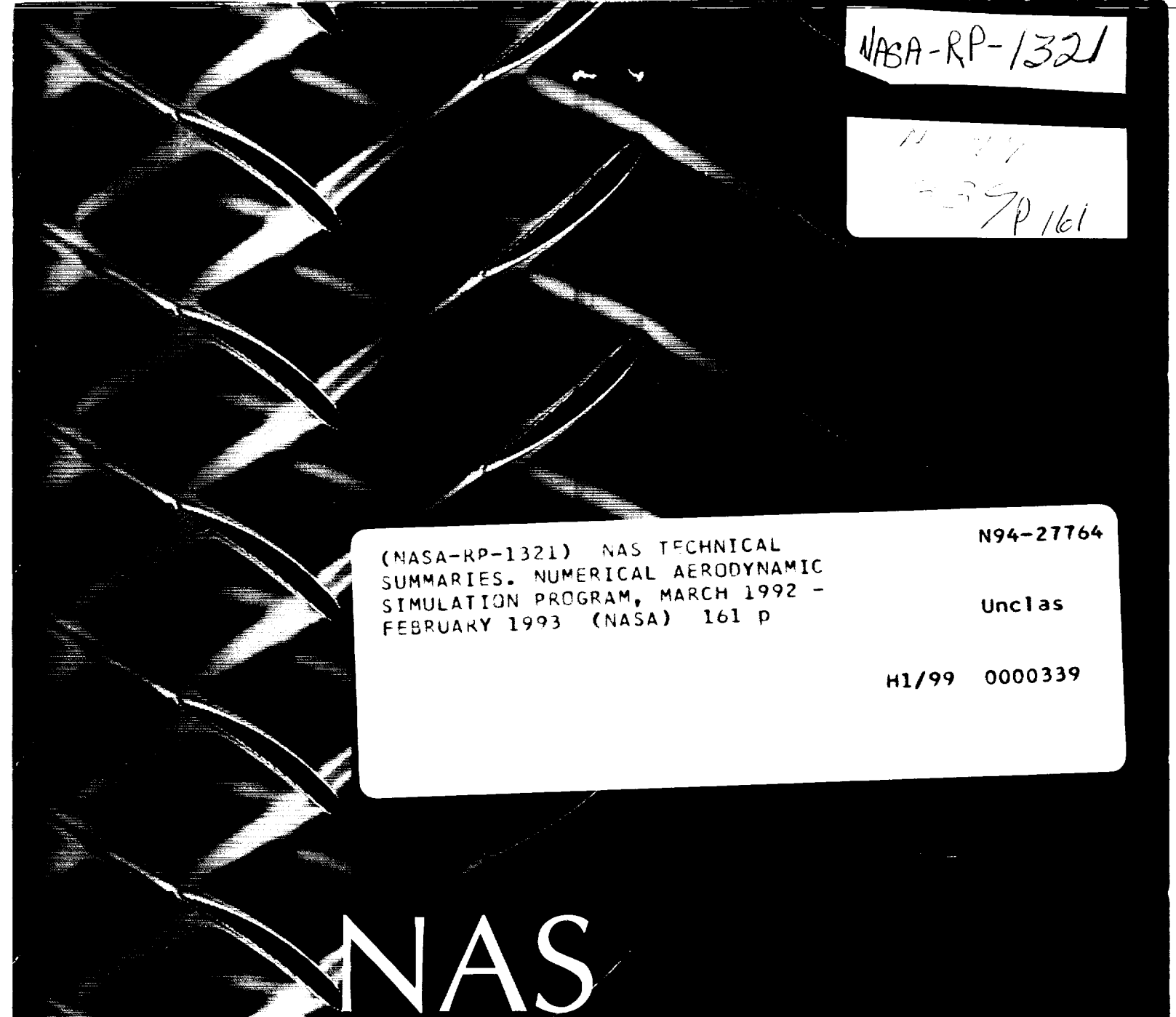

NAS Technical Summaries

Numerical Aerodynamic Simulation Program

March 1992 – February 1993

The use of color graphics is a powerful and flexible visualization tool for the science of computational fluid dynamics. Without color graphics, the millions of numbers which form the supercomputer solutions to the studies contained in this report and on the cover would be virtually incomprehensible.

On the cover: Nateri K. Madavan is a researcher with the MCAT Institute at NASA Ames Research Center. The cover image is from Madavan's summary, "Unsteady Multistage Turbomachinery Applications," on page 77.

NAS Technical Summaries

Numerical Aerodynamic Simulation Program

National Aeronautics and Space Administration
Ames Research Center

Preface

NASA created the Numerical Aerodynamic Simulation (NAS) Program in 1987 to focus resources on solving critical problems in aeroscience and related disciplines by utilizing the power of the most advanced supercomputers available. The NAS Program provides scientists with the necessary computing power to solve today's most demanding computational fluid dynamics problems and serves as a pathfinder in integrating leading-edge supercomputing technologies, thus benefiting other supercomputer centers in government and industry.

During the 1992–93 Operational Year, the scientific community was given access to a Cray-2 and a Cray Y-MP. The Cray-2, a first generation supercomputer, had four processors, 256 megawords of central memory, and a total sustained speed of 250 million floating point operations per second. The Cray Y-MP, a second generation supercomputer, had eight processors, 256 megawords of solid state device memory, and a total sustained speed of 1 billion floating point operations per second. Because of its higher performance, the Cray Y-MP delivered 67 percent of the total number of supercomputer hours used by the NAS scientific community during the 1992–93 Operational Year.

The 1992–93 Operational Year concluded with 399 high-speed processor (HSP) projects and 91 parallel (PAR) projects representing NASA, the Department of Defense, other Government agencies, private industry, and universities. This document—the NAS Technical Summaries—provides a glimpse at some of the significant scientific results for the year.

The content of the NAS Technical Summaries for the 1992–93 Operational Year has been expanded from previous years. Traditionally, this report contains selected scientific results computed using HSP resources. This is the first edition to also contain results computed using PAR resources. An icon above the text of each technical summary indicates the resource used— represents HSP, and represents PAR.

The organization of the summaries also differs from previous years. Traditionally this report was organized alphabetically by principal investigator. This edition is organized by research disciplines and alphabetically within each discipline to make the book more functional.

Additional copies of the NAS Technical Summaries for this year and for previous years are available on request. Contact the NAS Documentation Center at NASA Ames Research Center, MS 258-6, Moffett Field, CA 94035-1000, or via email addressed to doc-center@nas.nasa.gov, or telephone (415) 604-4632.

Number of Cray Projects by Category

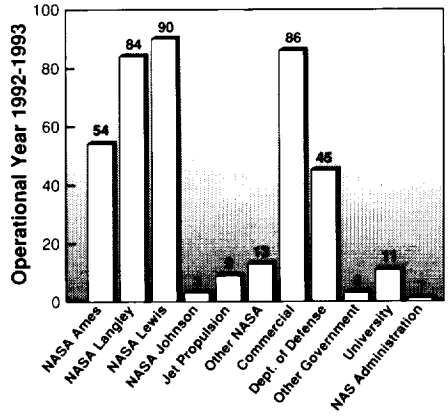

Number of Cray Projects by Discipline

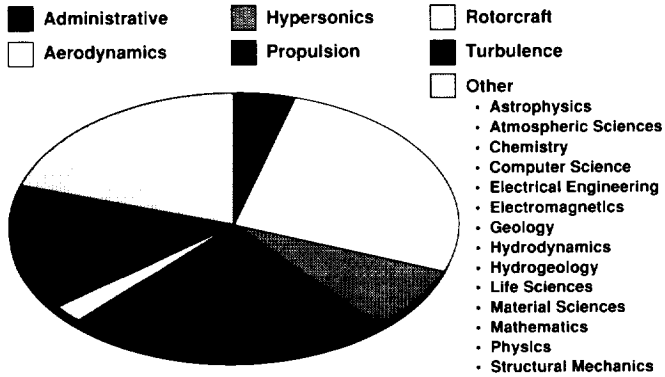

Number of Parallel Projects by Category

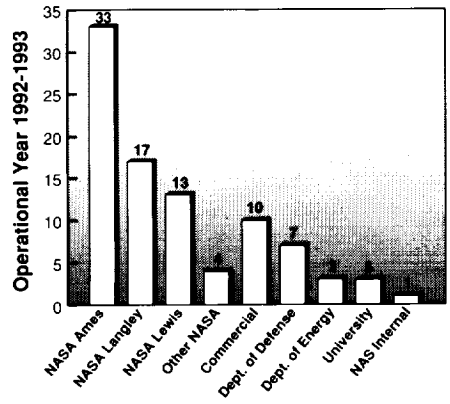

Number of Parallel Projects by Discipline

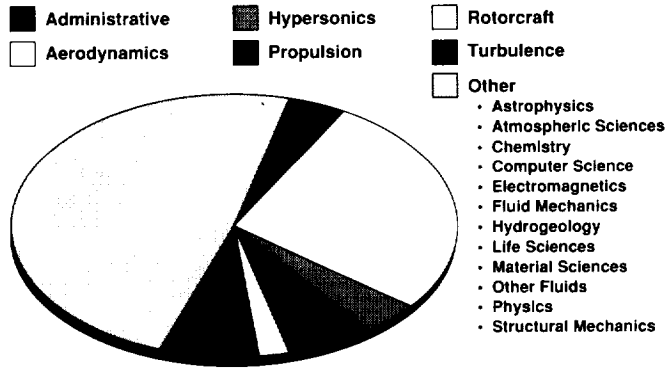

Table of Contents

Aeronautics: Hypersonics, Subsonics, Supersonics, Transonics

Hypersonics

General: Astronautics, Astronomy, Atmospheric Science, Chemistry, Computer Science, Electromagnetics, Fluid Mechanics, Hydrodynamics, Life Science, Reactive Flow, Space Science, Structural Mechanics

Astronautics

Astronomy

Atmospheric Science

Aeronautics

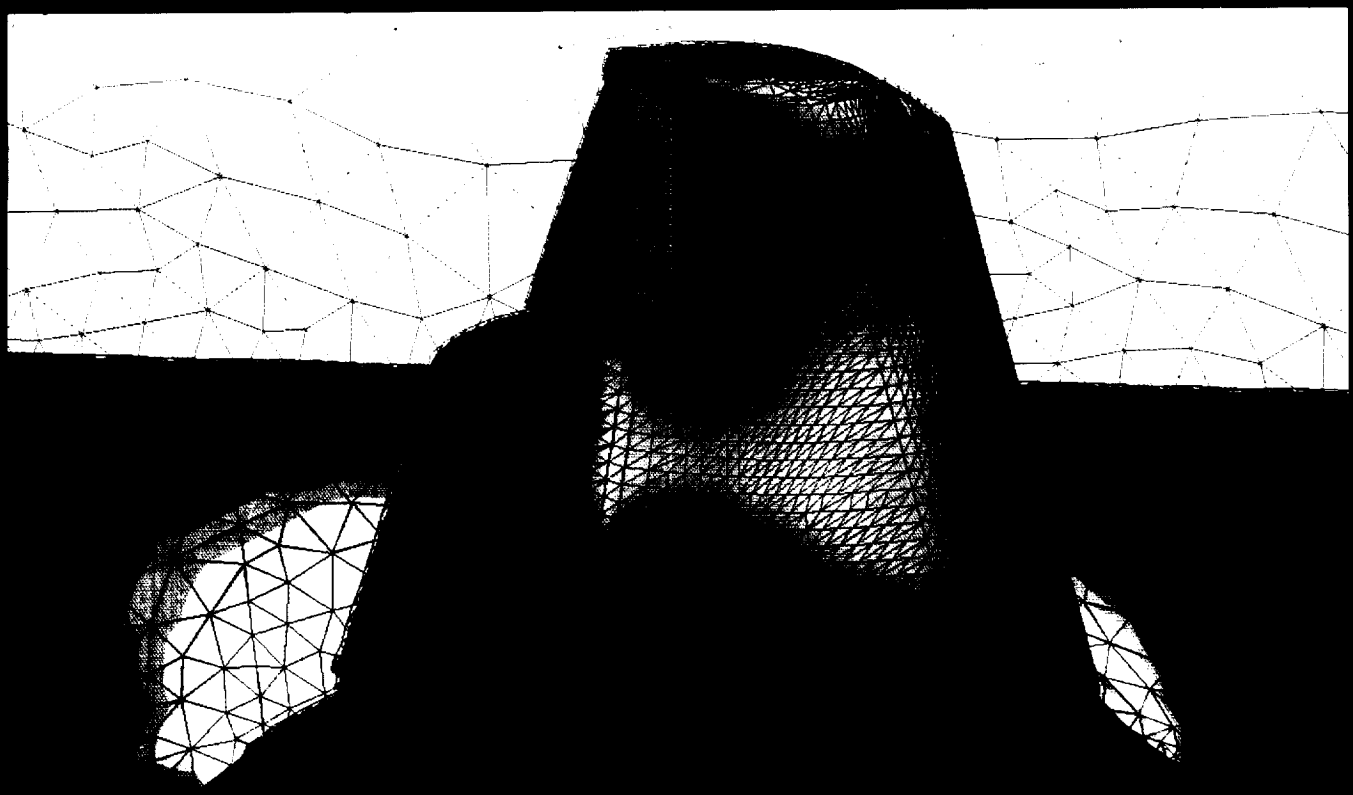

Basic Research

Numerical Solution of Three-Dimensional Maxwell Equations

Ramesh K. Agarwal, Principal Investigator
Co-investigators: Mark Shu and Mark R. Axe
McDonnell Douglas Corporation

Research Objective
To develop computational codes capable of predicting the electromagnetic (EM) signature of an aerospace vehicle. Such a code would be of great value in the design and development of fighter aircraft and missiles because a greater number of candidate configurations could be considered and evaluated with a reduction in cost and design time.

Approach
Three-dimensional (3-D) Maxwell equations were solved by employing mature computational fluid dynamics technology. Specifically, a compact, higher-order, finite-volume, time-domain/frequency-domain, multizone method was used to compute the EM field about scattering bodies.

Accomplishment Description
The EM scattering code was extended to calculate the scattering from geometrically and electrically complex two-dimensional (2-D) and 3-D objects. Accomplishments included 2-D EM scattering calculations from lossless and lossy dielectric objects such as dielectric cylinders, coated cylinders, and treated ducts. Also accomplished were the 3-D EM scattering calculations from perfectly conducting bodies such as spheres, cone spheres, finite cylinders, and almonds. Especially noteworthy were the 3-D EM scattering calculations from an F-15.

Significance
The project represents the development of a leading-edge technology in computational EM, and it will have substantial impact on the development of both fighter aircraft and missile programs.

Future Plans
A CFD-based Maxwell solver will be developed and validated to calculate the radar cross sections of complete, real-world 3-D configurations.

Publication
Huh, K. S.; Shu, M.; and Agarwal, R. K.: A Compact High-Order Finite-Volume Time-Domain/Frequency-Domain Method for Electromagnetic Scattering. AIAA 30th Aerospace Sciences Meeting, Reno, Nev., AIAA Paper 92-0453, Jan. 1992.

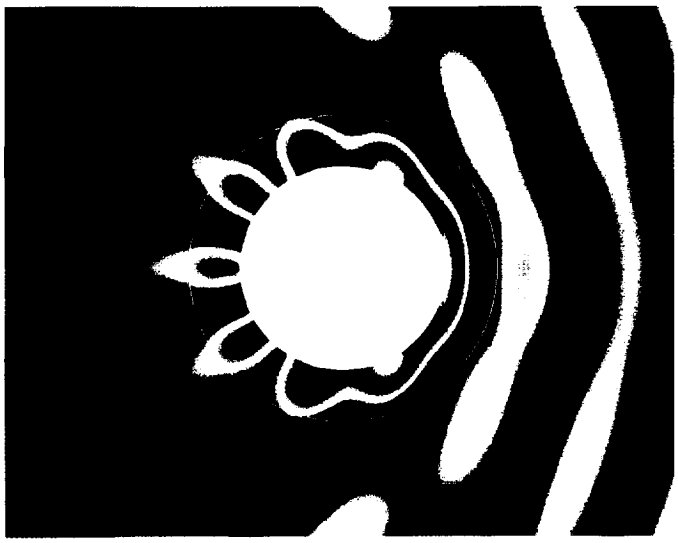

Amplitude of the magnetic field about a lossy coated perfectly conducting cylinder. The circular white line represents the edge of the dielectric. Red represents maximum amplitude and blue represents minimum amplitude.

Amplitude of the electric current on the surface of a perfectly conducting sphere. Red represents maximum amplitude and blue represents minimum amplitude. The white contour lines represent electric current contours of equal amplitude in the near field.

Simulation of Acoustic Scatter

Harold L. Atkins, Principal Investigator
NASA Langley Research Center

Research Objective
To evaluate the performance of a newly developed nonreflective inflow/outflow boundary condition for multi-dimensional unsteady flows.

Approach
A fifth-order shock-capturing finite-difference method was used to simulate flow over a sphere that either produced sound or reflected an incident sound wave. The boundary condition applied at the outer boundary was designed to allow waves to exit the domain without reflection and, at the same time, allow desired inbound waves to be prescribed. The boundary condition was evaluated by comparing two solutions in which the outer boundary was applied at different distances from the sphere.

Accomplishments Description
Simulations were performed for oscillating spheres and spheres interacting with plane waves. The figures show an acoustic plane wave that propagates from right to left and impinges upon the sphere to produce a scatter wave. The upper half of each figure corresponds to a case with the outer boundary at 13 sphere radii; in the lower half, the outer boundary is 9 radii. The boundary condition was designed on the premise that only isolated acoustic and convective waves of a single, known orientation exist. This test case consisted of two sets of waves with different orientations and gave a fair indication of how the boundary condition performs at off-design conditions. At the resolution illustrated in the figures, the difference between the two solutions was roughly three orders of magnitude below the amplitude of the scatter wave. Grid-refinement studies were performed to investigate the accuracy properties of the high-order method and the nonreflective boundary conditions. A typical case required about 40 minutes processing time to allow the plane wave to cross the domain and establish a periodic scatter wave and required less than 10 megawords of memory. Additional execution time was required when temporal analysis of the scatter wave was desired.

Significance
The present boundary condition allows the computational domain to be reduced to the minimum region required to simulate the nonlinear, near-field solution. This simulation should reduce the cost of predicting noise produced by aerodynamic flows.

Future Plans
The high-order method will be coupled with a Kirchhoff integral method for predicting the far-field noise. The initial tests will determine how much simulation data must be saved for input to the Kirchhoff method. This testing will be followed by a simulation of a high-speed jet.

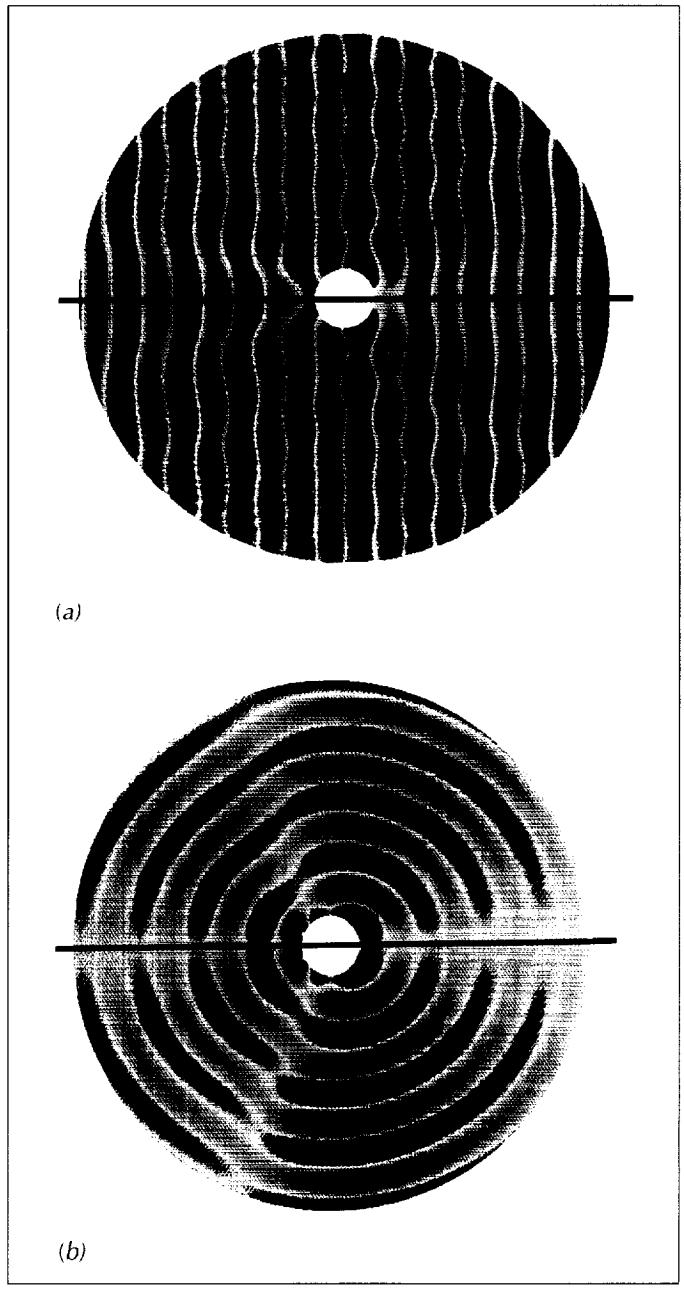

Perturbations produced by a plane wave impinging on a sphere. The upper half of each figure shows a case with the outer boundary at 13 sphere radii; the lower half of each figure shows the outer boundary at 9 sphere radii. Both the (a) density and (b) v component of velocity are on the order of ±0.001.

A Three-Dimensional Implicit Unstructured Euler Solver

Timothy J. Barth, Principal Investigator
Co-investigator: Samuel W. Linton
NASA Ames Research Center/Sterling Software Systems

Research Objective
To develop an efficient numerical scheme for solving the Euler equations of gas dynamics on unstructured meshes using a preconditioned minimum residual matrix solver.

Approach
The Euler equations were discretized on arbitrary tetrahedral meshes using a finite-volume approach with upwind dissipation added to stabilize the scheme. The algorithm exhibited second-order spatial accuracy on sufficiently smooth meshes. An implicit time-stepping strategy, which approached Newton's method for large time steps, was used. This strategy required the solution of a sequence of large sparse matrix equations. To solve the equations, a generalized minimum-residual method with incomplete lower-upper preconditioning was used.

Accomplishment Description
A computer code was designed, developed, and implemented on a range of computer architectures including vector and parallel machines. The computer code was used in the computation of aerodynamic flows about wings and helicopter blades at subsonic and transonic speeds. Using the implicit solution strategy, rapid convergence to steady state was demonstrated. The first figure shows the temporal convergence history of the algorithm for subsonic flow over multiple spheres.

Significance
The use of unstructured meshes permitted the calculation of aerodynamic flow over complex geometries (see the second figure). Moreover, the improved efficiency of the algorithm permitted the calculation of these flows using modest resources.

Future Plans
Plans include the modification of the code for computation of viscous flow including the effects of turbulence. In addition, the code will be modified to support computations in a nonheterogeneous computing environment.

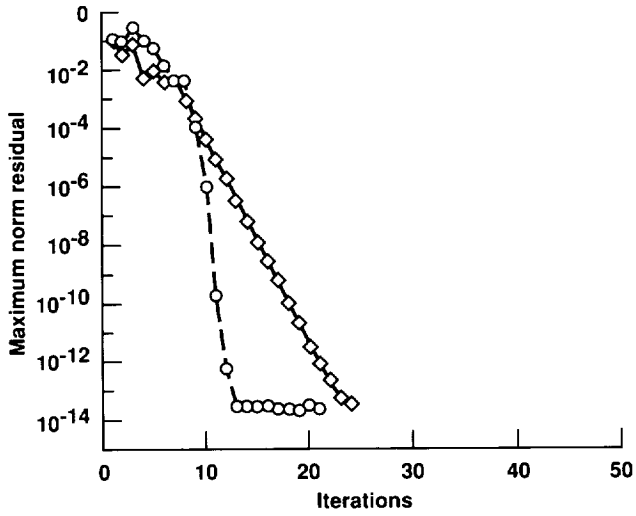

Convergence history of the implicit scheme. The dashed and solid lines depict the convergence history of the scheme with first- and second-order space differencing, respectively.

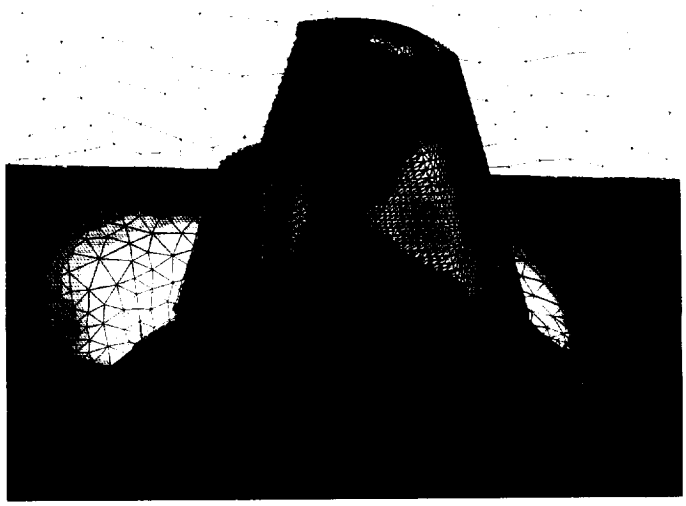

Surface mesh on the wing and fuselage portion of a Boeing 737 aircraft with high-lift devices deployed.

Simulation of Supersonic Jet Screech

Alan B. Cain, Principal Investigator
Co-investigators: William W. Bower and William W. Romer
McDonnell Douglas Aerospace

Research Objective
To simulate supersonic jet screech and provide detailed data for modeling receptivity and shock–vortex interactions.

Approach
Several algorithms were examined. A formulation based on upwind-biased, conservative, finite-volume spatial differentiation in combination with Runge–Kutta time integration produced the best results.

Accomplishment Description
Self-sustained screech oscillations were simulated and reasonably matched the frequency measured in NASA Langley experiments. Both axisymmetric and rectangular nozzle flows were examined. The fully expanded jet Mach numbers considered were 1.05, 1.20, and 1.60 for nozzles designed for perfect expansion at Mach numbers of 1.00, 1.30, and 1.35, respectively. Analysis is in progress for the acoustic spectra and direction characteristics. In the rectangular case, the initialization of the flow field produced an initial varicose mode that gradually evolved into a dominant sinuous mode consistent with the predictions of linear theory. Typical runs required 64 megawords of memory and 20–100 Cray Y-MP hours.

Significance
The screech prediction tool is important for the design of tactical aircraft. Eliminating screech substantially reduces nozzle maintenance costs. A preliminary design tool must generate analysis solutions quickly on a workstation; thus good models of the basic phenomena are essential. The present simulations are a starting point for detailed information to guide analytical modeling of the shock–vortex interaction and the nozzle lip receptivity.

Future Plans
Further analysis of the current results is needed to determine the spectral and directivity characteristics. New simulations for a round jet to examine mode switching will help define current simulation capabilities.

Publication
Cain, A. B.: Computation of Supersonic Jet Screech. Proceedings of the ASME Fluids Engineering Forum on Computational Aero- and Hydro-Acoustics Meeting, Washington, D.C., June 1993.

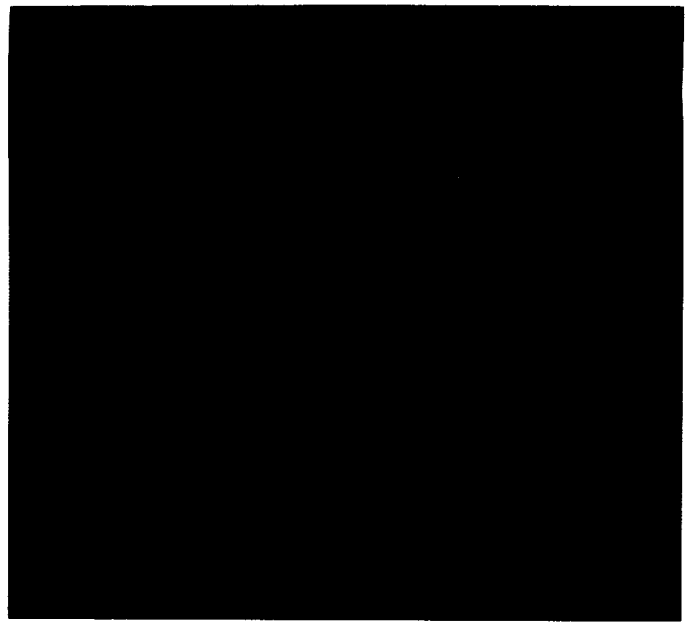

Pressure and vorticity contours for a rectangular nozzle: design Mach number = 1.35, fully expanded jet Mach number = 1.60, red = maximum pressure, blue = minimum pressure.

Efficient Constrained Aerodynamic Design

Richard L. Campbell, Principal Investigator
Co-investigators: Leigh A. Smith and Raymond E. Mineck
NASA Langley Research Center

Research Objective

To evaluate a new approach to constrained aerodynamic design of complex configurations at multiple design points using advanced computational fluid dynamics (CFD) codes.

Approach

The objective is approached in two parts that will eventually be merged: (1) evaluation of the Constrained Direct Iterative Surface Curvature (CDISC) design method for three-dimensional (3-D) applications and (2) investigation of automated multipoint design approaches. The CDISC method generates and modifies target pressure distributions to meet flow and geometry constraints. It includes an option for minimizing an objective function by adjusting the constraint values during the design process. The basic direct iterative surface curvature (DISC) design method is used to modify the configuration to match the new target pressure distributions. Several approaches to employ the CDISC method at multiple design points and determine what additional adjustments to the constraints may be required are being investigated. For these studies, the CDISC method is coupled with a thin-layer Navier–Stokes code (TLNS3D) and an unstructured-mesh Euler code.

Accomplishment Description

The design codes were applied to configurations at subsonic, transonic, and supersonic speeds. These cases included several dual-point design studies with the goal of defining an automation strategy for efficient multipoint design. Results for a redesign of a subsonic transport wing at a Mach 0.82 and a lift coefficient of 0.55 are shown in the figures. The solutions were obtained on a 193 × 49 × 49 grid, which required about 24 megawords of memory and about 1.25 Cray-2 hours to reach the convergence criteria of four orders of magnitude reduction in the residual. Mach number contours for the baseline wing are shown in the first figure. The yellow and red regions indicate Mach numbers greater than 1.25 and 1.30, respectively. The shock just aft of midchord extends to the symmetry plane, with the maximum strength occurring between about 25 and 50 percent of the semispan. The Mach number contours for the CDISC design (second figure) indicate that the shock has been significantly weakened over the inner half of the wing (all Mach numbers are below 1.30). This weakening and a slight redistribution of the spanwise loading reduced the inviscid drag of the wing by about 12 percent. This redesign involved 12 design cycles and required about 16 percent more time than the baseline analysis.

Significance

Results indicate that the CDISC method could provide an efficient alternative to numerical optimization for constrained design of aerodynamic configurations. The CDISC method eliminates the need to define or modify the target pressures required by the DISC approach and can reduce the central processing unit time required.

Future Plans

Multipoint design approaches will be evaluated at cruise and off-design conditions that include separated flow. The CDISC method will be installed in the multiblock version of TLNS3D for more complex geometries.

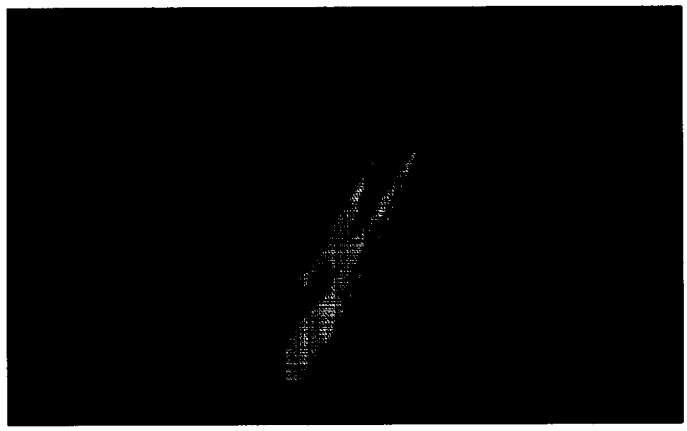

Mach number contours for baseline wing, Mach = 0.82.

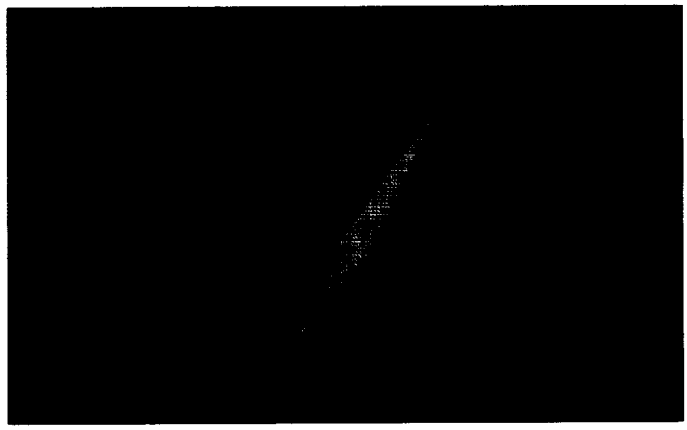

Mach number contours for CDISC redesign, Mach = 0.82.

Computation of Helicopter Rotor and Wake Flows

Frank Caradonna, Principal Investigator
Co-investigators: K. Ramachandran, J. Bridgeman, and D. Poling
U.S. Army Aeroflightdynamics Directorate, AVSCOM/Flow Analysis, Inc./Woodside Summit Group, Inc./The Boeing Company

Research Objective
To use large-scale computational models of the limiting flow phenomena of helicopters and tilt rotors to determine the various flow losses and vibratory loading mechanisms with sufficient accuracy to permit reliable design and to obviate the need for extensive testing.

Approach
Individual flow models were assembled and validated to build a total flow solver. Two unique methods were used in this work. Vortex embedding—an extension of potential methods that permits the free convection of the wake with no dissipation and no grid restrictions—was used to predict the hover and forward-flight performance of rotors. Vorticity confinement—an extension of Euler/Navier–Stokes codes that counteracts the effects of numerical dissipation—was used to model wake formation and blade–vortex interactions. Combined, the two methods provide accurate near-blade solutions and a wake-convecting, compressible "far" field that includes interaction effects.

Accomplishment Description
The most extensive computational fluid dynamics (CFD) hover validations were performed using the HELIX-I code to compute the performance of the UH-60A rotor. These methods were applied to the analysis of the hover performance of the new RAH-66 helicopter and revealed unsuspected regions of rotor power sensitivity. These computations required about 5 megawords of memory and 6 Cray-2 hours to compute a typical performance polar. The first forward-flight loads computations and comparisons with flight data were made using the HELIX-II code to compute the flow on the AH-1G. A typical run required about 15 megawords of memory and about 10 Cray-2 hours. The first vortex formation and blade–vortex interaction computations were performed using the code TURNS_CONFINE. Confinement efficiently maintained the identity and strength of vortex structures and increased the higher harmonic loading of the blade–vortex interactions. The runs required about 10 megawords of memory and 4 Cray-2 hours.

Significance
To improve rotor performance, a more detailed knowledge of the various drag mechanisms is required. The present computations are the most accurate wake solvers of any CFD method and provide a detailed analysis of rotor drag. This should provide a new capability to design and evaluate advanced rotor configurations with minimal experimental development.

Future Plans
Computational design studies will be performed. Accuracy and efficiency improvements will be made in the HELIX-II forward-flight code. Vorticity confinement methods will be applied to improve blade–vortex interaction computations and viscous flow effects. Confinement solvers will be combined with vorticity embedding solvers to provide a comprehensive rotor flow method.

(a)

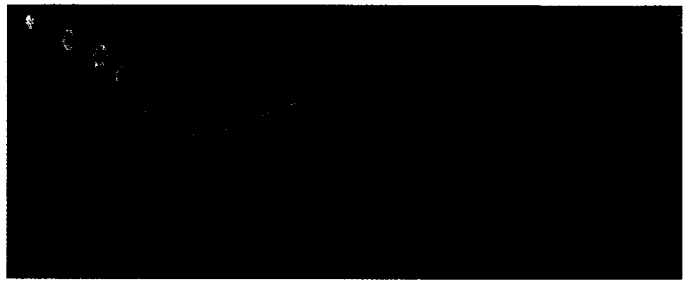

(b)

Vorticity contours of a vortex generated by a wing tip computed (a) without and (b) with the use of confinement.

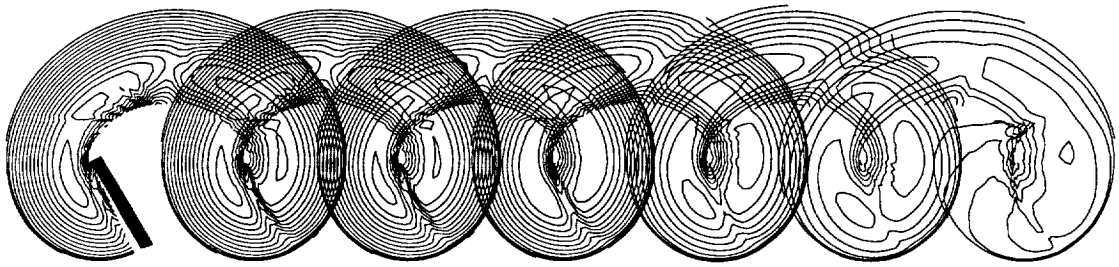

Wake structure evolution of a starting rotor solution. Periodicity is achieved in 6 revolutions, by which time blade–vortex interactions are clearly seen.

High-Incidence Static/Dynamic Roll Computations

Neal M. Chaderjian, Principal Investigator
Co-investigators: John Ekaterinaris, Yuval Levy, and Lewis B. Schiff
NASA Ames Research Center/Naval Post Graduate School/Stanford University

Research Objective

To develop a validated computational methodology to predict and investigate high-angle-of-attack vortex aerodynamics for static-roll and dynamic-roll motions of simple wing–body geometries.

Approach

Time-dependent, three-dimensional, Reynolds-averaged Navier–Stokes (RANS) equations were utilized to compute high-incidence vortical flows about a 65-degree-sweep delta wing at 15 degrees angle of attack. The Navier–Stokes simulation (NSS) code integrated the RANS equations using either the implicit Beam–Warming algorithm or a diagonal version developed by Pulliam and Chaussee. Turbulent flow conditions were treated with the Baldwin–Lomax turbulence model and the Degani–Schiff modification, which accounted for the cross-flow separation.

Accomplishment Description

The NSS code was used to compute the viscous flow about a delta wing in roll with free-stream Mach number = 0.27, angle of attack = 15 degrees, and Reynolds number = 3.67 million (based on the wing root chord). Investigations were carried out at several static roll angles up to 42 degrees of roll and a large-amplitude (40 degree), high-rate (7 hertz (Hz)) forced roll motion. The first figure shows the leeward-side vortices with helicity-density contours for the dynamic case at its maximum roll angle. Primary, secondary, and tertiary vortices are evident. The flow topology was verified by experimental oil-flow patterns. Static and dynamic computational surface pressures were in excellent agreement with experimental data, as were the forces and moments. The second figure compares the computational and experimental rolling moment coefficients for the static and dynamic cases. The negative slope of the static rolling moment curve indicates that the wing is statically stable in roll under the flow conditions. The dynamic rolling moment exhibits a significant hysteresis due to rate effects. The computational and experimental rolling moments move along their respective curves in a counterclockwise direction, indicating that the motion is damped. The areas under these curves represent the damping energy and agree within 3 percent. No vortex breakdown was observed in the computations or the experiment. Each static case was solved on an 800,000 point grid with a diagonal algorithm and required 26 hours (8,000 steps) on a Cray Y-MP.

Significance

Highly accurate computational results were obtained for a delta wing in static and dynamic roll. This step is the first toward an experimentally validated computational method for computing static-roll and dynamic-roll motions of aircraft, which will eventually be applied to wing rock.

Future Plans

A similar study will be carried out where vortex breakdown occurs (30 degrees angle of attack) and free-to-roll motions, including wing rock, will be computed.

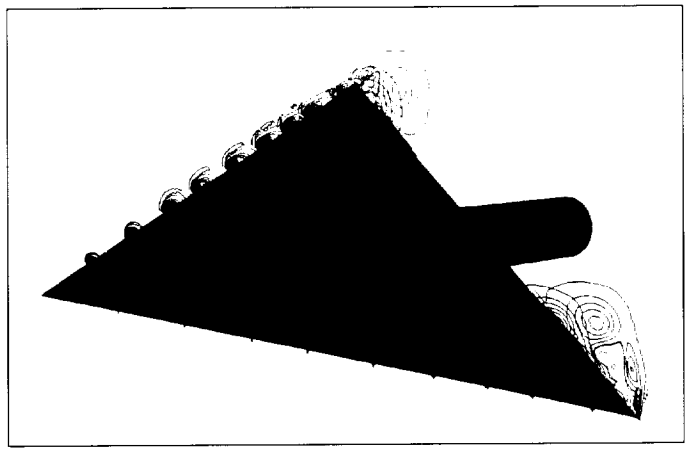

Helicity-density contours at roll angle (ϕ) = -40 degrees. Flow conditions: Mach = 0.27, Reynolds number = 3.67 million, dynamic roll amplitude = 40 degrees, and frequency = 7 Hz. Green contours = clockwise flow rotation and blue contours = counterclockwise flow rotation.

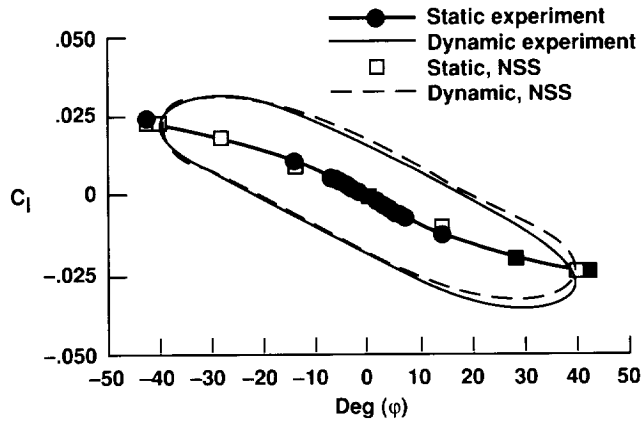

Static and dynamic rolling moment comparisons between computation and experiment. Flow conditions: Mach = 0.27, Reynolds number = 3.67 million, dynamic roll amplitude = 40 degrees, and frequency = 7 Hz.

Cavity Aeroacoustic Loads Prediction

Richard D. Crouse, Principal Investigator
Northrop Corporation

Research Objective
Experiments performed on aircraft weapons bay cavities have demonstrated the presence of powerful acoustic pressure waves. An effort was established to develop and execute a set of procedures to calculate the unsteady aeroacoustic flow-field environment using computational fluid dynamic methods.

Approach
The flow field within and around the cavity and the full aircraft is calculated using existing three-dimensional (3-D) Navier–Stokes flow codes. The time-varying pressure field is transformed with a fast-Fourier transform to a frequency domain. This procedure will allow the identification of the frequencies and the amplitude of the varying pressure.

Accomplishment Description
A 3-D grid was generated around the U.S. Air Force Innovative Weapons Cavity (IWC) model, including the open weapons bay cavity, consisting of 661,586 grid points. An optimum blocking structure was defined using six blocks. The viscous wall spacing was determined and correctly resolved the boundary layer. Computations on the model were completed and gave a steady-state solution. The time-accurate solution was started from this steady solution. Early results indicated excessive damping, which was probably due to a problem with the turbulence model, and the solution was halted. Only 10 Cray-2 hours were used and each run required 32 megawords of memory.

Significance
Acoustic loads prediction is needed when considering the increased performance levels of advanced tactical air vehicles. The study results provide an extremely useful tool to aid in new vehicle design. This computational means will enable solutions to be calculated on a variety of topologies and over a vast flight regime. It will not make empirical results present-case dependent, nor simply recalculate old data. Rather, it will be applicable in all stages of aircraft design, such as further analysis of existing geometries, development of present configurations, and research in future programs.

Future Plans
The turbulence model in the code will be corrected for time-accurate flow. The time-varying solution of the flow in a cavity in an entire aircraft will be completed. The results will be compared to wind tunnel test results of this model in early 1994.

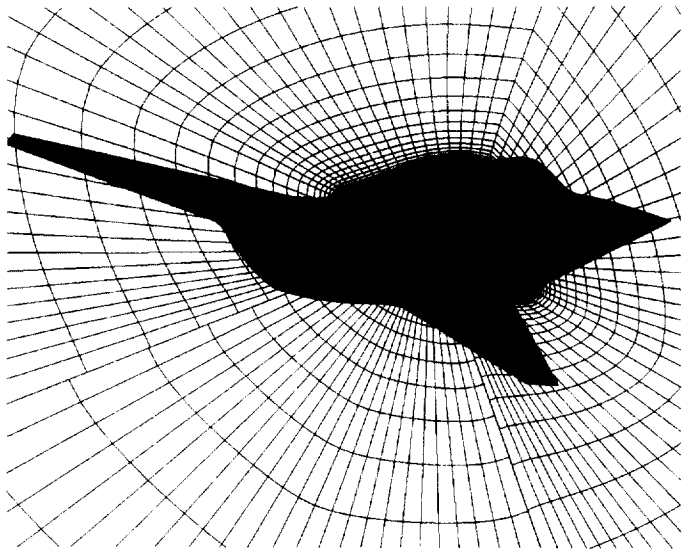

Three-dimensional grid lines around the U.S. Air Force IWC model.

High-Fidelity Space Shuttle Simulation

Daniel F. Dominik, Principal Investigator
Co-investigators: K. Rajagopal, S. Vuong, J. Wisneski, C. Olling, G. Hock, and J. Sikora
Rockwell International, Space Systems Division

Research Objective
To develop a full-scale, high-fidelity asymmetric model for the Space Shuttle Launch Vehicle (SSLV) and to predict the transonic aerodynamic loads during ascent by performing Navier–Stokes computations at full-scale flight Reynolds number.

Approach
A model with many fine geometry details of the SSLV was built using the ICEM/computational fluid dynamics (CFD) computer assisted design (CAD) and grid software. The multizonal grid was smoothed using the GRIDGEN3D software. Most, but not all, of the interzonal boundaries are aligned. The numerical solutions were obtained using the Reynolds-averaged Navier–Stokes formulation of the USA-RG3D code with the algebraic Baldwin–Lomax turbulence model. Initial calculations were without plume simulation; later calculations will include simulation of the three Space Shuttle main engine (SSME) plumes and the two solid rocket booster (SRB) plumes. Results will be correlated with available flight test and wind tunnel data.

Accomplishment Description
The SSLV model simulated the forward and rear attached hardware connecting the Orbiter, the external tank (ET), and the two SRBs. The primary protuberances on the body surfaces, including the liquid oxygen feedline on the right side of the ET, were also modeled. These geometry details enhanced the simulation accuracy of the multibody flow field. This complete, asymmetric grid model contained 237 zones and approximately 5 million points. The USA-RG3D flow solver was used to simulate the turbulent, flight Reynolds number transonic flow over the geometry. The model was broken into 6 sections and no section required more than 64 megawords of main computer memory. Each section had overlapping zones and the solutions were updated by cycling through the sections to ensure proper communication. Numerical solutions were computed for the redesigned solid rocket motor and advanced solid rocket motor configurations. The model enabled simulation of sideslip conditions. For each configuration, solutions were computed at Mach = 1.25 and Mach = 1.05 with 0 and 4 degrees of sideslip.

Significance
There was good correlation with experimental results. The detailed definition of the airload distributions and the insight into the complex three-dimensional flow physics illustrate the benefits that can only be obtained from this type of detailed CFD simulation.

Future Plans
Computations with variable specific heat gaseous SRB and SSME plume simulations are in progress now and are expected to improve further the correlation with test data.

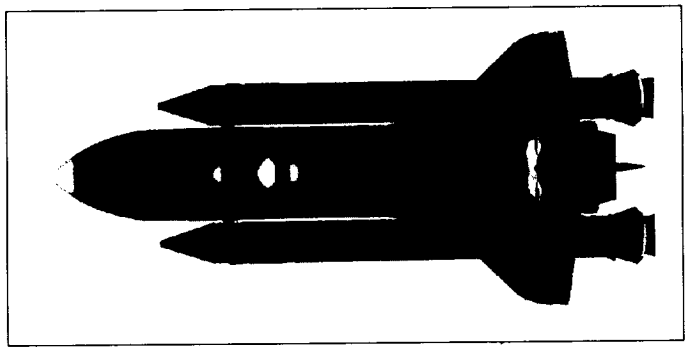

Surface pressure coefficient at Mach = 1.25, angle of attack = –5.1 degrees, sideslip = 0 degrees (without plume simulation) (gray = –0.75 and white = 0.75).

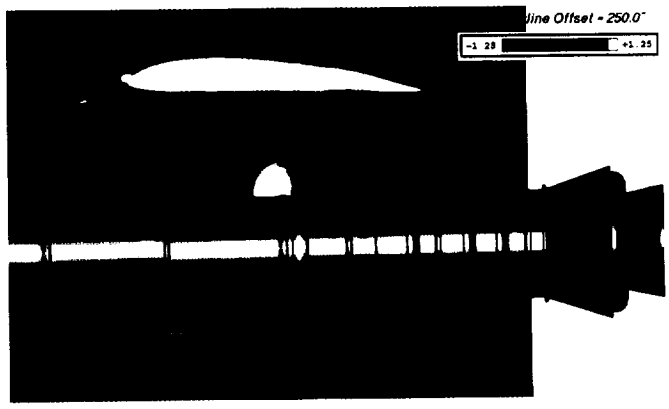

Pressure coefficient between wing and SRB at y = 250 in. for Mach = 1.25, angle of attack = –5.1 degrees, sideslip = 0 degrees (without plume simulation).

Aerodynamic Optimization of Supersonic Aircraft

Thomas A. Edwards, Principal Investigator
Co-investigators: Samson H. Cheung and I. C. Chang
NASA Ames Research Center/MCAT Institute

Research Objective
To apply computational fluid dynamics (CFD) technology to aerodynamic design problems for the High-Speed Civil Transport (HSCT). The problems include aerodynamic optimization and sonic boom minimization.

Approach
For aerodynamic design optimization, the CFD code was used as an analysis module for aerodynamic performance estimates. A numerical optimization routine based on sequential quadratic programming directed design modifications based on the sensitivity gradient vector and imposed constraints. For sonic boom minimization, a similar approach was used, but the objective function was related to the sonic boom signature. This function required additional analysis modules that would accept the CFD solution in the near field and extrapolate the pressure disturbance to ground level. The design variables were related to the aircraft equivalent area distribution, which was related in a non-unique way to the actual aircraft geometry.

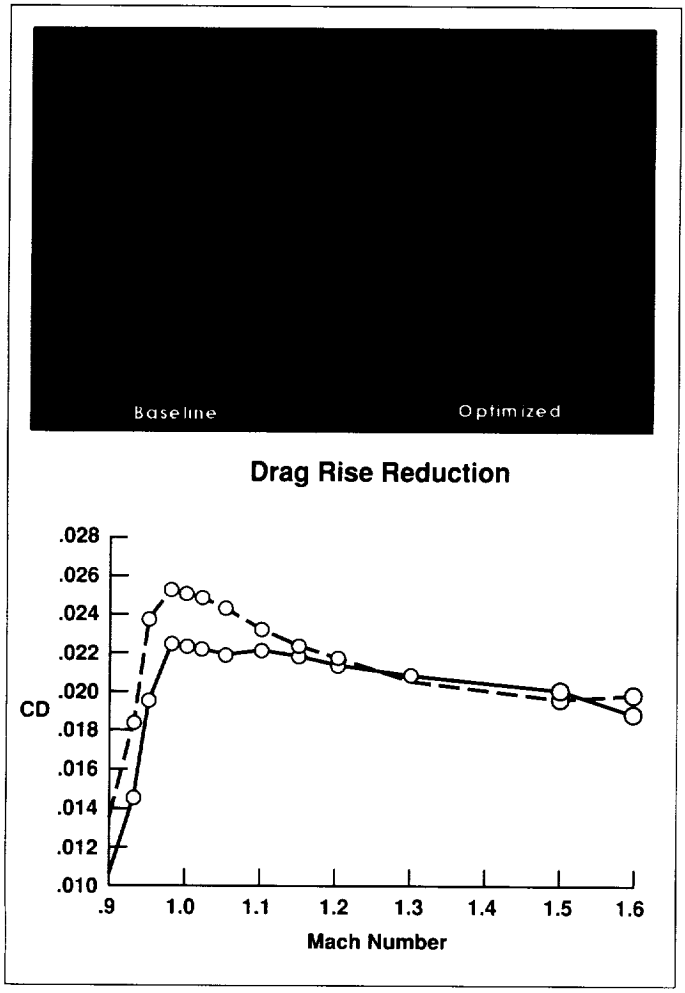

Comparison of a supersonic/transonic wing–body surface pressure distribution before and after drag minimization redesign. Contours: Mach = 1.0, α = 3.5 degrees.

Accomplishment Description
Both optimization processes were established and applied to HSCT design problems. Design optimization required many function evaluations so it was essential that the computer time per flow solution was kept to a minimum. This was done by vectorizing the code to the greatest extent possible, using efficient solution algorithms and moderately resolved grids. A typical solution for inviscid flow about an HSCT was obtained in about 3 minutes of Cray-2 time. However, a comparatively simple design problem required hundreds of function evaluations, so the computer time required for the optimization process was 5–10 hours or more, depending on the number of design variables and the complexity of the optimization problem.

Significance
Automated design optimization tools allow the computer to perform what would otherwise be a time-consuming, labor-intensive process, freeing the designer to explore a broader range of design issues, evaluate new concepts, and achieve performance improvements that would otherwise be unattainable.

Future Plans
The design capability will be applied to advanced HSCT concepts to explore the tradeoffs between aerodynamic performance and sonic boom loudness. The effects of structural deflections will be included in aerodynamic shaping, and multidisciplinary design optimization tools will be developed and applied to HSCT configurations.

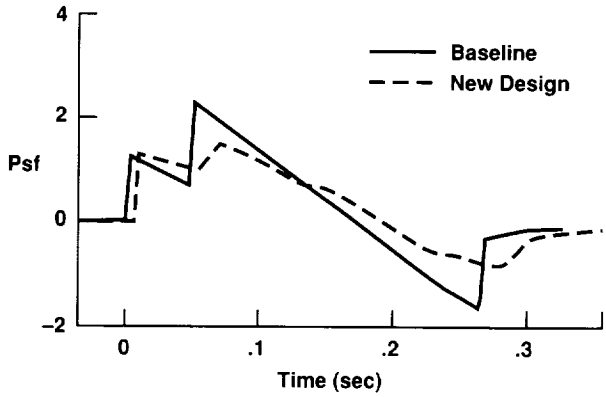

Comparison of sonic boom signatures at ground level for baseline HSCT and the new design optimized for low sonic boom.

Three-Dimensional Turbulent Double-Fin Interactions

Datta Gaitonde, Principal Investigator
Co-investigator: Joseph Shang
WL/FIMM, Wright Patterson AFB

Research Objective
To examine the flow-field structure arising out of the interaction of a turbulent boundary layer with intersecting shocks of equal strength. The ability of the chosen method to provide practical engineering estimates of mechanical and thermal loading is also investigated.

Approach
The three-dimensional, mean compressible Navier–Stokes equations in mass-averaged variables were solved with a high-resolution scheme for the inviscid fluxes, central differencing for the viscous fluxes, and an implicit relaxation-based time integration method. The examination was focused on a Mach 8 interaction for which high-quality experimental data were available for validation. Sensitivity of the solution to mesh resolution was examined.

Accomplishment Description
The flow fields past two symmetric configurations with 15- and 10-degree fins were simulated. With the exception of heat transfer rates in regions of large crossflow, the agreement with experiment was very good. An analysis of the 15-degree configuration was performed. A complex flow field was revealed with interesting features pertaining to the kinematic structure including the existence of two relatively small secondary vortices near the center of the interaction.

Significance
Three-dimensional turbulent interactions are common in supersonic applications such as inlets and wing–body junctures. The accompanying effects are often undesirable. A detailed understanding of the kinematic and dynamic structure of flow fields will provide the insight needed for control and may thus suggest improvements in the design and performance of practical devices.

Future Plans
The present interaction will be verified at different values of relevant parameters (including shock strength and Mach numbers). Preliminary indications are that the overall structure remains similar, but the details exhibit significant variation—particularly in local topological features. The sensitivity of the flow structure to variations in turbulence modeling will also be examined.

Publication
Gaitonde, D.; and Shang J.: Calculations on a Double-Fin Turbulent Interaction at High Speed. AIAA Paper 93-3432, Applied Aerodynamics Conference, Monterey, Calif., Aug. 1993.

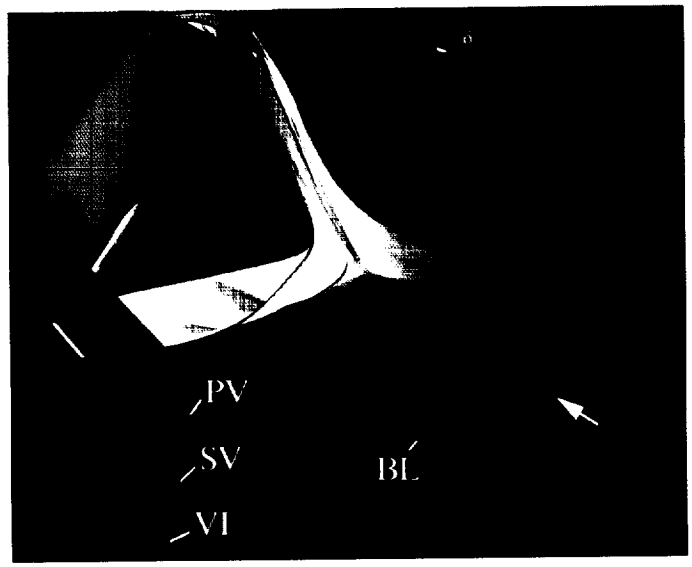

Ribbons exhibiting flow features: BL = boundary layer, VI = vortex interaction, SV = secondary vortex, PV = primary vortex.

Design-By-Optimization Method

Philip B. Gingrich, Principal Investigator
Rockwell International, North American Aircraft Division

Research Objective
To develop and validate a three-dimensional (3-D) numerical optimization design method applicable to complete aircraft configurations.

Approach
A multiblock, implicit time-marching Euler and Navier–Stokes solver is coupled with a gradient-based, constrained optimization technique. Perturbation functions, with an associated design variable, operate on the surface grid. The optimizer determines the design variable set that minimizes a composite function formed with the objectives and constraints. To simulate an inverse procedure, the objective is the root-mean-square difference between the current and a specified target pressure distribution.

Accomplishment Description
A 3-D design-by-optimization method was developed for application to complete aircraft configurations. The design capability has been applied to the F-16XL-2 with a baseline laminar flow control (LFC) glove. A coarse (160,000 points) multiblock Euler grid was developed. The baseline analysis at Mach 1.9 and 3 degrees angle of attack indicated swept isobars that would promote boundary layer transition due to crossflow. To increase laminar flow potential, a flat-top-design pressure distribution was specified for the forward midspan region of the wing. Design studies were conducted at several span stations to determine the appropriate shape functions and constraints. The required number of global optimizer iterations was typically of the order of the number of design variables. For a design at one wing station, 0.5–2.0 Cray Y-MP hours were required, using 20 megawords of memory.

Significance
Nonlinear design methods have not kept pace with computational fluid dynamics analysis capability. Emerging direct inverse and numerical optimization techniques will reduce design cycle time for projected subsonic and supersonic aircraft.

Future Plans
The feasibility of using the numerical optimization technique to minimize drag will be investigated. Appropriate shape function sets and constraints will be established.

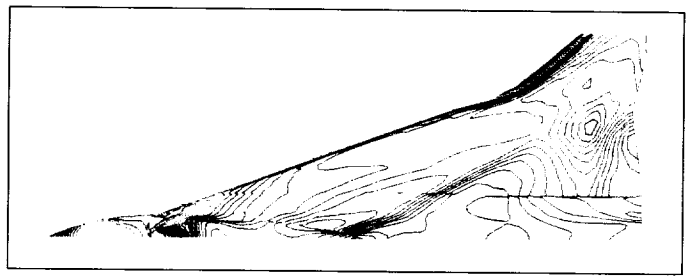

(a)

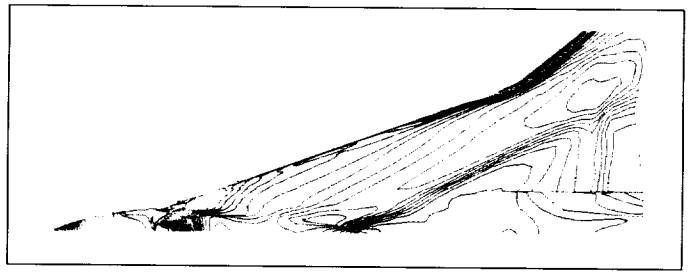

(b)

Upper surface isobars on F-16XL-2 with LFC glove at Mach 1.9, 3 degrees angle of attack for the (a) constant-pressure optimization inverse and (b) baseline. Contour increment = 0.02.

F/A-18 Store Carriage Analyses

David Halt, Principal Investigator
Co-investigators: Mori Mani and Todd Michal
McDonnell Aircraft Company

Research Objective
To investigate the viability of unstructured grid methods and Chimera methods in the modeling of a complex, fluid flow field around an F/A-18 with an array of stores in the stowed position.

Approach
In the unstructured grid approach, the Delaunay grid generation method was used along with a finite-element flow solver, MDFENS. In the Chimera grid approach the "line intersection" method was used to cut the hole in the background grid (the wing grid zone) and set up the fringe boundaries for the Navier–Stokes time-dependent (NASTD) multiblock flow solver.

Accomplishment Description
The unstructured grid for the full configuration F/A-18 with pylon and store used 38,162 grid points and 220,118 tetrahedra in the half plane. The surface Mach contours are shown in the first figure for an Euler solution with a free-stream Mach number of 0.84 and 0 degrees angle of attack. The Chimera solution used 28 zones. The pylons and a store were constructed using a Chimera grid and the remaining zones were constructed from a nonoverlapping grid. The outboard pylon and store grids intersected and a hole was generated in each zone. Both the pylon and the store create a hole with the wing grid. The Euler solution is shown in the second figure for a 0.7 free-stream Mach number and 0 degrees angle of attack. The solution is smooth and continuous across the zone boundaries.

Significance
The unstructured grid Euler solution demonstrates the level of complexity that can be modeled using unstructured grid technology with flexible control of local grid spacings. The Chimera solution demonstrates the three-dimensional capability using the NASTD flow solver and the flexibility to include or exclude a number of stores and pylons or part of the geometry from the solution without generating a new grid each time. This method will reduce the cost and increase the efficiency in obtaining a new solution each time.

Future Plans
Each methodology for the unsteady case of store separation for the F/A-18 aircraft will be demonstrated.

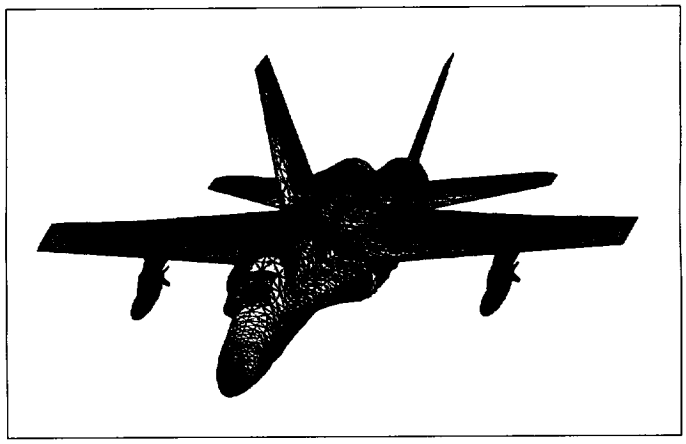

F/A-18 unstructured grid surface Mach contours at free-stream Mach number 0.84 and 0 degrees angle of attack; blue = Mach 0.5 and below, red = Mach 1.0 and above.

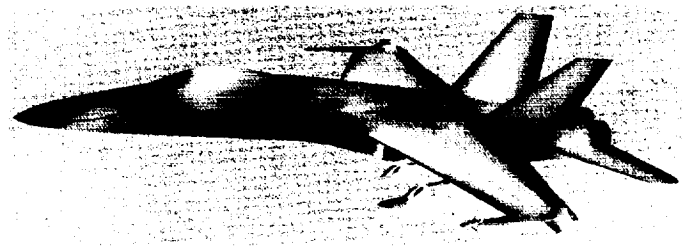

NASTD Chimera grid surface pressure contours on a fighter geometry with pylon, store, and tip missile; black = 0.37, white = 1.34.

Lifted Ethylene Jet Diffusion Flames

Carolyn R. Kaplan, Principal Investigator
Co-investigator: Elaine S. Oran
Naval Research Laboratory

Research Objective
To demonstrate the capability to simulate the phenomenon of flame lift-off and to study the mechanism by which a lifted flame is stabilized.

Approach
The model solved the multi-dimensional time-dependent reactive-flow Navier–Stokes equations coupled with submodels for soot formation and radiation transfer to simulate unsteady axisymmetric ethylene air-jet diffusion flames. The convection terms were solved using the barely implicit correction to the flux corrected transport algorithm. The effects of thermal conduction, molecular diffusion, and viscosity are included through explicit finite-differencing formulations. The radiative heat flux was found from a solution of the radiation transfer equation using the discrete ordinates method. The soot formation and growth model are based on a set of coupled ordinary differential equations describing soot nucleation, surface growth, and coagulation.

Accomplishment Description
Simulations were conducted for jet inflow velocities ranging from 5 meters/second to 100 meters/second for three different fuel-jet dilutions. The computations show that (1) the base of the flame stabilizes in a stoichiometric region, (2) the flame lift-off height increases linearly with jet exit velocity, and (3) the height at which the flame stabilizes increases with fuel-jet dilution. In all cases, the laminar flame base is anchored in a turbulent region of the gas jet. The stabilization heights compare favorably with experimental measurements reported in the literature. The computations support an extinction theory of flame stabilization, in which the flame is quenched when the rate of heat conduction to the sides of the flame exceeds the rate of heat production due to chemical reaction.

Significance
The physical mechanisms responsible for flame stabilization are still controversial. Past work has involved experimental measurements of flame lift-off height, and stabilization mechanisms have been deduced from these experiments. This work constitutes the first numerical simulation of flame lift-off and may provide more insight into the stabilization mechanisms.

Future Plans
Further analysis of the stabilization mechanism will be deduced from the simulation data. The model will be used to evaluate the effect of co-flow velocity on the dynamics of jet diffusion flames.

Publication
Kaplan, C. R.; Baek, S. W.; and Oran, E. S.: Dynamics of an Unsteady Buoyant Ethylene Jet Diffusion Flame. AIAA Paper 93-0109, Jan. 1993.

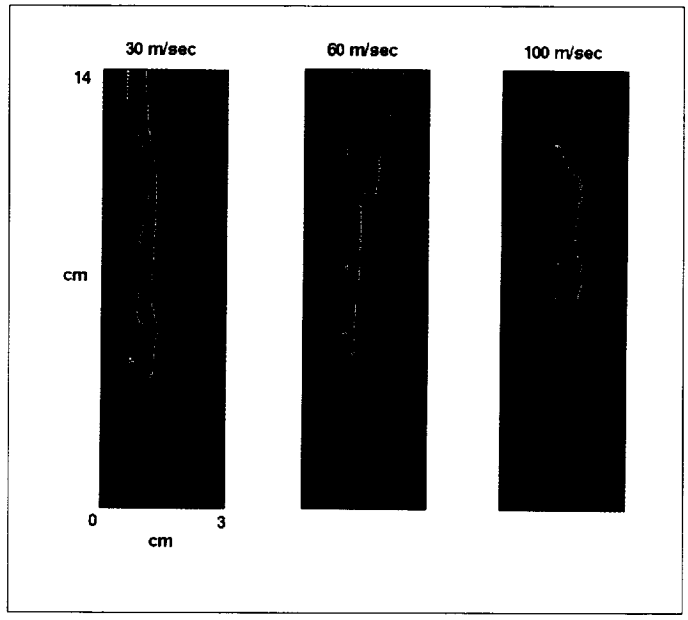

Temperature contours show the effect of jet inflow velocity on flame lift-off height.

Unstructured Grid/Flow Solver Calibration

Steve L. Karman, Jr., Principal Investigator
Co-investigators: Doug Howlett and Elizabeth A. Robertson
Lockheed Engineering and Sciences Company

Research Objective
To demonstrate the capability to numerically model complex three-dimensional (3-D) time-dependent, multibody flow fields using unstructured grid methods.

Approach
An unstructured Cartesian grid computational fluid dynamics (CFD) code was used to analyze complex two-dimensional (2-D) and 3-D multibody flow fields. The grids were generated by recursively refining a root Cartesian cell that encompassed the entire domain. The subdivision was initially based on user defined boundary spacing. Later, the grid was refined based on flow-field gradients or movement of a body through the domain. The flow solver used upwind differencing. The 2-D solver used a point-implicit time-integration scheme that made use of Jacobi subiterations for improved stability. The 3-D flow solver used a multistage Runge–Kutta time-integration scheme. Multigrid can be used for steady-state problems.

Accomplishment Description
Various 2-D problems were solved to prove the concept. One of the more difficult 2-D problems attempted was the AGARD 03 test case, which consisted of a NACA 0012 airfoil run at a free-stream Mach number of 0.95 and an angle of attack of 0 degrees. The flow field was symmetric from top to bottom and contained a normal shock in the wake. Grid convergence studies performed by other researchers showed the normal shock to appear 3.35 chord lengths aft of the airfoil trailing edge. This investigation placed the shock at 3.4 chord lengths back, a difference of 1.5 percent. In the first figure, the final grid with 33,517 active cells and normalized velocity contours from this study are given. The primary focus of the 3-D work was the grid-generation process. Although the grid-generation procedures are still being developed, some preliminary solutions were computed. In the second figure, the inviscidly computed, steady-state velocity magnitude contours on the surface and on the symmetry plane of a 3-D generic wing/store configuration are shown.

Significance
The development of an unstructured CFD capability will greatly reduce the analysis time for complex 3-D geometries and flow fields. Automatic grid generation will permit the timely evaluation of parametric studies of complex geometries and the analysis of phenomena such as store separation.

Future Plans
The calibration of the 3-D Cartesian-based unstructured-grid code will continue. Various steady-state solutions for complex geometries will be analyzed. The time-accurate moving body capability will be added and calibrated. Long-term plans are to include a viscous analysis capability.

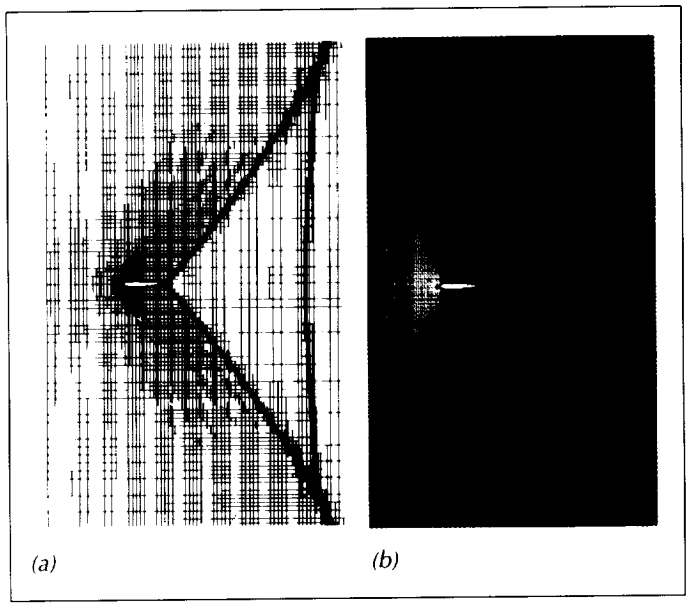

Results of AGARD 03 test case for a 2-D code; (a) adapted grid and (b) velocity magnitude.

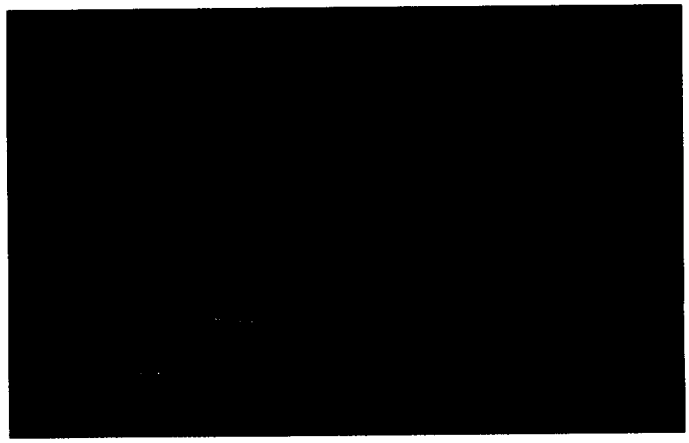

Velocity magnitude contours on the surface and the symmetry plane of a generic wing/store configuration.

Simulation of Flow About an Airborne Observatory

Stephen P. Klotz, Principal Investigator
Co-investigator: Christopher A. Atwood
NASA Ames Research Center

Research Objective
To assess, using computational fluid dynamics (CFD), effects of an open telescope bay on the aerodynamics and aero-optics of a Boeing 747-SP, the aircraft platform for the Stratospheric Observatory for Infrared Astronomy (SOFIA).

Approach
Computations were performed on a sting-mounted aircraft without empennage. The telescope was mounted behind the wings and the engines were powered. Solutions were computed by OVERFLOW and used the diagonalized Beam–Warming numerical scheme and Baldwin–Lomax turbulence model in the code. A shear-layer version of the Baldwin–Lomax model simulated the effects of turbulence in the cavity-port shear layer.

Accomplishment Description
The original design concept for SOFIA placed the telescope cavity forward of the wings and immediately behind the cockpit. Recent work focused on computations with the telescope mounted behind the wings because locating the cavity there required fewer structural modifications. Nevertheless, an aft-mount cavity configuration has potential problems associated with (1) radiative scattering from the engine plumes, (2) a boundary layer that is optically thicker, and (3) strong oscillatory flow in the vicinity of the empennage. The figure shows the geometrical configuration used in the computations and the contours of surface pressure coefficients and engine plume temperatures at SOFIA cruise-flight conditions. The cavity was fitted with an internal shear-layer ramp and demonstrated broadband acoustic behavior similar to the forward-mounted design. However, a region of separated flow is apparent immediately downstream from the cavity aperture. Optical clarity of the infrared telescope was also investigated. There is some degradation of clarity in the near-infrared regime if the telescope is mounted behind the wings.

Significance
The use of CFD in the design of SOFIA has provided information that is difficult to obtain experimentally. The generality of the methodology has attracted industry interest for applications ranging from the stealthy internal carriage of stores to the design of airborne laser platforms.

Future Plans
The Boeing 747-SP horizontal and vertical stabilizer geometry will be included in the computations during the next year. Calculations will focus on a detailed investigation of the separation region behind the cavity and fluctuating loads on the aircraft empennage.

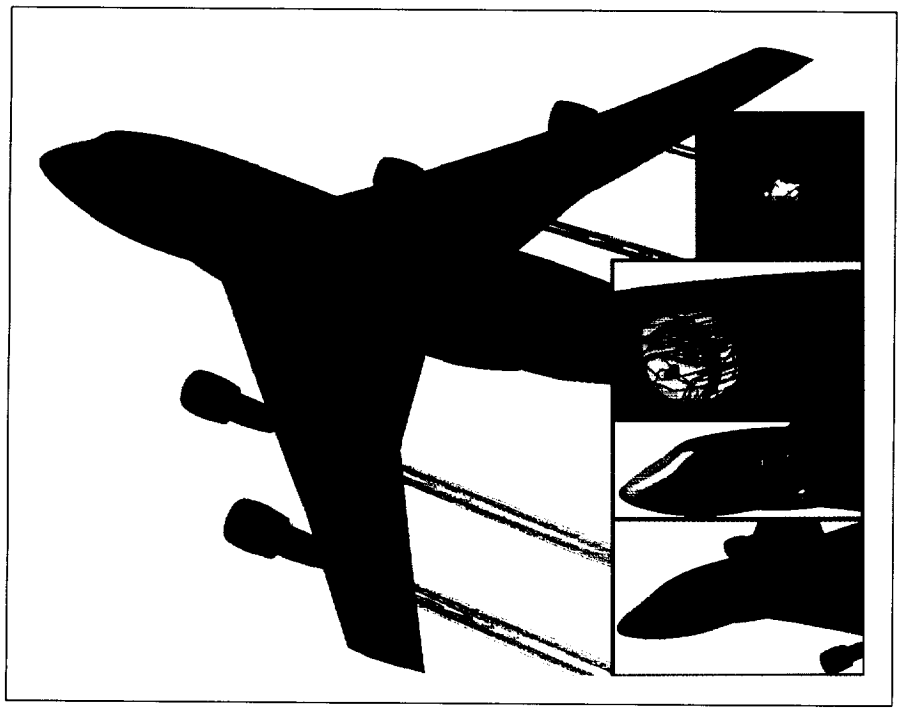

Contours of SOFIA surface pressure coefficients and normalized plume temperatures: magenta = high, blue = low. Insets (top to bottom): instantaneous diffraction pattern; instantaneous streamlines near the cavity; quiet cavity (forward mount); and rectangular cavity (forward mount).

Finite-Element Euler Solver for a Distributed Memory Computer

Rainald Lohner, Principal Investigator
Co-investigator: Alexander Shostko
George Washington University

Research Objective
To develop a three-dimensional (3-D) unstructured-grid generator in the multiple-instruction/multiple-data (MIMD) context.

Approach
The advancing-front grid generation technique was used in conjunction with unstructured grid load balancing and domain partitioning methodologies with the host-nodes parallel model. Moreover, distributed data structures were used for the parallel 3-D grid generation.

Accomplishment Description
The unstructured-grid generator prototype was developed and ported to the MIMD context. The algorithm used a background grid as the means to separate spatially different regions, enabling the concurrent, parallel generation of elements in different domains. After generating elements in parallel in the different domains, the empty interdomain regions were gridded in parallel. Several difficulties were overcome by extending the two-dimensional grid generator to three dimensions. Load balancing was improved by optimization of initial subdivision, similar to heat conduction methodology. In 3-D, only a fraction of the total mesh could reside in any one processor at a given time. Thus, the grid is kept in the processors, where it was generated. A numbering method for the generated nodes and elements was developed and yielded a unique identification for each node and element generated on all processors. Optimal tolerance for the interfaces and predefined maximum effort to be spent affect the quality of the generated grid. The total execution time is still under investigation. New visualization tools for debugging complex geometries and for postprocessing were developed for the 3-D subdomain/interface grid generation.

Significance
For the first time, 3-D grid generation was ported to the MIMD context.

Future Plans
Grid generation for complex 3-D geometries will be tested and benchmarked. Front-end preprocessing of the background grid will be developed for better load balancing in cases with coarse background grids and background sources.

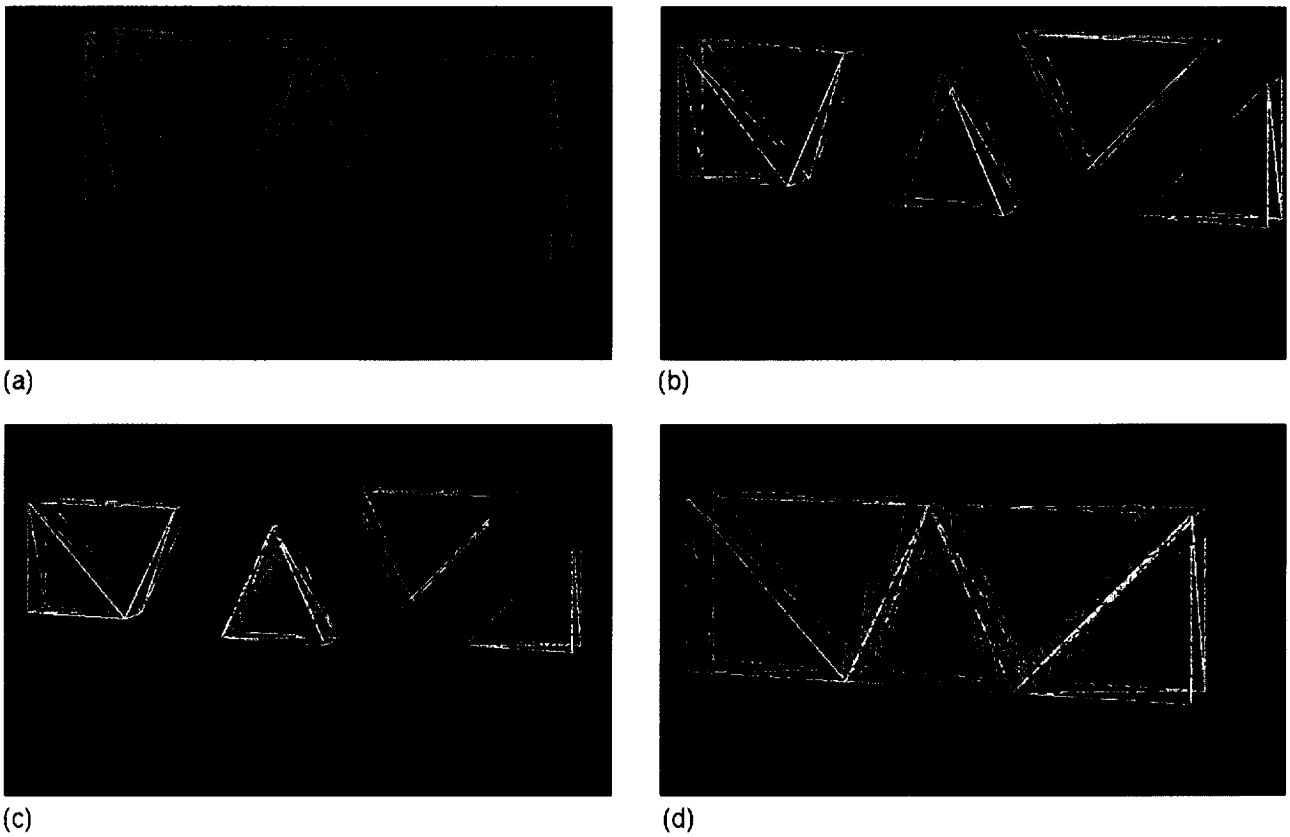

Parallel grid generation. (a) Domain definition and background grid. (b) Subdomain grids after parallel generation. (c) Interface and subdomain grids after parallel generation. (d) Assembled grid.

Space Shuttle Flow Field

Fred W. Martin, Jr., Principal Investigator
Co-investigators: P. Buning, W. Chan, I. Chiu, R. Gomez, J. Slotnick, E. Ma, D. Pearce, T. Wey, and M. Kandula
NASA Johnson Space Center

Research Objective
To improve the numerical modeling of the Space Shuttle Launch Vehicle (SSLV) ascent aerodynamic environment by improving the geometric resolution of the vehicle.

Approach
The OVERFLOW-Chimera scheme is used to obtain flow fields about the SSLV in the Mach number range 0.6–4.5, with particular emphasis on the transonic range. ICEM-computational fluid dynamics (CFD), a computer-aided design (CAD)-based grid generation package, was used to produce the surface grid. The resulting grid has, on average, a four inch resolution along the surface. The hyperbolic volume grid generator HYPGEN was used to create the volume grids.

Accomplishment Description
A 113-grid system comprised of approximately 16 million points was generated. Hyperbolic volume grids were used to resolve the boundary layer features. The hyperbolic volume grids communicated with Cartesian grids, which captured flow features between the bodies and communicated with a relatively coarse farfield grid. A thin-layer Navier–Stokes solution of the SSLV during ascent was initiated.

Significance
The ICEM-CFD model was the first complete CAD model of the entire SSLV. The model included all surface protuberences larger than four inches because of the geometric sensitivity observed in previous solutions. The CAD model exceeds the geometric fidelity of the wind tunnel model used to develop the original aerodynamic data for the SSLV.

Future Plans
Flow-field calculations using the 113-grid system are under way for a Space Transport System-50 flight case including the Space Shuttle main engine and solid rocket booster plumes. Comparison with available wind tunnel data and flight measurements will be used to verify the accuracy of the grid system and flow solver. The required accuracy for this solution is to be within 5 percent of the wing's ultimate capability.

Publications
1. Pearce, D. G. et al.: Development of a Large-Scale Chimera Grid System for the Space Shuttle Launch Vehicle. AIAA Paper 93-0533, 1993.
2. Kandula, M.; and Buning, P.: Evaluation of Baldwin–Barth Turbulence Model with Thin-Layer Navier–Stokes Computation of an Axisymmetric Afterbody-Exhaust Jet Flowfield. AIAA Paper 93-0418, 1993.
3. Slotnick, J. P.; Kandula, M.; Buning, P. G.; and Martin, F. W., Jr.: Numerical Simulation of the Space Shuttle Launch Vehicle Flowfield with Real Gas Solid Rocket Motor Plume Effects. AIAA Paper 93-0521, 1993.

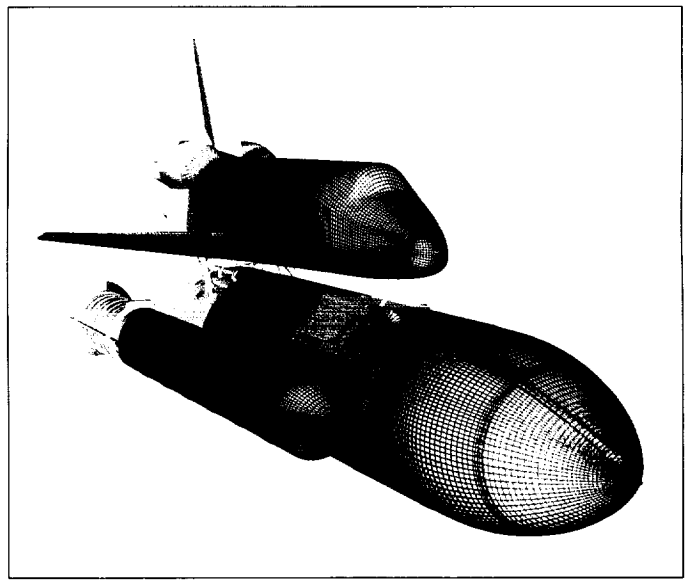

Surface grids on the SSLV.

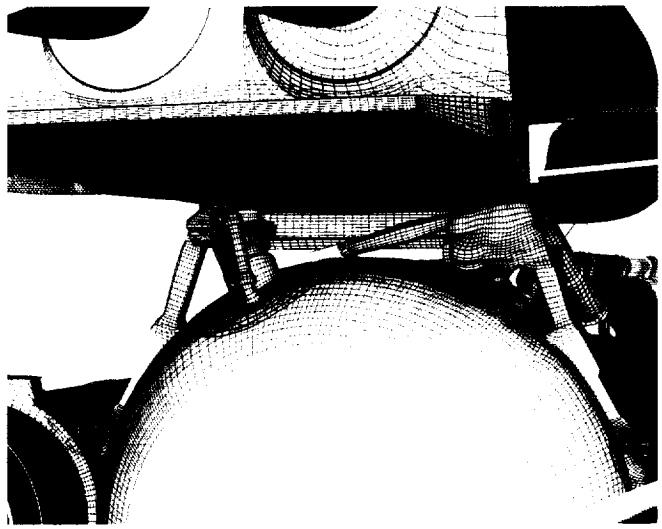

Surface grid topology of aft attach hardware.

Direct Computation of Aerodynamic Sound Generation

Parviz Moin, Principal Investigator
Co-investigators: Sanjiva K. Lele, Tim Colonius, Brian E. Mitchell, and Jonathan B. Freund
NASA Ames Research Center/Stanford University

Research Objective

The prediction of the sound produced by turbulent flow requires a detailed knowledge of acoustic source terms. Computation of both the acoustic sources and far-field sound using the unsteady Navier–Stokes equations allows direct validation of aeroacoustic theories, and will help provide noise control strategies.

Approach

Accurate computation of far-field sound and near-field hydrodynamics requires the Navier–Stokes equations to be solved using accurate numerical differentiation and time-marching schemes, with nonreflecting boundary conditions. Sixth-order compact finite-difference schemes were used to evaluate spatial derivatives and time was advanced with a fourth-order Runge–Kutta scheme. Nonreflecting boundary conditions developed for the two-dimensional (2-D) linearized Euler equations were modified for use with nonlinear Navier–Stokes computations of open flow problems.

Accomplishment Description

The numerical scheme, which was previously validated on several model problems, was used to compute the sound generated by a 2-D spatially developing subsonic mixing layer. The layer was forced at its most unstable frequency and its first three subharmonics, causing a highly organized structure (nearly periodic in time). Vortices were formed and underwent pairing twice at fixed locations downstream from the inflow boundary. The sound sources associated with the flow were computed. The figure shows the vorticity contours in the near field, indicating the formation of vortices and the two pairings. Also plotted in the figure are the contours of the dilatation outside the near field, showing the acoustic waves that are generated by the flow. The most intense sound is produced by the second pairing. This computation required 200 hours on the Cray Y-MP with a core memory of 10 megawords.

Significance

The computation of the sound generated by the 2-D mixing layer represents the first time that direct numerical simulation has been used to compute the sound generated by a turbulent shear flow. The results will shed light on the nature of the sound generation by flows with noncompact vorticity fields and will allow a critical evaluation of the accuracy of aeroacoustic theory in predicting the sound generated by turbulent shear flows.

Future Plans

Computations of the sound sources in a three-dimensional round jet are under way. Techniques for reducing computational cost are being investigated, including the development of a hybrid numerical scheme which solves a convected wave equation for the far field and the Navier–Stokes equation in the near field and matches the two solutions.

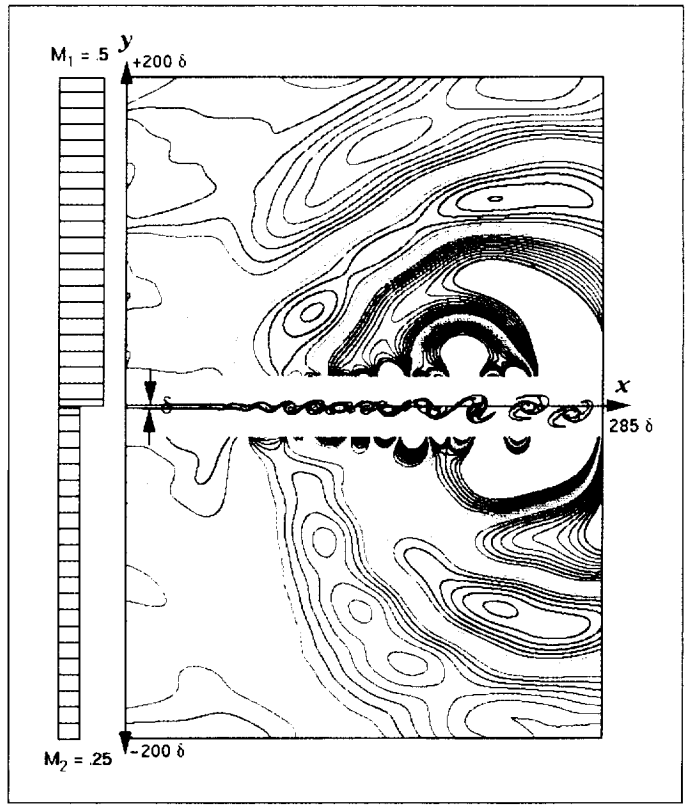

Contours of near-field vorticity and far-field dilatation in the 2-D mixing layer.

Computational Fluid Dynamics of F-18 Flow Field

Yehia Rizk, Principal Investigator
Co-investigators: Scott Murman and Ken Gee
NASA Ames Research Center

Research Objective
To use computational fluid dynamics (CFD) to study the effects of engine inlet flow on the external flow field around the F-18 aircraft and to gain more understanding of the vortex-induced tail buffet phenomenon, including the effect of installing a leading edge extension (LEX) fence.

Approach
Simulation of the complete flow field around the F-18 was achieved by coupling the external flow and the internal flow through the engine inlet. A Chimera grid zonal scheme was used to add necessary grids to the existing system to simulate the flow through the inlet duct up to the compressor face. Boundary conditions allowing the specification of the mass flow were used. A weak coupling between the aerodynamics and structures was used for the tail buffet study. A time-accurate Navier–Stokes solver combined with Chimera was used for the aerodynamics. The resulting airloads were used as a forcing function to compute the structural response of the flexible vertical tail using modal analysis. Chimera was also utilized to investigate the effect of the LEX fence to reduce tail buffet.

Accomplishment Description
The results indicate a strong coupling of the engine external and inlet flows, especially at the maximum power engine setting. Increasing the mass flow rate through the inlets caused the LEX vortex breakdown location to move progressively downstream; this movement is consistent with trends observed in flight tests. Time accurate computations show that buffet frequency is proportional to airspeed. At flight speed, tail buffet is observed because the airload frequency is close to the tail's first natural frequency of bending. Computations also show that installing the LEX fence introduces an unsteady vortex interaction which results in reducing the airload frequency compared to the tail's natural frequency. Coarse grid computations typically consumed about 100 Cray Y-MP hours and about 12 megawords of central memory.

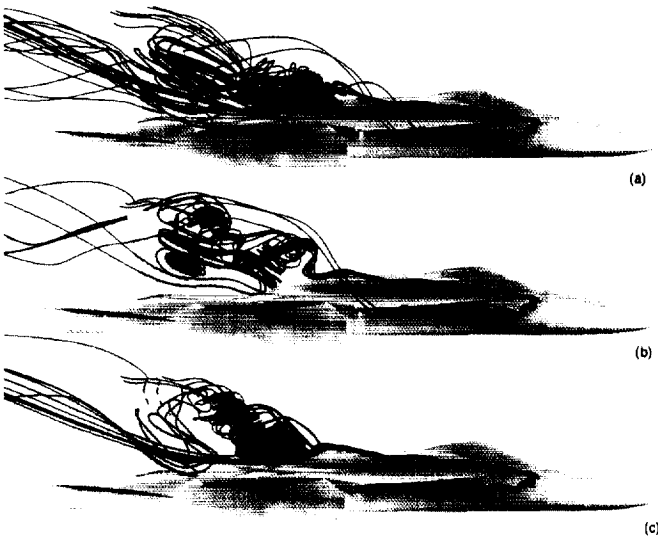

Inlet mass flow rate on LEX vortex; $M_\infty = 0.243$, $Re = 11.0 \times 10^6$, $\alpha = 30.3$ degrees. (a) Faired inlet; (b) flight idle; (c) maximum power.

Significance
Inclusion of the effects of engine inlet flow improved the correlation between CFD results and flight data. CFD results also provided more understanding of the vortex/tail interaction. This increased understanding will lead to more effective means of controlling or alleviating the buffet and preventing premature tail structure fatigue for current and future high-performance aircraft.

Future Plans
The effect of grid refinement on the flow-field structure will be examined. Also, the computational method will be generalized to account for a strong structural/aerodynamic coupling.

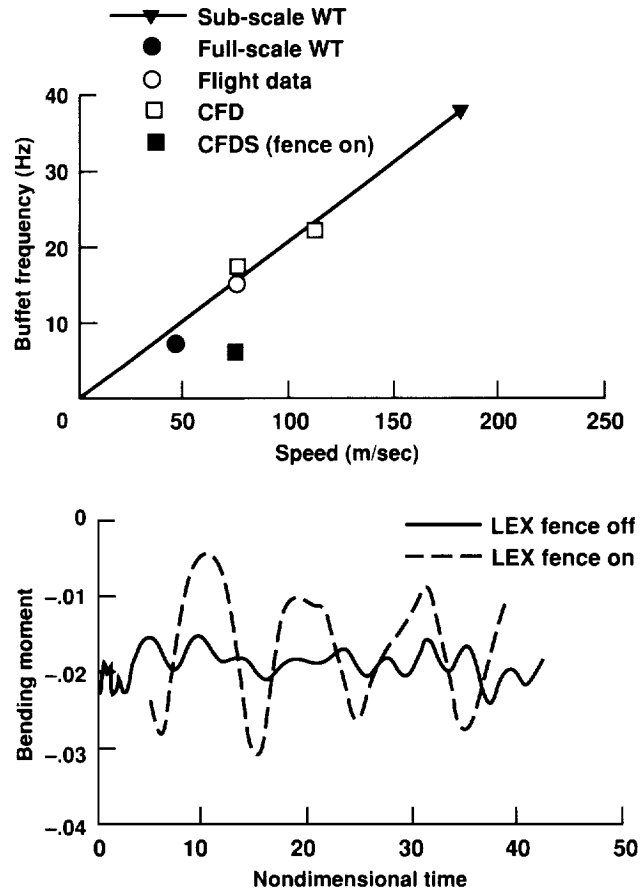

Effect of LEX fence on vortex-induced buffet frequency.

Wings with Control Surfaces

David M. Schuster, Principal Investigator
Lockheed Engineering and Sciences Company

Research Objective
To develop a computational aerodynamics method to analyze and design aeroelastic wings with multiple deflected control surfaces.

Approach
Wing geometries with specified leading- and trailing-edge control surfaces were modeled by allowing the computational grid to shear between control surfaces and by assuming that there was no gap along the hinge line. The models were analyzed using an existing Euler/Navier–Stokes aeroelastic analysis method (ENS3DAE). This method computed steady or unsteady aerodynamic loads and the structural deflections that resulted. These loads and deflections were used to determine the aerodynamic and structural performance of the wings.

Accomplishment Description
This method was applied to the aeroelastic design of an advanced fighter wing for efficient operation at steady, transonic maneuver flight conditions without degrading the wing's transonic cruise performance. A set of leading- and trailing-edge control surface deflections in conjunction with an aeroelastic twist distribution were defined to obtain optimal aerodynamic performance at a specified maneuver flight condition. The predicted aerodynamic loads, along with the structural deflections required to obtain the optimal aerodynamic performance at this flight condition, were used to compute the bending and torsional stiffness characteristics of the wing using an inverse structural design procedure. From this computation, an unloaded jig shape for the wing was extracted, which, under cruise loading, deflected to the optimal cruise geometry of the wing. Upon deflection of the control surfaces and adjustment of the flight conditions to the maneuver design point, the wing aeroelastically deflected to the appropriate shape for optimal maneuver performance.

Significance
The interaction of controls, structures, and aerodynamics is an important design consideration for modern commercial and military aircraft. The method studied demonstrates an efficient scheme for implementation of complex-flow aerodynamic analysis methods into the design environment.

Future Plans
Parallel processing will be employed to couple the aeroelastic method with a finite-element computational structural mechanics method to perform more detailed fluid–structure interaction analyses and designs.

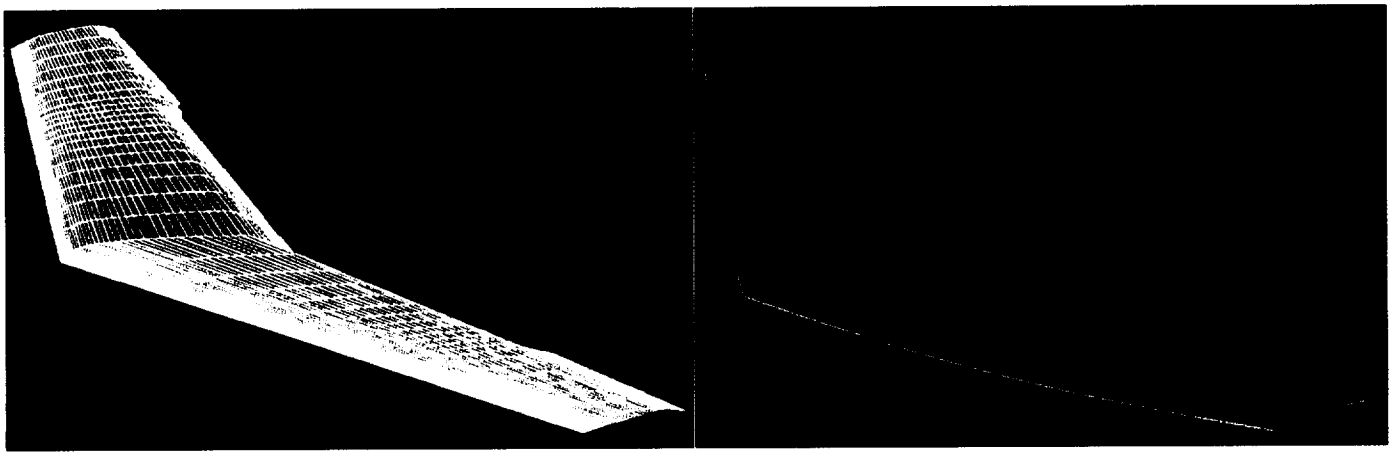

Surface grid for a wing with deflected control surfaces and aeroelastic pressure coefficient contours on a fighter wing design at transonic maneuver flight conditions. Pressure coefficient ranges from –1.0 (blue) to 1.0 (magenta) with an increment of 0.1 between contours.

Sonic Boom Predictions for High-Speed Civil Transport

Michael J. Siclari, Principal Investigator
Co-investigator: Kamran Fouladi
Grumman Corporate Research Center/Lockheed Engineering and Sciences Company

Research Objective
To develop a fast Euler solver capable of accurately predicting sonic boom pressure signatures generated by complex aircraft geometries.

Approach
The unsteady three-dimensional Euler equations were solved explicitly within the context of a finite-volume multistage Runge–Kutta integration scheme using local time stepping and residual smoothing to accelerate convergence. An implicit upwind marching scheme was utilized along with an axial multiblock approach to facilitate the modeling of complex geometries including multiple lifting surfaces, inlets, exhaust, and engine nacelles.

Accomplishment Description
Grid spreading that occurs with conventional grid topologies results in poor resolution of the flow field downstream of an aircraft without the use of millions of grid points. The current approach retains resolution of the flow field so that pressure signatures can be predicted at one to two body lengths below the aircraft. These near-field pressure signatures are then extrapolated to the ground using atmospheric propagation programs based on linear theory. The magnitude and shape of sonic boom signatures generated by candidate low-boom High-Speed Civil Transport designs can be evaluated using this method.

Significance
This innovative grid topology reduced grid spreading and shock smearing and resulted in accurate field computations several body lengths downstream of an aircraft. The speed of this computational fluid dynamics method for supersonic flows is ideally suited for the design optimization environment.

Future Plans
New research will be carried out to couple this methodology with a nonlinear design optimization program to design aircraft shapes with optimum aerodynamic performance and minimum sonic booms.

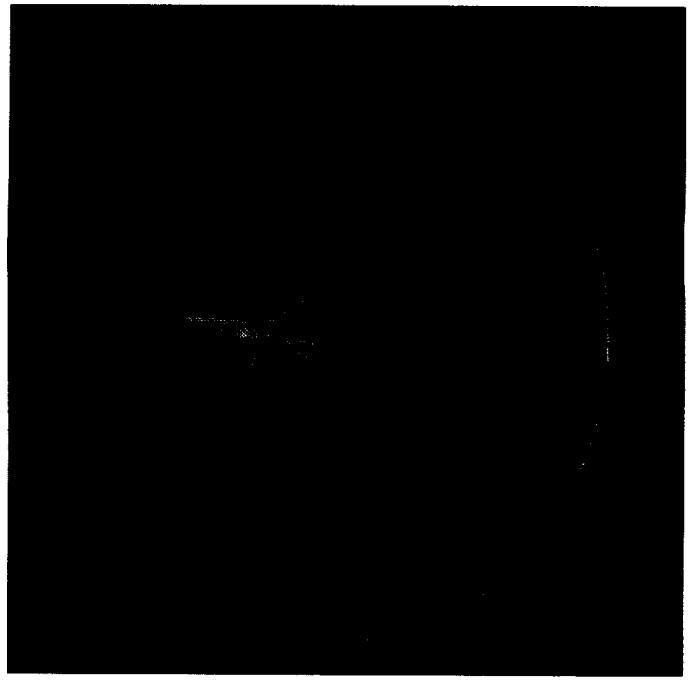

Pressure propagation behind a supersonic vehicle.

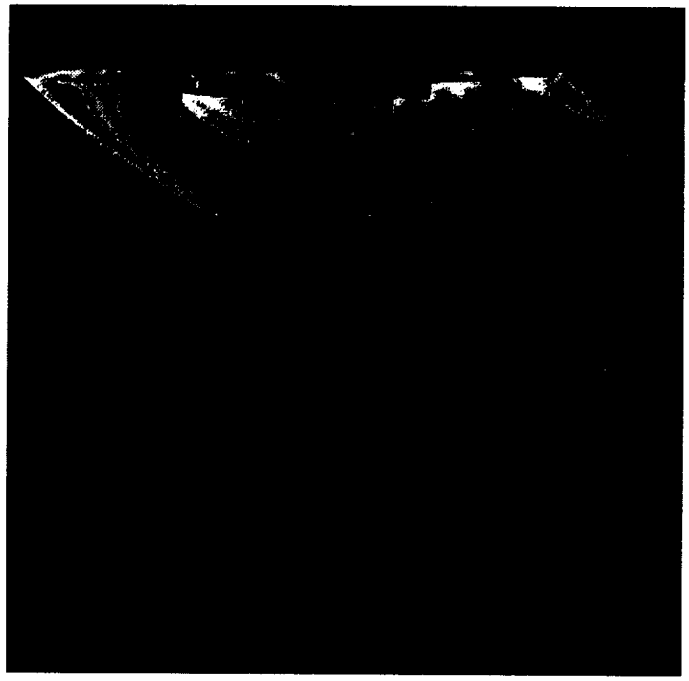

Pressure propagation below a supersonic vehicle.

Navier–Stokes Equations for Jet Acoustics

Eli Turkel, Principal Investigator
Co-investigator: Ehtesham Hayder
ICOMP/NASA Lewis Research Center

Research Objective
To investigate the noise generated by and the stability properties of a jet subject to perturbations. This requires coupling the near-field solution, which is nonlinear, with a linear far-field solution. Because of the large range of scales that are present one must use higher order numerical methods.

Approach
The fully time-dependent Navier–Stokes equations were solved with a high-order finite-difference method that was fourth-order accurate in space and second-order accurate in time. The algorithm was extended from one to several space dimensions using a splitting method. The fluxes were extrapolated at the boundaries to keep the formal order of accuracy. Various boundary conditions were compared at the outflow boundary to prevent waves from being reflected and contaminating the interior solution. The goal was to simulate aerodynamic noise associated with a supersonic jet flowing into a subsonic free stream. The computations were done in two stages. First, a mean state of the field with steady inflow boundary conditions was computed, then the transient behavior of the flow was calculated using a boundary condition that was a time-dependent perturbation of the initial boundary condition. The perturbation could be either a sinusoidal perturbation or a perturbation based on the eigenmodes of the linearized problem.

Accomplishment Description
Planar and axisymmetric jets were considered. For the planar case, the jet Mach number was 1.5 and the Reynolds number was 1.27 million. Solutions were obtained for steady-state calculations and a time-dependent simulation. Results for the axisymmetric jet simulations were similar to those of the planar jet case. The original algorithm was extended to be fourth-order accurate in space for the viscous and inviscid terms and was compared with the solutions for a flat-plate calculation. Several radiation boundary conditions were also considered. For a nondimensional time of 200 and a $150 \times 200 \times 7$ grid for a domain 25 jet diameters long, 8 megawords of memory and 16 processing hours were required.

Significance
The use of a higher order accurate scheme is essential to obtain accurate solutions with limited resources.

Future Plans
A major problem with three-dimensional Navier–Stokes equations is the treatment of a singular line. Future focus will be on the correct numerical treatment of a singular line and its application to jet acoustics.

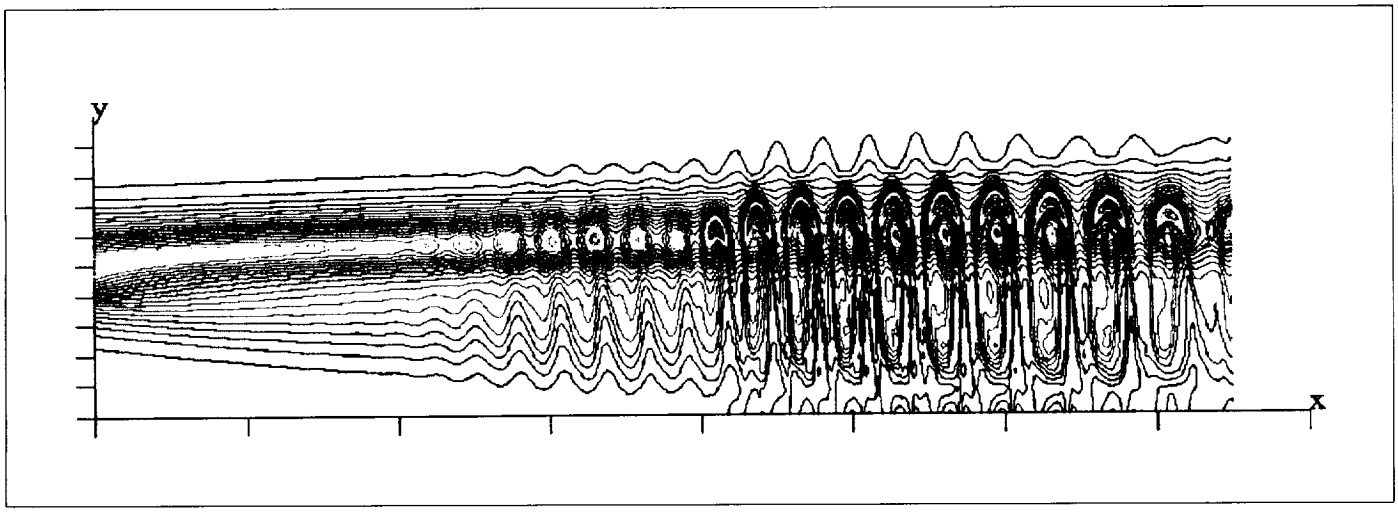

Subsonic jet simulation with high resolution in a large domain. Mach = 0.8, angle of attack = 0.0 degrees, Reynolds number = 1.02×10^4. Contour levels: dark blue = 0.0 and magenta = 1.6.

Block-Structured Approach for High-Lift Applications

Veer N. Vatsa, Principal Investigator
Co-investigator: Mark D. Sanetrik
NASA Langley Research Center/Analytical Services and Materials, Inc.

Research Objective
To demonstrate the feasibility of using a block-structured grid approach for computing viscous flows over high-lift configurations of practical interest.

Approach
A newly developed grid generation procedure with automatic blocking and compact grid enrichment capability was coupled to a cell-centered, finite-volume Navier–Stokes multiblock flow solver.

Accomplishment Description
High-quality grids suitable for high-Reynolds number viscous flows were generated for a three-element, high-lift airfoil configuration. The resulting grids varied smoothly across block boundaries, but maintained point-to-point continuity across block interfaces. Grid points were clustered in selected regions to resolve high gradients without propagating the grid points in the far field. This clustering resulted in compact grid enrichment. A multistage time-stepping algorithm with a multigrid acceleration technique was used to obtain steady-state solutions to the Reynolds-averaged Navier–Stokes equations. A field-equation type turbulence model (the Spalart–Allmaras model) was chosen to accommodate multiple layers of wall–wake boundary-layer interactions. The computed solutions compared well with independent calculations and correlated well with experimentally measured pressure and skin-friction data.

Significance
Block-structured grids with point-to-point continuity across block interfaces can be used to analyze complex aerodynamic configurations. This methodology offers the advantages of unstructured grids in its ability to accommodate complex configurations and cluster grid points in regions of interest while still maintaining the efficiency of structured-grid flow solvers.

Future Plans
This method will be applied to more complex configurations. An effort is under way to compute flow over a transport aircraft configuration and a High-Speed Civil Transport configuration.

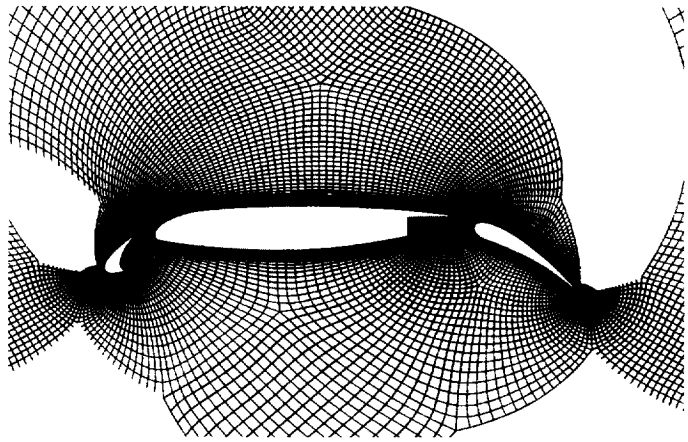

Partial view of a 20-block grid for a 3-element airfoil.

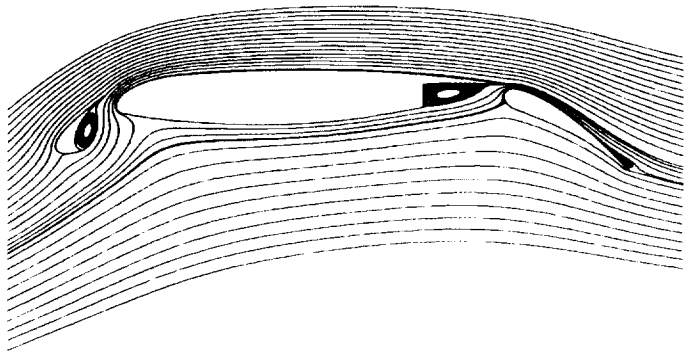

Particle traces for a 3-element airfoil; Mach = 0.2, angle of attack = 8.1 degrees, Reynolds number = 9.0 million.

Aeronautics

Hypersonics

Flow Fields Including Chemical Kinetics

Ramesh K. Agarwal, Principal Investigator
Co-investigators: Jerry E. Deese, Paul Schulte, T. Mark Walter, Thomas P. Gielda, and Hugh Thornburg
McDonnell Douglas Research Laboratories

Research Objective
To develop computational methods capable of accurate and efficient prediction of aerospace vehicle flow fields including chemical kinetic and propulsion effects.

Approach
The Reynolds-averaged Navier–Stokes equations were solved on body-conforming curvilinear grids using a finite-volume Runge–Kutta time-stepping algorithm. Euler, thin-layer, slender-layer, and full Navier–Stokes options were available. Complex configurations were modeled with a multiblock zonal implementation. Algebraic and two-equation turbulence models have been incorporated into the code. Nonequilibrium air, hydrogen–oxygen, and hydrocarbon chemical models were included. Ionization models were available for analysis of electromagnetic wave transmission through the flow field.

Accomplishment Description
Flow fields about a number of high-speed configurations were computed. Single-stage-rocket technology configurations were analyzed at angles of attack from 0 to 180 degrees. Several missile and launch vehicle configurations with plumes were analyzed to determine base drag. The figure shows the Mach number distribution in the symmetry plane of a launch vehicle with three boosters including the core and booster plumes. High-Mach number calculations were run for reentry vehicles requiring the nonequilibrium air chemistry model. Typical calculations required 20–40 megawords of memory and 10–20 Cray-2 hours.

Significance
High-speed, high-enthalpy flows are difficult to simulate experimentally. Accurate simulation of these flows will give designers an important computational data base on vehicle performance that cannot be obtained experimentally.

Future Plans
Chemistry models for solid-rocket-motor plumes will be incorporated into the code. Additional chemistry models will be added and validated.

Publication
Gielda, T. P.; Walter, T. M.; and Agarwal, R. K.: Single Stage Rocket Performance. AIAA Paper 92-1386, March 1992.

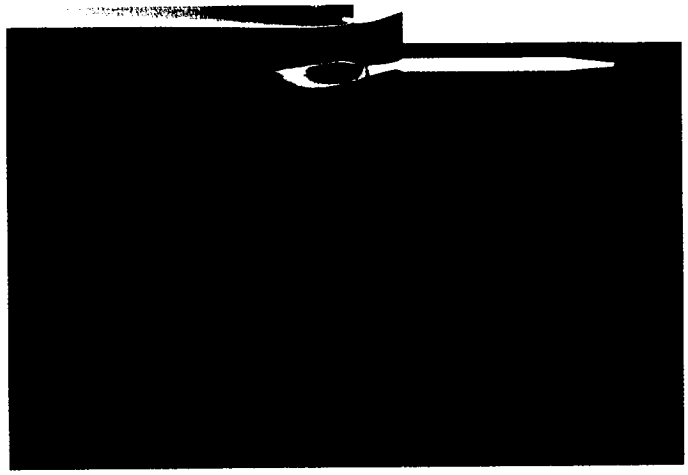

Mach number distribution in the symmetry plane of a launch vehicle with three boosters.

Three-Dimensional Compressible Turbulence Modeling

Jorge E. Bardina, Principal Investigator
Co-investigator: Thomas J. Coakley
MCAT Institute/NASA Ames Research Center

Research Objective
To verify and develop the baseline two-equation turbulence models that account for the effects of compressibility in high-speed turbulent flows. The focus is on the identification of models that are superior in their predictive capabilities of three-dimensional (3-D) turbulent flows.

Approach
Turbulence models were developed based on insight gained from experimental and theoretical research. A data base of high-speed turbulent flows was used in this investigation. Specific topics for the data base were high-speed attached boundary layers with pressure gradients, supersonic shear-layer mixing, and shock wave/boundary layer interactions (SWBLI). A 3-D compressible Favre-averaged Navier–Stokes code in a generalized coordinate system with two-equation turbulence models was used to predict the experimental SWBLI data base. The code was based on an implicit second-order total-variation-diminishing flux-difference splitting algorithm with an alternating symmetric Gauss–Seidel plane relaxation method and a diagonally dominant approximate factorization scheme in each plane. The characteristic-based boundary approximations were implicit.

Accomplishment Description
The computational method was validated against experimental data and two-dimensional simulations of a flat-plate boundary layer at Mach 5 and a compression corner at Mach 3. A set of Mach 8 numerical simulations of a 3-D SWBLI experiment generated with a single fin and an intersecting SWBLI experiment generated with two fins were computed. The turbulence models investigated were the zero-equation Baldwin–Lomax algebraic model, several forms of the k–ω two-equation turbulence model, and two low-Reynolds number k–ε two-equation turbulence models. The model corrections investigated were a length-scale correction, a rapid-compression correction, and a rotation correction.

Significance
Turbulence modeling is a critical technology needed to develop the National Aero-Space Plane. A critical task is the ability of the turbulence model to predict hypersonic viscous/inviscid interactions. These computations provide benchmark results to develop and implement two-equation turbulence models in the design.

Future Plans
Two simulation experiments are planned: (1) the interaction of two oblique shock waves with a thick turbulent boundary layer, and (2) the interaction of shock waves generated with two straight fins and a top wall with a thick turbulent boundary layer. A major consideration is the development of improved compressibility corrections in the turbulence models and the identification of models that have superior predictive capabilities.

Particle traces of Mach 8 intersecting shock waves and thick turbulent-boundary-layer interaction.

Waverider and Reference Model Computational Study

Charles E. Cockrell, Jr., Principal Investigator
NASA Langley Research Center

Research Objective
To conduct a computational study of (1) a Mach 4.0 viscous-optimized waverider model, (2) a configuration designed for shock attachment along the outer leading edge and high lift-to-drag ratios at the design Mach number, and (3) a non-waverider reference flat-top model. Performance characteristics of the configurations will be compared to illustrate the benefits of waverider flow-field properties.

Approach
Three-dimensional thin-layer Navier–Stokes (TLNS) and parabolized Navier–Stokes (PNS) solutions were obtained for the waverider and reference model configurations using the General Aerodynamic Simulation Program (GASP). Lift and drag values were obtained by integrating computational fluid dynamics (CFD) surface pressure predictions for each configuration.

Accomplishment Description
Solutions for the waverider and reference model configurations were obtained at Mach 4.0 at 0–10 degrees angle of attack. Solutions were obtained at Mach 2.5 and Mach 3.5 at 0 degrees angle of attack for the waverider model only. The CFD surface pressure predictions and the integrated lift and drag values for the reference model configuration were lower than those for the waverider model. The aerodynamic performance of the reference model configuration was slightly better than the waverider model because it had a lower drag for the same amount of lift. Flow-field solutions showed that the reference model exhibited the same waverider shock attachment properties because the planform shapes were identical. The planform shape of the waverider created shock attachment at the leading edge resulting in the aerodynamic performance advantage. Typical solution times required 2–3 Cray-2 hours and 10–20 megawords of memory.

Significance
The planform shape of the configuration is the property that gives the waverider an aerodynamic performance advantage over conventional hypersonic vehicles. This suggests that the bottom surface may be altered without a significant decrease in aerodynamic performance as long as the planform shape is maintained. A configuration can provide slightly better aerodynamic performance, but it does not necessarily have better propulsion airframe integration characteristics.

Future Plans
A computational study will be conducted for a Mach 4.0 waverider-derived vehicle with realistic vehicle components integrated.

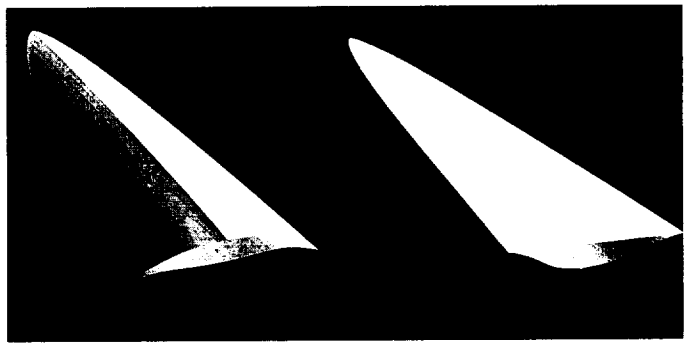

Mach 4.0 waverider model (left) and reference flat-top model (right).

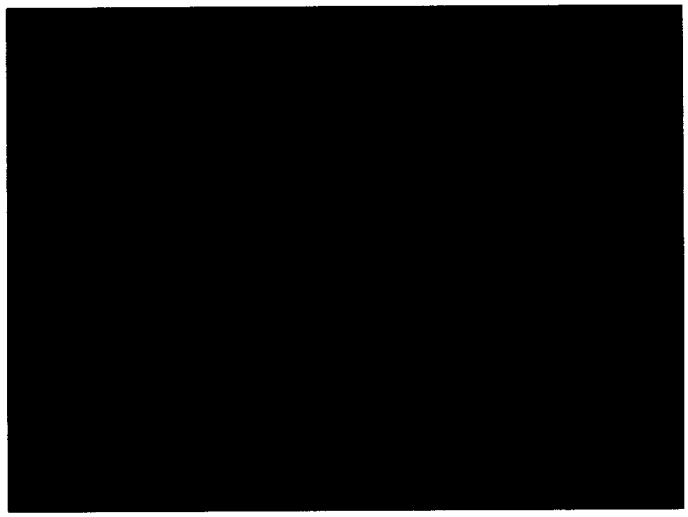

Static pressure values, nondimensionalized by free-stream pressure, ranging from 0.75 (blue) to 2.0 (red), for the waverider (top), reference model (bottom), at the centerline (left), and base of each model (right). The solutions are at Mach 4.0 and 1 degree angle of attack for the waverider model and 2 degrees angle of attack for the reference model.

Reentry Heating Effects on the Shuttle Orbiter

Peter A. Gnoffo, Principal Investigator
NASA Langley Research Center

Research Objective
To evaluate the capabilities and limitations of the Langley Aerothermodynamics Upwind Relaxation Algorithm (LAURA) program for calculating laminar convective heating over the Space Shuttle Orbiter in a hypersonic flight regime with strong equilibrium and nonequilibrum gas chemistry effects.

Approach
Flow field simulations at three trajectory points for Space Transport System (STS)-2 between Mach 24 and Mach 12 (72 to 55 kilometers altitude) were obtained with LAURA and calculated convective heating levels were compared to flight thermocouple data. A multiblock solution strategy partitioned the simulated flow field into manageable blocks that required only a fraction of the computer resources (time and memory) of a full-domain approach. Partitions were reassembled and a full-domain solution was generated from a nearly converged initial condition.

Accomplishment Description
Calculated laminar heating levels along 15 linear cuts on the windside and leeside shuttle surfaces were in generally good agreement with flight thermocouple data for laminar flow at all three simulation points. Transitional and turbulent flow on the deflected bodyflap below Mach 18 and on elevons below Mach 13 were not modeled. A factor of ten change in surface catalysis rates caused a 15–20 percent change in convective heating rates across this flight regime; the application of a radiative equilibrium wall boundary condition accentuated these differences. Typical resource requirements were 100–250 hours per case, 128 megawords of core memory, and 128 megawords of solid-state storage device memory. The code achieved concurrent central processing unit average values greater than seven in the multitask queue of the Cray Y-MP.

Significance
Multiblock methodology and simulation capabilities were established for future vehicle studies across the hypersonic flight regime.

Future Plans
Additional grid convergence tests and multidimensional grid adaption on leeside shuttle surfaces are planned.

Publications
1. Gnoffo, P. A.; Weilmuenster, K. J.; and Alter, S. J.: A Multiblock Analysis for Shuttle Orbiter Re-Entry Heating from Mach 24 to Mach 12. AIAA Paper 93-2813, July 1993.
2. Weilmuenster, K. J.; Gnoffo, P. A.; and Greene, F. A.: Navier–Stokes Simulations of the Shuttle Orbiter Aerodynamic Characteristics with Emphasis on Pitch Trim and Body Flap. AIAA Paper 93-2814, July 1993.

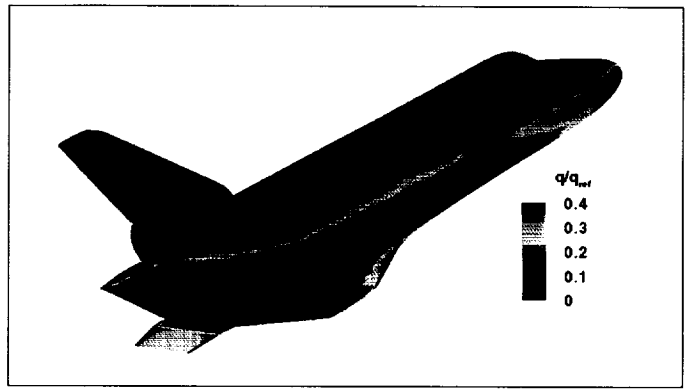

Heating levels over the shuttle surface at Mach 18.07 indicate cooling effects of the expansion leading up to the deflected bodyflap. A separation zone is evident in the form of a cool (dark blue) crescent in front of the bodyflap hinge line. Peak heating for this case occurs on the wing leading edge (dark red) in the vicinity of the bow-shock/wing-shock interaction region.

Particle Simulation of Hypersonic Rarefied Flow

Brian L. Haas, Principal Investigator
Co-investigators: Michael A. Fallavollita and William J. Feiereisen
Eloret Institute/Stanford University/NASA Ames Research Center

Research Objective

To develop and enhance a multiprocessor code for modeling three-dimensional (3-D) reactive flows about realistic vehicles during rarefied hypersonic aerobraking using the direct simulation Monte Carlo (DSMC) particle method. This code was applied to realistic flow scenarios to assess code performance, scaleup, and limits.

Approach

DSMC methods modeled a rarefied flow as a large collection of discrete particles traveling through space and interacting via collisions. New collision-selection rules and other algorithmic changes permitted efficient implementation on parallel-processing computers. The flow field was divided into a network of small, uniform, cubic cells. These cells were grouped into indivisible blocks of a fixed size. The load-balancing scheme then dynamically assigned various numbers of blocks to each processor to evenly distribute the computational work. Blocks tended to align with the free-stream direction to reduce diffusion and interprocessor communication. Sequential processing of cells within each block reduced memory requirements.

Accomplishment Description

The code was modified for the Intel Gamma machine to run with one processor serving both as a coworker and as the host for the rest of the machine. This permitted ready porting to other machines. As depicted in the first figure, steady 3-D simulations were performed of a Mach 24 flow past a blunted cone during aerobraking at 100 kilometers altitude in five-species reactive air. As plotted in the second figure, nearly perfect scaleup was observed up to 128 processors, although the costs of load balancing operations became excessive as more processors were used. By restricting the number of cells per block from 512 to 64, calculations for a given block remained within the memory cache of the processor, thus reducing costs which previously resulted from frequent accessing of main memory.

Significance

Because of limitations of the Navier–Stokes equations, continuum flow computation methods fail to accurately simulate rarefied flows associated with atmospheric entry of space vehicles or impingement of thruster exhaust upon satellite components. DSMC methods are particularly well suited to such scenarios, but they require excessive computational resources. This multiprocessor code enables affordable simulation of flows of engineering interest and exceeds the performance of an efficient vectorized DSMC code (for the Cray Y-MP) when running 64 or more processors. Good scalability permits implementation on larger machines and thus simulation of extremely large problems or unsteady flows.

Future Plans

Thermochemistry models for rotational, vibrational, and chemical relaxation will be enhanced in the code. Load-balancing algorithms will be improved to reduce interprocessor communication costs and increase throughput. Variable cell sizes within each block will be introduced to improve statistical accuracy when simulating flows with large density variations.

Temperature profile for flow about a blunted cone. Temperatures range from 1 to 125 times the free-stream value.

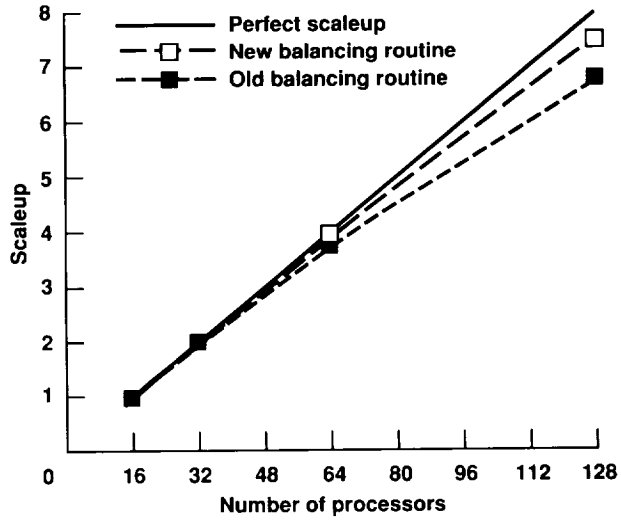

Performance scaleup for the blunted cone simulations. Comparisons between old and new load-balancing schemes.

Computation of Space Transport Vehicle Re-Entry Heating

William D. Henline, Principal Investigator
Co-investigators: Y.-K. Chen, G. E. Palmer, and S. M. White
NASA Ames Research Center/Eloret Institute

Research Objective
To apply three-dimensional (3-D) hypersonic flow computational fluid dynamics (CFD) tools to the computation of re-entry surface heating for hypersonic and space transportation vehicles. Material surface boundary conditions were applied to provide realistic estimates of aerothermal heat loads.

Approach
Hypersonic 3-D Navier–Stokes numerical solvers were used to test vehicle aerothermodynamic surface heat transfer computational modeling. Material surface and thermal response boundary-condition subroutines were developed to couple with the CFD flow code to represent the flow field plus heat shield aerothermodynamic response. The flow solver GASP2.0 was used to calculate surface heating, temperatures, and ablation rates for three calculations: shuttle tile gap heating, a coupled flow field with heat transfer and surface catalysis on a high-angle blunt cone, and a coupled flow field and ablation response for a hypersonic nosetip.

Accomplishment Description
For the shuttle tile gap heating calculation, the code was used to model the overlying hypersonic boundary layer at Mach 5 as air flowed over a tile gap. The downstream tile face was slightly elevated to create a step-type obstruction for the impinging flow. This calculation required a very fine numerical grid and tight tolerences on local time steps. Runs took approximately 1 Cray Y-MP hour for simple isothermal wall boundary conditions. The first figure shows the pressure field and associated velocity fields for the tile gap heating problem. GASP2.0 was applied to the hypersonic heating to an ablating graphite nosetip problem. This problem was difficult, and it required nearly 50 Cray Y-MP hours. GASP2.0 was applied to the computation of surface heating with catalysis on very-high-angle blunt cones. Surface heating distributions compared well with experimental data.

Significance
Valuable information on the sensitivity CFD algorithms to a wide range of different complex vehicle surface boundary conditions was gained. A specific coupling strategy was needed to efficiently obtain a solution for each problem. Only proper explicit updating of the CFD flow-field variables using relaxation techniques allowed any solution for coupled ablation problems.

Future Plans
The realism of material response boundary condition modeling will be extended. More efficient ways to couple the flow codes will be explored. Coupled problems will be extended to compute flows over more realistic 3-D flight body geometries and will be compared to experimental data and flight data.

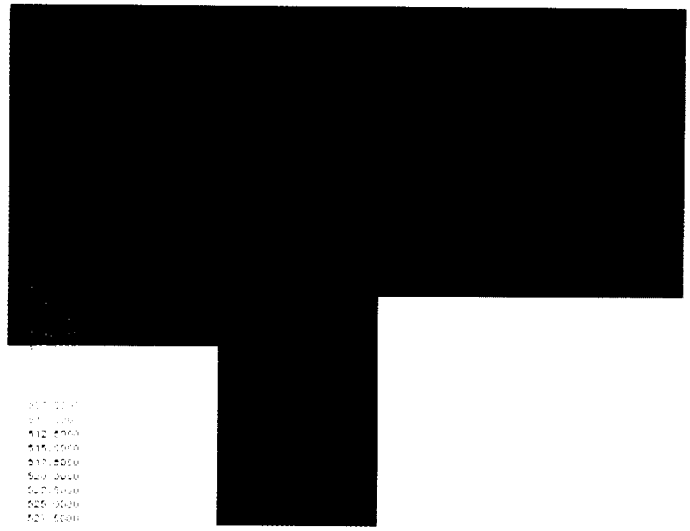

(a)

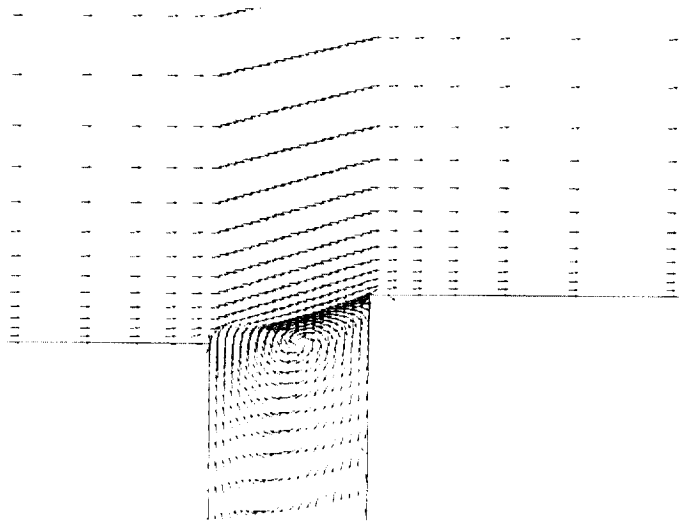

(b)

(a) Pressure and (b) velocity fields for Mach 5 air flow over a transverse tile gap with a step.

Powered Hypersonic Air-Breathing Configuration Studies

Lawrence D. Huebner, Principal Investigator
Co-investigator: Kenneth E. Tatum
NASA Langley Research Center/Lockheed Engineering and Sciences Company

Research Objective

To perform computational analyses of hypersonic air-breathing vehicles under simulated powered conditions. Three-dimensional (3-D) effects of inlet fairings on the powered aftbody and wings will be determined, as well as differences in plume characteristics at various points along a typical flight path.

Approach

The inlet-fairing effects and plume characterization studies were performed on Langley's Test Technique Demonstrator (TTD) using three different forebody/inlet representations and a common aftbody with wings at four representative Mach number/nozzle pressure ratio (NPR) combinations. Exhaust flow simulation was initiated with internal nozzles designed for each prescribed free-stream Mach number.

Accomplishment Description

Salient flow-field features about the TTD with a flow-ingested inlet are shown in the first figure. No strong shocks were created at the cowl leading edge, and pressurization of the aftbody lower surface due to the powered exhaust simulation is evident. The second figure compares the effects of inlet representation and powered flow conditions by using the exhaust mass-fraction contours at the body trailing edge. The faired-over inlet cases show slightly greater plume expansion in the vertical direction, but very comparable lateral expansion. There is a significant effect of plume expansion for increasing Mach number/NPR. At Mach 3.40, the plume remains attached only to the aftbody. At higher Mach numbers, the plume expands vertically and laterally, and at Mach 13.66 the entire lower surface of the aftbody and wings is engulfed in the exhaust flow. Solutions averaged about 1.5 Cray Y-MP hours and required about 7 megawords of memory.

Significance

Fairing over the inlet of a hypersonic air-breathing wind tunnel model is a viable approach to obtaining powered aftbody effects at supersonic and hypersonic speeds. Lower surface forebody flow-field differences that propagate downstream are isolated from the aftbody surface by the exhaust plume, resulting in minimal aftbody force and moment differences. The expansion of the exhaust plume over the vehicle lower surface and wings at increased Mach numbers may alter the aerodynamic characteristics of this type of vehicle.

Future Plans

Scramjet exhaust simulation techniques will be compared to assess differences in cold-gas and hot-gas exhaust simulation, including the modeling of the flow with scramjet combustion products.

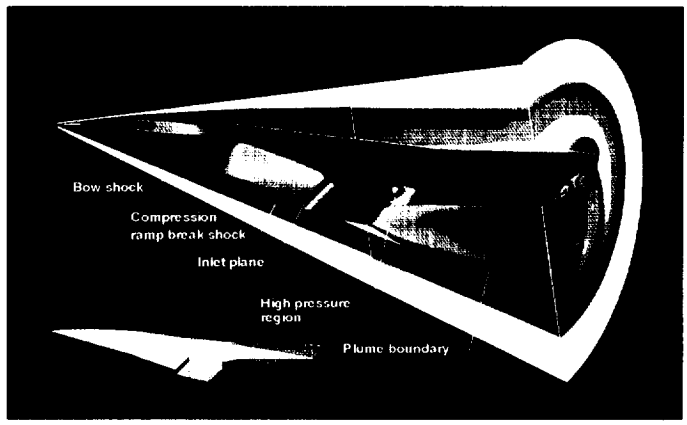

Flow-field Mach number contours (0 = blue to 5.9 = light pink), and surface pressures (0 = blue to 3,000 = light pink) for the TTD with a flow-ingested inlet, M_∞ = 5.92, NPR = 200.

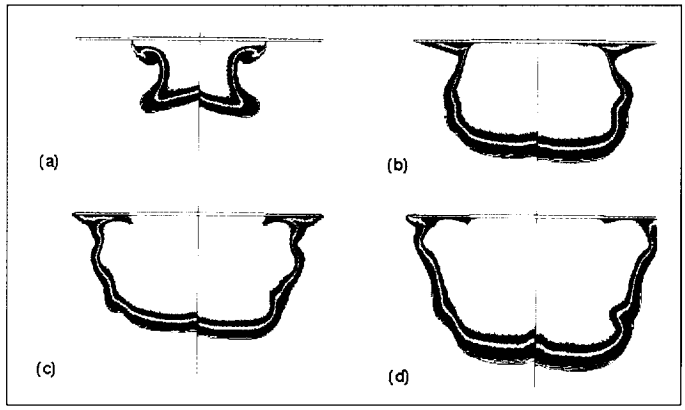

TTD body trailing edge exhaust mass-fraction contours; 0.01 = blue to 0.99 = light pink. (a) Flow-ingested inlet (left), faired-over inlet (right), M_∞ = 3.40, NPR 30. (b) Flow-ingested inlet (left), faired-over inlet (right), M_∞ = 5.92, NPR = 200. (c) Flow-ingested inlet (left), faired-over inlet (right), M_∞ = 10.14, NPR = 3,000. (d) Flow-ingested inlet (left), faired-over inlet (right), M_∞ = 13.66, NPR = 40,000.

Computational Performance Enhancement of a Scramjet Inlet

Ajay Kumar, Principal Investigator
Co-investigator: Dal J. Singh
NASA Langley Research Center

Research Objective
To conduct a numerical performance enhancement study of a sidewall compression scramjet inlet and to develop a design/optimization procedure.

Approach
A three-dimensional (3-D) Navier–Stokes code and a marching Euler code were used to assess numerically the impact of curved sidewalls on the performance of a baseline swept-sidewall compression scramjet inlet at Mach 4 conditions. In addition, a systematic 3-D design procedure was developed by optimizing performance for a two-parameter inlet design utilizing a flow-field analysis based upon the Euler equations. A viscous solution of the inviscidly optimized inlet was obtained and compared with the baseline case. Effects of boundary-layer ingestion on the overall flow features and performance were also investigated.

Accomplishment Description
Turbulent flow-field solutions were generated by solving Reynolds-averaged Navier–Stokes equations to obtain inlet performance parameters such as total-pressure recovery, mass capture, and flow-field distortion. These parameters were used to assess the performance enhancement by modifying the planar-sidewall compression angle as a function of height, utilizing sidewall curvature, and employing both the forward-swept and backward-swept compression surfaces. This study indicated that both the viscous and inviscid solutions yielded similar performance trends. The resulting optimized inlet geometry yielded inlet performance improvements; however, inlet top-wall separation still persisted. The code for an average run used 20 megawords of memory and took about 15 Cray Y-MP hours.

Significance
This numerical study showed that enhanced performance is obtainable using curved-wall modifications to the standard planar-sidewall inlet design.

Future Plans
A constrained inlet design/optimization procedure consistent with multi-dimensional adverse pressure gradient separation criterion will be developed.

Publication
Korte, J. J.; Singh, D. J.; Kumar, A.; and Auslender, A. H.: Numerical Study of the Performance of Swept Curved Compression Surface Scramjet Inlets. AIAA Paper 93-1837, June 1993.

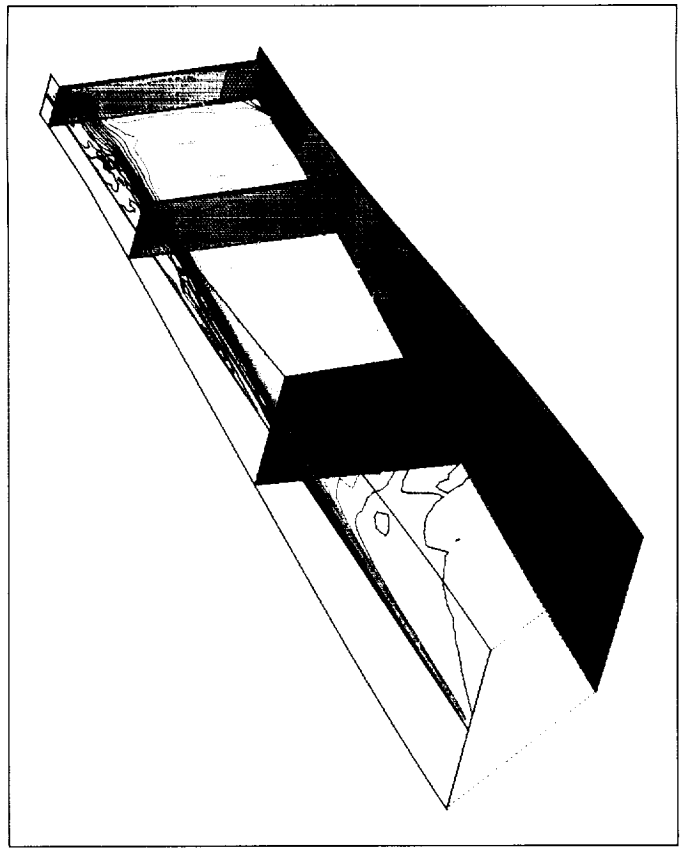

Scramjet inlet flow-field Mach contours.

Integrated Hypersonic Vehicle Simulation

Scott L. Lawrence, Principal Investigator
Co-investigators: Gregory A. Molvik, Johnny R. Narayan, and Bradford C. Bennett
NASA Ames Research Center/MCAT Institute

Research Objective
To develop reliable tools for numerically predicting hypersonic vehicle flow fields, including the effects of interactions between the airframe and propulsion flow fields. Where possible, the tools developed were used in-house to study the unique physics associated with hypersonic flight.

Approach
In addition to extending current capabilities by implementing models for physical effects not previously addressable (for example, hydrocarbon–air combustion chemistry), existing physical models were upgraded with more robust or more accurate models where deficiencies were identified. The basic suite of codes involved in this effort included the time-dependent flow solvers, TUFF and SPARK, and the space-marching flow solvers, STUFF and UPS.

Accomplishment Description
A finite rate hydrogen–air chemistry model was adapted for the purpose of analyzing the effect of turbulence–chemistry interactions in high-speed combustion. This model was initially implemented in the SPARK code and applied to two-dimensional and axisymmetric configurations involving hydrogen–air combustion reactions. The model was also added to the TUFF and STUFF codes and validated. Demonstration nose-to-tail calculations were performed for a hydrocarbon-burning waverider and were initiated for a hydrogen-burning National Aero-Space Plane-type vehicle. The Hypersonic Waverider Research Vehicle (HWRV) results (see figure) were obtained at power-on design conditions (Mach 8.0, altitude = 92,500 ft). The external flow, computed with a space-marching method, required 5 megawords of main memory and approximately 6 hours of Cray Y-MP time. The time-marching scheme required for the internal hydrocarbon scramjet flow employed a two-equation turbulence model, consumed approximately 103 hours of Cray Y-MP time, and used roughly 20 megawords of main memory. Tip-to-tail analysis of a generic, hydrogen-burning, hypersonic vehicle (power-on) configuration is under way. The forebody flow field was solved using TUFF and UPS. Nonequilibrium air with finite-rate chemistry is considered at a free-stream Mach number of 16. A scramjet engine consisting of three intake modules with swept sidewall compression is being considered for the power-on computations. The multizone TUFF code is being used for the inlet computations. The engine computation typically requires 12 Cray Y-MP minutes per time step.

Significance
The coupling of internal and external flow solvers provides the capability to capture interactions between the airframe and propulsion system that would be neglected if simulations were carried out separately. The HWRV results play a role in the design process through their use in calibrating the aerodynamics and propulsion modules of a systems analysis code.

Future Plans
Hydrogen-burning scramjet vehicle simulation will be completed. In conjunction with this work, other turbulence–chemistry interaction models will be investigated and some design problems associated with the scramjet combustor will be addressed.

Nose-to-tail analysis of a hypersonic waverider research vehicle; pressure contours, red = high, blue = low.

Efficiency Improvements of Boundary Layer Transition Predictions

C. C. Lee, Principal Investigator
Co-investigators: Shawn Hagmeier, Brad Hopping, and Charles Vaporean
McDonnell Douglas Corporation

Research Objective
To develop efficient predictions of three-dimensional (3-D) boundary layer transition using linear stability analysis (LSA).

Approach
Three-dimensional LSA (e^{Malik}) requires a high quality computational fluid dynamics (CFD) solution as input as well as estimates for the most unstable frequency of the disturbance. The LSA procedure is more efficient when an improved CFD grid stretching function, frequency and disturbance growth onset estimates, and automated frequency search procedures are used.

Accomplishment Description
Various CFD stretching functions were studied to optimize the CFD grid for LSA. The stretching function maintained adequate resolution of the near-wall region for accurate heat transfer and skin friction calculations and better resolved the boundary layer for LSA. There was up to a 40 percent decrease in the number of radial grid points required for proper LSA results. A disturbance frequency and onset of disturbance growth estimation were incorporated and have automated the frequency search for the most unstable disturbance.

Significance
Accurate prediction of transition is essential for hypersonic vehicle design. Improvements are necessary to make the 3-D LSA design process efficient. Frequency estimation is also useful to determine instrumentation requirements for flight test vehicles.

Future Plans
Other candidate stretching functions will be tested for greater efficiency. The process of 3-D LSA will be refined to allow its use in the design of hypersonic vehicles.

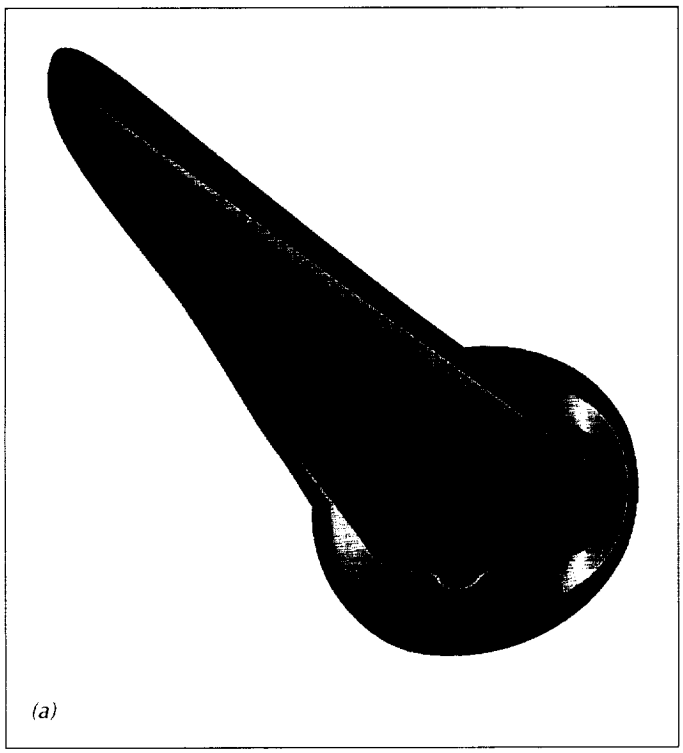

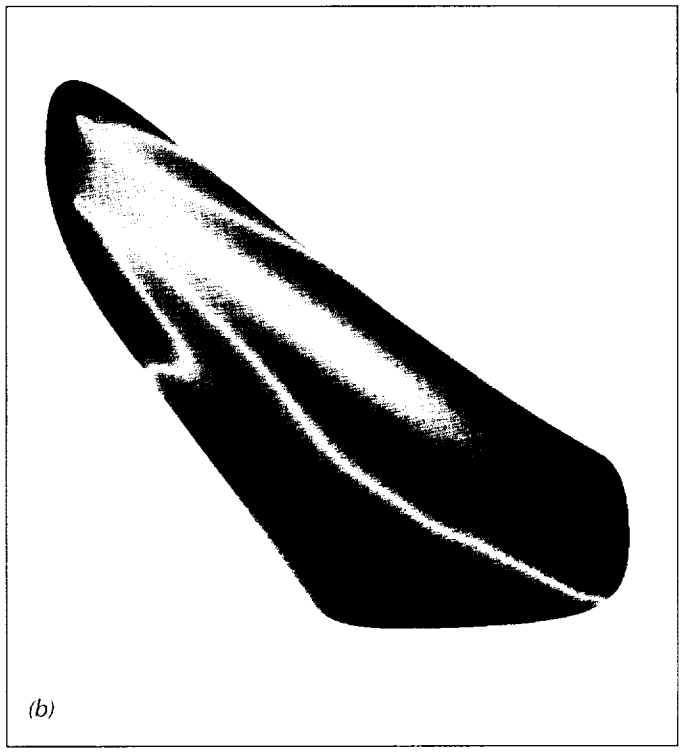

(a) Mach number distribution from 6 to 14 for a hypersonic flight test vehicle at a free-stream Mach number of 14. (b) Disturbance frequency distribution from 80,000 to 350,000 hertz. The disturbance frequency at hypersonic speeds is estimated using the velocity at the boundary layer edge and the boundary layer thickness.

Flow Past a Dynamic Multiple Body System

K. Kurian Mani, Principal Investigator
Co-investigator: J. W. Haney
Rockwell International, Space Systems Division

Research Objective
To study multiple body dynamics in the hypersonic flow regime with zonal decomposition.

Approach
In multibody dynamics analysis, the domain around bodies is divided into multiple computational zones. The zone boundaries and the grid nodes belonging to the adjacent zones may or may not align. The grid was generated using GENGRID. Once the basic grid structure was generated, nodal velocities were assigned to the grid points. At first only the edge points were calculated for the grid. From the edge points, the effect of all the component bodies will be calculated. Next, each of the bounding surfaces was treated individually. For a selected surface, the velocities of the points on the bounding curves were known from the previous calculation. The interior points on the surfaces were influenced only by the boundary points to maintain continuity of induced velocities. A smooth blending of the grid velocities was assured even if certain surfaces contained patches with prescribed velocities. The solution provided an instantaneous picture of the flow field with the effect of body dynamics on the flow field. This solution was achieved by accounting for the nodal velocities of the surface grid points using the unified solution algorithm code.

Accomplishment Description
The current study analyzed the flow field around a geometry system consisting of the SR-71 aircraft with a "piggy backed" waverider derivative at the aft end of the SR-71. The grid generation was very complex. Once a grid was obtained, the grid system was made flexible to accommodate the relative motion. An algorithm was developed to compute grid velocities across zonal boundaries. This algorithm was followed by a solution process accounting for flux crossings across cell surfaces in motion.

Significance
The study resulted in a method to analyze multibody dynamics using zonal decomposition and grid stretching without a great computational burden on the solvers.

Future Plans
The method will be extended to large relative motions.

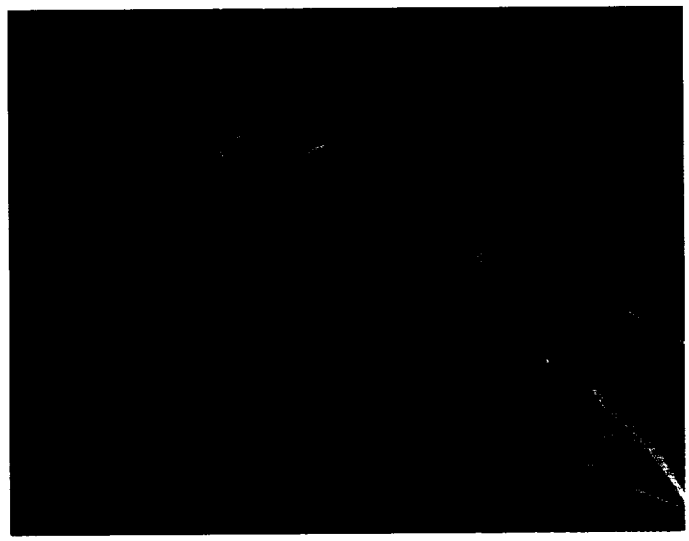

Mach contours on the SR-71 aircraft/waverider geometry at relative motion.

Performance Potential of Full-Scale Injectors

Charles R. McClinton, Principal Investigator
Co-investigator: David W. Riggins
NASA Langley Research Center

Research Objective

To evaluate the performance potential of realistic scramjet combustor injection strategies for flush-wall jets and intrusive (ramp) injectors using state-of-the-art simulation capabilities. An important goal is to gain understanding of the generation and evolution of vorticity in supersonic combustors and its role in the mixing process.

Approach

The three-dimensional Navier–Stokes family of SPARK reacting codes was used to model the complex flow physics in scramjet combustors for representative flight conditions and full-scale geometries corresponding to a high flight Mach number (Mach 14). Parametric studies of flush-wall and intrusive injector geometries were undertaken using full finite-rate H_2–O_2 chemistry. Performance potentials of the various strategies were obtained using an energy-based method. Detailed studies of vorticity generation and evolution were performed using subscale injector ramps.

Accomplishment Description

Flow fields for three full-scale candidate scramjet combustors were obtained and analyzed for mixing, combustion, and thrust potential. Details of the flow physics have been obtained and allowed in-depth interpretation of vortex mixing and combustion and comprehensive examination of flow losses. Stokes circulation law and moment-of-momentum checks provided confidence in modeling consistency for vorticity and vortex structures for a series of subscale injector ramps. A correlation between mixing and axial large-scale vorticity was developed.

Significance

This study of full-scale flight-scaled injector ramps and jets in supersonic reacting flows allowed the detailed comparative study of flow phenomena that contribute to mixing, burning, and thrust production for hypersonic air-breathing vehicles. In addition, the understanding of injector-generated large-scale vorticity and its contribution to fuel–air mixing was increased by the parametric investigation of subscale ramps in high- and low-enthalpy flows.

Future Plans

Computational studies of scramjet engines with various injector strategies will continue, including the specific modeling of a full-scale combustor/nozzle experiment for flight Mach 8 conditions.

Publications

1. Vitt, P. H.; Riggins, D. W.; McClinton, C. R.; and Rogers, C. R.: Validation and Application of Numerical Modeling to Supersonic Mixing and Reacting Flows. AIAA Paper 93-0606, Jan. 1993.
2. Riggins, D. W.; and Vitt, P. H.: Vortex Generation and Mixing in Three-Dimensional Supersonic Combustors. AIAA Paper 93-2144, June 1993.

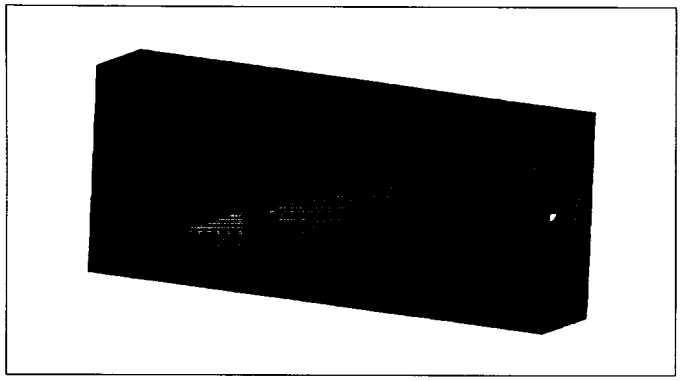

Pressure contours over full-scale ramps in a scramjet combustor.

Reaction-generated water mass fraction contours 18 cm downstream of the ramp base (ramp is approximately 36 cm long).

Hypersonic Computational Studies

Grant Palmer, Principal Investigator
Co-investigators: S. Sharma, C. Park, S. M. Ruffin, T. Gokcen, D. Babikian, S. Tokarcik-Polsky, and E. Venkatapathy
NASA Ames Research Center/Eloret Institute

Research Objective
To investigate a wide spectrum of phenomena relating to the computation of hypersonic, chemically reacting flows, including coupled radiation, vibrational relaxation, and the application of reacting gas flow solvers to space vehicle configurations.

Approach
Radiative transfer was coupled to an axisymmetric nonequilibrium flow solver for a nongray emitting and absorbing gas. The resulting set of integro-differential equations were solved using a modified Gauss–Seidel relaxation technique. In another study, a new vibrational relaxation model that accurately described relaxation in expanding base flows was developed using modified Schwartz, Slawsky, and Herzfeld vibration–translation transition rates and by considering both long-range and short-range intermolecular forces when computing vibration–vibration exchange rates. The performance of a drag device attached to a lunar return aerobrake was assessed using an effective gamma to simulate real-gas effects.

Accomplishment Description
The calculated spectra from the coupled radiation code qualitatively agree with those from both shock tube and Fire II flight experiment data. The new vibrational relaxation model showed substantial improvement over the standard Landau–Teller model when applied to expanding flows. The new model closely reproduced experimental data that showed an order of magnitude greater energy exchange rate than predicted by Landau–Teller. It was shown that by varying the drag-device panel length and deflection angle the drag coefficient of the lunar return aerobrake could be increased by a factor of 8.4. Resource requirements for a drag-device computation were 15 megawords of memory and 10 Cray Y-MP hours.

Significance
Coupled radiation and vibrational relaxation in regions of expansion are two areas that have not been successfully integrated into nonequilibrium flow solvers. This work represents a substantial advancement to the state of the art in these disciplines. The drag-device calculations provide information for a realistic vehicle configuration that may aid future design of these spacecraft.

Future Plans
The results of this work will be incorporated into future theoretical and applied hypersonic reacting-gas studies.

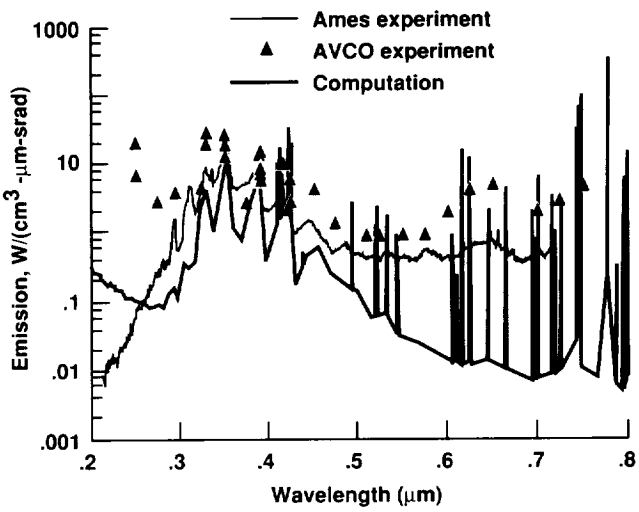

Emission at the peak radiation point.

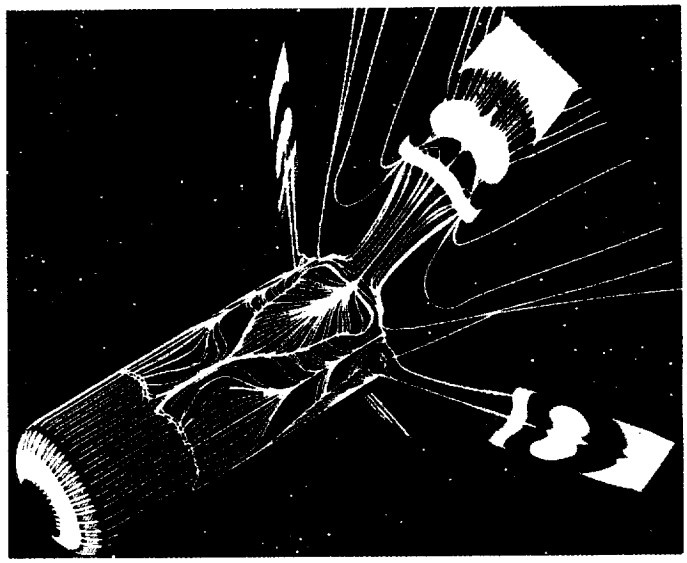

Calculated surface oil flow and surface pressure.

Computational Studies of Nonequilibrium Flows

Ramadas K. Prabhu, Principal Investigator
Co-investigator: George C. Olsen
Lockheed Engineering and Sciences Company/NASA Langley Research Center

Research Objective
To develop computer codes for the solution of two-dimensional and three-dimensional Navier–Stokes equations assuming the flow to be in chemical and thermal nonequilibrium, and to use these codes to determine aerodynamic and thermal loads on some critical components of hypersonic flight vehicles.

Approach
The Langley adaptive remeshing code and Navier–Stokes solver employed a cell-centered upwind scheme using Roe's flux difference splitting technique. This solver, together with the adaptive unstructured mesh generator, mesh enrichment, and mesh movement techniques, was very effective in capturing detailed flow features in complex flow situations.

Accomplishment Description
The perfect gas code was modified to include a five-chemical species and two-temperature air model. The code with no transport terms was completed, and several example cases were solved. The transport terms have been included in the code. This code was also vectorized for computational speed, and it is being used to determine type IV shock interference heating on the cowl leading edge of a hypersonic vehicle. The remeshing codes are being modified.

Significance
Knowledge of the magnitude of extreme aerothermal loads is a key element in the design of hypersonic flight vehicles. This project determined the aerothermal loads on some critical components and demonstrated the power of unstructured meshes in capturing intricate flow features.

Future Plans
Several examples of type IV shock interference will be solved to determine the heat flux amplification. These codes will be extended to three-dimensional flows.

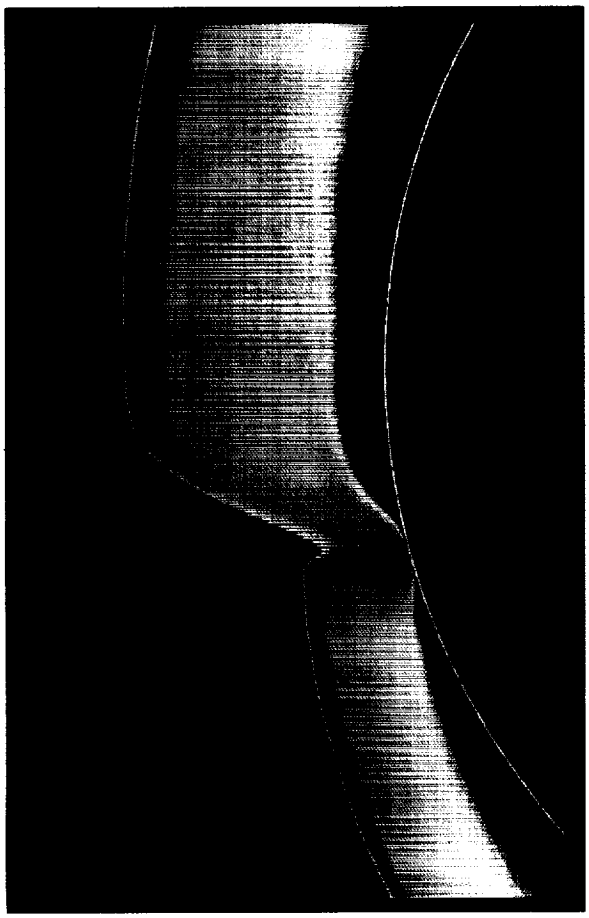

(a)

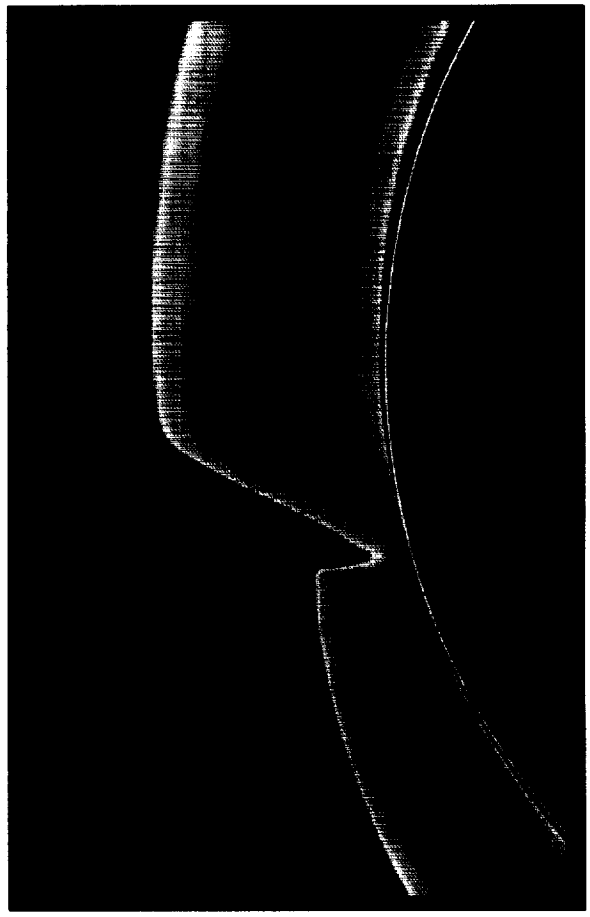

(b)

(a) Translational and (b) vibrational temperature contours for Mach 15 flow (with shock interference) past a 0.1-in.-radius body.

Validation of the Parabolized Stability Equation Method

C. D. Pruett, Principal Investigator
Co-investigator: C-L. Chang
Analytical Services and Materials, Inc./High Technology Corporation

Research Objective
To validate the nonlinear parabolized stability equation (PSE) method for transitional high-speed boundary layer flows.

Approach
Forced "second-mode" instabilities in a Mach 6.8 boundary layer flow along a sharp cone were investigated by two fundamentally different approaches: PSE and spatial direct numerical simulation (DNS). In PSE, the governing equations were approximate, but the solution was computationally efficient because of the use of marching methods. In spatial DNS, the compressible Navier–Stokes equations were solved in three dimensions and time by highly accurate compact-difference and spectral numerical methods. Results were compared with particular attention paid to the evolution of nonlinearly generated harmonics of the forced disturbance.

Accomplishment Description
Spatial DNS was a yardstick by which other tools were measured. Spatial DNS was used to assess the fidelity of the nonlinear PSE method. PSE treats both mean-flow nonparallelism and nonlinear wave interactions. Previously, DNS and PSE were studied for incompressible flows, but this study is believed to be the first comparison for high-speed boundary layer flows. The first figure compares PSE and DNS computations for forced transitional hypersonic flow along a sharp cone. The PSE computation is forced with a single symmetric pair of finite-amplitude oblique second-mode disturbances (identified as "T11"). All other harmonics arise spontaneously from nonlinear interactions. The PSE result (lines) is then compared to the DNS result (symbols). Agreement between the methods is superb for harmonic amplitudes and harmonic structures (second figure). The DNS required nearly 200 Cray-2 hours and 25 megawords of storage; the PSE computation required less than 2 Cray-2 hours.

Significance
The PSE method is a reliable and computationally efficient tool for investigating convectively dominated instabilities in high-speed boundary layer flows. The method remains valid well into the moderately nonlinear stage of laminar–turbulent transition. Moreover, results confirm that "oblique-mode breakdown" is a possible path to transition in high-speed compressible flows.

Future Plans
The complete laminar–turbulent transition process in high-speed boundary layer flows will be investigated combining PSE with spatial DNS. PSE will be used to compute the nonlinear initial stages of the transition process to derive a harmonically "rich" inflow condition for the spatial DNS. DNS will be used to compute the strongly nonlinear and breakdown stages of laminar–turbulent transition.

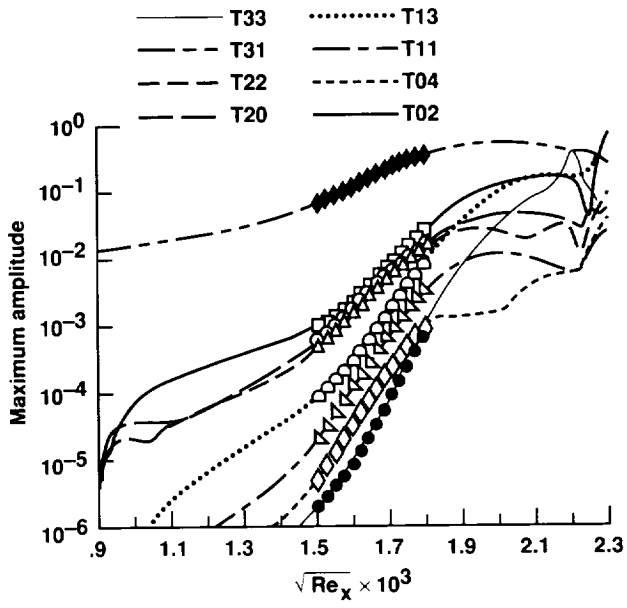

Maximum amplitudes of fundamental disturbance and selected harmonics as functions of root Reynolds number; lines = PSE, symbols = DNS. Legend: integers identify harmonics with respect to temporal frequency and spanwise wave number, respectively.

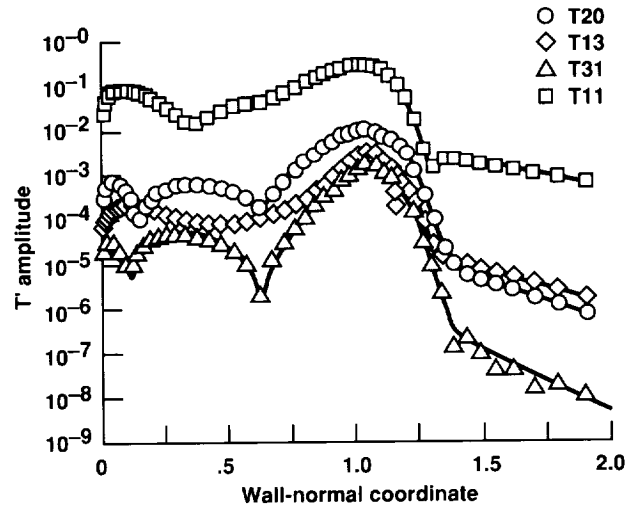

Amplitude envelope versus wall-normal coordinate of temperature components of fundamental disturbance and selected harmonics at $\sqrt{Re_x} = 1{,}742$.

Jet Interaction Aero-Optic Effects on Hypersonic Interceptors

R. P. Roger, Principal Investigator
Co-investigator: S. C. Chan
Teledyne Brown Engineering

Research Objective

To obtain flow-field predictions for a supersonic jet exiting into a hypersonic stream from a conical surface. Geometric configurations correspond to advanced concepts for defense interceptors on which jet thrusters are used for maneuver control. The second objective is to isolate effects that could adversely affect the performance of an on-board infrared seeker. Effects due to large angle of attack are of particular interest.

Approach

A three-dimensional full Navier–Stokes flow solver employing an upwind algorithm was used to predict the complex jet interaction flow field for the configuration. Computational fluid dynamics results were generated for wind tunnel test conditions to be compared to test data for the large recirculation region on the missile surface upstream of the jet. Subsequently projected tactical flight conditions were simulated.

Accomplishment Description

Computed results for the slot-cooled infrared seeker window in a triconic forebody compared well with surface pressure and temperature distribution data. Computed results for the large center-of-gravity thruster firing at 0.0 and 16.0 degrees angle of attack also compared well to force and moment data and to Schlieren photographs. The 16-degree angle of attack case required over 3 million grid points and was performed in 3 computational blocks. It required 200 Cray Y-MP hours and 52 megawords of memory for the largest block.

Significance

All proposed designs for advanced endoatmospheric interceptor concept developments employ infrared seekers and center-of-gravity thrusters. Use of center-of-gravity lateral control during "end game" is preferred because of the reduced sensitivity to target miss distance. For maneuvering target intercepts large lee-side angles of attack are necessary. In this configuration, the jet upstream recirculation region could extend onto or over the seeker window. This project investigated the fundamental flow-field structure for this phenomenon.

Future Plans

This project has been completed. Tactical flight environment predictions will be performed at a secure government computer facility.

Publication

Roger, R. P.; and Chan, S. C.: CFD Study of the Flowfield Due to a Supersonic Jet Exiting into a Hypersonic Stream From a Conical Surface. AIAA Paper 93-2926, 1993.

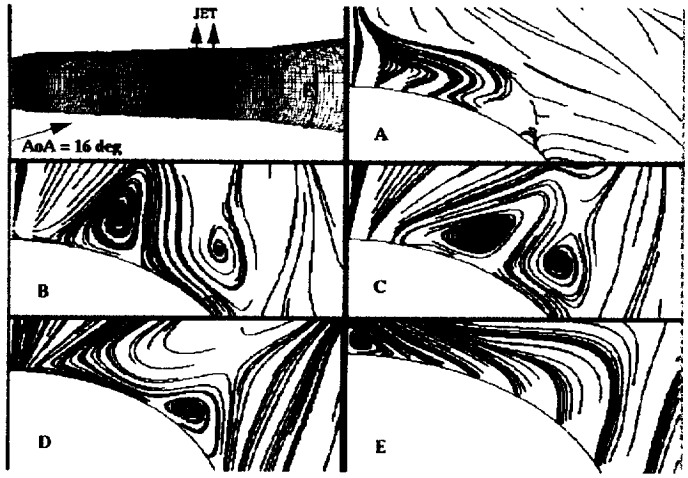

Complex flow features in several cross planes for the 16-degree angle of attack case.

Fuel Plume Imaging/CFD Comparisons

R. Clayton Rogers, Principal Investigator
Co-investigators: Robert D. Bittner and David W. Riggins
NASA Langley Research Center

Research Objective
To assess the fuel (hydrogen) distribution in a high-enthalpy (Mach 13.5) pulse facility using computational fluid dynamics (CFD) and Mie scattering of silicon dioxide particles. Both methodologies were analyzed on a quantitative basis to compare integrated fuel mixing. Because the amount of thrust provided by an engine is directly related to fuel mixing, the ability to quantify the degree of mixing with minimum uncertainty is imperative.

Approach
The SPARK codes were used to model this high-enthalpy flow field. The codes were used in a blocking algorithm, where the Navier–Stokes code was used only where the flow physics dictated. The calculations were for mixing only. A laser with a long pulse length illuminated silicon dioxide particles in the injected fuel through Mie scattering. The hydrogen jet was seeded with the silicon dioxide particles by preburning a silane–hydrogen mixture and adding enough oxygen to consume all the silane. The pre-burner outflow was modeled as a mixture of hydrogen and water. The CFD hydrogen-number density flux was then compared with the experimental Mie image intensity.

Accomplishment Description
A comparison of computational and experimental results three inches downstream from a pair of 10 degree swept ramp injectors is shown in the figure. The left side of the figure shows the CFD planar hydrogen-number density flux normalized by the total flux in that plane. The right side of the figure shows the experimental planar laser intensity normalized by the intensity integral in that plane. The CFD has slightly greater penetration, less spreading, and a larger jet core. The CFD jet lifted off the wall slightly more than in the experiment, but overall the agreement is very good. A procedure developed to deduce the integral mixing efficiency from an experimental image was applied to the CFD-generated image. A value of 0.46 was obtained, which agreed well with the CFD result of 0.44. Applying the procedure to the data image resulted in efficiencies between 0.48 and 0.53. This close agreement (±10 percent) with the CFD results was considered very good.

Significance
This was the first application of Mie imaging of a fuel plume with silicon dioxide particles. Eventually, CFD will be used to (1) predict how well fuel mixes in high-enthalpy flows, (2) dissect the details of the flow physics, and (3) determine what factors influence mixing. Long-pulse-length laser image correlation with Reynolds-averaged CFD is encouraging.

Future Plans
Recent tests of different geometries and crossflow plane locations to increase the high-enthalpy mixing will be analyzed. A study of the effects of two-phase flow on the results has also been proposed.

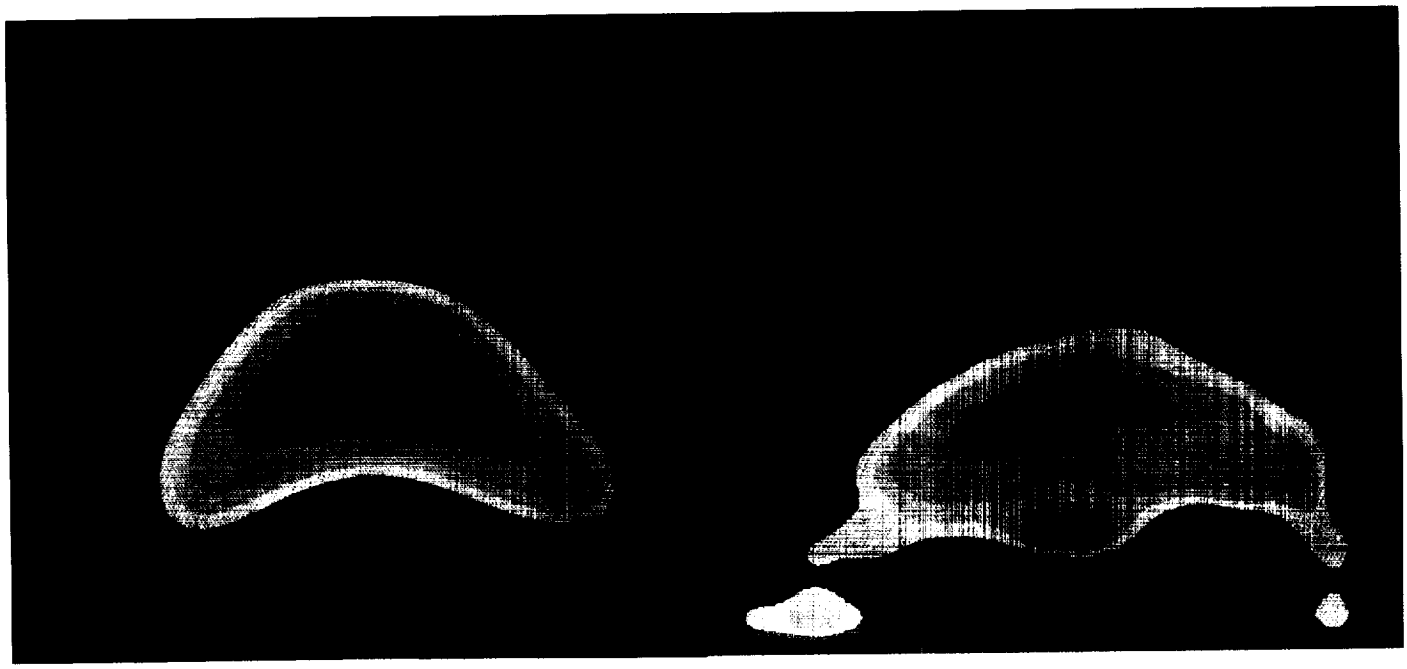

Comparison of CFD solution (left) and Mie imaging of fuel plume (right); red = high levels, blue = low levels.

Adaptive Unstructured Hypersonic Multigrid Solver

Rajiv Thareja, Principal Investigator
Co-investigators: Kenneth Morgan, Jaime Peraire, and Joaquim Peiro
Lockheed Engineering and Sciences Company/University of Wales/Massachusetts Institute of Technology/Imperial College

Research Objective
To further develop the FELISA system for the modeling of compressible flows using unstructured tetrahedral meshes.

Approach
The algorithm used a centered scheme along with an explicitly added artificial viscosity of matrix form. A multistage time-stepping scheme was used in combination with an unstructured multigrid algorithm in order to advance the solution to steady state. The system can be used to model flows from subsonic to hypersonic regimes. The figures show the computation of a Mach 0.5 flow over a model of the Grumman X-29 at an angle of attack of 5 degrees. A sequence of three meshes with 744,551, 245,422 and 103,379 tetrahedral elements was used in the computation. The fine mesh, two auxiliary meshes used for the multigrid scheme, and the surface density contours are shown.

Accomplishment Description
An unstructured mesh system was demonstrated as a powerful method for the computation of three-dimensional Euler aerodynamic flows. The scheme used a side-based data structure with minimal storage requirements. The practical usefulness of the method was dramatically improved by incorporating a multigrid acceleration procedure for the analysis of steady-state problems. A typical multigrid run required about 100–150 cycles to achieve convergence in about 3–4 Cray Y-MP hours using about 8 megawords of memory.

Significance
The algorithm can be used to model Euler flows over complex three-dimensional bodies using a series of unrelated unstructured meshes and multigrids to achieve rapidly converged solutions for flows across a wide range of flow speeds. The system (FELISA 2.0) is available for testing.

Future Plans
The scheme will be extended for highly stretched meshes to solve Navier–Stokes equations from subsonic through hypersonic flows.

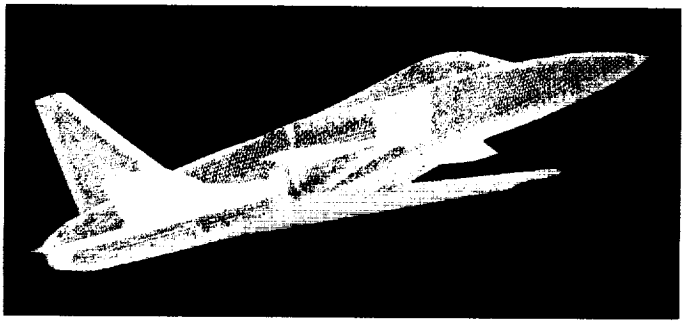

(a)

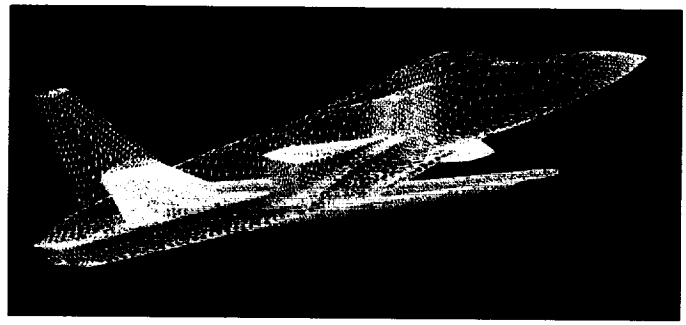

(b)

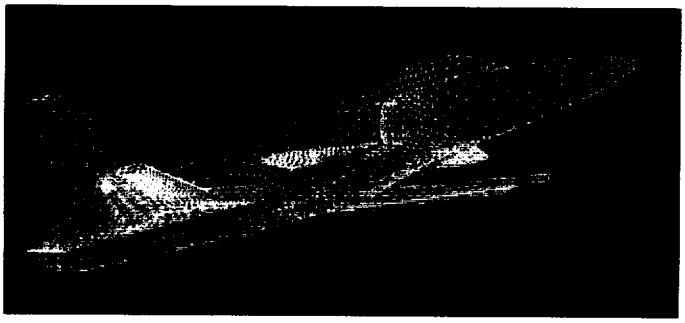

(c)

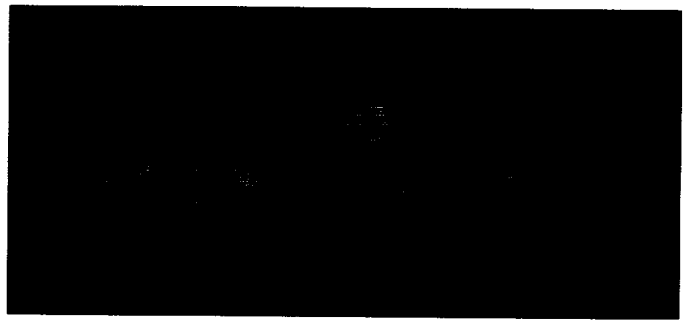

(d)

Grumman X-29 (a) surface mesh, (b) auxiliary mesh 1, (c) auxiliary mesh 2, (d) density contours.

Aerothermodynamic Benchmark for Candidate AMLS Vehicle

Richard A. Thompson, Principal Investigator
NASA Langley Research Center

Research Objective

To provide high-fidelity aerothermodynamic solutions over the forebody of a candidate Advanced Manned Launch System (AMLS) vehicle during reentry for validation of preliminary design efforts and to determine a starting point for follow-on analyses of the vehicle aft-end.

Approach

Solution of the time-dependent, thin-layer Navier–Stokes equations was achieved using the Langley Aerothermodynamic Upwind Relaxation Algorithm (LAURA). Models for chemically reacting flow were included to assess both equilibrium and nonequilibrium air effects. Wall temperatures were computed simultaneously with the flow-field solution using a radiation-equilibrium wall boundary condition. Calculations were performed for the vehicle near peak-heating flight conditions where design of the thermal protection system (TPS) is critical.

Accomplishment Description

Flow-field and surface heating predictions, including the effects of real-gas chemistry, were obtained for the vehicle forebody at a moderately high altitude (78 km) and angle of attack (32 degrees). Radiation-equilibrium wall temperatures were computed at these conditions assuming both equilibrium-air and finite-rate chemistry (seven species) in the shock layer. In the latter case, the vehicle surface was considered to be fully noncatalytic. The point-implicit solution strategy in LAURA complemented the macrotasking capabilities of the Cray Y-MP and Cray C-90. Sustained concurrent central processing unit usage was measured up to 15.07 out of 16 processors on the Cray C-90 using this multitasking approach. Typical solutions required up to 95 megawords of core memory with supplemental solid-state storage of 50 megawords. Complete solutions required on the order of 25 processing hours.

Significance

Surface pressures and heat-transfer rates were computed over the vehicle forebody for validating approximate engineering techniques used in preliminary design efforts. Wall temperatures computed at the peak-heating condition showed the current design to be within bounds of the thermal protection system limits. No regions of over-critical heating occurred on the forebody.

Future Plans

Aerothermodynamic analysis of the vehicle aft-end, including wings and tip-fin controllers, will be done. Investigation and validation of the approximate engineering design techniques will continue.

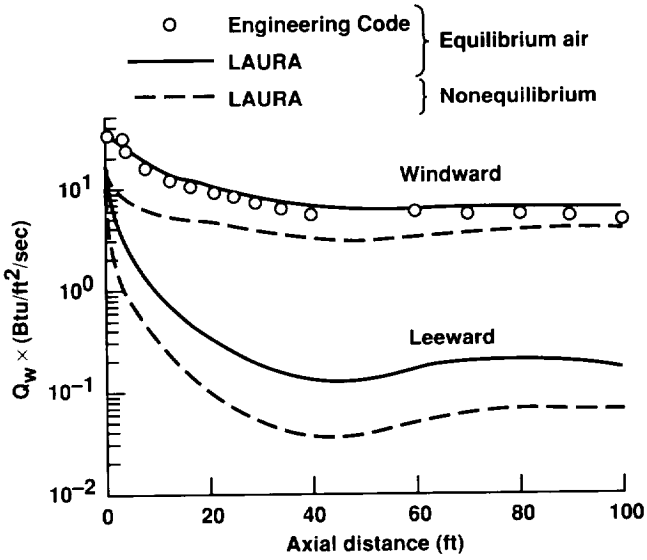

Comparison of computed heat-transfer distributions along the windward and leeward centerlines of the candidate AMLS forebody.

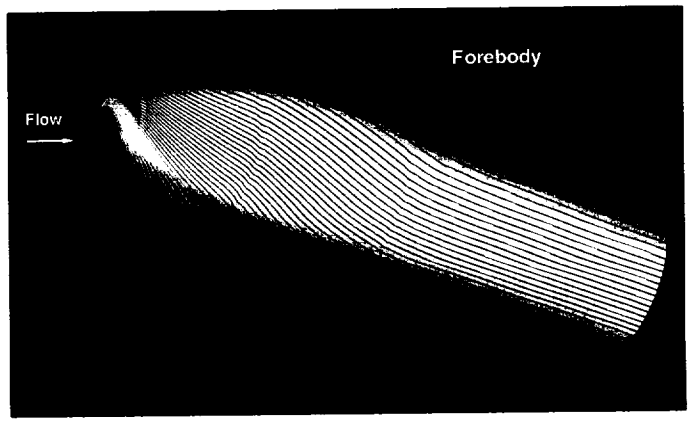

Contours of computed radiation-equilibrium wall temperatures for equilibrium air chemistry on the forebody. Highest wall temperature (1,650 K) is shown in red and the lowest (300 K) is in cyan.

Navier–Stokes Simulations of Orbiter Aerodynamic Characteristics

K. James Weilmuenster, Principal Investigator
Co-investigators: William L. Kleb and Francis A. Greene
NASA Langley Research Center

Research Objective
To develop and validate surface modeling, grid generating, and flow solving software for the aerodynamic analysis of winged entry vehicles.

Approach
Vehicle surface definition and control surface orientation were implemented through ICEM software. GRIDGEN and 3DMAGGS (three-dimensional multiblock advanced grid generation system) codes were used for grid generation. Fluid dynamic simulations were implemented through the Langley Aerothermodynamic Upwind Relaxation Algorithm (LAURA) code, which is appropriate for solving viscous, hypersonic flows in thermochemical equilibrium and nonequilibrium. Shuttle Orbiter wind tunnel and flight data were used as a validation data base.

Accomplishment Description
Flow-field solutions were obtained for the complete Orbiter configuration at flight conditions and for a simplified Orbiter shape at tunnel and flight conditions. Surface properties were integrated to determine the longitudinal aerodynamic characteristics of these configurations. A parametric study using the simplified Orbiter configuration showed increases in flight bodyflap trim angle over those required at tunnel conditions when compared with the wind tunnel based, pre-STS-1 aerodynamic data book. This study also showed that the increase in bodyflap trim angle was caused by an increased nose-up basic body pitching moment caused by real-gas effects. Computed aerodynamics for the complete Orbiter configuration were within 5 percent of the flight values and the bodyflap trim angle was predicted to within 10 percent of the flight value.

Significance
Ground-based facilities cannot simulate the aerothermal environment encountered by entry vehicles at hypersonic speeds. This study shows that the computational tools are in place to define accurately the longitudinal aerodynamic characteristics of such vehicles in this flight regime.

Future Plans
The technology developed in this study will be directly applied to the analysis of the Advanced Manned Launch System, HL-20, and other candidate winged entry vehicles.

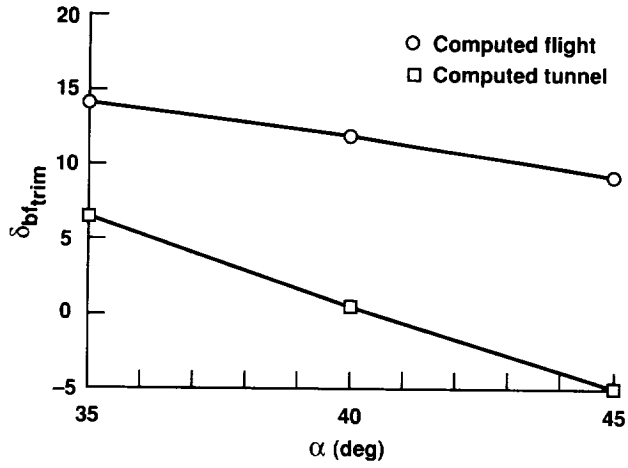

Comparison of computed Orbiter bodyflap trim requirements for tunnel and flight conditions as a function of angle of attack.

Modeling for High-Speed Transitional Boundary Layers

Thomas A. Zang, Principal Investigator
Co-investigator: Nabil M. El-Hady
NASA Langley Research Center/Analytical Services and Materials, Inc.

Research Objective
To apply the state-of-the-art dynamic modeling of small-grid scales to a transitional boundary layer at high speed. A central issue in large-eddy simulation (LES) is model development for the small subgrid scales. The model allows the transfer of the right amount of energy from the large to the subgrid scales, or vice versa, near the wall. In previous studies, the ad hoc manner in which the model constants or the model modifications have been treated was not satisfactory.

Approach
The subgrid scales were modeled dynamically in a temporal LES of transitional boundary-layer flow along a cylinder at Mach 4.5. The coefficients of the dynamic eddy-viscosity model were determined from the local information of the smallest resolved field. This was accomplished by filtering the equations of motion with a test filter having a width double that of the grid filter. The difference between the two resulting small-grid scale fields, which are related by the Germano identity, is the contribution by the scales of motion between the test and the grid scales. Both the formulations of Germano et al. and Lilly (least-square technique) were used for the dynamic modeling to compare and assess their results. The results of the LES were compared with accurate results from direct numerical simulations (DNS).

Accomplishment Description
The dynamic eddy-viscosity subgrid-scale model has been successfully applied to a high-speed transitional boundary layer. The coefficients of the dynamic model were qualitatively evaluated at various stages of the laminar turbulent transition process. The model gave the proper asymptotic behavior of modeled quantities near the wall and in the free stream, with no dissipative character in the linear and early nonlinear regions. A remarkable agreement exists between LES calculations and the accurate DNS results concerning the resolved Reynolds stresses, heat flux, and the time evolution of the skin friction. LES of the transitional flow along a cylinder at Mach 4.5 is achieved with one-sixth of the grid resolution used for DNS. A typical LES case for laminar breakdown takes about 20–25 CPU hours with central memory requirements from 2 to 8 megawords compared to 125 CPU hours and 30 megawords for DNS.

Significance
Simulation of temporal forced transition through laminar breakdown and beyond can be accomplished accurately and cheaply at high speeds. Location of transition onset (rise of skin friction), the length of the transition zone, and peak skin friction can be predicted accurately using dynamic LES modeling.

Future Plans
The LES method will be thoroughly tested with other state-of-the-art small-grid scale models and will then be extended to spatial transition.

(a)

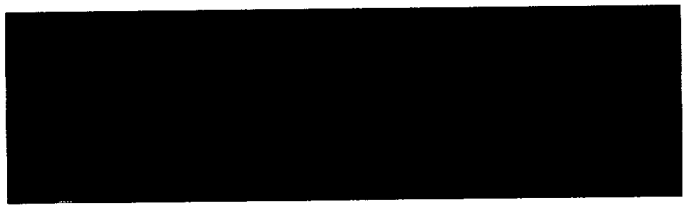

(b)

Spanwise vorticity flow structure in the middle of the skin friction rise from (a) DNS (96 × 48 × 144) and (b) LES (36 × 24 × 96). Mach = 4.5, t = 54.

DSMC Simulation of High-Altitude Plume Interaction

S. H. Konrad Zhu, Principal Investigator
Co-investigator: Leonardo Dagum
Rockwell International, Rocketdyne Division/NASA Ames Research Center

Research Objective
To characterize the flow field from two simultaneously firing reaction control system (RCS) engines on the Space Shuttle Orbiter during proximity operation about Space Station Freedom.

Approach
The direct simulation Monte Carlo (DSMC) method was applied to analyze the problem. PSiCM, a three-dimensional (3-D) particle simulation for rarefied flows, was used to obtain the flow-field solution.

Accomplishment Description
Solutions for the multiple RCS plume interactions were computed and demonstrated a complex, 3-D structure for the flow field from two RCS plumes separated by distances of 7.8 meters and 18.5 meters. The computational domain covered a downstream distance about the same as the separation distance. The solutions provide essential information about the near-field flow structure and physics for the concerned plume interaction. PSiCM was compared to experimental results for the interaction between two rarefied free jets. The computed flow fields show excellent agreement.

Significance
This work was prompted by the Space Station design and the possibility of excessive loads on the solar array caused by RCS plume impingement. These solutions indicate that there is still a significant interaction that suggests the practice of predicting the multiple-plume flow field as a linear superposition of each single RCS plume is inaccurate in the present Space Station design.

Future Plans
A parametric study of the multiple RCS firings will be done to provide a data base to establish an accurate engineering model for the Space Station design. A multizonal capability and an impingement capability will be added to PSiCM to extend computational domain further downstream.

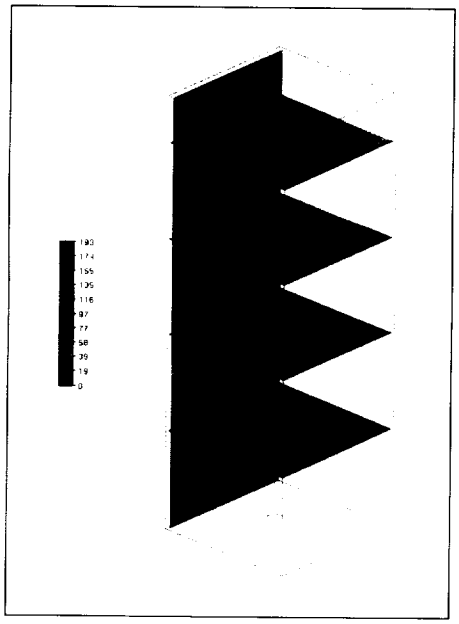

Density field from two RCS plume interactions separated by a distance of 7.8 meters. Half the flow field is presented. There is a 20 degree computation cutoff angle measured from the plume centerline. A shock is formed adjacent to the symmetry plane between the two plumes.

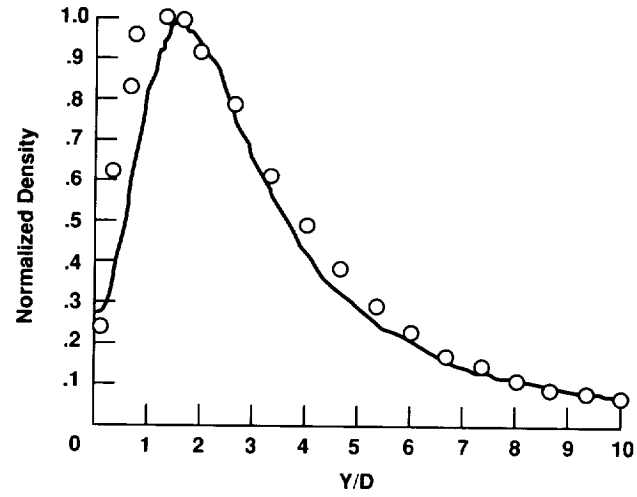

Density profile along the symmetry plane centerline between two interacting jets; circles = experimental data.

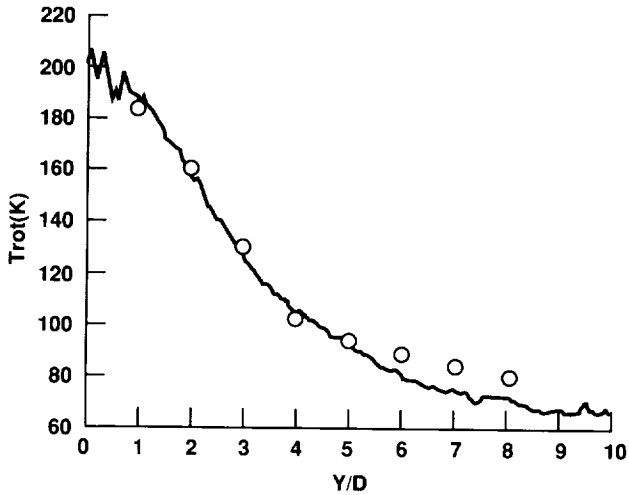

Rotational temperature distribution along the symmetry plane centerline between two interacting jets; circles = experimental data.

Subsonic High-Lift Analysis

Kenneth M. Jones, Principal Investigator
Co-investigators: Kevin Kjerstad and Victor Lessard
NASA Langley Research Center/ViGYAN, Inc.

Research Objective
To predict the flow characteristics of several high-speed research (HSR) configurations with attached-flow leading-edge flaps and vortical-flow leading-edge flaps at subsonic takeoff and landing conditions, and to compare the numerical and experimental data. Numerical methods were assessed as analysis and design tools for high-lift systems on HSR configurations.

Approach
Two approaches were used for numerical analysis. A three-dimensional (3-D), thin-layer, Reynolds-time-averaged Navier–Stokes code (CFL3D) was used to simulate an attached-flap HSR configuration on a two-block structured-volume grid. The 3-D Euler code USM3D was used to simulate a vortex-flap HSR configuration (including trailing-edge flaps) on an unstructured volume grid.

Accomplishment Description
The CFL3D code (with the Baldwin–Lomax turbulence model) was used to predict the forces and moments of the HSR configuration with an attached-flow flap over an angle-of-attack range from 0 to 20 degrees at Mach 0.22 and a Reynolds number of 1.4 million per foot. Surface pressures on the attached-flow flap compared well with experimental data except at higher angles of attack. The discrepancies at the higher angles of attack were due to the inability numerically to predict transition and capture the correct separation location for turbulence flow. The USM3D code was used to model leading-edge vortex flaps coupled with deflected trailing-edge flaps on a generic HSR configuration. At the design condition for the vortex flaps, USM3D accurately predicted the reattachment line of the primary vortex when compared to experimental flow visualization. Forces, moments, and surface pressures compared well with the experimental data.

Significance
Accurately modeling and predicting the effects of leading- and trailing-edge flaps of a High-Speed Civil Transport design are critical in meeting high-lift requirements at takeoff and landing.

Future Plans
Viscous effects for split leading- and trailing-edge flaps will be included using specialized domain decomposition techniques.

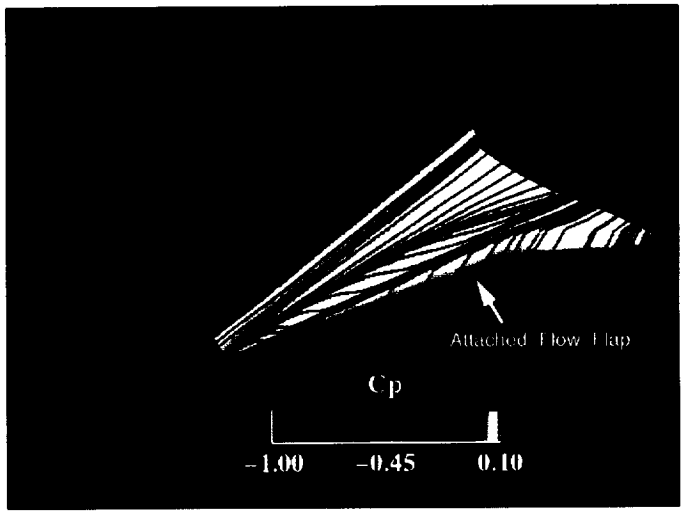

Pressure coefficient (Cp) contours and surface traces on an HSR configuration with attached-flow flaps; Mach = 0.22, angle of attack = 8 degrees, Reynolds number = 1.4 million per foot.

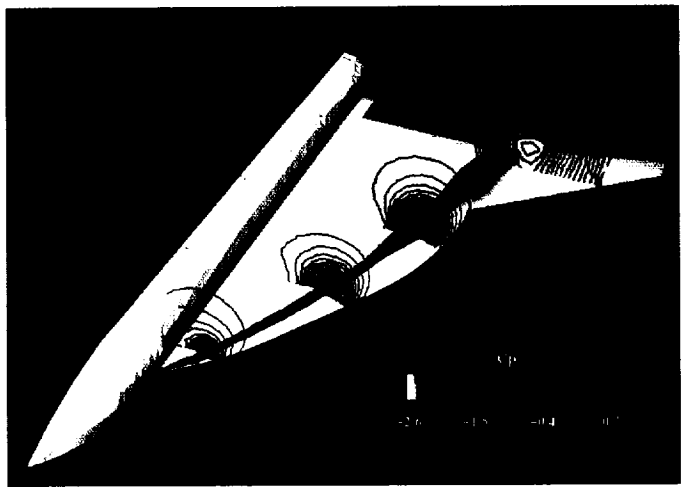

Pressure coefficient (Cp) contours on an HSR configuration with vortex flaps; Mach = 0.22, angle of attack = 12 degrees.

Analysis and Design of High-Lift Systems

Anutosh Moitra, Principal Investigator
Co-investigator: Wendy B. Lessard
High Technology Corporation/NASA Langley Research Center

Research Objective
To simulate the viscous subsonic flow about a representative High-Speed Civil Transport (HSCT) configuration with and without deployment of control surfaces. The concept of optimally deflecting the leading- and trailing-edge flaps to achieve attached flow was studied to improve the high-lift system performance of an HSCT aircraft.

Approach
A vortex-lattice technique (WINGDES and AERO2S) based on linear, attached-flow theory was used to determine the optimum flap deflection to provide maximum performance for specific flight conditions. The flow was simulated using CFL3D, which solved the three-dimensional, compressible, Reynolds-averaged Navier–Stokes equations.

Accomplishment Description
Numerical simulations for flow about a representative HSCT configuration with and without leading-edge flaps deflected were performed at Mach 0.08 and a Reynolds number of 640,000 at various angles of attack. As shown in the figure (left side), a reduced vortical flow field (approaching attached flow) results when the leading-edge flaps are optimally deflected. The computations correlated very well with the experimental coefficients at all angles of attack, and the predicted streamline patterns were similar to experimental oil flow results.

Significance
Accurate simulation and prediction of the vortex-dominated flow about an HSCT aircraft is essential to the design and analysis of high-lift systems.

Future Plans
An unstructured gridding technique will be applied to an HSCT configuration with the leading- and trailing-edge flaps deflected.

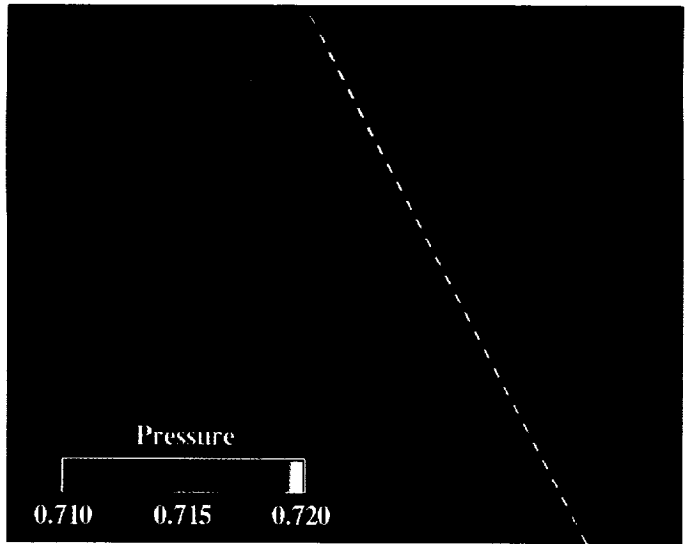

Total pressure contours for an HSCT configuration without leading-edge flaps deflected, angle of attack = 8.0 degrees (left), and with leading-edge flaps deflected, angle of attack = 9.7 degrees (right).

Aircraft Forebody Flow Control Technology

Lewis B. Schiff, Principal Investigator
Co-investigators: Ken Gee, Scott Murman, Gabriel Font, and Roxana Agosta
NASA Ames Research Center

Research Objective
To determine the effect of pneumatic forebody flow control on the flow field about a full aircraft geometry and simple configurations flying at high angle of attack using computational fluid dynamics (CFD).

Approach
The flow about an F-18 geometry with tangential slot blowing was computed using a multizone thin-layer Navier–Stokes code. The slot geometry was modeled in the computations. The jet conditions were introduced as boundary conditions in the slot grid. A computation using the isolated forebody was obtained for wind tunnel test conditions, and computations using the full aircraft geometry were obtained for flight conditions. Also, computations were carried out for simple bodies incorporating tangential slot blowing at high incidence.

Accomplishment Description
Computations were accomplished for the F-18 isolated forebody and complete F-18 configuration at wind tunnel and flight-test conditions. In the figure part (a), the computed surface flow pattern with blowing active on the left side of the isolated F-18 fuselage is shown. The flow is highly asymmetric on the nose of the aircraft. An analogous computation for the full F-18 configuration is shown in the figure part (b). Here, the asymmetric breakdown of the wing leading-edge-extension (LEX) vortices is clearly visible. The left LEX vortex breaks down in advance of the right vortex. Asymmetric flows generate large yaw moments on the aircraft, which have the potential of being exploited for enhanced control of the aircraft in high-angle-of-attack maneuvers. Computations were used to optimize the configuration of the slot location, as seen in the figure part (c). A comparison of the computed surface pressure distributions with data measured in the full-scale test is in the figure part (d). It shows excellent agreement with the experimental measurements.

Significance
The computations show the ability of CFD methods to model the complex high-angle-of-attack flow field. The computations, carried out in advance of the wind tunnel test, guided the design of the wind tunnel experiment. This illustrates how the coordinated use of computational and experimental methods can provide increased understanding of complex high-incidence flows.

Future Plans
Time-accurate, full aircraft computations at wind tunnel conditions are under way to more accurately resolve the interaction of the forebody vortex and the vertical tails. Computations for simple bodies are being done to investigate the basic physics underlying the development of the flow asymmetry at high angles of attack.

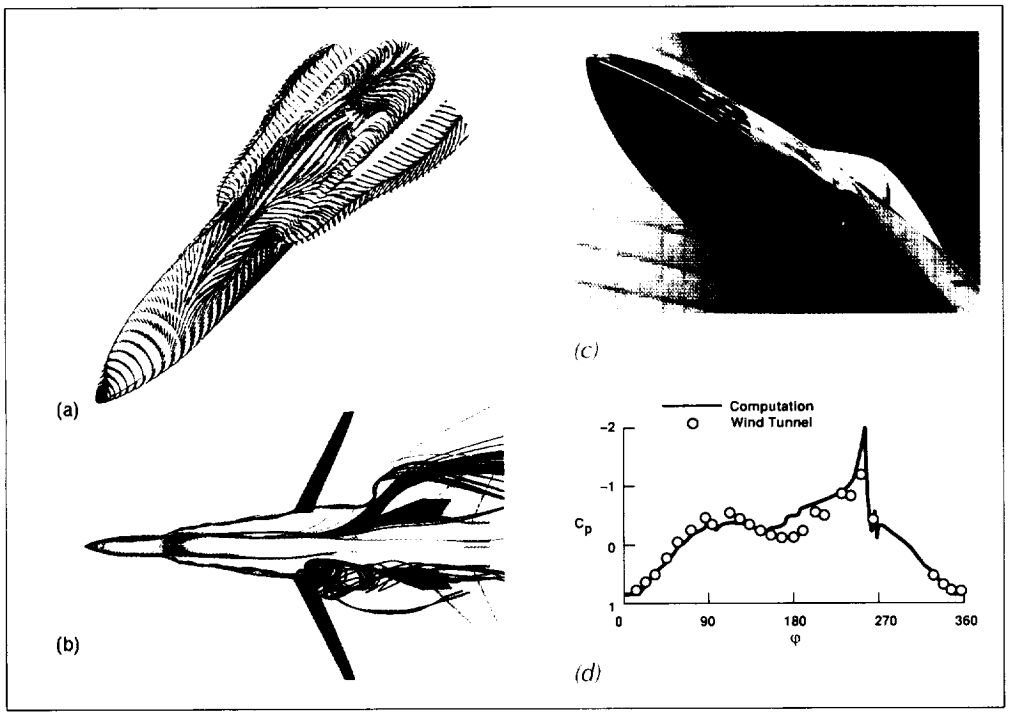

Slot blowing for enhanced aircraft high-angle-of-attack agility. (a) CFD prediction; (b) computed asymmetric flow with blowing; (c) wind tunnel test configuration; (d) CFD/wind tunnel comparison.

Steady and Unsteady Flows at High Angles of Attack

David T. Yeh, Principal Investigator
Rockwell International, North American Aircraft Division

Research Objective
To extend and validate a computational capability to assist in the design of advanced technology aircraft that are required to operate in a high-angle-of-attack flow environment.

Approach
The unified solution algorithms (USA) code and the ENSAERO code were used for high-angle-of-attack flow simulations. The USA code solved the three-dimensional Reynolds-averaged Navier–Stokes equations through an upwind, flux-difference, finite-volume approach coupled with a high-resolution total-variation-diminishing scheme. The ENSAERO code coupled the Navier–Stokes solutions with modal structural equations of motion for computing aeroelastic responses of flexible aerodynamic surfaces. The X-31 enhanced fighter maneuverability demonstration aircraft was the configuration studied. This configuration was chosen because of its inherently designed high-angle-of-attack characteristics and capabilities, the existence of a wind tunnel data base, and the ongoing flight-test program.

Accomplishment Description
The X-31 configuration was gridded and numerical solutions using the USA code were analyzed for prestall and poststall flight regimes and compared with wind tunnel and flight-test data. A nonaligned block interface technique was utilized to model multiple canard deflection angles where a cylindrical grid around the canard can be rotated about the hinge line. The effects of the movable canard on the aerodynamic control in the post-stall regime were demonstrated and validated with wind tunnel test data. Aeroelastic calculation of the structural response was initiated for applications such as the vertical tail buffet phenomena observed in high-angle-of-attack environments.

A simplified one-block grid was generated to focus on the demonstration of the aeroelastic simulation of the X-31. The aeroelastic computation was started from the rigid steady-state solution. The figure shows the rigid solution of a simplified X-31 under the free-stream conditions of Mach = 0.3 and angle of attack = 30 degrees. A typical computation required 25 megawords of memory and 30 Cray Y-MP hours.

Significance
This study paralleled the X-31 flight-test program and established and extended computational fluid dynamics capability for analysis of high-angle-of-attack flow phenomena. This study will have significant impact on current and future advanced aircraft design.

Future Plans
The study will be extended to include structural response in an unsteady vortex dominated flow environment based on the current rigid solution.

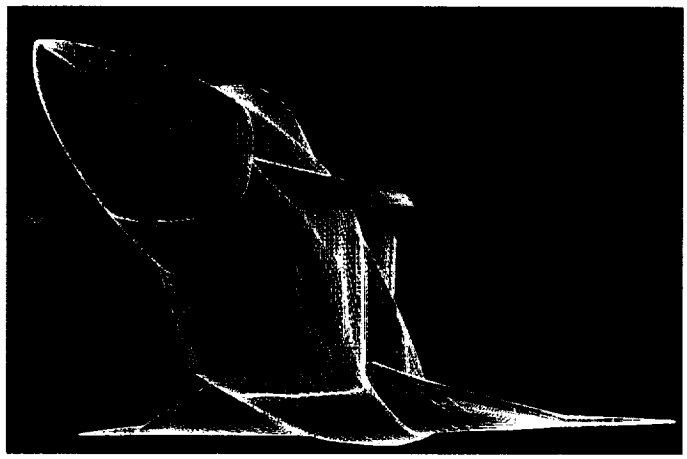

Pressure contours for a simplified X-31 rigid model.

CFD Applications to HSCT Design and Analysis

Dharmanshu L. Antani, Principal Investigator
Co-investigators: Shreekant Agrawal, David L. Rodriguez, Ramesh K. Agarwal, and Raymond Hicks
McDonnell Aircraft Company/NASA Ames Research Center

Research Objective
Computational fluid dynamics (CFD) codes are calibrated and validated for supersonic wing designs to improve the cruise aerodynamic performance of a High-Speed Civil Transport (HSCT) configuration. A three-dimensional (3-D) Navier–Stokes code for the analysis of current HSCT configurations was applied for a highly loaded condition. A 3-D Navier–Stokes code was calibrated and validated to analyze high-lift concepts for HSCT configurations and to provide design guidelines for improving aerodynamic performance of the high-lift system.

Approach
A 3-D wing optimizer was used in conjunction with an advanced CFD code to improve the aerodynamic performance of an HSCT wing originally designed using linear theory. The new wing design was performed with an Euler code in the presence of the fuselage. The improved wing was tested in the NASA Ames 9- by 7-Foot Supersonic Wind Tunnel to validate the design optimization methodology. A Navier–Stokes code was used to analyze a current HSCT configuration in a 2.5 G flight condition to predict aerodynamic loads for future application to structural design. A 3-D Euler/Navier–Stokes code with available data was used to analyze an HSCT high-lift configuration.

Accomplishment Description
The 3-D Euler-based wing–body optimizer was used to design a new HSCT supersonic wing with a predicted improvement in the supersonic cruise lift-to-drag ratio of about 5 percent (compared to a linear-theory designed wing) based on flight Reynolds number conditions. An analysis of the wing using a Navier–Stokes solver predicted an improvement in performance. Navier–Stokes solutions were obtained for a current HSCT wing–body configuration in 2.5 G subsonic, transonic, and supersonic flight conditions for prediction of aero loads. Results compared well with wind tunnel data. Euler solutions were obtained for a high-lift HSCT configuration and were compared to experimental data. Several cases were analyzed in each area of study. An average job run for the wing optimization and aerodynamic loads prediction required 8 Cray Y-MP hours and 64 megawords of central memory.

Significance
This method shows large potential for improving aerodynamic performance of HSCT configurations originally designed using a linear method. Accurately modeling nonlinear aerodynamics is the key to this success. CFD-based design optimization methods will minimize expensive wind tunnel tests. Once verified, spanwise loading from CFD predictions will have a strong impact on the low-weight structural design of the wing.

Future Plans
Wing and fuselage design optimization methods will be improved. Wing design methods in the presence of nacelles and diverters will be developed and applied. Wing–body design optimization methodologies will be validated against 1993 supersonic wind tunnel tests.

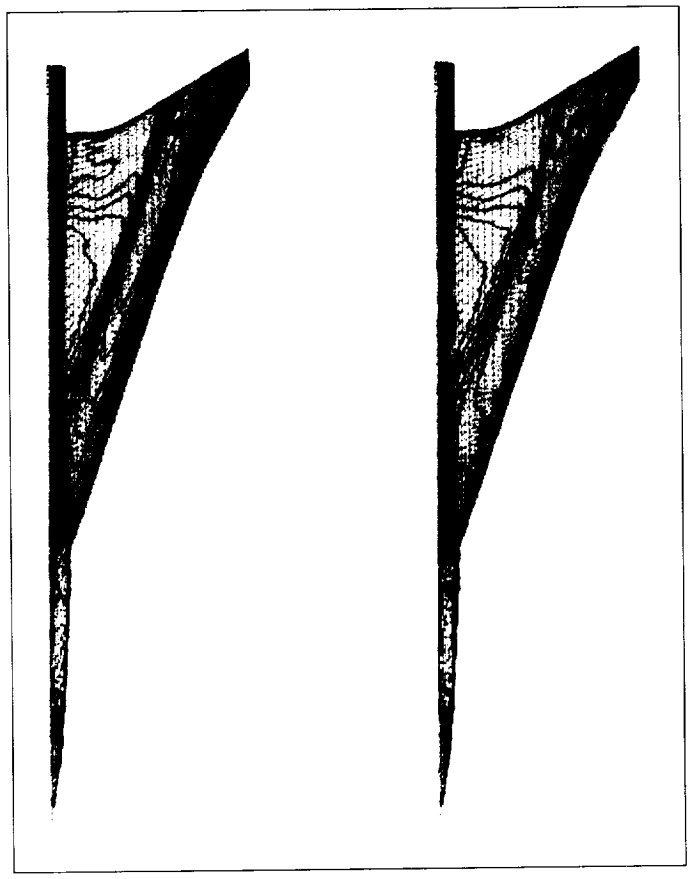

Pressure contours on upper surface of baseline (left) and modified (right) wings.

Transonic Flow Around a Delta Wing

Osama A. Kandil, Principal Investigator
Old Dominion University

Research Objective
To predict steady and unsteady, transonic, vortical flows around delta wings in the moderate- to high-angle-of-attack range. A complex shock-vortex system develops in the transonic-flow regime, which is important for the performance of the new generation of super-maneuver aircraft. Experimental measurements of transonic flows around a 65-degree cropped delta wing show that the shock system appearing over the wing consists of a ray shock wave beneath the leading-edge primary vortex and a transverse, time-dependent shock wave (known as a terminating shock).

Approach
The unsteady, compressible, full-Navier–Stokes equations were solved with an implicit, upwind, flux-difference, finite-volume scheme (FTNS3D). The scheme was a modified full-Navier–Stokes solver of the CFL3D program.

Accomplishment Description
A 65-degree swept-back, sharp-edged, cropped delta wing of zero thickness was considered for the computational solutions. The cropping ratio was 0.15. An O–H grid of $1 \times 258 \times 584$ in the wraparound, normal, and axial directions was used. The minimum grid size normal to the wing surface is 5×10^4. The figure shows the results for a wing at 20 degrees angle of attack, Mach 0.85, and Reynolds number 3.23×10^6. A plane-of-geometric-symmetry view of the computed surface pressure and Mach contours along with particle traces of the leading-edge vortex core is shown. The terminating shock and the supersonic pocket ahead of the wing are clearly captured along with the vortex breakdown of the leading-edge core. The computed surface pressure is in good agreement with the existing experimental data, and a complete reconstruction of the flow field behind the terminating shock was presented for the first time. The effects of the angle of attack and Mach number were also studied.

Significance
Prediction and study of transonic flows around delta wings are important to increase the performance quality of the new generation of super-maneuver aircraft. Unlike the low-speed regime, vortex breakdown in the transonic flow regime occurs at moderate angles of attack and is caused by shock waves.

Future Plans
Work is under way to study the transonic flow around delta wings undergoing pitching, rolling, and combined oscillations with high amplitudes and during the vortex-breaking mode. Coupling the computational fluid dynamics with the wing dynamics will also be considered.

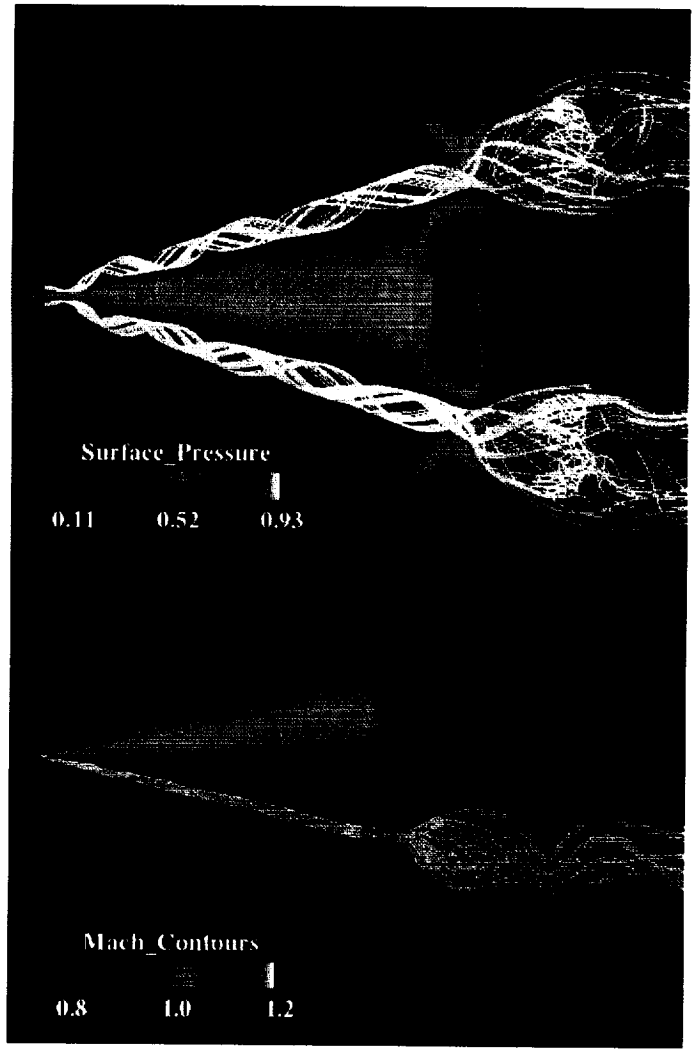

Surface pressure, Mach contours, and particle traces on wing and symmetry planes; $M_\infty = 0.85$, Reynolds number = 3,230,000, $\alpha = 20$ degrees.

Aeronautics

Propulsion

Simulation of Turbomachinery Flows

John J. Adamczyk, Principal Investigator
Co-investigators: Tim Beach, Mark Celestin, Kevin R. Kirtley, Rick Mulac, Wai-Ming To, Jeff Yokota, and Aamir Shabbir
NASA Lewis Research Center/Sverdrup Technology, Inc./ICOMP

Research Objective
To develop a flow model to analyze the flow field within multistage/single-stage turbomachinery.

Approach
In a parallel effort, an unsteady code based on the computational tool V-STAGE was developed to investigate the effect of unsteadiness on turbomachines. V-STAGE is a finite-volume cell-centered scheme that solves the average-passage equation system. These simulations will be used with experimental data to develop better average-passage equation system models.

Accomplishment Description
The effect of tip clearance on stall in a high-speed fan and the blade redesign on a one-and-a-half-stage turbine were studied. Simulations of two types of bypass fans, a compact two-stage high-speed compressor, and an unsteady simulation of a high-speed single-stage fan were completed. A four-stage high-speed compressor was analyzed. Typical run times were in excess of 20 Cray Y-MP hours per completed case and required up to 20 megawords of memory.

Significance
The design of advanced turbomachinery components requires the development of a three-dimensional model that can predict the complex flows associated with these devices. A model was developed to answer many of the issues associated with the flow field within single-stage and multistage turbomachinery.

Future Plans
Refinements to V-STAGE will include higher order turbulence models and closure models for the deterministic stresses. V-STAGE-unsteady is being used to simulate unsteady flow through a blade row.

Density distribution of an advanced high-speed compressor rotor.

Investigation of Scalability of Parallel Turbomachinery Codes

Richard A. Blech, Principal Investigator
Co-investigators: Edward J. Milner, Scott E. Townsend, and Angela Quealy
NASA Lewis Research Center

Research Objectives
To develop a parallel, portable version of the average-passage turbomachinery code and investigate the scalability of this code on several parallel architectures.

Approach
A distributed-memory, message-passing programming model was used. Portability was achieved through use of the Application Portable Parallel Library (APPL). Initial demonstrations focused on the inviscid, single-blade-row code (ISTAGE) on several parallel computers. The experience gained from this exercise will be used to develop a parallel, viscous, multistage (MSTAGE) version of the average-passage code.

Accomplishment Description
A parallel version of ISTAGE was demonstrated on the NASA Lewis Hypercluster, the NASA Lewis Intel iPSC/860, and the Intel Delta machines. A fine-grain partitioning of the grid in the axial direction was used. The grid size used was 120 × 11 × 11. A speedup of about 12 was achieved on all three machines using 20 processors. The code was run using up to 60 processors on the NAS iPSC/860, which increased the speedup to about 15. The results are summarized in the figure. A larger problem size would likely result in better performance. The larger cases were not run, however, so that the focus could be shifted to the viscous code, MSTAGE. A coarse-grain parallel version of MSTAGE was developed by running individual blade rows on separate processors. A four-blade-row compressor simulation was demonstrated on the Hypercluster and a network of IBM RS6000 workstations. Four processors were used in each case. Speedups of 3.91 and 3.78 were achieved on the Hypercluster and the RS6000s, respectively. More significantly, an overall performance of 44 MFLOPS, 30 percent of the Cray Y-MP single processor performance, was achieved on the four RS6000s. This translates to a performance/cost ratio of 220 MFLOPS per million dollars for the RS6000s versus 50 MFLOPS per million dollars for an eight-processor Cray Y-MP. APPL was used for all these cases, allowing the same parallel code to run on four different parallel computers without additional programming.

Significance
The initial demonstration of the ISTAGE code shows that significant performance improvement is possible using parallel processing. The results for the viscous code, MSTAGE, on the RS6000 workstations offer hope for a cost effective alternative to supercomputers. A parallel version of the average-passage code will allow more cost effective execution by industry, as well as within NASA Lewis for applications such as integrated computational fluid dynamics and experiments and numerical propulsion system simulators. Parallel processing is also an important first step toward developing codes which can be run interactively.

Future Plans
The parallel blade-row version of MSTAGE is operational, and will be used in the ICE project for computational fluid dynamics calculations of the Low Speed Compressor Facility. A fine-grain parallel version of MSTAGE is currently being tested. This version will be better suited to massively parallel processors, and will be demonstrated on the Hypercluster, Intel iPSC/860, and Delta machines. An interesting comparison will be the performance of the coarse-grain version of MSTAGE on a few powerful processors versus the fine-grain version using many lower-performance processors.

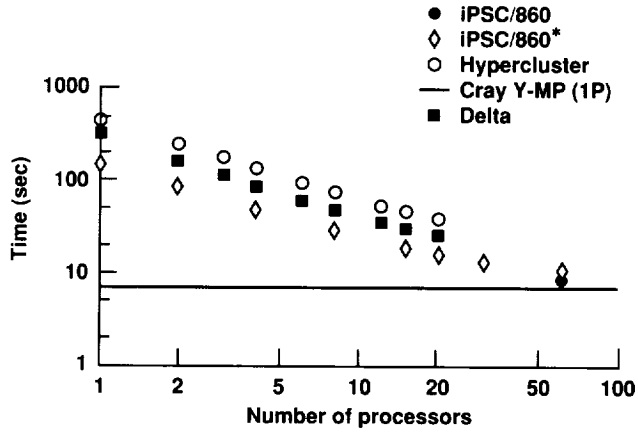

*Compiler and algorithm optimizations

Timings for the ISTAGE code on several parallel computers; 20 iterations on a 120 × 11 × 11 grid.

Subsonic Transport Propulsion/Airframe Integration

Pieter G. Buning, Principal Investigator
Co-investigators: Lie-Mine Gea, Cathy Maksymiuk, and W. R. Van Dalsem
NASA Ames Research Center/McDonnell Douglas Corporation

Research Objective
To test and refine the application of overset grid methodology to Navier–Stokes flow simulation for subsonic transport wing–body–pylon–nacelle geometries.

Approach
Pylon and nacelle grids were added to a suitably refined wing–body grid generated using McDonnell Douglas grid generation capabilities. The Air Force PEGSUS grid-joining code was used to cut holes in the wing–body grid to accommodate the pylon and nacelle. The Ames Research Center OVERFLOW code was then employed to compute the flow on the overset grids.

Accomplishment Description
The OVERFLOW flow solver was first validated in comparison to the Langley Research Center thin-layer Navier–Stokes code for wing–body configurations. Methodology was established for adding pylon–nacelle grids, and comparisons were made with wind tunnel and flight-test data. Areas in need of additional investigation were identified. In addition, a new time-step scaling was implemented that accelerates convergence to steady state (in some cases by a factor of four).

Significance
The capability for investigating propulsion–airframe integration issues through Navier–Stokes flow simulation was established.

Future Plans
This effort is being extended to develop gridding strategies for automatic generation of overset structured grids for propulsion–airframe integration applications.

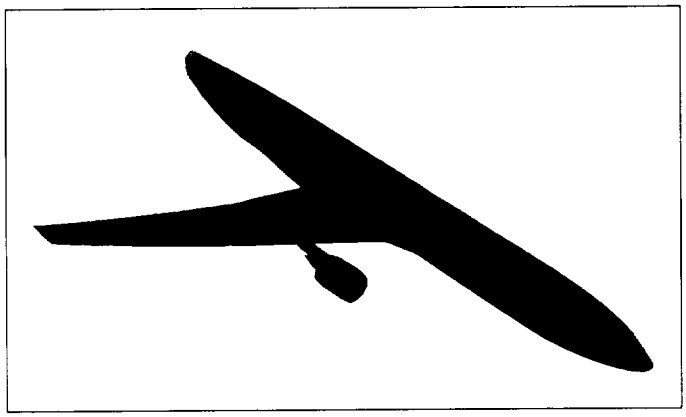

Surface pressure on a subsonic transport; Mach = 0.85, Reynolds number = 49 million (based on chord).

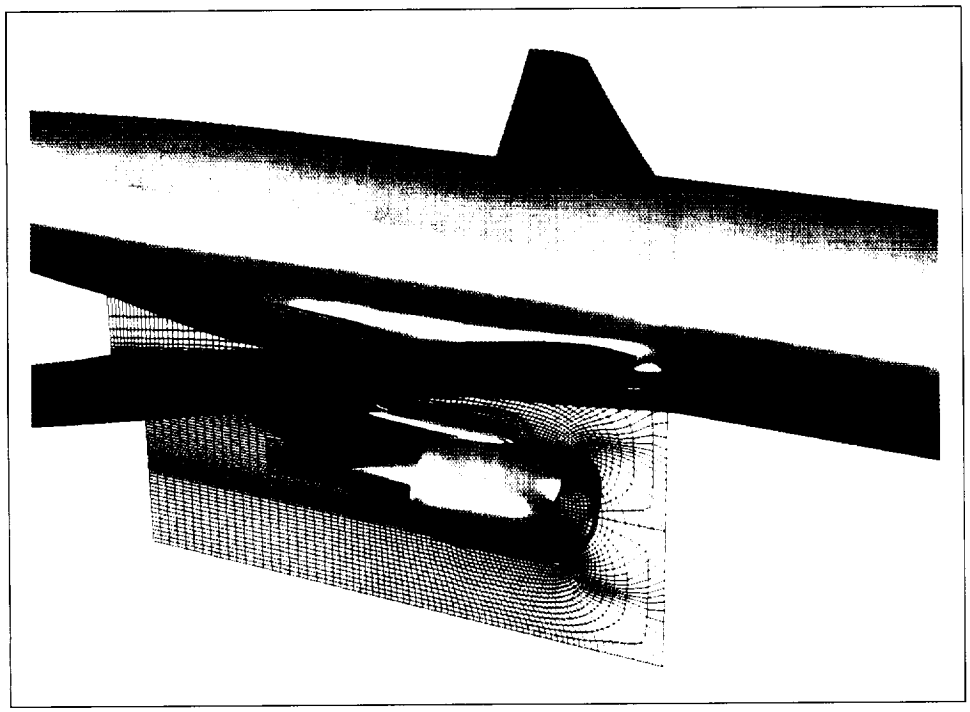

Overset grids on nacelle symmetry plane.

Pulsed Detonation Wave Augmentor Concept

Jean-Luc Cambier, Principal Investigator
Co-investigators: Henry G. Adelman and Gene P. Menees
Eloret Institute/NASA Ames Research Center

Research Objective

To investigate the use of unsteady waves in a supersonic combustor (scramjet), in order to enhance mixing and combustion rates. In this concept, blast waves are produced at the end of small detonation tubes embedded in the combustor walls and propagated into the main combustor stream. The interaction between the strong pressure waves and the mixing layer stimulates the formation of mixing vortices, while shock-heating of the mixture allows for very rapid combustion. The detonation tubes are rapidly cycled and triggered in sequence.

Approach

Preliminary computational fluid dynamics studies of various generic engine configurations were performed to estimate the effectiveness of the concept and to identify the key elements for future parametric studies. The numerical simulations were performed using a two-dimensional, time-accurate Navier–Stokes code, coupled to the full chemical kinetics of hydrogen–air combustion.

Accomplishment Description

The studies demonstrated the validity of the concept for a specific engine configuration, shown in the figures, where a short detonation tube was located beneath the fuel layer of a scramjet engine. The wave diffracted at the tube exit and decayed into a blast wave. The exiting shock was transmitted through the fuel layer, which it compressed and heated to ignition temperature. A rapid burning occurred at that location, and it is clearly seen in the figure (a). The fuel layer was then pushed and rolled-up by the transmitted shock, creating a large vortex. After only 275 microseconds, the fuel layer had significant amounts of vorticity and stretching present—both contribute to mixing enhancement (figure (b)). The shock heating was also very efficient at stimulating the combustion, which was seen to occur at several locations. Another important feature was the transmittal of a shock within the fuel layer. This particular feature may be used in other engine configurations, such as external combustion.

Significance

Strong, unsteady shocks are a powerful mechanism for stimulating the mixing and combustion in a scramjet combustor. This may lead to the design of shorter, lighter engines, with higher performance at high flight speeds. The detonation tubes also significantly contribute to the engine thrust, and they have minimal operating penalties.

Future Plans

We will investigate these unsteady interactions in more detail, using sophisticated nonequilibrium, compressible turbulence models. Other configurations will also be studied, notably external combustion and the stimulation of hydrocarbon combustion.

Publication

Cambier, J. -L. et al.: Numerical Simulations of a Pulsed Detonation Wave Augmentation Device. 29th AIAA Joint Prop. Conference, Monterey, CA, June 1993, AIAA Paper 93-1985.

(a)

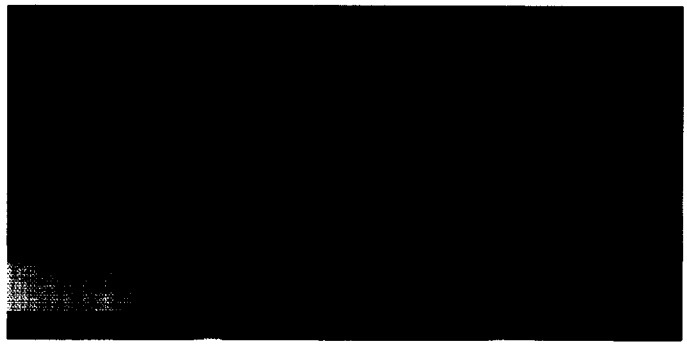

(b)

Temperature contours, at (a) 75 and (b) 275 microseconds.

Evaluating Nozzle Drag Using Computational Fluid Dynamics

Jeffrey A. Catt, Principal Investigator
Co-investigators: Tracy J. Welterlen and Brett W. Denner
Lockheed Engineering and Sciences Company

Research Objective
To define a methodology that uses computational fluid dynamics (CFD) to predict jet-induced nozzle drag. The methodology should accurately predict the difference between two operational exhaust system conditions as compared to test data.

Approach
Using the HAWK3D flow solver, three-dimensional full Navier–Stokes solutions of several F-16 jet effect test points were obtained. Two configurations simulating a reference "zero-nozzle drag" configuration and the actual nozzle installation were evaluated at two Mach numbers. The drag of each configuration was calculated by integrating pressure over surfaces that represented the metric portion of the model. Drag increments between the two configurations were compared to tested drag increments.

Accomplishment Description
Comparisons of predicted afterbody pressure distributions with pressure data gathered during jet effects testing showed that HAWK3D accurately modeled jet entrainment. Balance readings for incremental drag differences also matched test data very well. These comparisons showed the validity of using CFD to predict jet-induced drag increments. However, highly accurate computational procedures must be applied in a rigorous manner to achieve valid results. The computational model must accurately reflect the test environment, especially in the definition of the tested model. It is important that drag is evaluated on only those portions of the model that are force sensitive. Tracking quantities of merit (drag, for this study) as a solution progresses provides needed insight on convergence. This tracking is critical for jet-induced drag evaluation, because numerical quantities can indicate convergence long before fluctuations in afterbody pressure distribution damp out. Convergence of a typical 2.5 million point problem required approximately 20,000 iterations, 92 megawords of memory, and 300 Cray Y-MP hours.

Significance
Propulsion integration is a driving technology in the development of advanced fighter aircraft. This is evident in the design of the F-16 afterbody, which requires that the nozzle be cleanly integrated into the airframe. Predicting drag characteristics with CFD provides cost-effective and timely input into the design process and provides risk reduction before manufacturing is initiated. CFD may prove to be a viable alternative to wind tunnel testing.

Future Plans
Preliminary CFD results show that refinements to external nozzle shaping can result in significant station improvement. Work is continuing through the prediction of jet-induced drag of advanced nozzle concepts installed on the F-16.

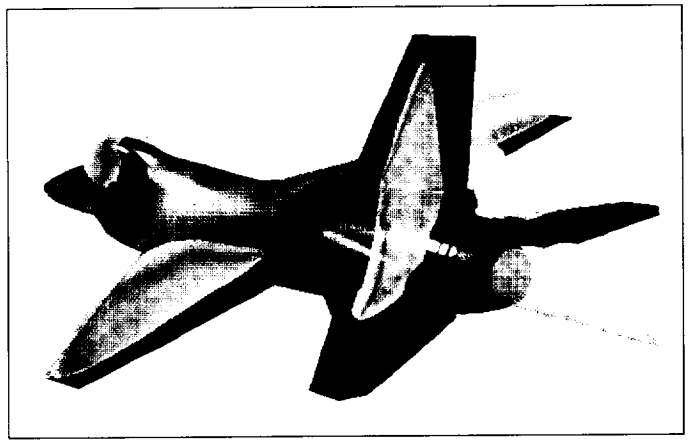

Surface pressure contours and sonic regions produced on the F-16 at Mach 0.9; low pressure regions = blue, high pressure regions = magenta.

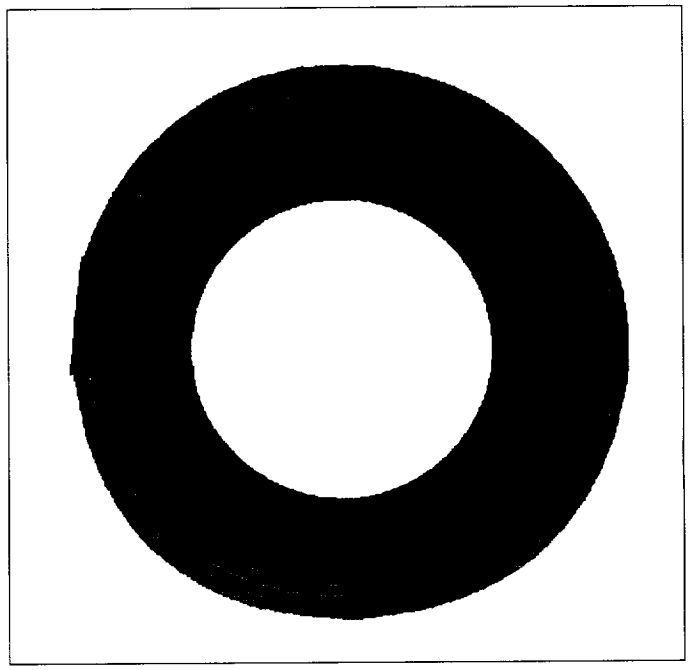

CFD predicted nozzle pressure contours (left) compared with test data (right). Test contours interpolated from 40 pressure taps.

CFD for Engine–Airframe Integration

Richard D. Cedar, Principal Investigator
Co-investigator: Craig M. Kuhne
General Electric Aircraft Engines

Research Objective
To develop an analytical tool to determine the mutual aerodynamic interaction between an engine and an airframe. Emphasis is on the development of an analysis system that can be integrated into the engine–airframe design process.

Approach
The current computational fluid dynamics (CFD) based design and analysis systems at General Electric Aircraft Engines were used to assess the mutual aerodynamic interaction of isolated components (engine inlets, exhaust systems, clean wings). This assessment was pursued using the Chimera domain decomposition technique to build the complete configuration from the isolated component grids. The PEGSUS code was used to determine the interpolation coefficients required by the Chimera method, and the CFL3D code was used as the flow solver.

Accomplishment Description
An advanced high-bypass-ratio engine was tested in the NASA Langley National Transonic Facility wind tunnel. Three-dimensional Euler and Navier–Stokes calculations were performed for the isolated engine, the clean-wing airframe (with no engine installation), and the complete configuration (airframe including the engine and pylon). Comparisons with test data showed that the major aerodynamic interactions were predicted. These included an increase in the wing upper-surface Mach numbers inboard of the installation and a reduction outboard (see figure) due to the engine installation. A typical Navier–Stokes solution takes about 20 Cray-2 hours and 64 megawords of memory.

Significance
Assessment of engine and airframe aerodynamic interaction is critical for optimum aircraft design.

Future Plans
Work is in progress to make more efficient use of the computational grid while concentrating the grid in the areas where it is deficient for high-quality Navier–Stokes solutions. Further evaluation of the results is planned when test data become available from a highly instrumented model of the MDC cooperative study aircraft that is to be tested in the NASA Langley 16-Foot Wind Tunnel.

Publications
1. Ostrander, M. J.; and Cedar, R. D.: Analysis of a High Bypass Ratio Installation Using the Chimera Domain Decomposition Technique. AIAA Paper 93-1808, June 1993.
2. Cedar, R. D.; Dietrich, D. A.; and Ostrander, M. J.: Engine/Airframe Installation CFD for Commercial Transports. An Engine Manufacturers Perspective. SAE Aerotech '93, Sept. 1993.

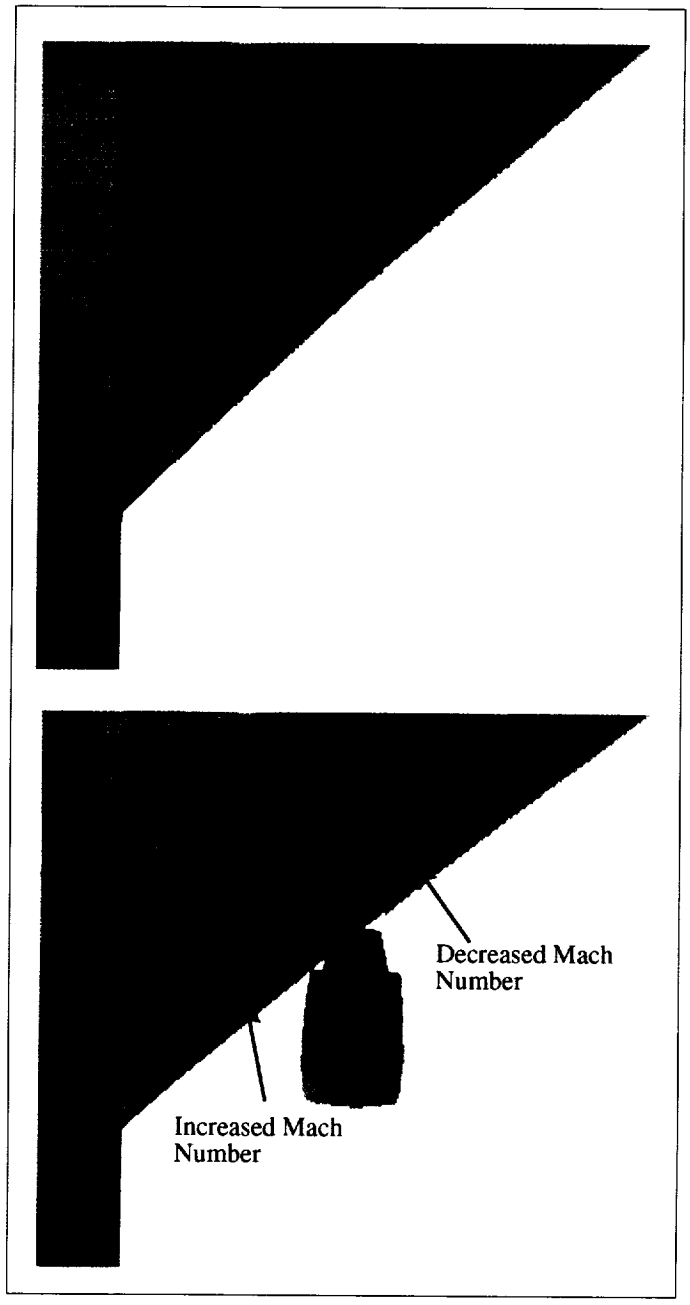

Surface pressure distribution on the (top) clean wing and (bottom) installed engine configurations.

Computation of Separated Nozzle Flows

C. L. Chen, Principal Investigator
Co-investigators: S. R. Chakravarthy and C. M. Hung
Rockwell International Science Center/NASA Ames Research Center

Research Objective
To understand separated overexpanded nozzle flows using a time-accurate Reynolds-averaged Navier–Stokes solver.

Approach
The equations solved were the unsteady, axisymmetric Reynolds-averaged Navier–Stokes equations. The time-accurate unified solution algorithm (USA) Navier–Stokes code was employed to calculate the separated nozzle flow. Time accuracy was required to study the transient flow and the unsteady nature of the separated flow. The USA code, which is a finite-volume multizonal Navier–Stokes solver, utilizes a high-resolution total variation diminishing scheme. The code was validated from low subsonic to hypersonic flows.

Accomplishment Description
The axisymmetric overexpanded nozzle flows were studied, and the flow structures of the startup and throttle-down processes were examined. During the impulsive startup process, observed flow features included the Mach disc, separation shock, Mach stem, vortex core, contact surface, slip stream, initial shock front, and shocklet. The movement of the Mach disc was not monotonical in the downstream direction. For a range of pressure ratios, hysteresis phenomenon occurred; different solutions were obtained depending upon different processes (see accompanying figure).

Significance
The separated flow structures associated with the hysteresis phenomenon were revealed. A typical time-accurate calculation to reach final-state solution required 40 Cray Y-MP hours and 10 megawords of memory.

Future Plans
The bifurcation diagram will be further investigated and examination of three-dimensional flow structure will be continued.

Publication
Chen, C. L.; Chakravarthy, S. R.; and Hung, C. M.: Numerical Investigation of Separated Nozzle Flows. AIAA Paper 93-3016, July 1993.

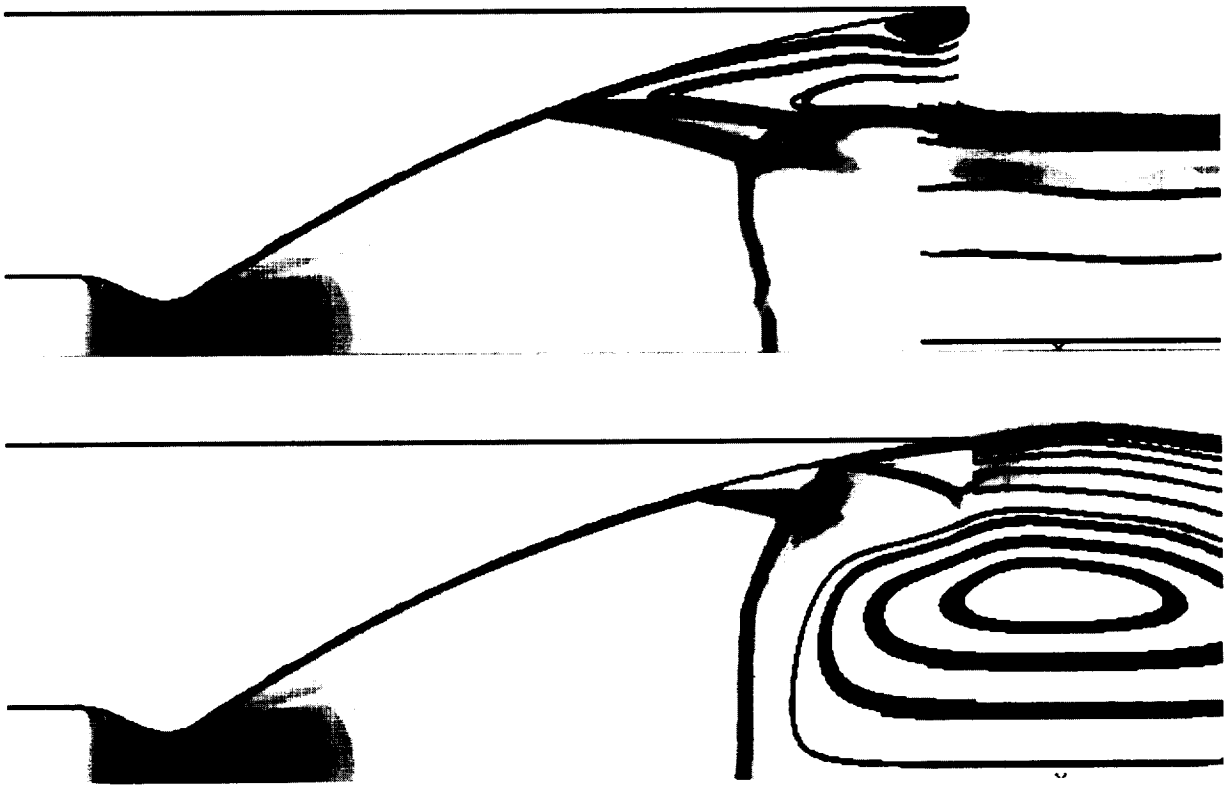

Schlieren-type snapshots and streamlines at pressure ratio = 45. (top) Startup. (bottom) Throttle down.

Inverse Design of Installed Nacelle

H. C. Chen, Principal Investigator
Co-investigators: T. Y. Su, T. J. Kao, and D. A. Naik
Boeing Commercial Airplane Group/NASA Langley Research Center/ViGYAN, Inc.

Research Objective
To reshape an installed nacelle to achieve a specified nacelle pressure distribution.

Approach
The flow solver was a general, multiblock, multigrid Euler code (GMBE) developed for the analysis of complete airplane configurations with underwing turbofans. GMBE was coupled with the direct iteration surface curvature algorithm, and the resulting new code (GMBEDS) was used for the inverse design of a turbofan nacelle installed on a transport airplane.

Accomplishment Description
GMBEDS was executed successfully for a generic low-wing transport with two different turbofan nacelles (bypass ratio 6). The analysis run from the first installed nacelle was used to obtain the initial pressure distribution. This nacelle provided the initial geometry from which to start the design iteration. The pressure distribution from an analysis of the second installed nacelle was used as the target. The goal was to see how close the GMBEDS-designed nacelle would be to the target nacelle. The volume grid contained approximately 1.2 million grid points and was composed of 32 blocks. A typical analysis of 500 multigrid steps for third-order convergence takes 220 minutes and 20 megawords of memory on the Cray Y-MP. The analysis after each design iteration requires only first-order convergence. Typically, 5–10 iterations are required. The figure shows how the initial and target pressures compare with those of the designed nacelle after six design iterations.

Significance
The computational fluid dynamics code developed in this project is an effective tool for the inverse design of installed turbofan nacelles. The computational cost of the design is of the same order as that of the analysis.

Future Plans
The same methodology will be applied to a chosen multiblock Navier–Stokes code.

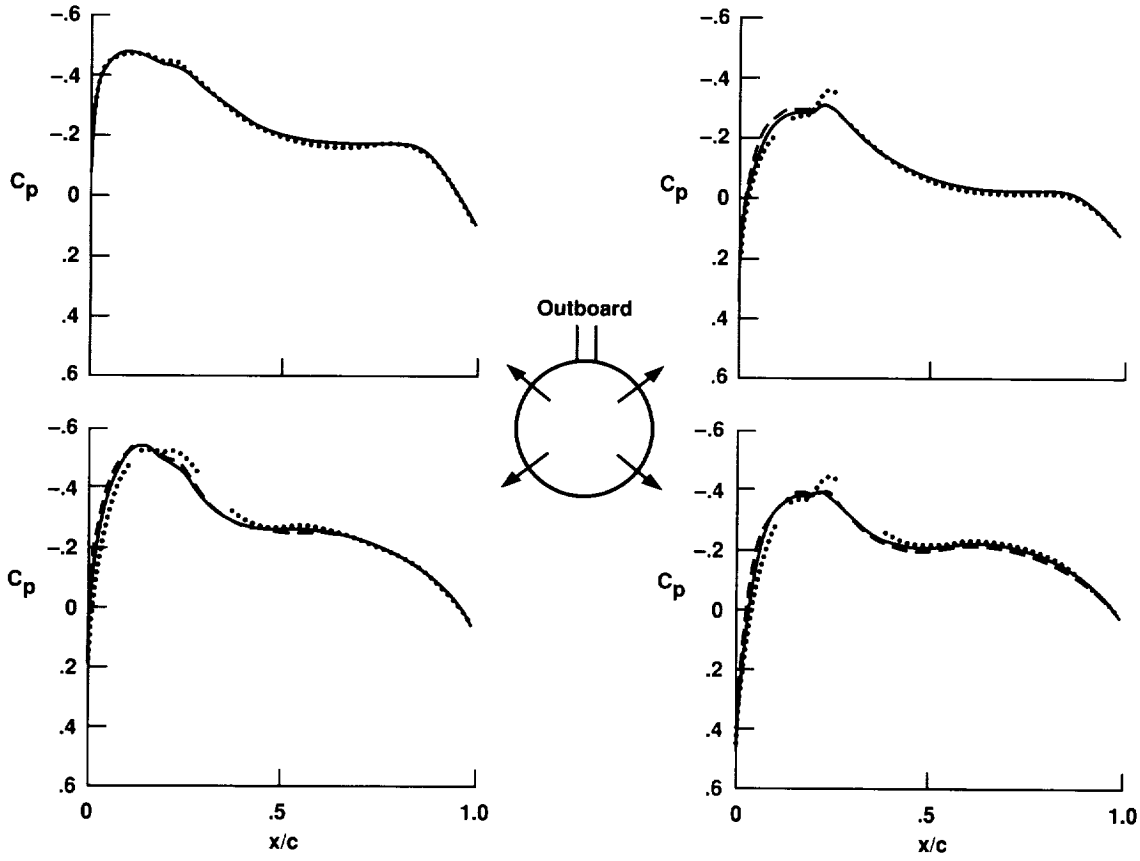

Pressure comparison for installed nacelle design; free-stream Mach number = 0.85, angle of attack = 0.5 degrees. Dotted line = initial, solid line = target, dashed line = design.

Airframe/Inlet Aerodynamics

Wei J. Chyu, Principal Investigator
Co-investigators: Tom I-P. Shih and David A. Caughey
NASA Ames Research Center/Carnegie Mellon University/Cornell University

Research Objective
To develop the analytical capability to predict integrated performance of forebody–inlet systems for highly maneuverable aircraft.

Approach
Navier–Stokes codes were adapted and developed using two numerical approaches, one with the F3D Navier–Stokes code combined with the Chimera grid-embedding technique, and the other with a finite-volume method with multiblock and multigrid diagonal implicit schemes.

Accomplishment Description
Studies were made on (1) an inlet boundary layer bleeding with one or multiple flat plates with circular holes that vent into a plenum, (2) an inlet flow through a highly contoured and offset super-elliptic diffuser with a newly developed three-dimensional finite-volume Navier–Stokes code, and (3) a transonic flow around the forebody–inlet of the AV-8B II Harrier aircraft.

Significance
The study permitted analysis of complex inlets, making possible the investigation of a broader range of design variables associated with integration of the forebody and inlet systems and inlet performance with boundary layer control.

Future Plans
Efforts will focus on code validation cases with various turbulence models to determine the effects on the flow physics and inlet performance.

Publications
1. Chyu, W. J.; Howe, G. W.; and Shih, T. I-P.: Bleed Boundary Conditions for Numerically Simulated Mixed-Compression Inlet Flow. J. of Propulsion and Power, vol. 8, 1992.
2. Wang, L.; and Caughey, D. A.: Multiblock/Multigrid Euler Method to Simulate 2D and 3D Compressible Flow. AIAA Paper 93-0332, Jan. 1993.
3. Mysko, J. M.; Chyu, W. J.; and Chow, C. Y.: Navier–Stokes Simulation of External/Internal Transonic Flow on the Forebody/Inlet of the AV-8B Harrier II. AIAA Paper 93-3057, July 1993.
4. Chyu, W. J.; Rimlinger, M. J.; and Shih, T. I-P.: Effects of Bleed-Hole Geometry and Plenum Pressure on Three-Dimensional Shock-Wave/Boundary-Layer/Bleed Interactions. AIAA Paper 93-3259, July 1993.

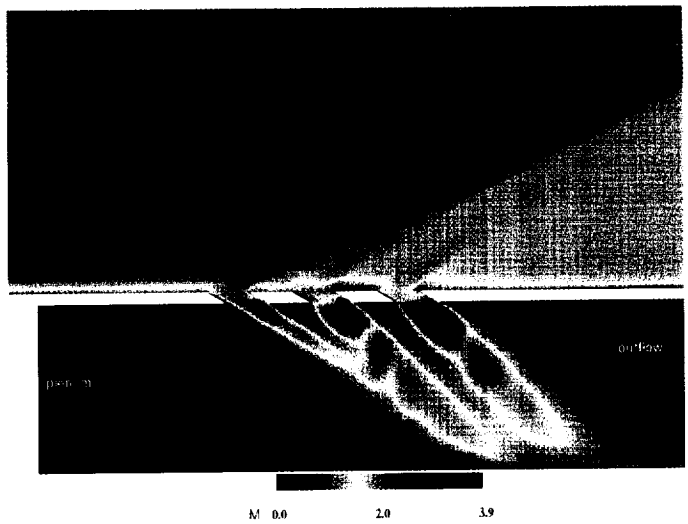

Boundary layer bleed through multiple slanted circular holes.

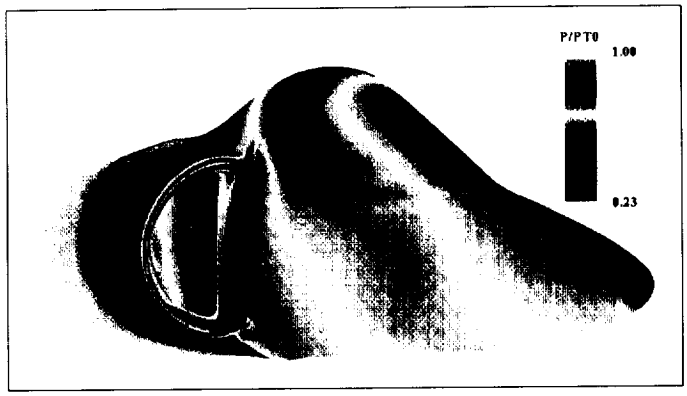

AV-8B II Harrier forebody-inlet surface pressure.

Three-Dimensional High-Speed Plume–Propulsive Flow Fields

Sanford M. Dash, Principal Investigator
Co-investigators: Neeraj Sinha, Brian J. York, Robert A. Lee, Ashvin Hosangadi, and Donald C. Kenzakowski
Science Applications International Corporation

Research Objective
To establish and advance computational methodology for the simulation of steady and transient chemically reacting, multiphase, high-speed plume–propulsive flow fields. Advanced turbulence models and new techniques for simulating nonequilibrium thermochemical and multiphase flow processes are being developed.

Approach
The CRAFT implicit/upwind code with strongly coupled, large-matrix inclusion of multi-equation turbulence models and chemical species was extended to incorporate particulate nonequilibrium capabilities using Eulerian and Lagrangian formulations. In addition, a gas–liquid formulation was incorporated with rate-dependent vaporization and combustion. For steady problems, Eulerian particle formulation and Reynolds-stress-based turbulence modeling was utilized. For nonsteady problems, the Lagrangian particle formulation with large-eddy-simulation based turbulence modeling was utilized.

Accomplishment Description
Grid methodology was upgraded to provide zonal patching in a dynamic framework. Particulate methodology was upgraded to account for volumetric contributions, and a new Lagrangian solver was incorporated and integrated with a solid-propellant ball-grain formulation. Large-eddy-simulation subgrid stress models were incorporated for transient studies. Problems analyzed included rocket plume–propulsive flows, ducted rockets, and plume–launcher interactions. The upgrades produced unique computational capabilities for steady and transient combusting/multiphase flows. Each run required 30–120 megawords of memory and 10–50 Cray Y-MP hours, depending on the grid dimensions and the number of chemical species included.

Significance
CRAFT plays a major role in missile design, in vertical launcher design, and in propulsive system design. It also supports major hypervelocity gun programs.

Future Plans
Multiphase flow modeling will be significantly advanced. Volumetric contributions, particle–particle interactions, and combustion modeling will be emphasized, as well as strong coupling to ablative boundaries and a detailed treatment of particle–surface interactions. Advanced work on droplet formation at transient interfaces will also be performed.

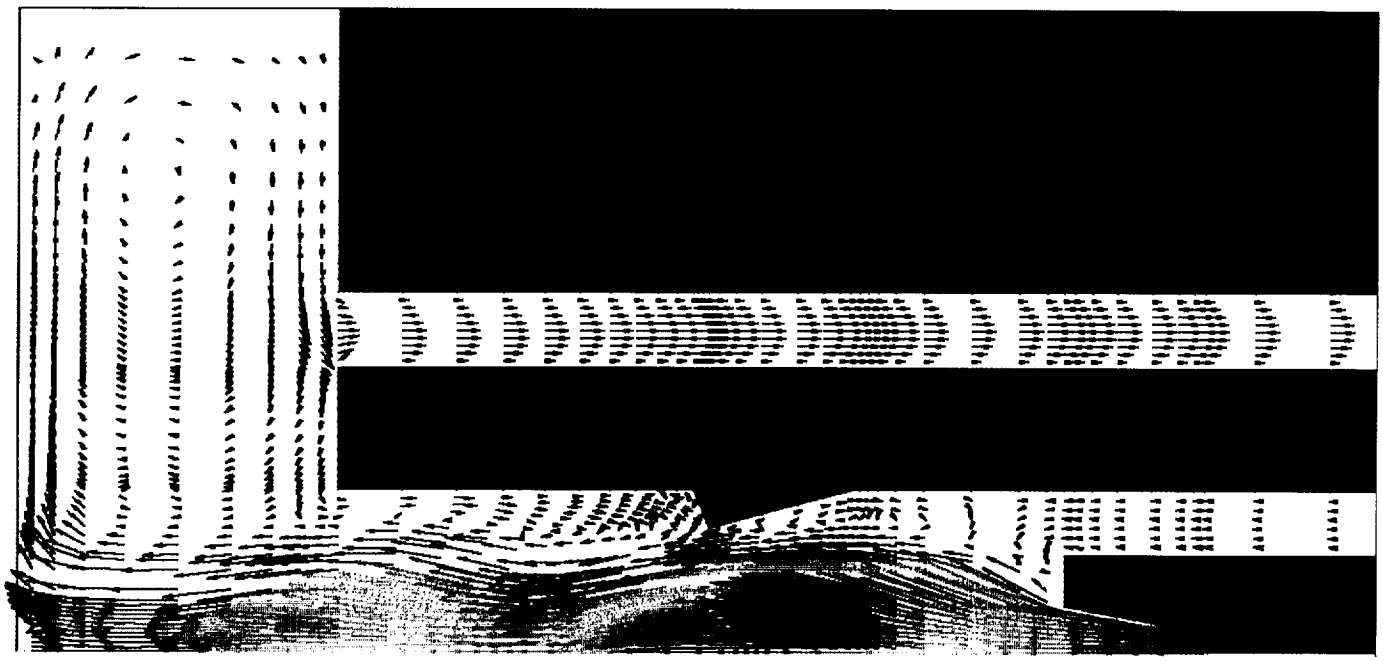

Interaction flow field for a rocket plume in a vertical launcher. Velocity vectors colored by Mach number.

Turbine-Blade Tip Clearance Flows

Frederik J. de Jong, Principal Investigator
Co-investigator: Tony Chan
Scientific Research Associates, Inc.

Research Objective
To analyze the tip clearance region flow for the gas generator oxidizer turbine (GGOT) blade and to study advanced concepts to reduce tip clearance losses.

Approach
The finite-difference form of the compressible, three-dimensional Navier–Stokes equations was solved for a single blade row in a rotating frame of reference using a linearized block-implicit alternating-direction-implicit procedure. The grid was generated by stacking a series of two-dimensional grids from hub to casing; grid points were clustered near solid boundaries and in the tip clearance region. At the inflow boundary, located approximately one axial chord from the blade leading edge, flow profiles were specified, while at the outflow boundary the static pressure was prescribed.

Accomplishment Description
Results were obtained for the baseline GGOT blade at the full-scale Reynolds number on a grid containing approximately 216,000 points: 90 points in the streamwise direction (36 points on the blade), 60 points in the circumferential direction (30 points on the blade), and 40 points from hub to casing (12 points in the clearance region). Particle traces in the near-tip region showed vortical flow behavior of the fluid which passed through the clearance region and exited at the downstream edge of the gap. In an effort to reduce clearance flow losses, the mini-shroud concept, which added a fence to the pressure side of the blade at the blade tip, was proposed. Calculations performed on the GGOT geometry with the minishroud, however, indicated that the minishroud had only a marginal effect on the tip clearance losses at the design tip clearance. Calculations at larger tip clearances are currently in progress. Each calculation required approximately 10 Cray Y-MP hours and 11 megawords of memory.

Significance
The ability to predict accurately the tip clearance flow and to perform parametric studies on changes in the geometry (both blade shape and tip clearance) is essential to the design of high-performance turbines.

Future Plans
Further three-dimensional simulations will be performed to assess the effect of tip clearance and to study additional advanced concepts.

Publication
Chan, Y.-T.; and de Jong, F. J.: Navier–Stokes Analysis of an Oxidizer Turbine Blade with Tip Clearance with and without a Mini-Shroud. Presented at the 11th Workshop for Computational Fluid Dynamics Applications in Rocket Propulsion, Huntsville, Ala., April 1993.

Pressure contours and particle traces on the baseline GGOT blade.

Interaction of Turbulence and Chemical Reaction

Richard L. Gaffney, Jr., Principal Investigator
Co-investigators: Jeffery A. White, Sharath Girimaji, and J. Phillip Drummond
Analytical Services and Materials, Inc./Institute for Computer Applications in Science and Engineering/NASA Langley Research Center

Research Objective
To investigate the interaction of turbulence and chemical reaction in high-speed turbulent chemically reacting flows.

Approach
The Favre-averaged Navier–Stokes equations and 8-species continuity equations with an 18-step reaction model were solved to provide various mean quantities in chemically reacting flows. A k–ε turbulence model for the Reynolds stresses provided part of the interaction of turbulence and chemical reaction. The effects of temperature fluctuations on the mean species reaction rate were modeled by an assumed marginal probability density function (PDF) for temperature. The temperature variance that affected the shape of the PDF was determined from the solution of an equation for the enthalpy variance.

Accomplishment Description
Assumed Gaussian and beta PDFs were used to model the effects of temperature fluctuations on chemical reactions in turbulent flows. Results indicated that the effects of temperature fluctuations either increase reaction rates or decrease them depending on the mean temperature, the fluctuation intensity, and the reaction mechanism under consideration. Numerical simulations indicated that in hydrogen–air reactions, temperature fluctuations can have a significant effect on the ignition delay time. These fluctuations directly affect scramjet combustor length and efficiency. Simulations of a hydrogen–air coaxial jet configuration were completed. Typical calculations took 60 megawords of memory and 40 Cray Y-MP hours of computer time.

Significance
Temperature and species fluctuations can influence the performance of a scramjet by affecting chemical reaction rates. The effects of temperature and species fluctuations must be understood and modeled appropriately to optimize scramjet performance.

Future Plans
This work will be extended to include the effects of species fluctuations and determine the effect that they have on scramjet performance.

Publication
Gaffney, R. L., Jr.; White, J. A.; Girimaji, S. S.; and Drummond, J. P.: Modeling Turbulent/Chemistry Interactions Using Assumed PDF Methods. Joint Propulsion Conference, Nashville, Tenn., AIAA Paper 92-3638, 1992.

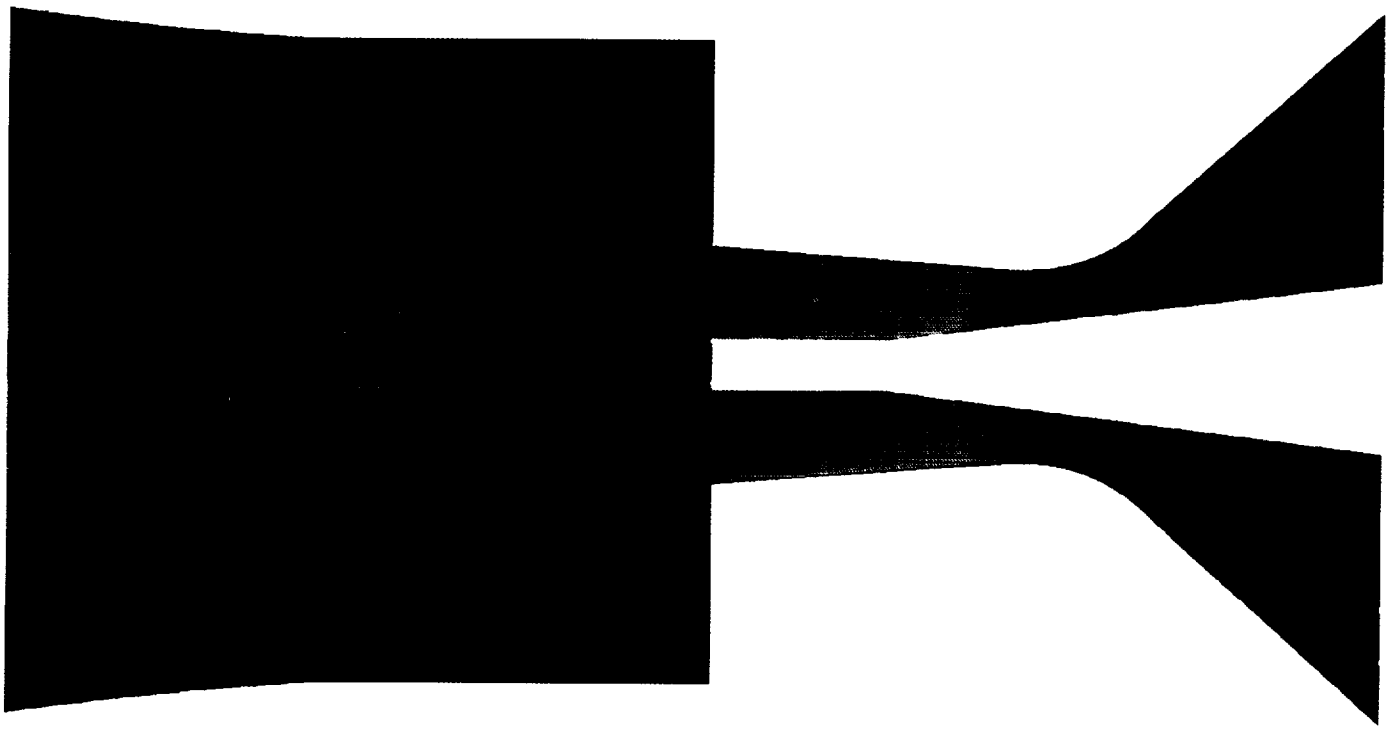

Mach contours inside the outer (vitiated air) nozzle and downstream of the exits of the hydrogen and air nozzles (solution inside the hydrogen nozzle not shown). Dark blue = low Mach number, red = high Mach number.

Unsteady Turbomachinery Computations

Karen L. Gundy-Burlet, Principal Investigator
Co-investigator: Akil Rangwalla
NASA Ames Research Center/MCAT Institute

Research Objective
To investigate unsteady rotor–stator interaction in multistage turbomachines.

Approach
The three-dimensional (3-D) Navier–Stokes codes, STAGE-3 and ROTOR-4, incorporate the most modern, high-order (third-order spatial and second-order time-accurate) upwind-biased schemes for the solution of the thin-layer Navier–Stokes equations. The schemes were set in an iterative implicit framework. The codes used a multizone grid with some zones moving relative to others. Information was transferred between the various zones using temporally- and spatially-accurate zonal boundary conditions.

Accomplishment Description
A fine-grid 3-D calculation of a turbine stage was completed; however, the numerical results indicated that twice as many points would be needed in the radial direction to obtain sufficient accuracy for a turbine-loss calculation. Because of insufficient computational resources, this grid refinement was not carried out. A fine-grid 3-D calculation of a multistage compressor was initiated. Initial results from the code compared well with experimental data for time-averaged surface-pressure distributions, but the unsteady flow field was still developing. The code required 16 megawords of memory and 70 megawords of solid-state device memory for the 1.8-million point grid. A typical converged solution was estimated to require approximately 500 Cray Y-MP hours for a converged time-averaged solution. The figure shows preliminary instantaneous surface pressures within the compressor.

Significance
Unsteady turbomachinery flow fields are extremely complex, especially in the latter stages of multistage turbomachines. Wake–wake and wake–airfoil interactions cause complex time-varying forces on the downstream airfoils. It is important to understand these interactions to design turbomachines that are light, compact, reliable, and efficient.

Future Plans
The 3-D computation of the flow within the multistage compressor is continuing. On completion of the 2.5 stage compressor computation, the results will be compared with experimental data from a 2.5 stage compressor investigated. Future computations will include a 4.5 stage compressor geometry and a multistage/multi-airfoil turbine computation.

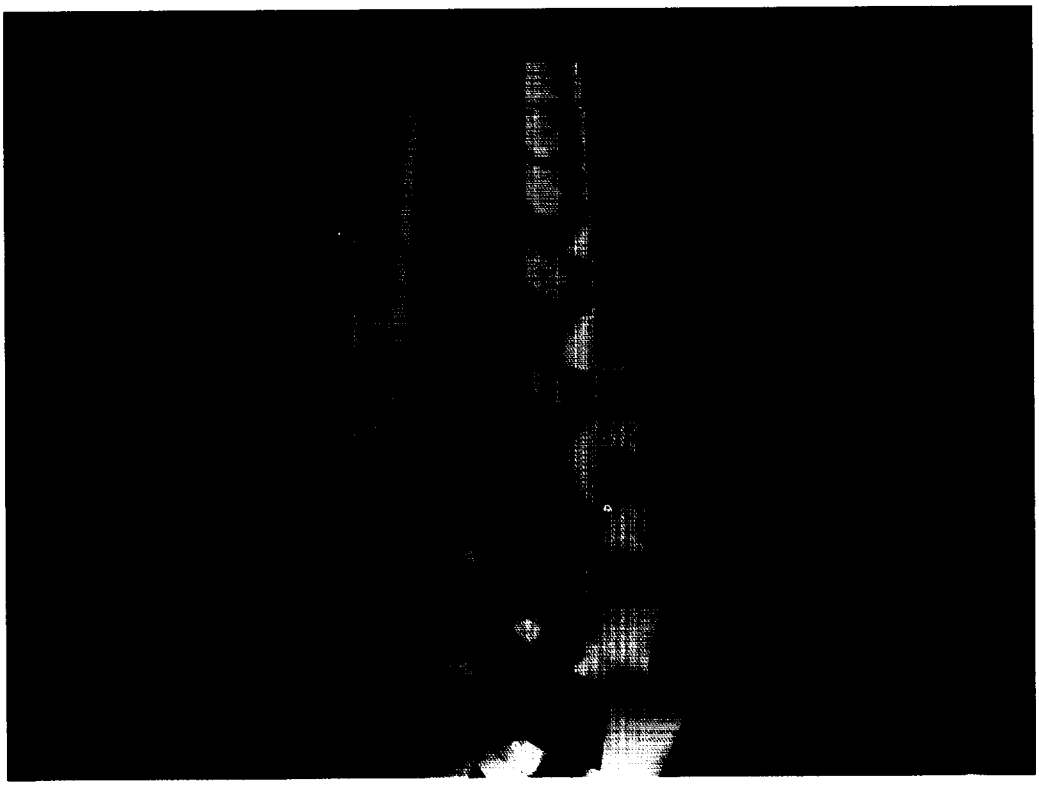

Preliminary instantaneous surface pressures in a 2.5 stage compressor.

Three-Dimensional Transonic Compressor Stage Flows

Chunill Hah, Principal Investigator
Co-investigators: J. Loellbach, S. L. Puterbaugh, and W. W. Copenhaver
NASA Lewis Research Center/ICOMP/WL/FIMM, Wright Patterson AFB

Research Objective
To simulate numerically the unsteady flow field inside a transonic, high-through-flow axial compressor stage, and to compare computed results with available experimental data.

Approach
The three-dimensional, unsteady Navier–Stokes equations are solved on structured grids using second-order accurate implicit time integration, third-order accurate upwind differencing for the inviscid fluxes, and second-order accurate centered differencing for the viscous fluxes. A two-equation turbulence model with a low-Reynolds-number modification is used for turbulence closure.

Accomplishment Description
The numerical method simulated the unsteady flow field inside a transonic, high-through-flow compressor stage consisting of 20 low-aspect-ratio rotor blades and 31 stator blades. For the simulation, a set of two rotor blades and three stator blades were used, along with a time-lagged periodic boundary condition. The flow fields at three typical operating conditions (near choke, near peak efficiency, and near stall) were computed. Approximately 630,000 grid points were used for each calculation. A typical run required approximately 300 hours of single CPU time and 32 megawords of memory on a Cray Y-MP. Time-averaged quantities from the computed results compare well with those of the experimental data. The figure shows the instantaneous static pressure distribution on the blade and hub surfaces for two different time steps at the near-peak-efficiency operating condition. Small differences can be seen between different passages at the same time step and between corresponding passages at different time steps, illustrating both the non-periodicity and the unsteadiness of the computed flow field.

Significance
This work is a direct extension to unsteady flow analysis of an existing steady Navier–Stokes solver that has been tested and applied for a wide range of turbomachinery flows. Unsteady analysis is necessary for accurate flow-field prediction for closely coupled blade rows within a stage or between successive stages.

Future Plans
Efforts are under way to analyze the unsteady effects of various inlet flow distortions and to perform design optimizations.

Publications
1. Hah, C.: Unsteady Aerodynamic Flow Phenomena in a Transonic Compressor Stage. AIAA Paper 93-1868, June 1993.
2. Hah, C.; and Puterbaugh, S. L.: A Critical Evaluation of a Three-Dimensional Navier–Stokes Method as a Tool to Calculate Transonic Flows Inside a Low-Aspect-Ratio Compressor. AGARD Proceedings, 1990.
3. Copenhaver, W. W.; Hah, C.; and Puterbaugh, S. L.: Three-Dimensional Flow Phenomena in a Transonic High-Through-Flow Compressor Stage. ASME J. Turbomachinery, vol. 115, no. 2, 1992.

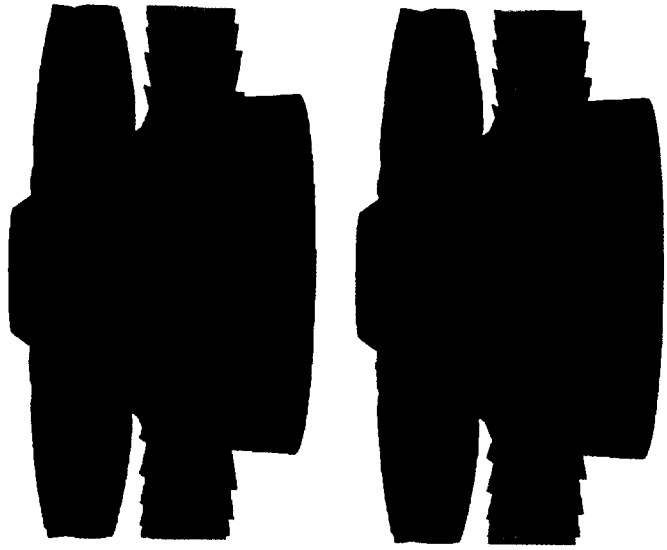

Instantaneous static pressure distributions at two different time steps.

Evaluating High-Angle-of-Attack Inlet Characteristics

Doug G. Howlett, Principal Investigator
Co-investigators: Brett W. Denner and Chris L. Reed
Lockheed Engineering and Sciences Company

Research Objective
To establish a rigorous methodology for evaluating shock–boundary layer interaction using the three-dimensional full Navier–Stokes flow solvers HAWK3D and CDFalcon. This project served as a validation exercise for the newly developed CDFalcon flow solver.

Approach
Flow-field predictions were obtained using CDFalcon and HAWK3D. CDFalcon is a finite-volume flow solver similar to HAWK3D. Validation of these codes focused on their ability to model complicated flow phenomena. A test condition at Mach 0.3 and 30 degrees angle of attack was chosen because it produced a strong normal shock that interacted with a separation bubble downstream of the inlet cowl lip. Since inlet performance and basic airflow are highly dependent upon the ability to model accurately shock–boundary layer interaction and separation, accurate analysis of this condition is a demanding test for any flow solver. Analysis of these solutions consisted of obtaining a converged solution on a grid that was not optimized for separated flow, adapting the grid to local flow gradients, interpolating the existing solution onto the adapted grid, and resolving the flow field.

Accomplishment Description
Predicted flow characteristics showed good agreement between HAWK3D, CDFalcon, and test data. Flow-field phenomena in and around the inlet developed as anticipated. CDFalcon predicted duct surface pressure distributions that showed good agreement with test data. Although HAWK3D analyses are not complete, they show that all primary flow field features have been captured. Duct pressure distributions, pressure recovery, and compressor face distortion were tracked as solutions converged and were very near or approaching tested values.

Significance
High-angle-of-attack maneuver flight conditions produce complex flow fields that are difficult to predict numerically. Recursive grid adaptation can overcome this limitation, but it usually imposes unwieldy increases in computational requirements. Single-step grid adaptation provides a practical way to achieve accurate results for these solvers. The most desirable solution would be an efficient unstructured-grid flow solver with automated grid refinement capability.

Future Plans
The HAWK3D solution of this flow field and the use of similar procedures to analyze advanced boundary layer management concepts for fighter aircraft application will be pursued.

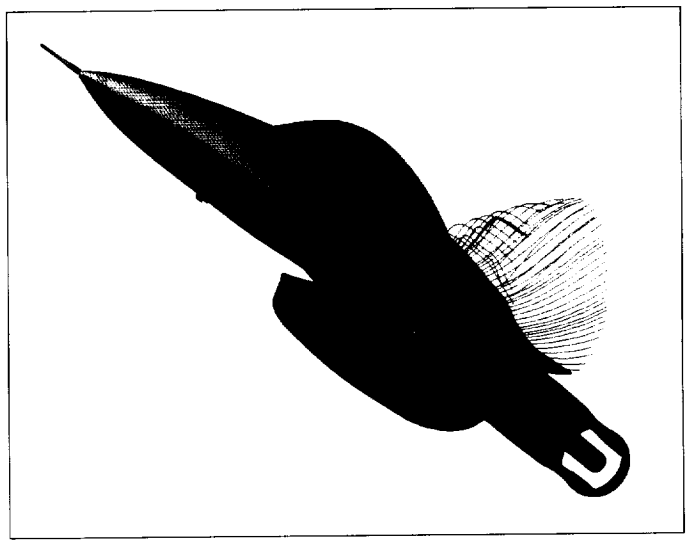

Surface pressure contours and strake vortex particle traces. Blue = low pressure regions and magenta = high pressure regions.

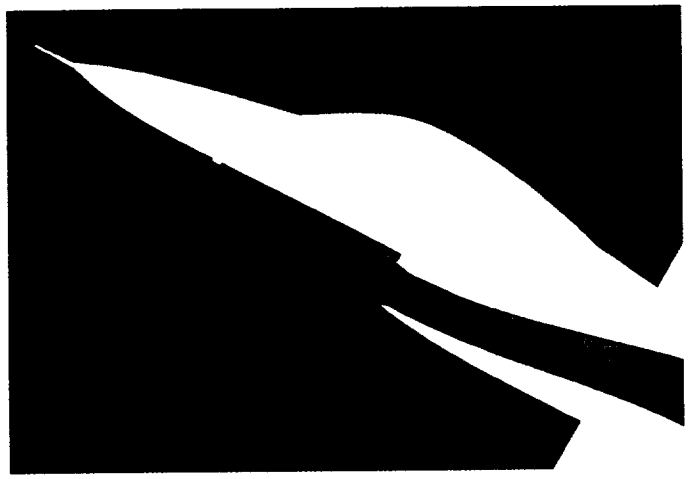

Centerline Mach contours show significant lip separation and a subsequent normal shock. Blue = static regions and magenta = the maximum Mach (approximately 1.5).

Computational Analysis of a Tip-Engine Configuration

J. Mark Janus, Principal Investigator
Co-investigators: Animesh Chatterjee and Chris Cave
Mississippi State University

Research Objective

To perform a computational flow analysis of a design concept centered around induced drag reduction and tip-vortex energy recovery.

Approach

The tested geometry was a semispan model having an unswept, untapered wing with a tip-mounted SR-2 blade design high-speed propeller in a pusher configuration. The flow conditions were set to Mach 0.70 and angles of attack ranging from approximately –2 to 4 degrees. The flow model solved the unsteady three-dimensional Euler equations, discretized as a finite-volume method, utilizing a high resolution approximate Riemann solver for cell interface flux definitions. The numerical scheme was an approximately factored block, lower–upper implicit Newton iterative-refinement method. Multiblock domain decomposition was used to partition the field into an ordered arrangement of blocks. Block–block relative motion was achieved using local grid distortion.

Accomplishment Description

Three configurations were analyzed: (1) a baseline fuselage–wing, (2) a fuselage–wing–nacelle, and (3) a fuselage–wing–nacelle propfan. In order to correlate adequately the relationship between angle of attack and interference effects, several numerical simulations at differing inflow angles were necessary. Data collected from the numerical solutions included aerodynamic force coefficients, propeller performance coefficients, and flow-field maps. Integration of surface pressure to obtain the coefficients was satisfactory for all but the drag calculations. Very good agreement has been obtained with configuration lift comparisons. An excellent correlation with the expected wind tunnel interference effects was found by comparing a free-flight simulation and a simulation including tunnel walls. The processing rate on a Cray Y-MP for each iteration of each time step was approximately 22,000 computational cells per second. A typical steady run took 15 Cray Y-MP hours and required 10 megawords of internal memory and 40 megawords of solid-state storage device memory. Unsteady runs took about 25 Cray Y-MP hours.

Significance

NASA wind tunnel tests have indicated large reductions in induced drag for wings with tip-mounted engines. This study used numerical simulation to investigate innovative methods for significantly reducing the induced drag of wings. Numerical simulations similar to those of the NASA investigation were performed to corroborate their data and to obtain insight into the performance enhancing mechanisms involved. Calculations were performed to complement NASA's results and to help guide future NASA research and system studies that address induced drag reduction technologies and vortex hazard alleviation studies.

Future Plans

Thus far, all solutions obtained have been inviscid; therefore no physical flow separation at the wing tip has been modeled. This separation may have a pronounced effect on the lift-off and trajectory of the tip vortex. Efforts are presently under way to obtain a viscous solution in an attempt to better determine the precise physics of the tip-vortex and its lift-off from the solid surface. Also under way are efforts to quantify better induced drag using a wake integral technique in lieu of surface pressure integration.

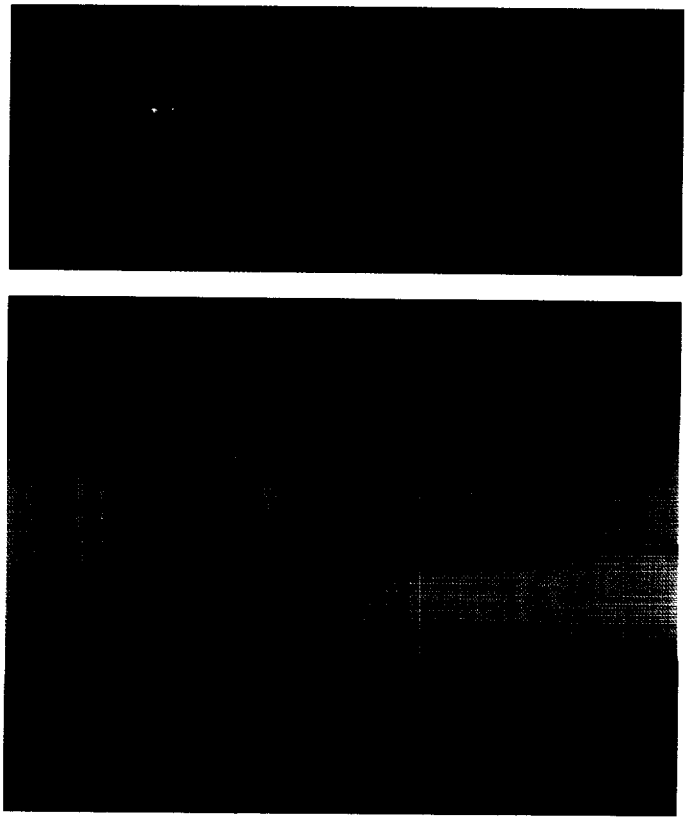

Fuselage–wing–nacelle–propfan shaded surface pressure contours (Mach = 0.7, angle of attack = 4 degrees).

Studies of Mixing and Combustion in Supersonic Flows

Jinho Lee, Principal Investigator
Sverdrup Technology, Inc.

Research Objective
To simulate numerically various three-dimensional (3-D) turbulent/chemically-reacting and nonreacting (mixing) flow fields inside supersonic combustors to investigate possible fuel–air mixing/combustion enhancement techniques to increase thrust. Different aspects of the turbulent and finite-rate chemistry models and their influence on combustor predictions are studied.

Approach
The analysis was performed using a reactive propulsion code based on the lower–upper scheme RPLUS. The effects of hydrogen–air chemical reactions were modeled using a 9-species/14-reaction finite-rate chemistry model. A modified zero-equation Baldwin–Lomax model was used to model the effects of turbulence. The inverse square length scale relationship was used to extend the turbulence model into a 3-D regime, and a simple gradient-diffusion relationship was used to model turbulent mass diffusion. A multiple-block structured-grid approach was used to model complex flow geometries.

Accomplishment Description
Steady mixing enhancement mechanisms used in existing wall mounted fuel injector designs were analyzed. The mixing characteristics of the transverse injector model, the multiple rectangular swept-ramp injector model, and the swept-ramp injector model were studied. A typical swept-injector model geometry, the flow condition, and the three-block grid system are shown in the first figure. This injector/combustor configuration was simulated using a three-block two-species (air–air) turbulent nonreacting model using 220,000 cells, approximately 13 megawords of memory, and 10 Cray Y-MP hours. A typical streamwise cross-section contour of the predicted injected gas mass fraction is compared with experimental data in the second figure.

Significance
The Baldwin–Lomax algebraic turbulence model predicted the near-wall turbulence in the near-equilibrium region of the combustor, but the model formulation was weak in predicting the mixing-layer behavior and the non-equilibrium behavior around the injectors. There was reasonable agreement between the predictions and the experimental data. The swept-injector design had superior mixing behavior over a typical transverse injector design, and enhanced mixing was developed through the streamwise vorticity generated by the swept ramp.

Future Plans
Effects of parameters in the injector exit conditions, injector model, and injector grid distribution on the streamwise vorticity generation will be studied. Mixing behavior modifications caused by physical models and their effectiveness in modeling combustor environments will also be studied.

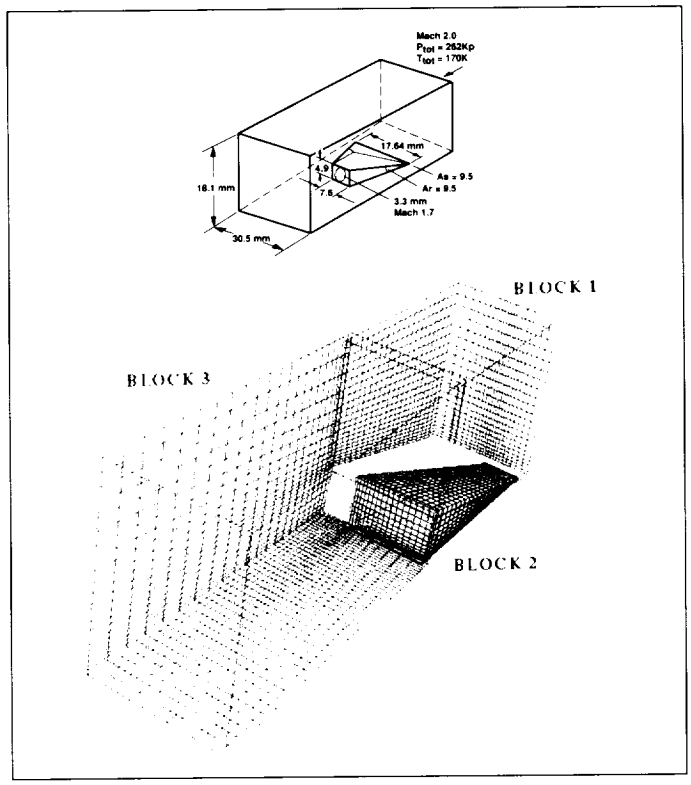

Mach 2.0, 9.5-degree swept-ramp streamwise injector model and a typical three-block grid system.

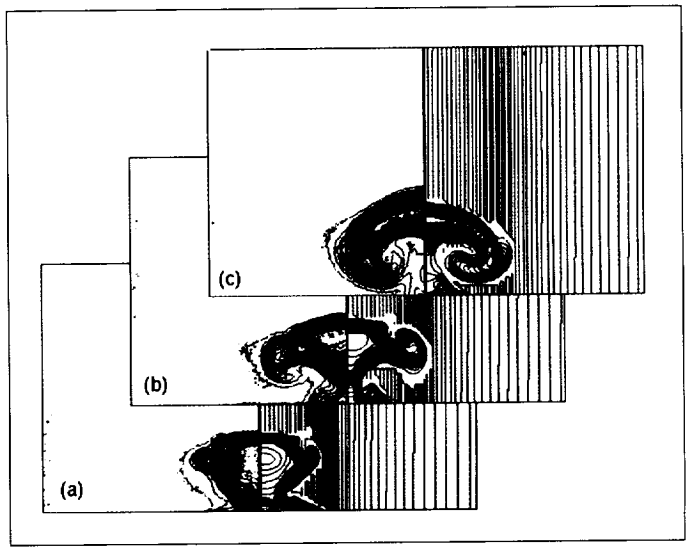

Streamwise injected mass-fraction contour comparisons; experimental data (left) and computed solution (right). Nondimensional streamwise locations: (a) 1.06, (b) 2.13, and (c) 3.19. Mass: black = 0.0 to white = 1.0.

Turbulent Base Heating Computational Fluid Dynamics

E. D. Lynch, Principal Investigator
Co-investigators: R. Lagnado and Y. Hsu
Rockwell International, Rocketdyne Division

Research Objectives
To predict the level of base fuel entrainment and heating to be anticipated under conditions characteristic of National Launch System (NLS)-like vehicles and to examine the physical behavior of turbulence models appropriate to those systems.

Approach
Traditional approaches for predicting base heating have used empirically based correlations to scale existing flight data. However, the configuration and flow conditions for modern launch systems are significantly different than previous configurations in how densely the engines are packed, the type of exhaust gases, and the degree of overexpansion of the nozzle plumes. The unified solution algorithm computational fluid dynamics (CFD) code was used to model the NLS base region flow at 10,000 and 50,000 feet altitude to predict the level of base heating. Full Navier–Stokes, three-dimensional (3-D), 200,000-grid-point analyses were made of the geometry, including all 6 nozzles and their external contours. The effects of the physical models were found through parametric axisymmetric analyses with various turbulence and kinetics models.

Accomplishment Description
The results of the computations showed little fuel entrainment into the base region and inconsequential base heating at either altitude. At 10,000 feet the nozzle plume was overexpanded and an oblique shock formed downstream in the nozzle plume. The vehicle airstream was responsible for driving a 3-D recirculation region in the base; however, no fuel was driven into the base. At 50,000 feet the plumes were underexpanded and interacted in the line between the plumes, but the level of base entrainment was insufficient to raise the base temperature above acceptable limits. These 3-D base-heating analyses required an average of 50 Cray Y-MP hours and 20 megawords of memory.

Significance
Use of fuel-rich turbine exhaust gases and film cooling to cool the nozzle walls in NLS-like launch systems could result in hot gases recirculating and burning in the vehicle base region and could lead to an unacceptable level of base heating. These CFD analyses indicated that base heating was not a significant issue and prevented a costly redesign of the NLS.

Future Plans
Future analyses will employ turbulence models more appropriate to defining the flow field in combusting flows such as vehicle base regions.

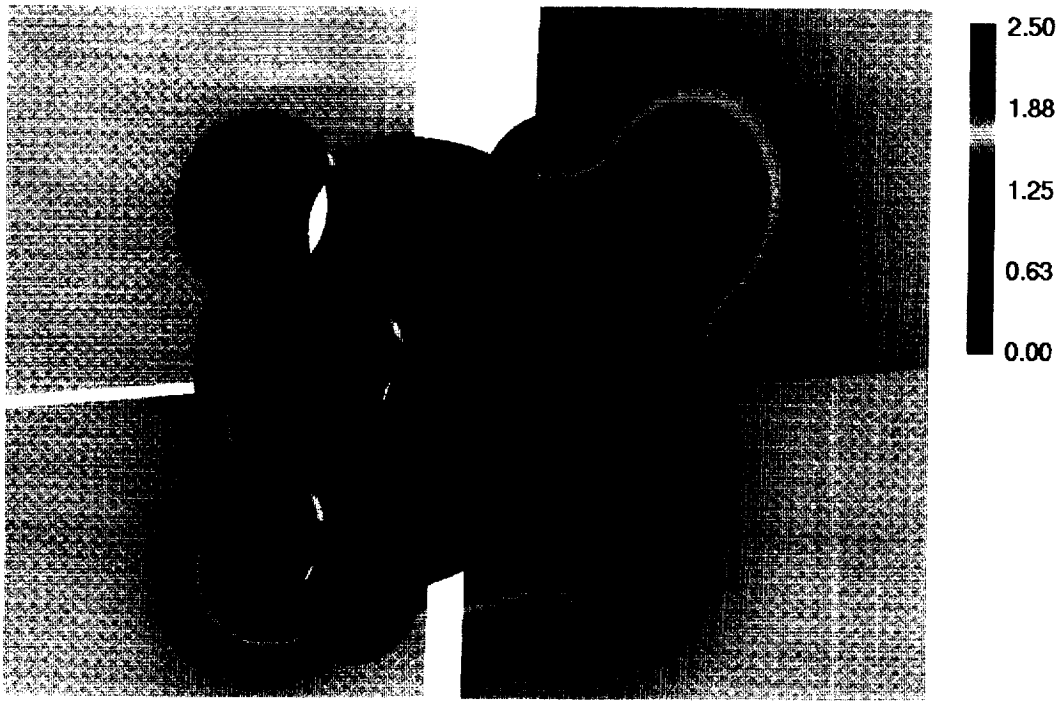

Mach number contours at 50,000 feet altitude in planes proceeding outward from vehicle base.

Unsteady Multistage Turbomachinery Applications

Nateri K. Madavan, Principal Investigator
Co-investigator: Sanjay Mathur
MCAT Institute/NASA Ames Research Center/Iowa State University

Research Objective
To evaluate the capabilities of the CM-2/CM-5 in predicting unsteady flows in multistage turbomachines.

Approach
In recent years, the ROTOR and STAGE families of codes have been developed at NASA Ames Research Center for the prediction of unsteady flows in turbomachines. These codes solve the thin-layer Navier–Stokes equations in a time-accurate manner using state-of-the-art upwind algorithms and zonal methodologies. Implementation of these codes has been limited to vector machines. The thrust of the present research is toward implementation of these codes on the CM-2/CM-5 and toward algorithm modifications to exploit the CM-2/CM-5 architecture to improve run-time performance and decrease overall computing times. Although three-dimensional capability remains the eventual goal, the focus here is on the two-dimensional STAGE2 code.

Accomplishment Description
Migration of the STAGE2 code to the CM-2/CM-5 was completed and the flow in a 3.5 stage experimental compressor was computed. Code migration included selecting optimal data structures and bookkeeping strategies, revisions to the algorithm that were necessitated by the CM-2/CM-5 hardware, and thorough checking of the interim results with the Cray version. The current implementation on the CM-2 incorporates the communication compiler for improved zonal boundary information transfer and the new slicewise compiler. The communication compiler has not been incorporated in the CM-5 implementation. Several routines in the STAGE2 codes result in extremely poor performance on the CM-2 when coded entirely in CM FORTRAN. Significant performance improvements were achieved by replacing the FORTRAN code with calls to the CM FORTRAN utility library.

Significance
A time-accurate, implicit algorithm for the Navier–Stokes equations in two dimensions was successfully implemented on the CM-2/CM-5. The algorithm used multiple overlapped and patched zones and high-order upwind techniques. Modifications to the original algorithm resulted in more optimal performance on the CM-2/CM-5.

Future Plans
Future plans include algorithm developments for improved performance and extensions to three dimensions.

Publication
Madavan, N. K.: Unsteady Turbomachinery Flow Simulations on Massively Parallel Architectures. Computing Systems in Engineering, vol. 3, nos. 1–4, 1992, pp. 241–249.

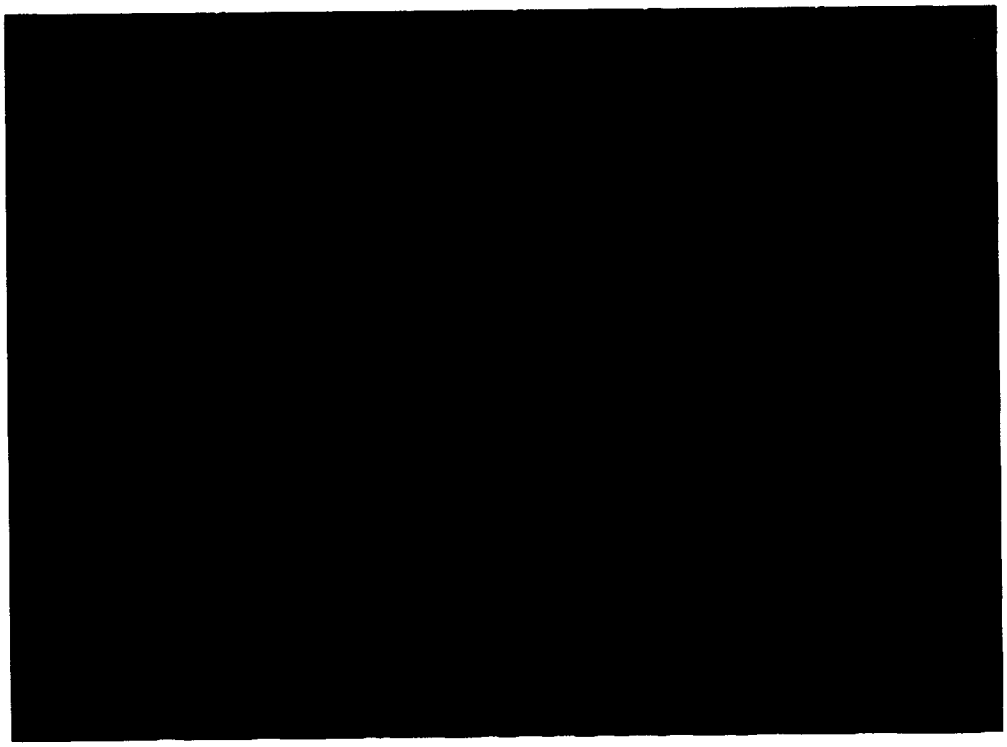

Entropy contours in a 3.5 stage axial compressor. Results from a two-dimensional multistage calculation.

Base Pressurization Methods for Scramjet Combustors

Charles R. McClinton, Principal Investigator
Co-investigator: Paul Vitt
NASA Langley Research Center/Analytical Services and Materials, Inc.

Research Objective
To use computational fluid dynamics (CFD) modeling to evaluate parametrically seven different methods of decreasing pressure drag on step expansions in supersonic combustor flows at Mach 16. Main fuel injection combustion effects and step height variation were also evaluated.

Approach
The General Aerodynamic Simulation Program was used in the steady-state elliptic, full-Navier–Stokes mode for all the computations in this study. Most of the cases were modeled as two-dimensional flow fields, but calculations were also made for two three-dimensional flow fields, to evaluate the effect of relieving around a single jet. All the cases involved turbulent inflow and finite-rate hydrogen–air chemistry. Comparisons were made with empirical and analytical closed-form models to anchor the results with an established experimental data base.

Accomplishment Description
The numerical simulations of the base pressurization designs focused on providing flow visualization, which was used to enhance the understanding of the flow physics that occurred in the near-base region. The designs used supersonic slot or circular orifice fuel injection, axial transpiration (bleed) from the face of the step, vertical transpiration along the wall downstream of the step, and a combination of supersonic slot from the step lip and axial bleed beneath. The effects of fuel flow rate, mainstream combustion, and variation in step height to combustor height ratio were also evaluated. The numerical results predicted the expected flow features and gave insight into the physics that determine the base pressure. The figure compares flow fields that result for no base injection, showing the large low-pressure recirculation region, to the flow fields for axial base bleed with two mass flow rates (right), and to the mixed supersonic/subsonic base injection case (lower left). Each solution required 10 megawords of memory and between 6 (supersonic injection) and 20 (subsonic injection) Cray Y-MP hours.

Significance
This study provides guidance for future design of base pressurization systems and indicates how the injection will affect the local flow fields. Also demonstrated are some of the possible limitations of pressurizing the base and the value of CFD solutions as a tool for understanding the interaction of complex flow physics.

Future Plans
The study will be enlarged to include evaluation of scramjet combustor injection methods at high flight Mach numbers.

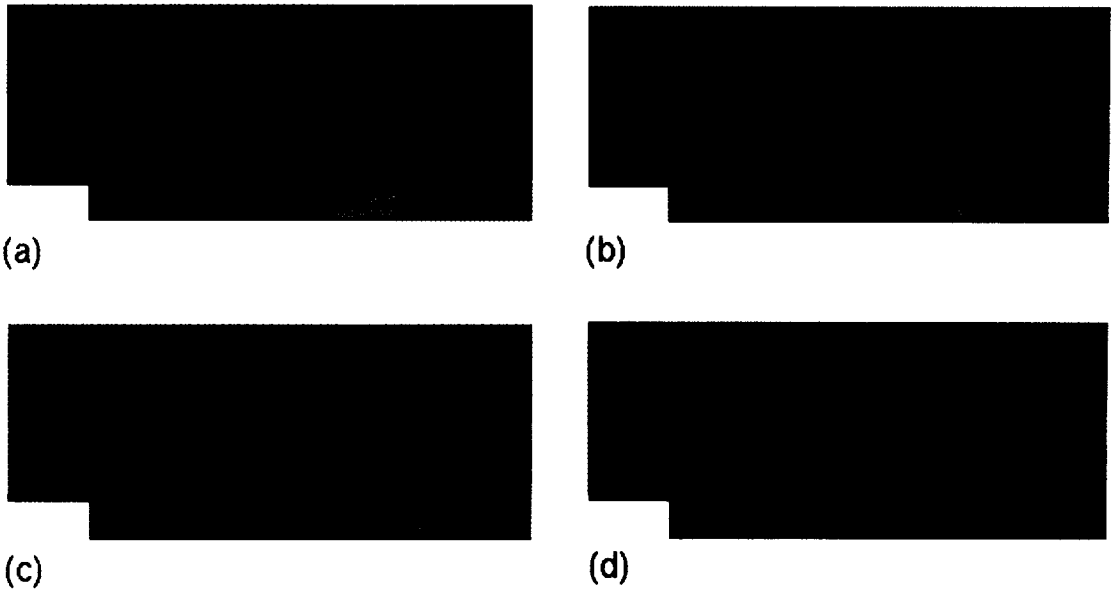

(a) Streamlines over pressure contours for flow over a two-dimensional backward-facing step in a scramjet combustor with a flight Mach number of 16; blue = low pressure and red = high pressure. (b) Effect of bleeding hydrogen fuel from the base at a fuel equivalence ratio of 0.036. (c) Base bleed rate of 0.068. (d) Pressure and streamlines for a case with a Mach 2 supersonic fuel slot at the step lip and base bleed below it at a fuel equivalence ratio of 0.05.

Simulation of Scramjet Combustor Flow Field

Charles R. McClinton, Principal Investigator
Co-investigator: S. Srinivasan
NASA Langley Research Center

Research Objective
To simulate scramjet combustor flow fields using the General Aerodynamic Simulation Program (GASP) flow solver and to assess the combustor performance.

Approach
GASP, a state-of-the-art computational fluid dynamics (CFD) code, was used to simulate high-speed scramjet combustor flow fields for comparison with the experimental Planar Laser-Induced Iodine Fluorescence Images (PLIIF) and with the results obtained using the SPARK flow solver. The evaluation effort was methodically completed by choosing several test cases to encompass both the high- and low-enthalpy flow regimes. The result for the low-enthalpy case is shown here.

Accomplishment Description
A simulation of normal injection of air at sonic conditions (staged at the University of Virginia) into a Mach 2 low-enthalpy airstream was performed. The mixing simulation took approximately 10 Cray Y-MP hours and about 6 million words of central memory. Good agreement with the experimental PLIIF images was obtained for both the low- and high-enthalpy cases. The figure compares the CFD and PLIIF of the injected air mole fraction contours along the plane of symmetry.

Significance
The GASP flow solver was successfully applied to simulate high-speed combustor flow fields. The results obtained from the simulation were compared with the experimental data, and they yield confidence in the use of GASP for routine scramjet flow-field simulations.

Future Plans
The GASP flow solver will be used to simulate several high-enthalpy scramjet combustor flow fields. Detailed comparisons of the CFD results with Mie scattering images obtained experimentally will be performed.

Publication
Srinivasan, S.; Bittner, R. D.; and Bobskill, G. J.: Summary of the GASP Code Application and Evaluation Effort for Scramjet Combustor Flowfields. AIAA Paper 93-1973, June 1993.

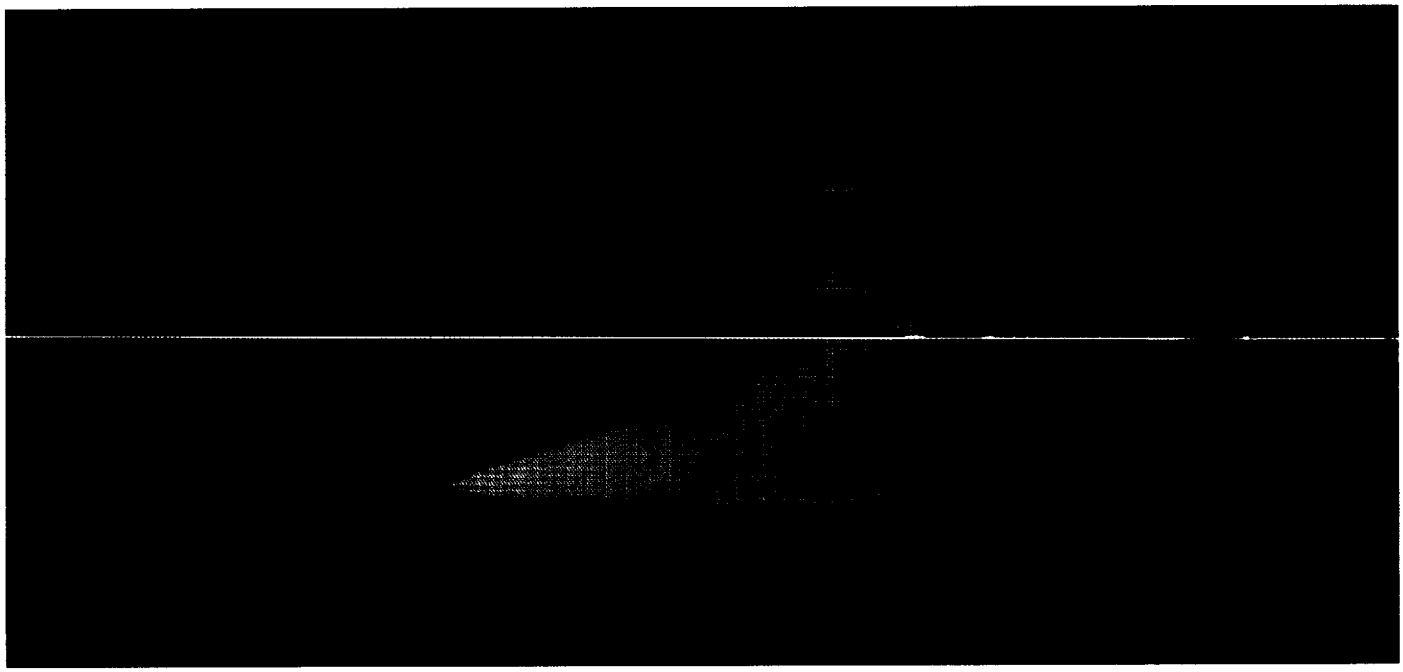

Comparison of CFD (top) and PLIIF (bottom) injectant mole fraction contours along the centerline in the streamwise direction.

Parallel Simulation of Unsteady Combustion

Suresh Menon, Principal Investigator
Co-investigator: Sisira Weeratunga
Georgia Institute of Technology/NASA Ames Research Center

Research Objective
To utilize the parallel code to simulate combustion instability in ramjet engines and then to implement a dynamically adjusting active secondary fuel-injection controller. The benefits and problems associated with the use of highly parallel distributed processing machines for unsteady simulations of combustion will be determined.

Approach
A large-eddy simulation (LES) model for unsteady compressible reacting flows was implemented on the Intel iPSC/860. The explicit finite-volume numerical scheme solved the axisymmetric form of the Navier–Stokes equations and a thin-flame model for premixed combustion. A one-equation model for the subgrid turbulent kinetic energy was used to model the unresolved subgrid momentum and heat fluxes.

Accomplishment Description
It is possible to realize a highly scalable, distributed memory, data parallel implementation for a class of explicit time integration schemes used in unsteady combustion simulations. A geometry-tailored, two-level data partitioning strategy was adopted to deal with the L-shaped computational space and has resulted in a very efficient implementation, in spite of the added complexity. The implementation is general enough to be portable to any multiple-instruction/multiple-data parallel computer that supports processor-to-processor communication primitives. Parallel computers such as the Intel iPSC/860 appear to provide a scalable, yet reasonably low-cost, alternative to traditional vector supercomputers for simulations of unsteady flow phenomena, except in the critical area of external input/output performance. For combustion simulation with a one-equation subgrid model, 64 nodes of the iPSC/860 achieved performance much better than a single-processor Cray Y-MP, and, with 128 nodes, the performance exceeded a single processor Cray C-90. A simulation with a 640 × 120 grid using 64 nodes required about 40 central processing unit hours to obtain enough data for statistical analysis.

Significance
The parallel simulation model allows the exploration of unsteady combustion in a parameter space that was uneconomical and difficult to accomplish with the available resources on the Cray computers. A new approach to simulate combustion in the subgrid was developed and is uniquely suited for parallel computations. Coupling the subgrid combustion model with the parallel LES model will result in a new simulation capability.

Future Plans
Simulations of unsteady combustion with the subgrid combustion model will be carried out. A secondary fuel-injection controller based on a theoretical model will be coupled in parallel to the simulation model so that the controller will learn while the simulation is going on and inject an optimized secondary fuel stream to suppress the combustion instability.

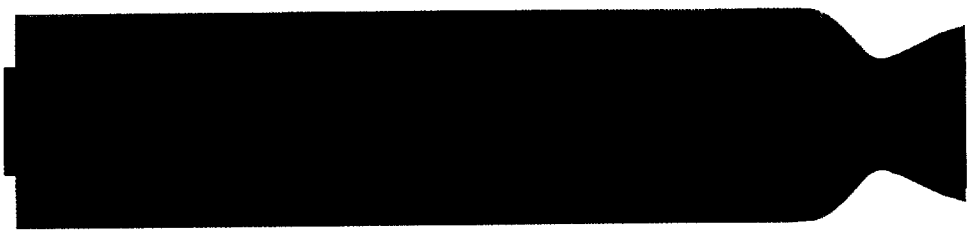

Flame propagation in an axisymmetric ramjet: yellow = product, red = flame, cyan = fuel.

Vortex motion in an axisymmetric ramjet.

Unsteady Combustion in a Ramjet

Suresh Menon, Principal Investigator
Co-investigator: Thomas M. Smith
Georgia Institute of Technology

Research Objective
To simulate and investigate unsteady combustion and combustion instability in a three-dimensional (3-D) ramjet engine and to characterize the effects of the 3-D flow field on the premixed flame structure.

Approach
An explicit, finite-volume scheme was used to solve the 3-D unsteady, compressible Navier–Stokes equations using a large-eddy simulation (LES) technique. A compressible eddy viscosity was used to model the unresolved momentum and heat subgrid fluxes. Premixed combustion was simulated using a thin-flame model in which the turbulent flame speed explicitly appears as a function of the laminar flame speed and the subgrid turbulent kinetic energy.

Accomplishment Description
Unsteady combustion in a 3-D ramjet engine was simulated for conditions that were studied earlier using axisymmetric and two-dimenional (2-D) ramjet configurations. For stable, unsteady combustion (characterized by low-amplitude, low-frequency pressure oscillations), the vortex motion in the shear layer was quite different in 3-D flows when compared to 2-D flows. In 3-D flows, conversion of the fuel into product was more efficient due to 3-D mixing, and the vortices in the shear layer were smaller and more concentrated due to vortex stretching effects. In spite of these flow-dominated differences, the analysis of the flame structure in 3-D flows showed that the flame sheet tended to be predominately 2-D (cylindrically shaped). This result agreed with data obtained by direct numerical simulation of flame propagation in temporal mixing layers and homogeneous isotropic turbulence, which showed that the flame sheet was highly 2-D with the vorticity vector aligning with the intermediate strain direction while the flame sheet was normally aligned with the most compressive strain direction. A simulation with a grid resolution of 192 × 64 × 16 cells needed approximately 22 megawords of memory and required about 75 hours on the Cray C-90 to obtain enough data for statistical analysis.

Significance
Statistical results suggest that the flame structure in complex 3-D flows has a preferred tendency to become a 2-D cylindrical shape. This tendency suggests that a 2-D simulation model, corrected for the out-of-plane vortex stretching effect, may be able to predict the statistical properties of premixed flame as in a 3-D flow. This ability would result in a major reduction in computational resource requirements and perhaps make LES of premixed flames a practical engineering tool.

Future Plans
The 3-D LES data base will be used to develop a new approach to carry out 2-D LES of premixed flames that include the effects of out-of-plane vortex stretching. Active control of combustion instability in the 3-D ramjet will also be investigated using a secondary fuel injection controller that was investigated earlier in axisymmetric flows.

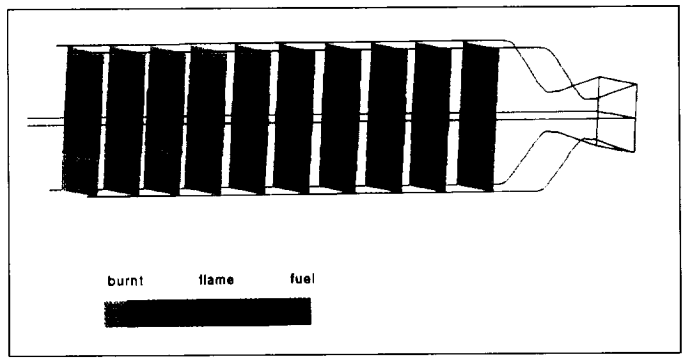

Flame propagation in the combustion chamber of a ramjet at various streamwise locations; yellow = product, red = flame, and cyan = premixed fuel.

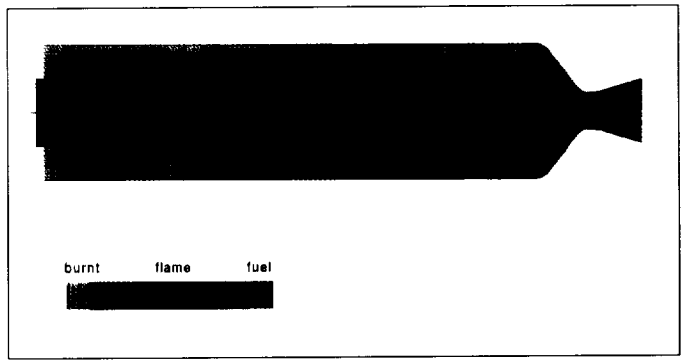

Middle spanwise plane showing the flame structure and the vortex motion (shown as contour lines) in the combustor.

Three-Dimensional Parallel Mixing Computations

John C. Otto, Principal Investigator
NASA Langley Research Center

Research Objective

To develop a parallel version of the three-dimensional chemically reacting, computational fluid dynamics, Navier–Stokes code, SPARK, and to use the parallel code to examine a nonreacting, fuel-mixing problem.

Approach

SPARK was moved from the sequential supercomputing environment of the Cray, where it runs on a single processor, to the distributed memory environment of the Intel iPSC/860 hypercube. The parallel efficiency of the code was measured when the problem size was scaled with the number of processors and when the problem size was constant. Performance was also compared to the sequential performance on a single processor of the Cray Y-MP. SPARK was used to examine a mixing enhancement strategy for scramjet engine applications. This mixing involved adding a swirling component to the supersonic fuel jet prior to injecting it at an angle of 30 degrees into a Mach 2.0 flow in a rectangular duct. An algebraic eddy-viscosity turbulence model was added to the code to model the turbulence in the region where the fuel–air mixing occurs. Mixing efficiency was computed as a function of axial distance to determine if the swirl enhanced the fuel–air mixing. The hydrogen fuel envisioned for use in scramjet engines was modeled by helium in the experiment.

Accomplishment Description

The parallel efficiency of SPARK asymptotes to a value of about 67 percent when a power-law viscosity model is used and the global problem size scales with the number of processors. When Wilke's mixture viscosity is used, the computational requirement is significantly higher and the parallel efficiency is asymptotic to about 76 percent. The performance of the code has been compared to that of a single processor of the Cray Y-MP. When the power-law viscosity model is used, the parallel code operates at 95.3 MFLOPS on 32 processors and at 161.5 MFLOPS on 64 processors. On a single processor of the Cray Y-MP, the problem that was run on 32 processors of the hypercube ran at a rate of 146.5 MFLOPS. The parallel code was used to study a fuel mixing problem. Two swirl levels and a nonswirling case have been examined. The mixing efficiency has been observed to increase as the swirl level increases. For the swirling cases, the mixing efficiency was significantly higher than for the nonswirling case. Initial comparisons between the numerical solutions and flow visualization data taken in the experiment show the development of similar flow structures. All comparisons to this point have been qualitative.

Significance

The code efficiency has been shown to be fairly good and the parallel code offers another resource for solving very large problems. Swirl enhances the mixing levels of the fuel. Qualitative comparisons to experimental data show the development of similar structures, but are insufficient to validate the numerical solutions.

Future Plans

Work is under way to port the SPARK code to other parallel computers, including the CM-5 and the Kendall square research KSR1. The code will also run on the Intel Paragon machines to solve very large problems that cannot be readily solved on conventional supercomputers.

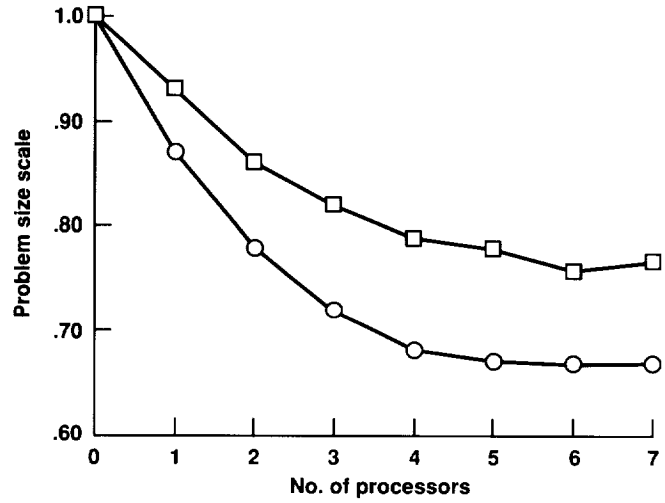

Parallel efficiency versus the hypercube order when the problem size scales with the number of processors; squares = mixture viscosity, circles = power-law viscosity.

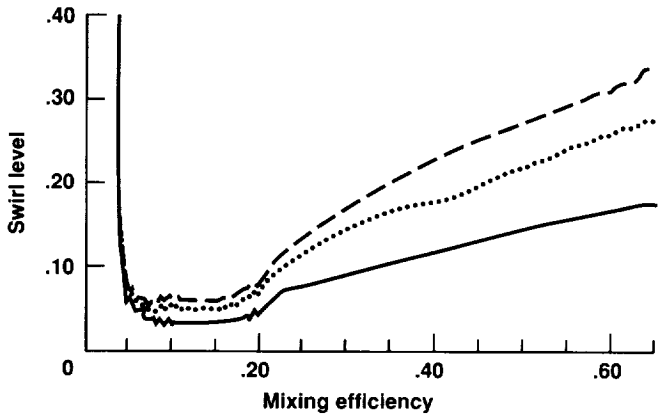

Mixing efficiency versus axial distance from the duct inlet; solid = no swirl, dotted = low swirl, dashed = high swirl.

Launch Vehicle Base Flow Simulations

Thanh T. Phan, Principal Investigator
Co-investigator: Timothy J. Ventimiglia
General Dynamics, Space Systems Division

Research Objective
To develop an accurate and economical technology capable of numerically simulating the complete flow field around a multibody launch vehicle interacting with its multi-engine plumes.

Approach
The three-dimensional Reynolds-averaged Navier–Stokes flow solver, FALCON, was used to simulate the flow field over an entire launch vehicle. The code employed a finite-volume, cell-centered, upwind-differencing scheme that includes a k–kl turbulence model. The GRIDGEN codes were used to create the initial multiblock structure grid. As the solution evolved, the adaptive version of the EAGLE code was used to adapt the grid to the flow gradients.

Accomplishment Description
Perfect gas simulations were extended to include the effects of the forebody for the Atlas II launch vehicle at several altitudes. The results showed that the forebody significantly alters the flow in the base region and therefore must be included to obtain a realistic base flow solution. Flow gradient grid adaptation was proved to greatly enhance the quality of the solutions, especially at higher altitudes where the plumes expand to greater size and create stronger interactions. A typical simulation required approximately 46 megawords of memory and 90 Cray Y-MP hours.

Significance
Currently, the environment in the base region of a launch vehicle is predicted with very large uncertainties. These uncertainties lead to designs of thermal protection systems that include many overconservatisms. This research will provide valuable understanding and information which can help in the design of optimal protection systems that can be used with higher confidence.

Future Plans
Perfect-gas simulations for the Atlas II configuration, which include four solid-rocket boosters, are planned. Real-gas effects will also be modeled to capture plume interactions more accurately.

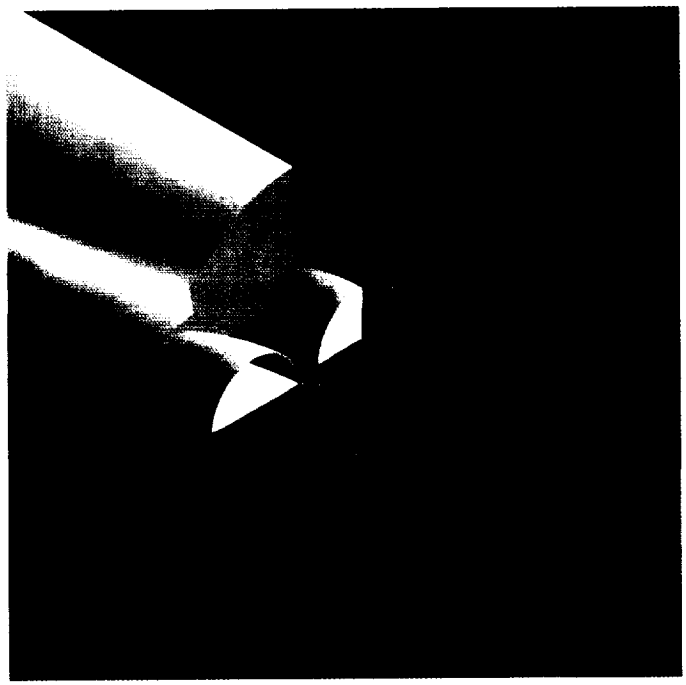

Mach number contours in the base region at 54,000 feet; free-stream Mach number = 2.1.

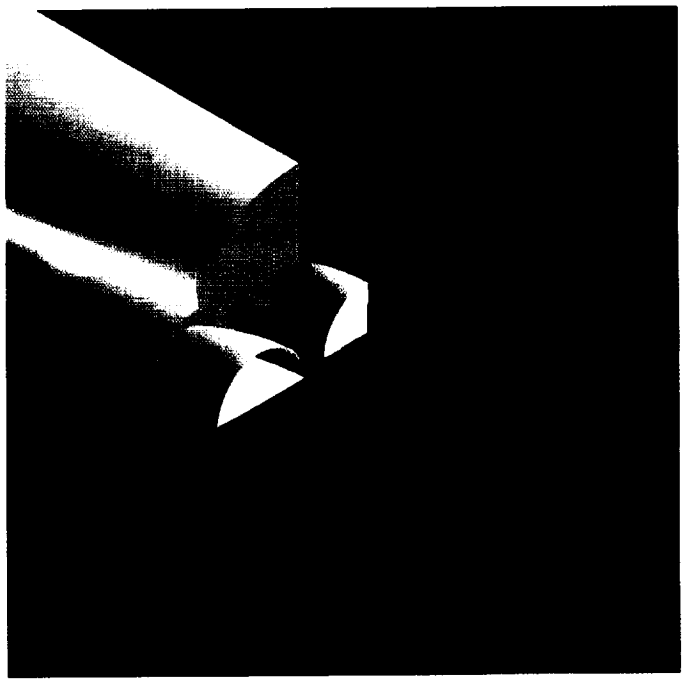

Temperature contours in the base region at 54,000 feet; free-stream Mach number = 2.1.

Flow in Turbine-Blade Coolant Passages

Tom I-P. Shih, Principal Investigator
Co-investigators: Mark A. Stephens and Kestutis C. Civinskas
Carnegie Mellon University/NASA Lewis Research Center

Research Objective
To develop and evaluate advanced computational tools to study three-dimensional (3-D) flow and heat transfer inside coolant passages of turbine blades.

Approach
When 3-D flow fields inside geometrically complex turbine-blade coolant passages are computed, the hours involved in the grid generation process account for most of the time required to obtain a solution. To reduce grid generation time, overlapping structured (Chimera) grids were employed with solutions to the compressible Navier–Stokes equations obtained by the OVERFLOW and PEGSUS codes.

Accomplishment Description
The OVERFLOW code was adapted to be used to compute flow fields in coolant passages of turbine blades that have steady-state solutions with respect to a rotating frame of reference. The Chimera grid approach was ideally suited for the design and analysis of coolant passages because the grid generation process was reduced from about one month for a continuous multiblock grid to a few days for a Chimera grid. Also, parametric studies to optimize locations for pin fin and divider wall were performed without generating new grids because grids about pin fins and divider walls can be easily moved. Finally, because each overlapping grid was structured, very efficient relaxation schemes were available to generate solutions. A typical 3-D computation for the coolant passage required about 30 megawords of memory and 3–5 Cray Y-MP hours.

Significance
Currently, coolant passages are designed by using either quasi-one-dimensional analyses or multidimensional analyses with simplified geometries. This study produced a code that allows the correct geometry to be analyzed in a timely and cost-effective manner.

Future Plans
Accuracy of predictions will be improved by using turbulence models that account for rotation and streamline curvature. The physics of flow and heat transfer inside coolant passages will be studied.

Publications
1. Steinthorsson, E.; Shih, T. I-P.; and Roelke, R. J.: Enhancing Control of Grid Distribution in Algebraic Grid Generation. Int. J. Numer. Methods Fluids, vol. 15, 1992, pp. 862–868.
2. Stephens, M. A.; Rimlinger, M. J.; Shih, T. I-P.; and Civinskas, K. C.: Chimera Grids in the Simulation of Three-Dimensional Flowfields in Turbine-Blade-Coolant Passages. AIAA Paper 93-2559, June 1993.

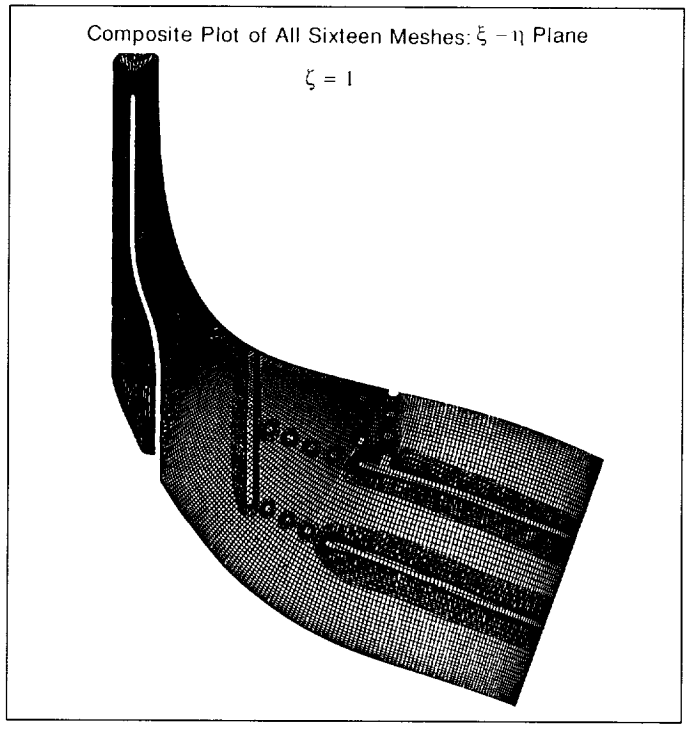

Two-dimensional view of a Chimera grid along the midplane of a coolant passage.

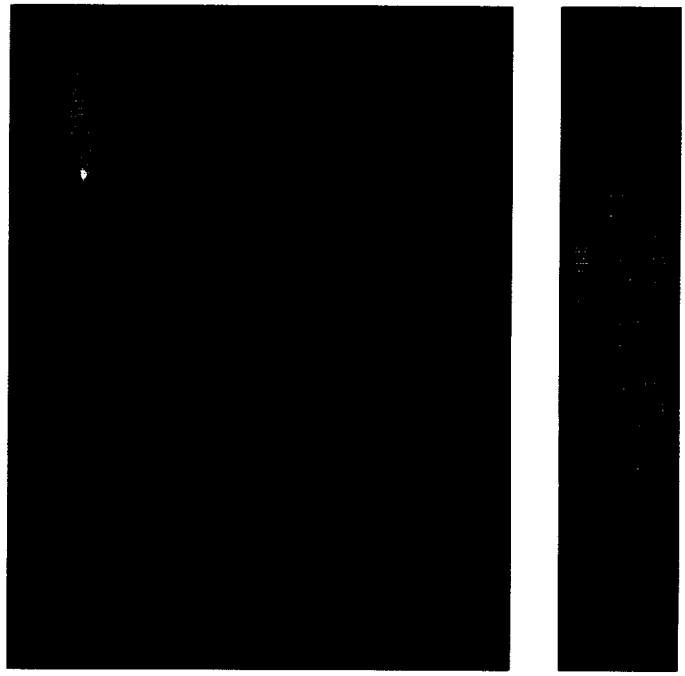

Mach number contours along the midplane of a coolant passage.

Jets-In-Crossflow Mixing

Clifford E. Smith, Principal Investigator
Co-investigators: Daniel B. Bain and James D. Holdeman
CFD Research Corporation/NASA Lewis Research Center

Research Objective
The objectives of this work were to identify improved mixing schemes for rich-burn/quick-mix/lean-burn combustors applicable to advanced aircraft engines and to assess the effects of design parameters on mixing effectiveness. Efforts were focused on jet mixing in rectangular cross-sectional geometries.

Approach
Numerical parametric studies were performed on different orifice configurations. The computational analyses were performed using a three-dimensional Navier–Stokes flow solver (CFD-ACE) capable of analyzing turbulent reacting flows in complex geometries. The numerical results were examined using an interactive visualization package (CFD-VIEW).

Accomplishment Description
Over 60 orifice configurations were analyzed and assessed. The modeled geometry consisted of a rectangular duct with a row of jets on the top and bottom walls. Isothermal flow conditions were assumed. Systematic, parametric analyses were performed, consisting of variations in (1) orifice lateral alignment (in-line and staggered), (2) jet-to-mainstream (J) momentum flux ratio (16, 36, 64), (3) orifice aspect ratio (4:1, 2:1, 1:1, circle), (4) jet-to-mainstream mass flow (MR) ratio (2.0, 0.50, 0.25), and (5) orifice spacing-to-duct height (S/H) ratio ($0.125 \leq S/H \leq 1.5$). The numerical calculations were performed with grids varying in size from 50,000–150,000 cells that required approximately 2–4 Cray Y-MP hours and 10–15 megawords of memory.

Significance
At optimum S/H, in-line lateral arrangements produced faster initial mixing than non-impinging, staggered arrangements due to their smaller geometric orifice size. Previous publications show that $S/H(\sqrt{J})$ is a practical design parameter for mixing optimization even at high MR, and increasing J improves initial mixing at optimum S/H.

Future Plans
The effect of mass flow ratio and aspect ratio on mixing effectiveness will be assessed, and emission characteristics will be inferred from existing cold-flow data.

Publication
Bain, D. B.; Smith, C. E.; and Holdeman, J. D.: CFD Mixing Analysis of Axially Opposed Rows of Jets Injected Into Confined Crossflow. AIAA Paper 93-2044, June 1993.

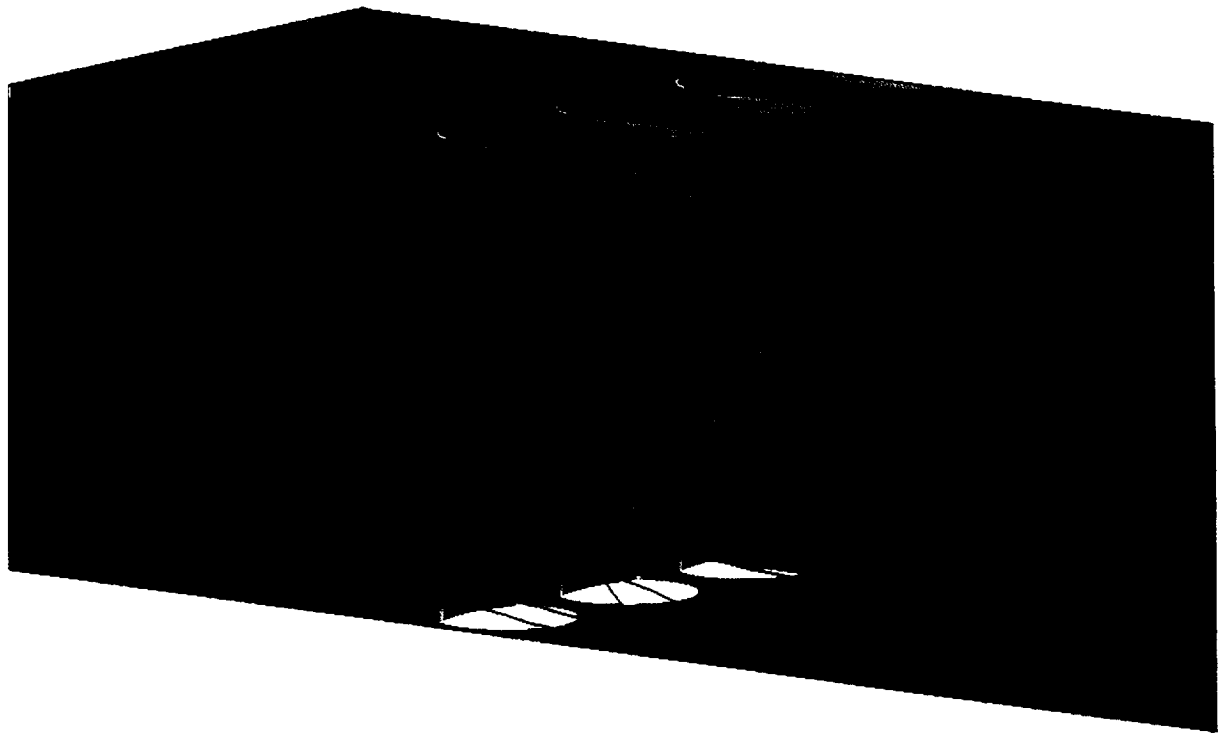

Typical jet mixing numerical results. In-line circular orifices: S/H = 0.375, J = 36, MR = 2.0. Jet mass fraction: red = 0.0 to blue = 1.0.

Flow Phenomena in Turbomachinery

C. S. Tan, Principal Investigator
Co-investigators: S. Arif Khalid and Ted Valkov
Massachusetts Institute of Technology

Research Objective

To investigate the role of compressor endwall flow in setting the pressure rise capability in axial compressors, and to characterize the unsteady flow phenomena involved in blade row interaction in turbomachinery.

Approach

For compressor endwall flow, three-dimensional Reynolds-averaged Navier–Stokes simulations of isolated compressor blade passages were done using the VSTAGE finite-volume compressible flow solver. Techniques were developed to quantify the effect of clearance and loading on the endwall flow field. For unsteady flow, direct Navier–Stokes simulations were done for passage flows with and without upstream wakes at Reynolds numbers 5,000–50,000. An algebraic turbulence model was incorporated in the solver and the simulations were repeated for Reynolds numbers of about 1,000,000. Results were compared to those from the direct calculations to take into account the uncertainty inherent to turbulence models.

Accomplishment Description

The compressor endwall flow computations were used to develop an extension of the boundary layer displacement thickness concept to quantify blockage in axial compressors. The loss in the shear between the leakage and passage flow is the source of blockage associated with the leakage vortex core. Increasing the clearance substantially affects the sensitivity of the endwall flow field to increases in passage pressure rise. Typical computations used 8 megawords of memory and 6 Cray Y-MP hours. The unsteady flow over the suction surface of the stator blade was dominated by a moving row of vortical disturbances produced at the leading edge upon interception of the wake. The strength of the disturbances over the suction surface was reduced by tailoring the pressure gradient over the foremost part of the blade, and could be virtually eliminated by removing boundary-layer fluid from the foremost part of the suction surface. Typical direct simulation computations required 64 megawords of memory and 4 Cray Y-MP hours.

Significance

Flow in the endwall regions is known to have a critical influence on axial compressor performance, and this study established causal links between clearance and stall onset. Turbomachinery design may be improved if the effects of unsteadiness on the performance metrics are taken into account. Control strategies identified in our study may be used to alleviate pressure fluctuations.

Future Plans

We will assess the importance of different mechanisms of blockage present in the endwall region. Casing treatment will also be studied. Three-dimensional simulations of the unsteady flow in wake-stator interaction will incorporate a full model of the upstream wakes, including interaction with streamwise vortices.

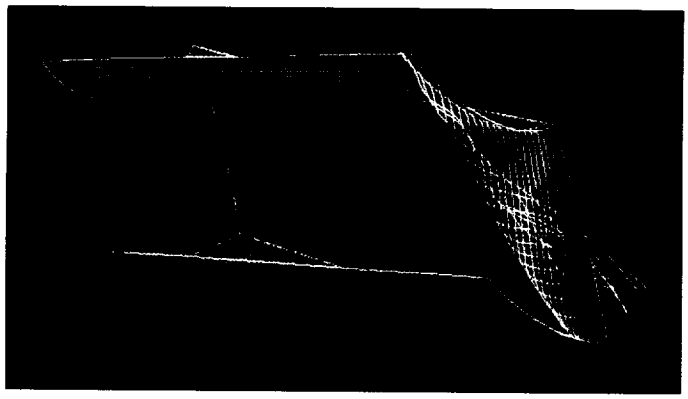

Particle traces in clearance vortex and contours of rotary total pressure coefficient in the trailing-edge plane. Red = 0.0, blue = –0.5.

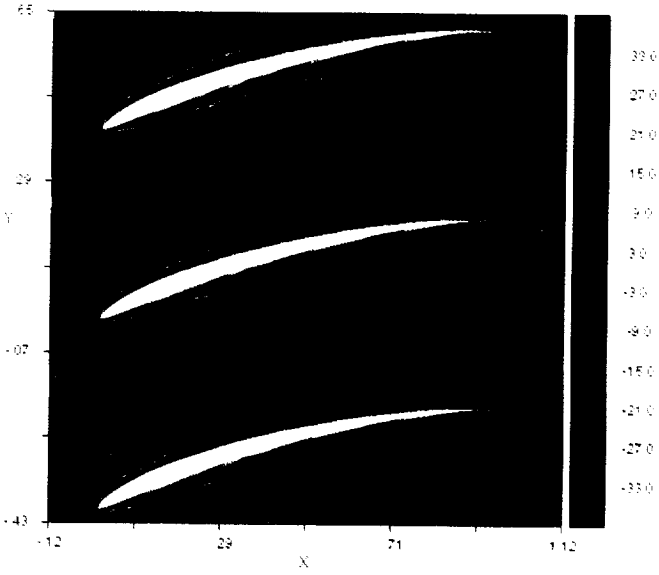

Disturbance vorticity contours showing the principal features of the unsteady flow during wake–stator interaction.

(1-2)

Hydrocarbon Scramjet Combustor Flows

Jong H. Wang, Principal Investigator
Rockwell International, North American Aircraft Division

Research Objective
To validate Navier–Stokes methodology for predicting hydrocarbon scramjet combustor flows.

Approach
The unified solution algorithm (USA) code is applied to existing combustor-flow test cases to validate the code and provide direction for future development of numerical and chemical models.

Accomplishment Description
A hydrocarbon scramjet combustor was numerically investigated. The combustor was first modeled as a two-dimensional (2-D) flow with the fuel-injector opening adjusted for a correct fuel–air ratio. Several chemical kinetics models were investigated for the oxidation of ethylene fuel. For a fuel–air ratio below 0.76, the predicted wall surface pressure was in good agreement with experimental data. However, for a higher fuel–air ratio, the predictions began to deviate from the data, and in the main combustor the wall pressure was underpredicted by 50 percent. This deviation indicated that the mixing for the 2-D numerical model was much less than that for the physical flow model. To investigate the effects of three-dimensional (3-D) flow, a 3-D numerical study was performed. The detailed configuration of the combustor, including all the fuel injectors, was considered in the numerical model. The grid system consisted of 347,030 points. The model was divided into two parts that required 5 and 14 megawords of memory, respectively. The solutions took 125 Cray Y-MP seconds per iteration and the entire process took about 130 hours to converge. The predicted wall surface pressure for the 3-D model compared better with data than the predicted pressure for the 2-D model. The maximum difference between the predictions and the data was about 20 percent. The discrepancy could have been due to the grid resolution, chemistry, or turbulence models. Further study is required to evaluate the effects of each parameter.

Significance
Efficient hypersonic combustors are essential to the design of air-breathing hypersonic vehicles. Flow physics complexity and efficient mixing and combustion require an accurate and robust computational tool.

Future Plans
Three-dimensional combustor flows with the effects of chemical and turbulence models will be studied at various flow conditions.

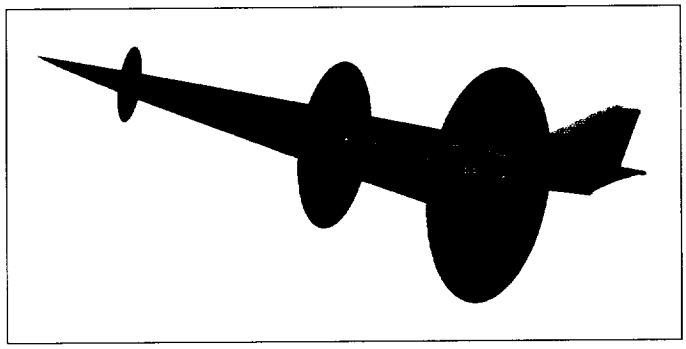

(a)

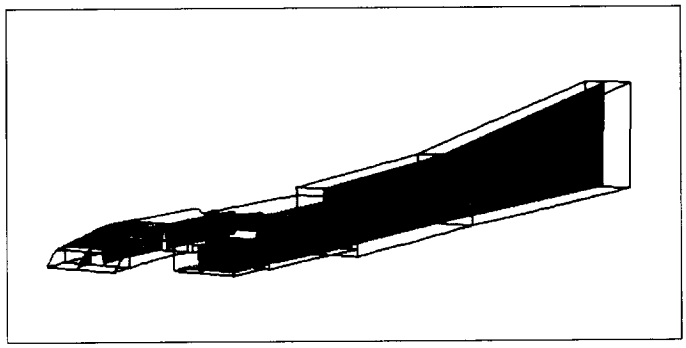

(b)

Mach number contours for a hypersonic vehicle at Mach 8. (a) Vehicle external flow Mach number contours. (b) Engine internal flow temperature contours.

Chimera Domain Decomposition Applied to Turbomachinery Flow

Kurt F. Weber, Principal Investigator
Co-investigator: Dale W. Thoe
General Motors Corporation, Allison Gas Turbine Division

Research Objective
To port the advanced compressor analysis code COM3D to the Intel iPSC/860 and evaluate its performance on a distributed memory, multiple-instruction/multiple-data (MIMD) stream architecture.

Approach
The purpose of this project was to apply the idea of domain decomposition using Chimera grid embedding to couple the calculated solutions of local flow fields in gas turbine fans and compressors. The equations were solved using Pulliam's diagonal version of the implicit approximate factorization algorithm of Beam and Warming. A composite mesh for complex flow fields was generated using the Chimera grid embedding technique. The code worked with the output from the multiple grid data management code PEGSUS, which established the interpolation between individual grids. The flow field was geometrically decomposed and grids were generated for the individual elements of a gas turbine compression system. PEGSUS was run to set up the interpolations for mesh boundary communication. For parallel processing, data decomposition can then be applied and the parallel processors distributed so the solution on each mesh is calculated concurrently.

Accomplishment Description
The best approach for applying a parallel Chimera code to turbomachinery was to base it on the parallel code, POVERFLOW. The POVERFLOW host program, the main program for the nodes, and the coding to update the Chimera boundary points were documented. Ten 32-node hours on the Intel iPSC/860 were used to calculate a 2-grid simulation of a GMA 3014 wing–nacelle configuration with the nacelle grid embedded in the wing O-grid. Learning and documenting the code and completing an initial calculation were necessary before upgrading the code to calculate turbomachinery flow.

Significance
The use of three-dimensional flow codes for aerodynamic design improvements in aircraft gas turbine engine compressors and fans has become more widespread. Increased emphasis is on extending the capability of analyses by coupling previously isolated flow-field calculations to determine the effect of coupling on component performance. Cost-effective parallel computers allow the use of complex turbomachinery flow calculations in the routine design processes.

Future Plans
POVERFLOW will be modified for turbomachinery calculations. Multiple grid parallel capability for turbomachinery flow can best be acquired by modifying the Chimera code, as opposed to porting our in-house serial flow code.

Static pressure contours and particle traces for a wing and simplified GMA 3014 nacelle configuration.

Turbofan Compression System Simulation Using Chimera Domain Decomposition

Kurt F. Weber, Principal Investigator
Co-investigator: Dale W. Thoe
General Motors Corporation, Allison Gas Turbine Division

Research Objective
To perform validation studies of a Navier–Stokes code that simulates the flow through the low-pressure compression system of a turbofan engine. Special emphasis was placed on the simulation of the flow field for the GMA 3007 engine.

Approach
A fully viscous three-dimensional (3-D) finite difference code was applied to the solution of compressor and fan flow fields. The equations were solved using Pulliam's diagonal version of the Beam–Warming implicit approximate factorization algorithm. Flow-field data were interpolated between grids using the Chimera grid embedding technique. The code worked with the output from the multiple grid data management code PEGSUS.

Accomplishment Description
A 3-D embedded grid Navier–Stokes code was applied to simulate transonic compressor flows. Fully viscous solutions with a very fine H-grid embedded in the clearance region were calculated for several designs of the low-pressure compression system of the GMA 3007 turbofan engine. Calculations included the flow through the fan rotor downstream through the flow splitter in the core and bypass ducts. The solutions show good agreement with component rig test data. The figure shows static pressure contours on the hub, fan rotor, and splitter surfaces. This multiple grid composite mesh used five individual grids. A typical calculation used 18 megawords of storage and required 18 Cray-2 hours for 2,500 iterations.

Significance
The use of 3-D flow codes for aerodynamic design improvements in aircraft gas turbine engine compressors and fans has become more widespread. However, the level of accuracy has not been high enough to reduce significantly the amount of testing required. Major improvements in performance or significant reductions in cost are unlikely unless the 3-D analyses focus on adequate resolution of the flow field and accuracy of the calculations. Accurate modeling of the flow field within compressor blade rows will provide the information needed to improve compressor performance.

Future Plans
An analysis for turbomachinery flow using Chimera domain decomposition that will run on massively parallel systems will be developed.

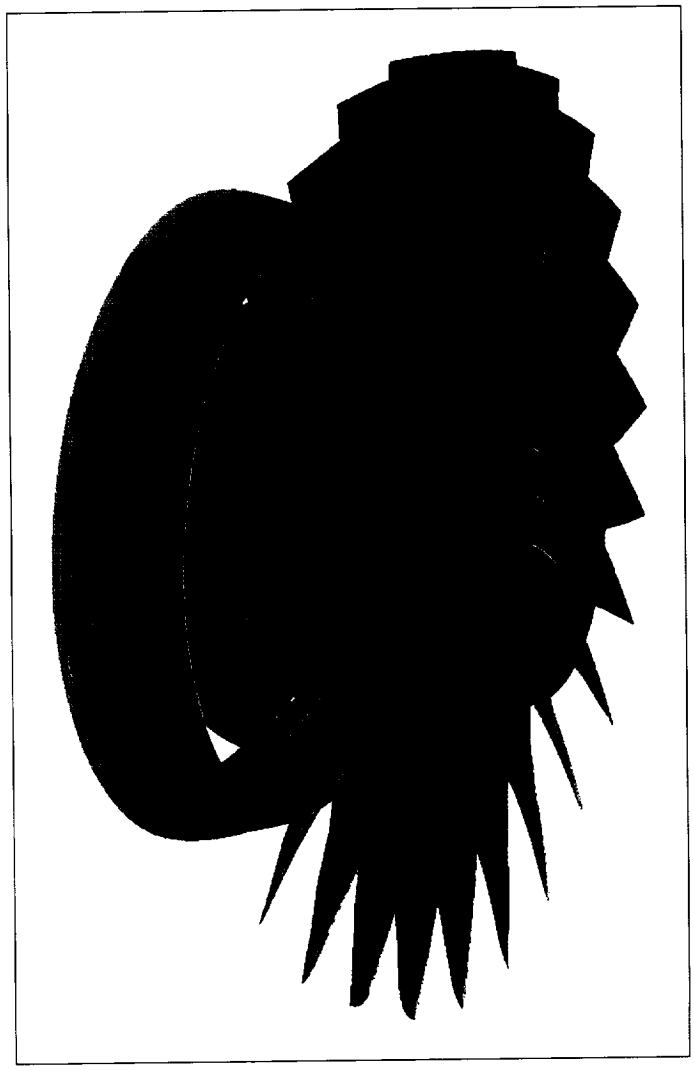

Static pressure contours for the GMA 3007 fan with a flow-field splitter; blue = low pressure, red and magenta = high pressure.

Multifunction Propulsion Systems

Perry A. Wooden, Principal Investigator
Co-investigator: Timothy P. Nobel
LTV, Aircraft Division

Research Objective
To investigate the performance of multifunction propulsion systems including cascade array thrust reversers, pivot-door thrust reversers, and long-cowl mixed flow nozzles in order to isolate a suitable technique for accurately predicting component performance.

Approach
A subscale model of a pivot-door thrust-reversing system was analyzed using computational fluid dynamics (CFD) methods and statically tested in a wind tunnel. The test hardware was a 40-percent-scale representation of an 18 degree sector of a high-bypass-ratio turbofan engine. The model instrumentation provided data comparisons with CFD predictions. Contiguous block interfacing eliminated linear interpolation errors.

Accomplishment Description
A full three-dimensional pivot-door analysis using PARC3D was completed. The figure shows a case with the pivot-door deployed at a 30 degree angle measured from the vertical position. Inflow conditions were set to an average total pressure and temperature was obtained during testing. The outflow condition was set to ambient, sea level condition at zero velocity. Particle traces were initiated at several positions along the fan duct. Large amounts of separated flow existed at the juncture of the lower fan duct wall and the fully deployed pivot-door. The particles released along the centerline traveled the complete door length, but the off-centerline traces revealed spanwise flow over the external portion of the door. The three GRIDGEN blocks generated for this problem were assembled into a single block to eliminate input/output and take advantage of the computer memory. The single block contained 1.3 million grid points requiring 32 megawords of memory. At a Courant number of 0.8, the solution took 5,000 iterations to converge four orders of magnitude. The computations required 40 Cray Y-MP hours to complete.

Significance
Thrust reversers represent the most common multifunction propulsion system application that enhances the overall effectiveness of both commercial and military aircraft. The pivot-door thrust-reverser concept is relatively new and offers weight benefits and reduced complexity.

Future Plans
Navier–Stokes simulations on the pivot-door configuration will be examined. Navier–Stokes calculations on a cascade array thrust reverser design will begin. The multifunction propulsion design investigation will be expanded to include a mixed-flow-nozzle experiment and computations.

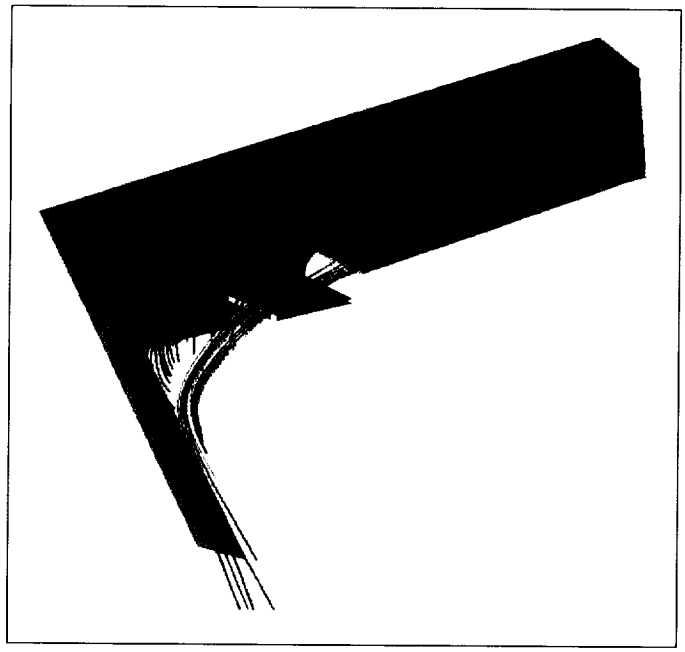

Particle traces for a 30 degree pivot-door Navier–Stokes solution with an inlet Mach number of 0.786.

Numerical Study of Thrust Vectoring Characteristics

David T. Yeh, Principal Investigator
Rockwell International, North American Aircraft Division

Research Objective
To extend and validate the Navier–Stokes methodology to predict the thrust-vectoring flow phenomena and to provide an assessment of turning efficiency and effectiveness as functions of paddle deflection and engine power settings.

Approach
The unified solution algorithm (USA) code was used to simulate the thrust-vectoring flow characteristics. The USA code solves the three-dimensional Reynolds-averaged Navier–Stokes equations through an upwind, flux-difference, finite-volume approach. A high-resolution total-variation-diminishing (TVD) scheme is incorporated to achieve a high-order spatial accuracy while maintaining numerical stability. The X-31 thrust-vectoring system is the focus of this study. This configuration was chosen because of the existence of a ground-test data base and the ongoing flight-test program.

Accomplishment Description
A blocked-grid approach was exploited to model the X-31 thrust vectoring system. A two-dimensional algebraic grid generation technique was utilized at each cutting surface to model the paddles with multiple deflection settings. The first figure illustrates a typical cross-sectional grid on a cutting surface, where a rectangular grid was created at the center to avoid a potential convergence problem associated with a singular axis. The study of the thrust deflection effectiveness was accomplished by sweeping one of the paddles into and out of the jet at constant deflection angles of the other two paddles. Data for the F404-GE-400 was used to define the boundary conditions at the nozzle throat for a prescribed power setting. Numerical solutions revealed the formation of diamond wave patterns throughout the exhaust jet. Numerical results show that turning efficiency decreases as paddle deflection increases, which is a result of stronger shocks at larger deflections. In the second figure, the surface pressure contours and grid for the X-31 thrust-vectoring system are illustrated. The top paddle was deflected 20 degrees into the jet while the other two paddles stayed at their neutral positions. A typical computation for this configuration requires 20 megawords of memory and 25 Cray Y-MP hours.

Significance
The numerical study parallels the ongoing X-31 flight-test program and establishes the computational fluid dynamics capability for analysis of thrust-vectoring flow phenomena. This study will have significant impact on current and future advanced aircraft design.

Future Plans
The control effectiveness of the thrust-vectoring system varies with altitude due to different nozzle pressure ratios. Numerical simulation will be performed at the flight conditions to provide a viable assistance to the in-flight control command.

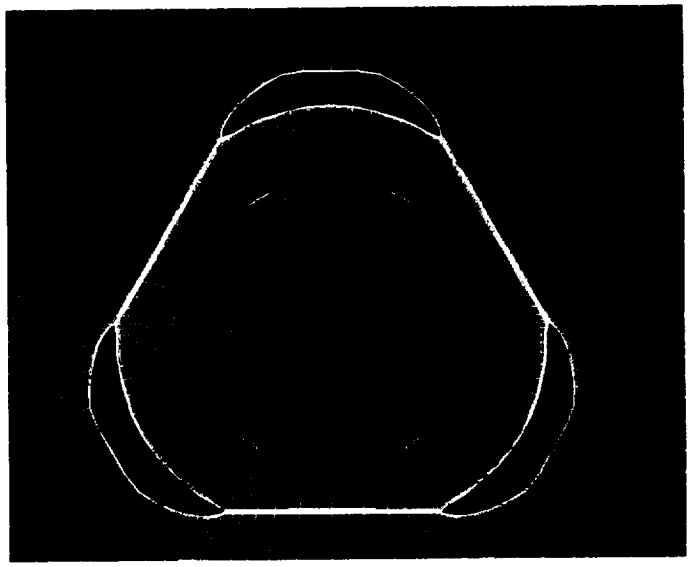

Typical grid arrangement on a cutting surface.

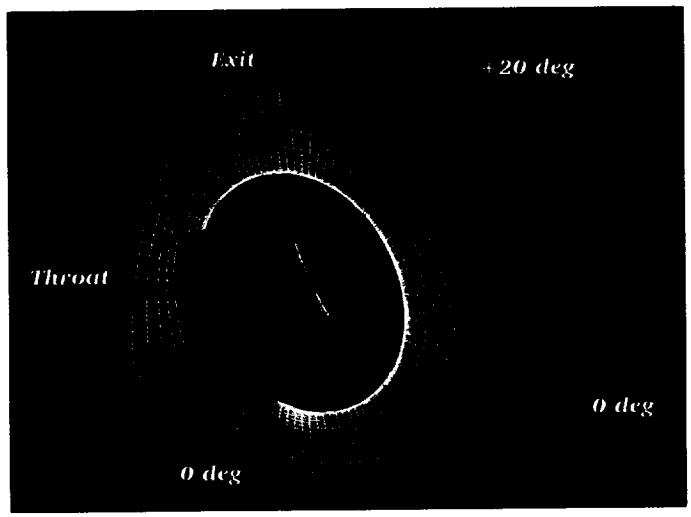

Pressure contours for the X-31 thrust-vectoring system. Contour levels are between 0.4 and 3.0.

National Aero-Space Plane External Burning Nozzle Studies

Shaye Yungster, Principal Investigator
ICOMP/NASA Lewis Research Center

Research Objectives
To provide a means for determining the sub-scale and full-scale performance of external burning nozzles at transonic flight conditions.

Approach
The Reynolds-averaged Navier–Stokes equations with finite-rate chemistry were solved using two- and three-dimensional (2-D and 3-D) multiblock, fully implicit codes based on the LU-SSOR factorization scheme. The spatial discretization was based on a second-order total variation diminishing scheme for the 2-D code, and central-differences with second- and fourth-order artificial damping for the 3-D code. The Baldwin–Lomax algebraic turbulence model was used in all the calculations. Most of the computations were carried out using a simple one-step combustion model.

Accomplishment Description
A computational model for the external fuel injection and combustion processes was developed and applied to three nozzle configurations: (1) a baseline cowl without a flame holder; (2) an extended cowl without a flame holder, and (3) an extended cowl with a flame holder. The numerical results were compared with experiments. The computed pressure distributions along the expansion ramp agreed favorably with the experimental data. Qualitative comparisons with experimental infrared images, such as those in the figures, were also conducted. This study showed that nozzle flows that include external burning can be adequately modeled using a 2-D formulation. Using this simplified approach, different configurations were analyzed quickly and inexpensively. A typical calculation required about 8 megawords of memory and 2 Cray Y-MP hours. At transonic speeds and without external burning 3-D effects become important because of nozzle overexpansion; thus a full 3-D analysis is required. For these cases, a multiblock version of the RPLUS3D code was used.

Significance
Nozzles similar to those on the National Aero-Space Plane are highly overexpanded at transonic speeds, resulting in large drag increases. One way to eliminate this drag is to increase the pressure along the afterbody by external combustion. Numerical simulations can provide details of the flow field, identify wind tunnel interference effects, determine scaling effects, and analyze advanced designs.

Future Plans
Determination of the full-scale performance of external burning nozzles at transonic flight conditions and investigation into the effects of various parameters on the thrust and normal forces acting on the expansion ramp and cowl are being investigated.

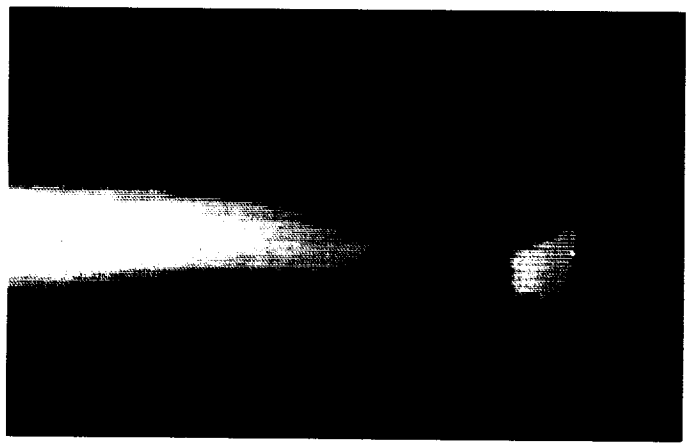

Experimental infrared image of external burning.

Computational results showing temperature contours: Mach = 1.2, nozzle pressure ratio = 6, external burning fuel pressure = 320 pounds per square inch.

Aeronautics

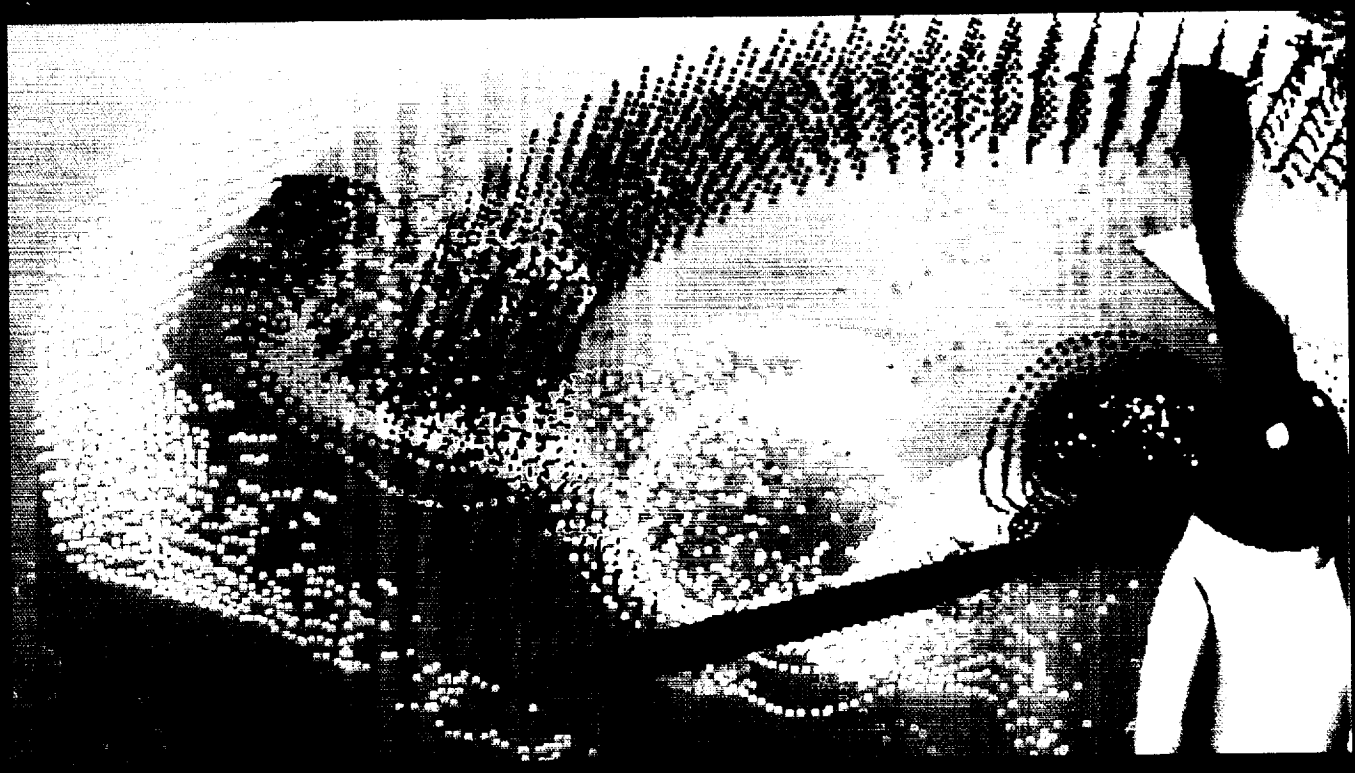

Rotorcraft

Aerodynamics and Acoustics of Rotorcraft

W. J. McCroskey, Principal Investigator
Co-investigators: J. D. Baeder, R. L. Meakin, V. Raghavan, and G. R. Srinivasan
NASA Ames Research Center

Research Objective
To develop and validate accurate, user-oriented viscous computational fluid dynamics codes for three-dimensional (3-D) unsteady aerodynamic flows about arbitrary rotorcraft configurations. Complex vortical wakes, shock waves, rotor–body interactions, and acoustic waves are included.

Approach
Advanced 3-D unsteady multizone implicit Navier–Stokes codes are used to simulate rotorcraft aerodynamics and acoustics under flight conditions that have not previously been treated satisfactorily. High accuracy and stability are achieved for rotor blades by using the transonic unsteady-rotor Navier–Stokes code, which features full upwinding, enhanced accuracy, and high computational efficiency. Complete rotorcraft are treated using the OVERFLOW code to solve the unsteady thin-layer Navier–Stokes equations and the DCF3D code (a new domain connectivity algorithm) to dynamically establish domain connectivity among the systems of fixed and rotating overset grids. In addition, special solution-adaptive grid clustering and wave fitting techniques are used to capture low-level radiating acoustic waves.

Accomplishment Description
A hypothetical, but realistic, set of flight conditions for the V-22 Osprey aircraft was established to facilitate rigorous testing of DCF3D, and to carry out an overset grid proof-of-concept tiltrotor simulation. Relative motion and interference effects between the V-22 airframe and rotor-blades were directly simulated within the context of an unsteady, thin-layer Navier–Stokes computation (see figure). The domain connectivity algorithm was verified to perform at rates equal to or greater than those realized previously for store-separation-like applications. The feasibility of carrying out unsteady Navier–Stokes analyses of rotorcraft problems has been demonstrated. The noise from five different rotor blades was examined in hover for a wide range of tip Mach numbers, including a detailed analysis of the nonlinearities that plague conventional acoustic theories. This study provided useful insight into the noise-generating mechanisms of the various blade shapes and the near-field wave front formations, and helped to define the limitations of the linear acoustic analogy.

Significance
The ability to simulate accurately the aerodynamics and acoustics of rotorcraft will allow quieter and more efficient vehicles to be designed at lower cost and less risk. Analysis of the flow separation on the V-22 Osprey aircraft has helped to avoid costly design errors.

Future Plans
More accurate and efficient simulations of rotorcraft aerodynamics and acoustics, with emphasis on blade–vortex interaction noise and rotor–body interference on tiltrotor aircraft will be developed.

Unsteady simulation of the V-22 Osprey tiltrotor aircraft aerodynamics in low-speed forward flight (helicopter mode). Small matrices of particles were released aft of an inboard and outboard blade-tip in a post-process flow visualization computation based on flow-field data from every 15th time step of the simulation. The particles are colored by time and highlight the structure of the rotor wake.

Calculations of High-Performance Rotorcraft

W. J. McCroskey, Principal Investigator
Co-investigators: J. D. Baeder, E. P. N. Duque, S. K. Stanaway, and G. R. Srinivasan
NASA Ames Research Center

Research Objective

To compute the viscous three-dimensional (3-D), unsteady flow field around advanced helicopters. Particular emphasis is placed on the transonic aerodynamics of high-performance rotor-blade tips, vortical wake structure, and rotor–body aerodynamics interference.

Approach

The unsteady 3-D Euler/Reynolds-averaged Navier–Stokes equations were solved by structured- and unstructured-grid methods, either in blade-fixed or inertial reference systems. The codes were validated through detailed comparisons with experimental data.

Accomplishment Description

The Reynolds-averaged thin-layer Navier–Stokes code OVERFLOW was applied to the Comanche fuselage. The first figure illustrates the surface pressure distribution over the front part of the aircraft. Areas in gray were not included in the calculation, thus they have no influence on the computed flow field. Significant progress was made in coupling an unstructured-grid rotor code to a structured-grid rotor code. In this case, a structured grid optimized for viscous-dominated flows is used for the near-body flows, while the unstructured grid is used for the inviscid flow fields away from the body. The two grid systems overlap and interpolate flow quantities at their boundaries. The second figure illustrates the structured/unstructured-grid system for a rotor in hover.

Significance

The Comanche helicopter is the Army's newest aircraft. Viscous fuselage calculations provide detailed flow-field information unattainable by other methods. These calculations can be used to help evaluate and improve aircraft performance. The hybrid structured/unstructured method incorporates the best features of each individual technology. Generally, structured grids perform much better for near body flows because the grid can cluster near the walls without severe time-step limits. The unstructured grids can refine around flow features more readily than the structured grids. This feature potentially allows more accurate wake calculations.

Future Plans

The unsteady flow field of the Comanche, including the rotor hub and blades in forward flight, will be computed and compared with future experiments. The structured/unstructured methodology will be validated for hover and forward flight and used to improve Chimera grid boundary update and connectivity. Dynamic grid adaption of the unstructured mesh will be implemented and demonstrated.

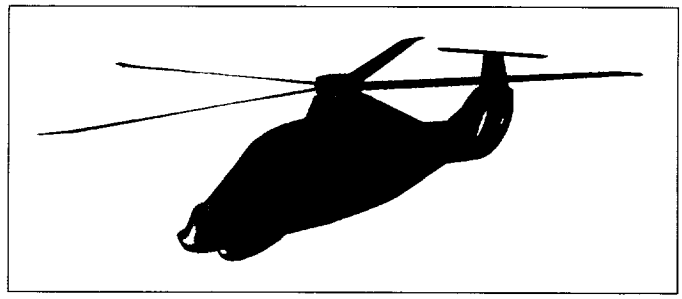

Surface pressure maps for the Comanche helicopter free stream; Mach = 0.26, Reynolds number = 14,000,000, angle of attack = 0.0.

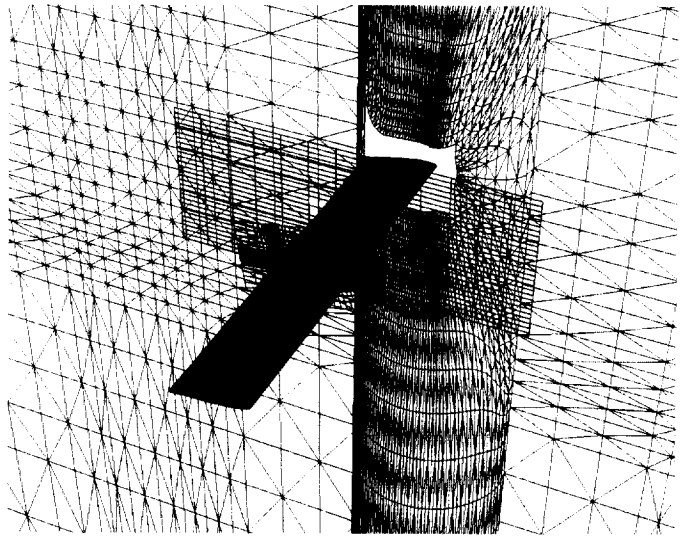

Unstructured/structured hovering rotor grid system.

Rotorcraft Drag Prediction

J. C. Narramore, Principal Investigator
Co-investigators: A. G. Brand, J. J. Shillings, and D. W. Axley
Bell Helicopter Textron, Inc.

Research Objective
To develop the capability to predict forces and moments including drag on complete rotorcraft vehicles.

Approach
Three-dimensional Navier–Stokes codes were used to perform steady and unsteady analyses of rotor blades and fuselages in flight and correlate these results with existing wind tunnel data. Both code and grid topology investigations were carried out.

Accomplishment Description
Research pertaining to the calculation of forces on three-dimensional rotor blades, fuselages, and other components, with special emphasis on the calculation of drag levels, was performed. Work was focused in four areas: developing an actuator disk model, modeling inlet flows, Navier–Stokes solutions to the flow about anhedral rotor tip shapes, and helicopter fuselage drag computations. To acquire methods to design advanced antitorque devices for helicopters, a ducted tail rotor actuator disk model based on Navier–Stokes techniques was developed. A typical solution required 8 Cray Y-MP hours and 10 megawords of memory. The figure illustrates the computed flow. Thrust was generated for this zero-angle-of-attack case moving from the port side of the disk to the starboard side aft of the disk (shown by the particle traces).

Significance
Computational fluid dynamic methods offer high potential for improved rotorcraft design and performance capabilities. This new technology should reduce vehicle costs, improve performance, reduce development times, increase aerodynamic responsiveness, and improve the quality of rotorcraft vehicles. Requirements for modern high-speed helicopters include fast rates of climb, high degrees of maneuverability, and improved performance. Accurate assessment of blade and fuselage drag in maneuvers, transonic flight, or at high angle of attack is crucial to rotorcraft predictive and design methodology. Results from detailed modeling of a ducted fan concept indicate that Navier–Stokes methods may be useful for the design of advanced helicopter antitorque devices. However, because of slow convergence at low Mach numbers, an incompressible Navier–Stokes methodology is also being pursued.

Future Plans
Chimera grid techniques will be incorporated into these modeling techniques. Wind tunnel data, including pressure and force comparisons, will be correlated for an incompressible Navier–Stokes method. Navier–Stokes codes will be used to investigate unsteady flows in a duct. Drag increments due to fuselage shape perturbations will also be computed.

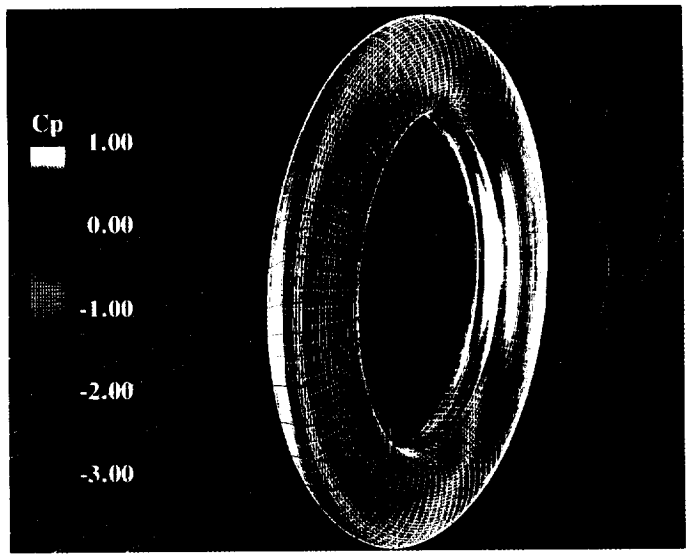

Thrusting actuator disk inside a faired duct with 6.8 pounds per square foot disk loading.

Dynamic Adaption for Three-Dimensional Unstructured Grids

Roger C. Strawn, Principal Investigator
Co-investigators: Rupak Biswas and Michael Garceau
RIACS/Stanford University

Research Objectives

To solve problems in rotary-wing aerodynamics where rotor-wake systems are extremely complex. Unlike a fixed wing, where the wake is rapidly convected downstream, a rotor operates in close proximity to its own wake. In order to accurately model these effects, computational methods must minimize any numerical dissipation that can artificially diffuse the vortices in the wake.

Approach

Numerical dissipation of the wake was minimized by using dynamic solution-adaptive grids and flow solvers that were appropriate for the resulting unstructured meshes. The solution-adaptive approach adds and removes points locally to provide higher resolution for moving flow features such as rotor-wake vortices. This local increase in grid resolution provides an excellent mechanism for minimizing numerical dissipation as long as the mesh points can be efficiently added and deleted from the mesh.

Accomplishment Description

An efficient procedure was developed for the simultaneous coarsening and refinement of three-dimensional (3-D) unstructured tetrahedral meshes. The mesh-adaption algorithm was implemented in C and used an innovative data structure consisting of a series of dynamically allocated linked lists. These lists allowed the mesh connectivity to be reconstructed rapidly when individual points were added or deleted. The data structure was based on edges of the mesh rather than the tetrahedral elements themselves and resulted in an efficient data structure and facilitated anisotropic mesh refinement and coarsening.

Significance of Accomplishment

The key to success for dynamic mesh adaption is the ability to add and delete points from the grid efficiently. For an unsteady flow, this coarsening/refinement step must be completed every few time steps, so its efficiency must be comparable to that of the flow solver. It must also have a reasonable memory requirement. The new mesh-adaption scheme has all these attributes. In addition, it can be applied to a variety of important NASA problems in areas other than rotorcraft aerodynamics.

Future Plans

The new mesh-adaption scheme is currently being used to compute large problems in rotor aerodynamics and acoustics. It is also being modified to run concurrently with the flow solver on the CM-5 parallel computer.

Publication

Biswas, R.; and Strawn, R. C.: A New Procedure for Dynamic Adaption of Three-Dimensional Unstructured Grids. AIAA 31st Aerospace Sciences Meeting, Reno, Nev., AIAA Paper 93-0672, Jan. 1993.

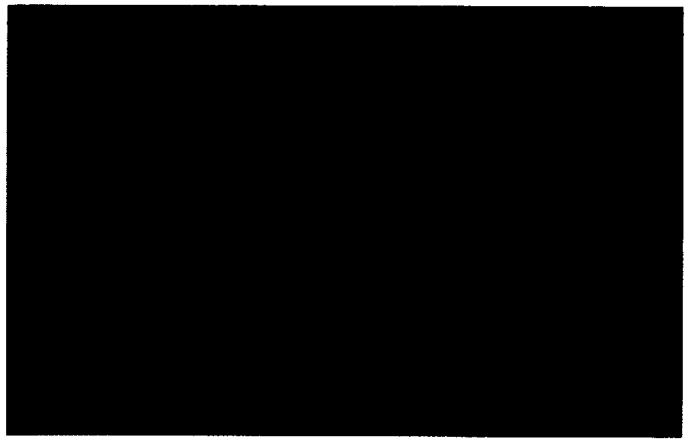

Mesh adaption for a 3-D NACA 0012 wing with inviscid sidewalls, $M_\infty = 0.85$, $\alpha = 1.0$ degree.

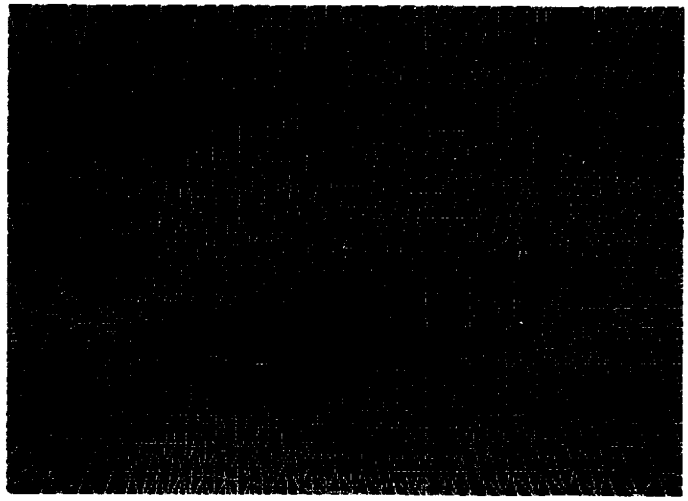

Side view of the final mesh after three refinement and two coarsening levels.

Simulation of a Complex Three-Dimensional Internal Flow Field

H. Tadghighi, Principal Investigator
Co-investigator: A. A. Hassan
McDonnell Douglas Corporation

Research Objective
To develop a predictive capability to analyze accurately and optimize efficiently complex internal flows for rotorcraft advanced antitorque systems.

Approach
The three-dimensional, Reynolds-averaged, zonal Navier–Stokes solver used for this study was NASTD. The solver algorithm is a time-dependent finite-volume implicit scheme based on upwind differencing. Baldwin–Lomax and k–ε turbulence models were employed in this study. To examine the complex internal flow created by the various components of the no-tail-rotor (NOTAR) concept antitorque system (such as highly curved inlet geometry, fairing, centerbody, and multibladed high-speed fan), analysis was performed for a range of mass flow rates with and without the influence of the swirl induced into the flow by the fan. The accuracy of the flow-field analysis was assessed using measured data.

Accomplishment Description
Several mass flow rates were evaluated using an actuator disk model to represent the existence of the fan. Analyses were performed with two turbulence models to investigate their effectiveness in improving the numerical simulation of the NOTAR antitorque system internal flow. Comparisons between measured data and the predictions indicated good agreement for a range of mass flow rates. The solution using the k–ε turbulence model improved the prediction of the flow-field features by more accurately capturing the separated flow regions observed in the measured data. The inlet-duct centerbody-fairing grid was comprised of 3 grid zones and contained approximately 0.7 million points. A typical solution with this mesh required 48 megawords of memory and up to 15 Cray-2 hours.

Significance
Accurate analysis of the complex flow field associated with the internal flow using the NASTD solver lends confidence in relying on a computational fluid dynamics technique for applications to problems of a similar nature. This provides valuable insight into the details of the flow and will furnish the designer with a viable tool to enhance the flow characteristics and the performance efficiency of the NOTAR antitorque system. The capability of NASTD to capture the features of the system's complex internal flow field is encouraging.

Future Plans
The NOTAR antitorque system internal flow will continue to be optimized by reducing interference effects between the inlet-fairing centerbody-fan components and optimizing duct surface contours. To reduce the intensive processing requirement for the k–ε model, the Baldwin–Barth one-equation turbulence model will be investigated for computational efficiency.

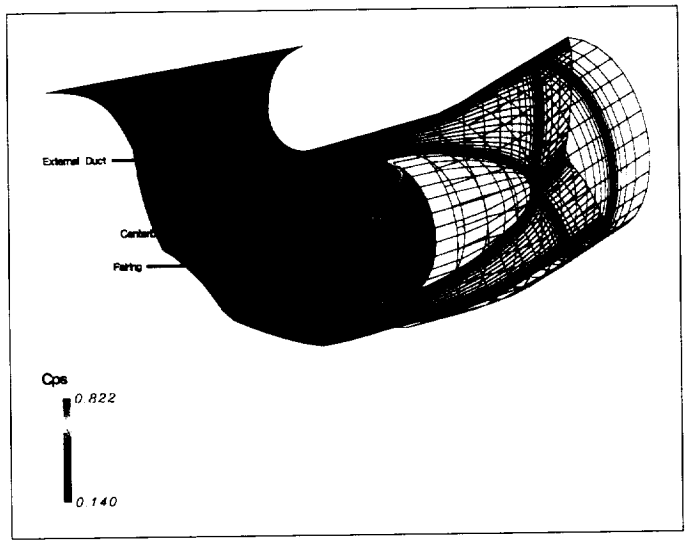

NOTAR antitorque system internal flow prediction at Mach = 0.2.

Aeronautics

Turbulence

Transition in a Highly Disturbed Environment

David E. Ashpis, Principal Investigator
Co-investigator: Philippe R. Spalart
NASA Lewis Research Center/Boeing Commercial Airplane Group

Research Objective
To understand the physical mechanisms of nonlinear stability and bypass transitions to provide guidance for engineering model developers.

Approach
Direct numerical simulations of controlled disturbances in the boundary layer were performed. Spatial simulations were performed using a Spalart's "fringe code." Numerical experiments simulating single frequency excitation (vibrating ribbon) and broad band excitation (blowing pulse) were performed. The disturbances were introduced on the wall by specifying localized suction/blowing. The flow field, frequency, and wavenumber spectra were computed for incompressible Blasius boundary layer flow.

Accomplishment Description
The original fringe code was modified to allow specification of time-dependent wall boundary conditions. Series of two- and three-dimensional runs were performed for a range of disturbance frequencies, amplitudes, and Reynolds numbers. Emphasis was on moderate and high levels of disturbances in the subcritical region. Computing resources varied according to the domain size, grid resolutions, and the length of simulation. Typical runs required 4–32 megawords of memory and 4–20 Cray Y-MP hours. Observations included some elongated streamwise structures in the pulse case, and a peculiar multiperiodic behavior in the low-frequency ribbon excitation case.

Significance
A highly disturbed environment prevails in flow in the gas turbine (for example, at the entrance to the turbine). Hence, conclusions obtained from the simulations of the associated nonlinear and bypass stability mechanisms are valuable for developers of models for applied engineering calculations.

Future Plans
Post-processing of the vast data acquired will be completed. Effects of factors such as pressure gradients and curvature will be studied. The studies will be extended to flows with heat transfer.

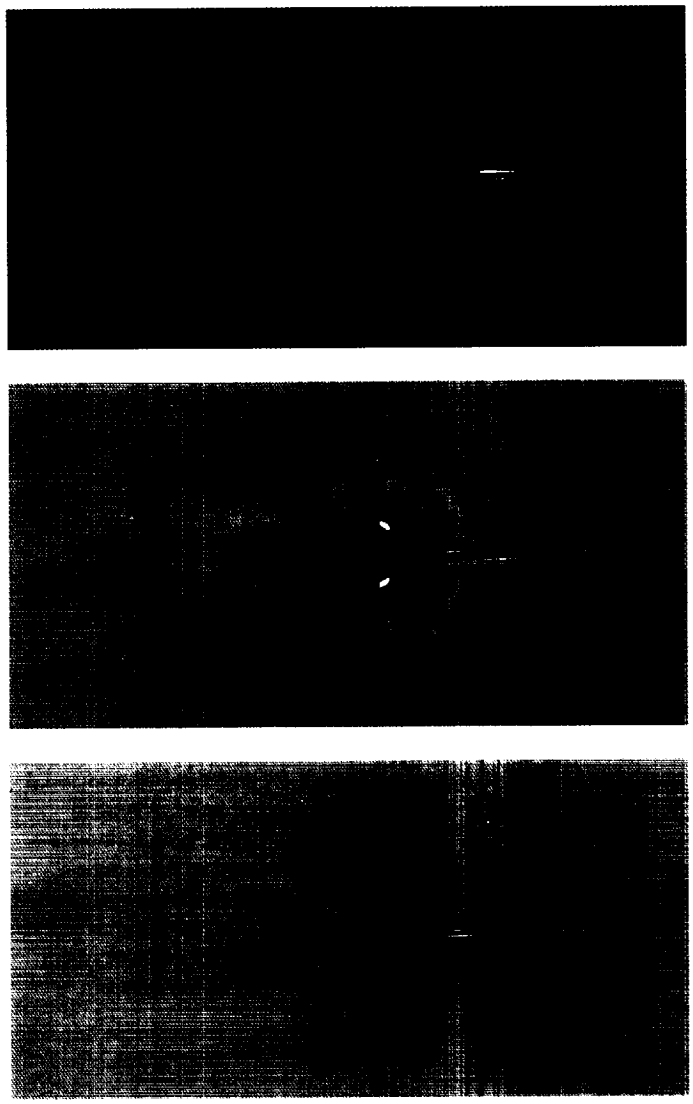

Flow structures generated by a blowing pulse in a Blasius boundary layer. Shown from top to bottom are u, v, w disturbance velocities in a horizontal x–z plane. Pulse is generated at a Reynolds number of 68,000. Domain range is from Reynolds numbers 30,000 to 305,000.

High-Speed Turbulent Reacting Flows

J. Philip Drummond, Principal Investigator
Co-investigators: Peyman Givi, Cyrus K. Madnia, Steven H. Frankel, and Virgil Adumitroaie
NASA Langley Research Center/State University of New York at Buffalo

Research Objective
To develop subgrid scale models for large-eddy simulations (LES) of turbulent reacting flows to make accurate predictions in practical engineering flows.

Approach
The investigation was based on probability density function (PDF) methods and results obtained from direct numerical simulations (DNS) were used for model validation. Computations of both incompressible and compressible flows in two- and three-dimensions were performed in homogeneous isotropic turbulent flows and spatially developing mixing layers. The numerical schemes were based on pseudospectral and hybrid spectral/finite-difference algorithms. The DNS-generated data were used in both a priori and a posteriori modes to validate LES predictions.

Accomplishment Description
Because of the demonstrated capabilities of PDF closures in homogeneous flows, their use was suggested as a subgrid scale model in LES of reacting flows. The subgrid scale models developed involved the use of a Smagorinsky-based, one-equation hydrodynamics model and an assumed Dirichlet PDF for the thermochemistry. The procedure required the solution of additional modeled transport equations for the subgrid turbulent kinetic energy and the subgrid species covariance. Results were obtained for both two-dimensional (2-D) and three-dimensional homogeneous turbulence and a 2-D mixing layer. A typical result for the shear layer is shown in the figure, which depicts contour plots of the chemical product formed in the reaction $A + B \rightarrow P$. The results suggested that better models were needed for the subgrid moments and for the formation of the joint scalar PDF. DNS requires 25 Cray Y-MP hours and 23 megawords of memory, whereas LES requires on the order of minutes of Cray Y-MP time.

Significance
DNS of high-Reynolds-number engineering flows with complex chemical kinetics is not possible in the foreseeable future. LES and PDF modeling offer an attractive, economically and computationally feasible means of making accurate engineering predictions. This work is one of the first attempts at incorporating PDF methods for LES of turbulent reacting flows.

Future Plans
Improved models for mixing and reacting in turbulent flows are currently being developed for use as subgrid scale models in LES. The use of such models in compressible reacting flows is also under investigation.

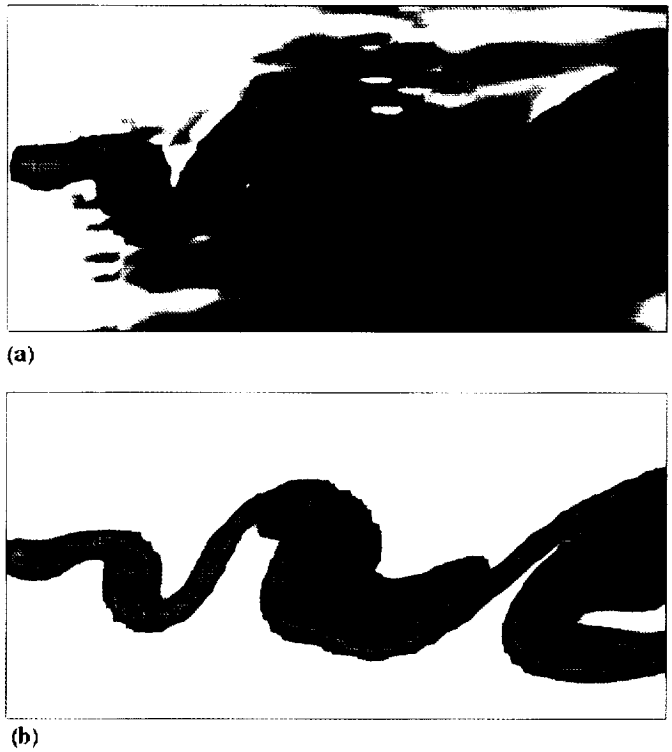

Contour plots of product mass fraction from (a) LES and (b) filtered DNS results.

Simulation of a Turbine-Blade Cooling Passage

Kai-Hsiung Kao, Principal Investigator
Co-investigator: Meng-Sing Liou
ICOMP/NASA Lewis Research Center

Research Objective
To predict the flow-field and heat transfer coefficients in a branched-duct test section that includes several significant features of a turbine blade cooling passage. Higher engine efficiency can be obtained at higher operating temperatures. Higher turbine inlet temperatures often require internal cooling in the blades and vanes. Effective design of internal cooling passages is greatly enhanced by the availability of dependable, validated computer codes.

Approach
A computer code based on a time-accurate, three-dimensional (3-D), finite-volume, high-resolution scheme for solving the compressible full Navier–Stokes equations was developed. The numerical formulation used a new advection upstream splitting method that improved the accuracy and efficiency of the flow solver. A 3-D Chimera grid-embedding technique was incorporated with the Navier–Stokes solver, subdividing into regions the physical domain of the flow field to accommodate an easily generated grid. The strategy from Chimera overset grids provides great flexibility in grid generation for complex configurations.

Accomplishment Description
The present Navier–Stokes solver was developed and validated for various two- and three-dimensional complex configurations. For the turbine blade cooling passage problem, a primary coarse grid system was generated using 18 structured grid blocks. Different grid topologies were used to resolve specific geometries. Because the overset meshes used were independent of each other, they could readily be embedded in arbitrary orientations. Consequently, grid points within solid boundaries were blanked or excluded from other overset grids. Communication through boundary interfaces between the separate grids was carried out using trilinear interpolation. The grid used for the simulation had about 160,000 points. Preliminary results clearly displayed the basic features, including the recirculation and separation regions. Typical runs required 3.5 megawords of memory and 3.7×10^{-5} Cray Y-MP seconds per grid point for each iteration.

Significance
This simulation provided insight into the physics of flow structures and examined heat transfer behaviors in a turbine blade cooling passage. The results enhance the accuracy of the design process and reduce the cost of experimental tests.

Future Plans
A finer mesh system is required to enhance the accuracy of the simulation. Various turbulence models will be considered to predict turbulent flow regions. Numerical results and experimental data for the velocity field and surface heat transfer coefficients will be compared.

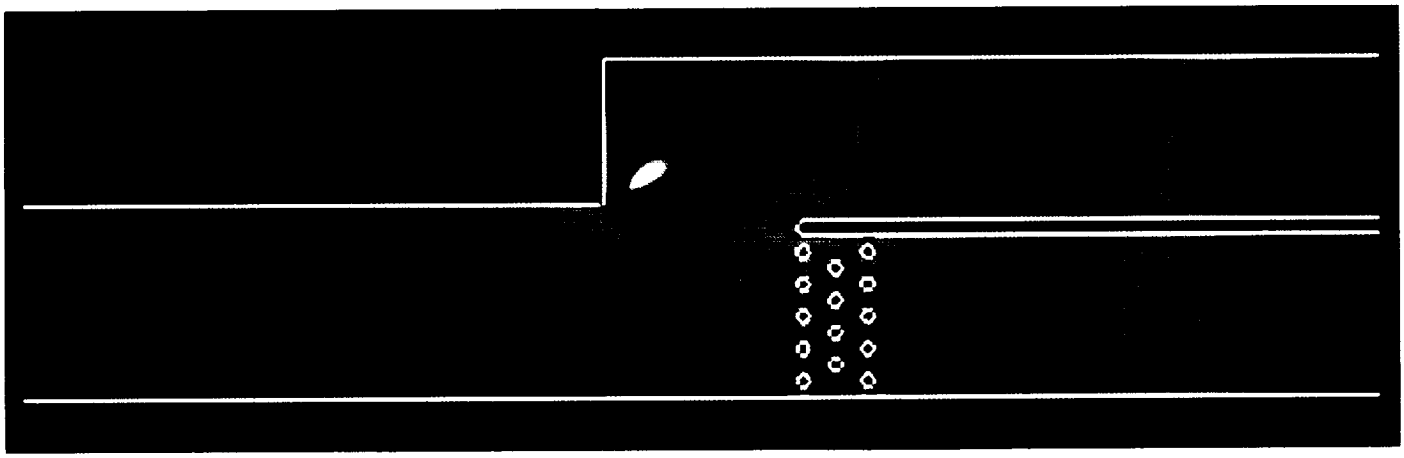

Temperature distributions in a turbine blade cooling passage with $M_\infty = 0.4$, Reynolds number = 45,000. Maximum temperature (white) = 0.75 K, minimum temperature (blue) = 0.65 K.

Numerical Simulation of Turbulence

J. J. Kim, Principal Investigator
Co-investigators: Robert D. Moser, R. S. Rogallo, Nagi N. Mansour, and J. R. Chasnov
NASA Ames Research Center/Center for Turbulence Research

Research Objective
To investigate the physics of turbulence in simple model flow situations and provide otherwise inaccessible turbulence data for use in modeling and other studies.

Approach
Direct numerical simulations and large-eddy simulations of turbulence in simple flow situations (currently homogeneous turbulence and turbulence in a plane channel) were performed by solving the incompressible Navier–Stokes equations using spectral numerical methods. The flow solutions were processed to extract relevant statistical data and to answer questions regarding the physics of turbulence.

Accomplishment Description
Several direct numerical simulations of homogeneous turbulence were performed. The decay of isotropic turbulence was simulated to determine the Reynolds number dependence of the decay power law. The results modified the k-ε turbulence model to reflect the observed dependence. Isotropic turbulence simulations were used to obtain Lagrangian velocity correlations. Large-eddy and direct simulations of homogeneous turbulence were used to study the convection of scalars, buoyancy driven flows, and simple combustion processes. These simulations were used to study self-similar turbulence decay at high Reynolds numbers, the "collapse" of eddies in stratified flows, and the behavior of probability density functions in reacting flows. Large-eddy simulations were used to address behavior of the largest scales in turbulent flows. Finally, simulations of nonisotropic turbulence were performed to provide better resolution in these cases. Two direct simulations of plane channel flow were performed. First, a channel at a Reynolds number of about 6,600 was simulated to study scalar transport in wall-bounded flows. Second, simulation of a channel at a Reynolds number of approximately 13,000 was begun.

Significance
In many flow situations turbulence is the controlling phenomenon, yet efforts to predict or control the effects of turbulence have had only limited success. These simulations provide important information needed to improve our understanding of and our ability to predict and control turbulence. Results from these simulations are being used to develop improved turbulence models and control strategies.

Future Plans
Simulations to provide turbulence data at higher Reynolds numbers and in new flow situations are planned. New algorithmic developments for parallel machines made as part of this project and the new Paragon hardware will increase our capability to study these important flows.

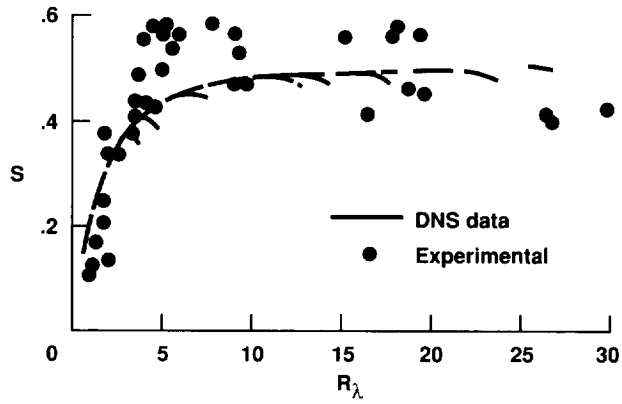

Velocity-derivative skewing; Reynolds number versus experimental data.

Receptivity, Transition, and Turbulence Phenomena

Linda D. Kral, Principal Investigator
Co-investigators: William W. Bower and John F. Donovan
McDonnell Aircraft Company

Research Objective
To investigate the physical processes in fluids through simulations of transition mechanisms or turbulence phenomena occurring in incompressible to supersonic flows.

Approach
Three areas were investigated: (1) boundary layer receptivity, (2) boundary layer transition, and (3) compressibility effects on turbulent boundary layers. To study boundary layer receptivity, the linearized Navier–Stokes equations were recast in spectral form and solved. For the studies in boundary layer transition and turbulence, direct and large-eddy simulation techniques were used. Different subgrid-scale models were investigated for the simulation of both transitional and turbulent boundary layers.

Accomplishment Description
The focus was on large-eddy simulations of supersonic turbulent boundary layers and boundary layer receptivity. Suppression of a Tollmien–Schlichting wave through the motion of a compliant surface and a springbacked membrane-compliant surface were simulated. Large-eddy simulations of supersonic, wall-bounded, turbulent flows were performed. Two compressible subgrid-scale models based on the Favre-filtered equations of motion for an ideal gas were tested. Higher order boundary conditions and adjustments in the computation of the viscous terms resulted in a more stable numerical scheme. The compressible Smagorinsky model and the structure function subgrid-scale model results agreed well with experimental data. In the first figure, a Smagorinsky model constant density surface is shown. Horseshoe-shaped structures similar to those found in incompressible boundary layers are visible. The second figure shows isovelocity surfaces of the streamwise velocity. The low-momentum fluid near the wall indicates low-speed streaks and shows regions of these streaks lifting away from the wall near the horseshoe-like structures. Typical supersonic large-eddy simulations required 10 Cray Y-MP hours and 6 megawords of memory when starting in the late stages of transition.

Significance
A better understanding of supersonic, turbulent boundary layers can lead to improved turbulence models.

Future Plans
The physics of the compressible, boundary layer transition process using direct numerical simulations and large-eddy simulations with the dynamic subgrid-scale model are being studied. Boundary layer transition over a curved surface will be simulated. The influence of localized wall heating to control transition is also under investigation.

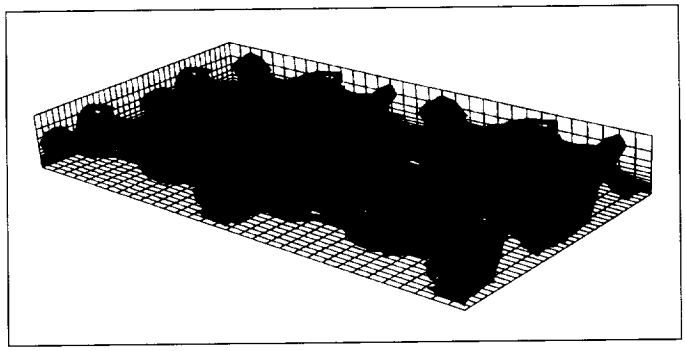

Constant density surface from a large-eddy simulation of a supersonic boundary layer.

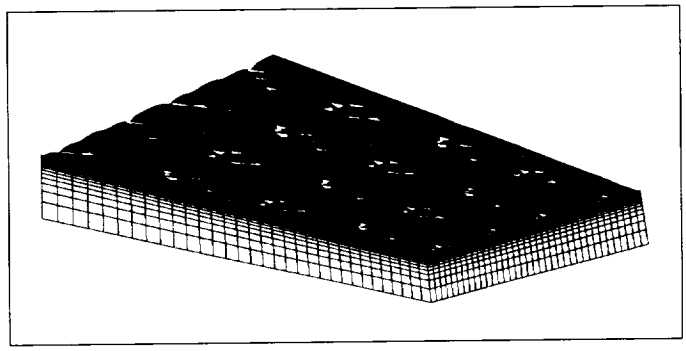

Isovelocity surface of streamwise velocity from a large-eddy simulation of a supersonic boundary layer.

Turbulence Modeling for Three–Dimensional Flow Fields

Linda D. Kral, Principal Investigator
Co-investigators: John A. Ladd, Mori Mani, and John F. Donovan
McDonnell Aircraft Company

Research Objective
To investigate turbulence models used in numerical simulations of complex viscous flows for critical aircraft components such as the forebody, wing, nozzle, inlet, diffuser, and afterbody.

Approach
A three-dimensional (3-D) zonal Navier–Stokes code, NASTD, with a two-equation turbulence model was used to predict turbulent flow fields around flight vehicles. An implicit, approximately factored, upwind scheme was employed to solve the 3-D, compressible, Favre-averaged Navier–Stokes and energy equations together with the k–ε two-equation turbulence model. In addition, a compressibility correction for free shear layers was implemented.

Accomplishment Description
The k–ε model was compared with other complex turbulent flow models. The compressibility correction worked well for high-speed mixing layers; however, when this correction was invoked for a high-speed boundary layer, the skin friction was significantly lower. Investigation of turbulent flow about an F/A-18 forebody at high angle of attack showed that the Jones–Launder k–ε model predicted flow features similar to the Baldwin–Lomax algebraic model. Investigation of a supersonic combusting shear layer showed that proper ignition delay was best predicted using the Chien low-Reynolds-number model. Calculations of a transonic supercritical airfoil showed that the algebraic Baldwin–Lomax and the two-equation model predicted the shock location and surface pressure distribution, but the results were extremely grid dependent. Calculations of a 3-D highly offset diffuser showed the ability of the Chien low-Reynolds-number model to predict accurately the flow-field features. A comparison of the total pressure at the diffuser centerline and engine face station is shown in the figure. The primary region of total pressure loss was similar, but the deficit was greater and more clearly defined in the algebraic model prediction since there was no eddy viscosity modeled in this region and the losses did not diffuse as quickly as in the two-equation model prediction. The algebraic model also predicted a spurious region of secondary flow. The two-equation model better predicted recovery and distortion parameters at the engine face. The calculation of the 3-D diffuser required approximately 10 Cray Y-MP hours and 14 megawords of memory for a converged solution using the two-equation turbulence model.

Significance
The data used to develop turbulence models were obtained from canonical flows and it is not clear how these turbulence models will perform for more realistic geometries. Successful simulation of turbulent flows on complex aircraft would provide a valuable design tool.

Future Plans
The performance of the code will be enhanced by improving the initialization process of the turbulence quantities and developing methods to handle local problem areas in the flow using an improved time-stepping procedure. Also, the So and Huang-Coakley k–ε low-Reynolds-number models and the Menter-blended two-equation model will be evaluated. The one-equation model of Baldwin–Barth will be evaluated for these complex flows. Finally, additional corrections for curvature and compressibility will be evaluated.

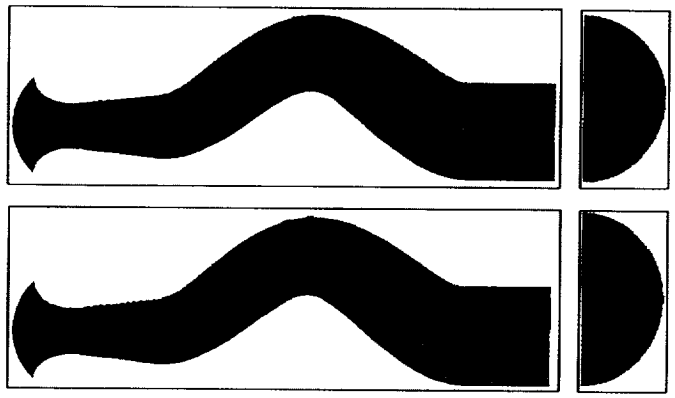

Comparison of total pressure contours along the centerline and at the engine face for a highly offset 3-D diffuser; (top) Baldwin–Lomax algebraic model prediction, and (bottom) Chien two-equation model prediction. Engine face total pressure contours are to the right of the figure.

Drag Reduction Mechanism by Riblets

Parviz Moin, Principal Investigator
Co-investigators: John Kim and Haecheon Choi
Center for Turbulence Research/Stanford University/NASA Ames Research Center

Research Objective

To perform direct numerical simulations of turbulent flows over riblets, to analyze the resulting flow data base, and to educe the mechanism of drag reduction by riblets. Such an understanding can potentially lead to the design of riblet configurations that yield even higher drag reduction.

Approach

Direct numerical simulation is used to simulate turbulent flows over riblet-mounted surfaces. A fully implicit finite-difference method is used to solve the unsteady incompressible Navier–Stokes equations in generalized coordinates.

Accomplishment Description

The computed drags on the riblet surfaces are in good agreement with the existing experimental data. The calculations with riblet spacing S = 40 and S = 20 with ridge angles of 60 degrees show 12 percent drag increase and 6 percent drag decrease, respectively. The mean-velocity profiles show upward and downward shifts in the log-law for drag-decreasing and drag-increasing cases. Turbulence statistics above the riblets are computed and compared with those above a flat plate. Differences in the mean-velocity profile and turbulence quantities are found to be limited to the inner region of the boundary layer. Velocity and vorticity fluctuations as well as the Reynolds shear stresses above the riblets are reduced in drag-reducing configurations. Quadrant analysis indicates that riblets mitigate the positive Reynolds-shear-stress producing events in drag-reducing configurations. From examination of the instantaneous flow fields, a drag reduction mechanism by riblet is proposed—riblets with small spacings reduce viscous drag by restricting the location of the streamwise vortices above the wetted surface so that only a limited area of the riblets is exposed to the downwash of high-speed fluid that the vortices induce. The total time per time step on the Cray Y-MP was 60 seconds. Thus, for each case with S = 20, approximately 200 Cray Y-MP hours were required to integrate 4,000 viscous time units, and 10 megawords of core memory and 40 megawords of disk scratch space were required.

Significance

The proposed drag reduction mechanism indicates that the skin friction on the wall can be significantly reduced by reducing the wetted surface area exposed to the downwash motion induced by the streamwise vortices above the wall or by weakening the strength of the streamwise vortices. Active and passive control strategies, aimed at influencing the streamwise vortices with the combinations of blowing and suction on the riblet surfaces, may be more effective in reducing drag.

Future Plans

We plan to investigate further other riblet configurations and active control strategies to achieve more drag reduction.

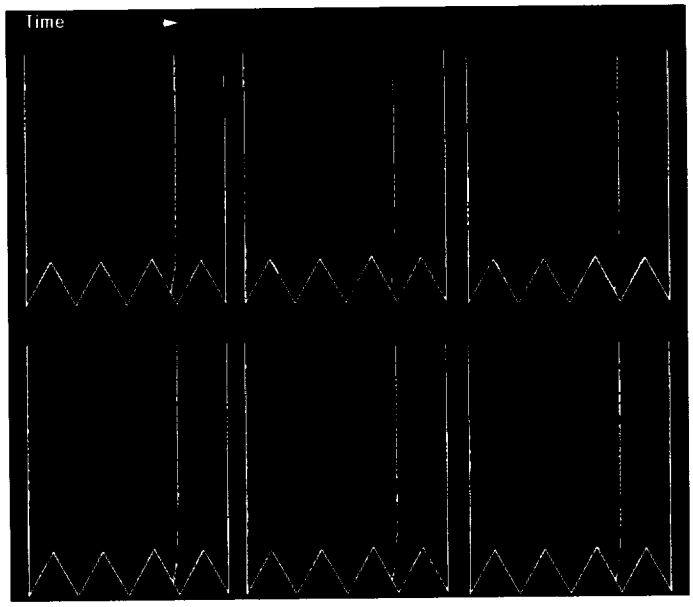

Streamwise vorticity evolution time sequence above riblets (S = 40, drag-increasing case) in coordinates moving with the structures. Flow is into the page. A strong streamwise vortex is formed in between riblets.

Turbulent Flow Over a Backward Facing Step

Parviz Moin, Principal Investigator
Co-investigator: Hung Le
Center for Turbulence Research

Research Objective
The objectives of this research are to perform a direct simulation of turbulent flow over a backward facing step with inflow and outflow boundary conditions, to generate a database for modeling, and to investigate the physics of turbulent reattachment.

Approach
A flat-plate boundary layer mean velocity profile was applied at a distance-10 step height prior to a step with superimposed random fluctuations. The fluctuations were derived using broadband spectra and were scaled to match all Reynolds stress components of a boundary-layer flow. Convective boundary condition was applied at the exit. The Reynolds number based on the step height was 5100. The simulation used approximately 13 megawords of memory and required 21 CPU seconds per time step on the Cray C-90 with 770 x 194 x 66 grid points.

Accomplishment Description
The statistical results (coefficient of friction, velocity, and turbulence intensity profiles) were in excellent agreement with the concurrent experiment at NASA Ames Research Center. The first figure shows a comparison of the simulated and experimental streamwise velocity. The mean reattachment length is 6h (h = step height). The second figure illustrates the high three-dimensionality of the flow near the reattachment with several imbedded streamwise vortices. Because of the low Reynolds number effects, a strong negative skin friction is seen in the recirculation region. At 20h downstream of the separation, the presence of the free-shear layer is still strong. In wall coordinates, the mean velocity profiles fall below the universal log-law, indicating that the flow has not fully recovered.

Significance
The simulations constitute a successful development and implementation of a method for direct computation of complex turbulent flows with inflow and outflow conditions. A comprehensive database has been archived for Reynolds averaged modeling and has up to third-order statistics.

Future Plans
The database will be analyzed to gain understanding of the physics of turbulent reattachment.

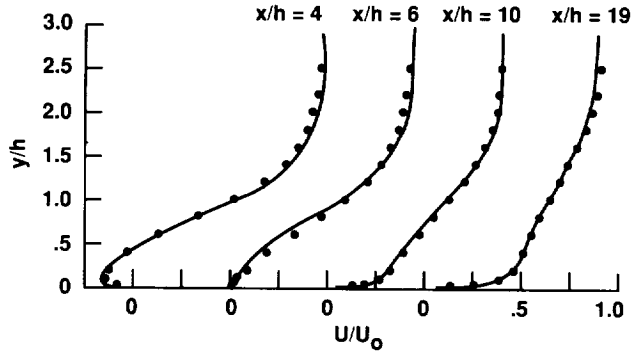

Comparison of streamwise velocity profiles; solid line = computation; dotted line = experiment.

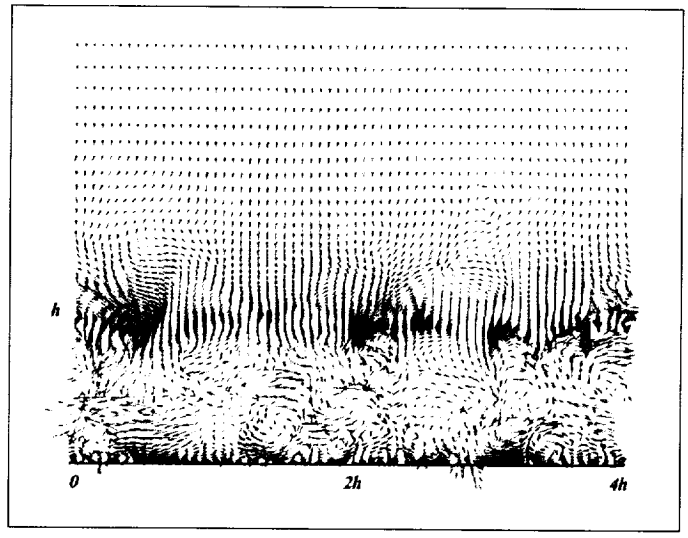

Instantaneous velocity vectors in the cross-flow plane at two step heights before reattachment. Streamwise velocity; blue = negative, magenta = positive.

Turbulence Simulation on the Connection Machine

J. Blair Perot, Principal Investigator
Co-investigator: Paul Malan
Stanford University

Research Objective
To use direct numerical simulation to investigate the fundamental fluid and heat transfer physics of wall–turbulence interactions.

Approach
The unsteady, incompressible Navier–Stokes equations and a passive scalar equation (for heat transfer) are solved using a second-order, finite-volume staggered-mesh approach in primitive variables. Time advancement is performed using a semi-implicit fractional-step method, and all the relevant scales of turbulent motion are resolved.

Accomplishment Description
A number of different boundaries were studied using grid sizes over 32 million nodes and obtaining turbulent Reynolds numbers as high as 375. Performance over a GFLOP was obtained on the CM-2, and initial results of over 500 MFLOPS were obtained using the CM-5. Detailed near-wall statistics, including Reynolds stresses, turbulent heat fluxes, and transport equation budgets, were calculated. Statistics exist for solid walls, free surfaces, permeable walls, and moving solid walls. The near-wall structures associated with kinematic effects, viscous effects, and energy transfer were fully identified. The understanding of these structures has lead to the development of a number of improved near-wall turbulence models.

Significance
Understanding and modeling near-wall turbulence is of vital importance to almost any engineering application which involves fluid mechanics. This work probes the fundamental physics of the wall–turbulence interaction and brings closer the development of rational near-wall turbulence models.

Future Plans
The effects of small mean shear on near-wall turbulence are under investigation. There are plans to evaluate large-eddy turbulence models and extend these studies to curved and rotating walls.

Publications
1. Perot, J. B.: Direct Numerical Simulation of Turbulence on the Connection Machine. Parallel Computational Fluid Dynamics 1992, Elsevier Publishing Co., 1993.

2. Perot, J. B.; and Moin, P.: A Near-Wall Model for the Dissipation Tensor. Eleventh Australasian Fluid Mechanics Conference, Hobart, Tasmania, Dec. 14–18, 1992.

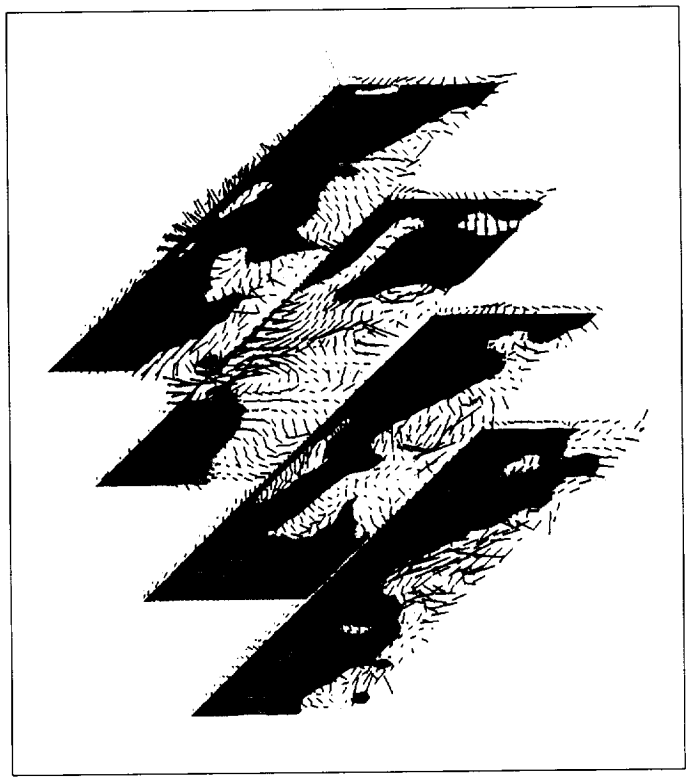

Velocity vectors and temperature contours in several planes extending perpendicularly from a shear-free wall.

Direct Simulations of Airfoil Flows

Man Mohan Rai, Principal Investigator
NASA Langley Research Center

Research Objective
To develop a methodology for performing direct simulations of compressible flow over complex geometries and to use this methodology to compute transitional/turbulent flows over a turbine airfoil subjected to moderate-to-high levels of free-stream turbulence.

Approach
High-order-accurate finite-difference methods were developed to perform direct simulations and large-eddy simulations of compressible transitional/turbulent flows over complex geometries.

Accomplishment Description
A computer program to compute transitional/turbulent flows over an airfoil cross section was constructed. Computations using this code (for subsonic Mach numbers and a prescribed level of free-stream turbulence) have been performed on a very coarse grid. Transitional/turbulent flow over a flat plate was previously computed using a direct simulation procedure. Free-stream turbulence to trigger the flows to transition was obtained numerically. The power spectrum obtained numerically only roughly approximated the Von Karman spectrum. The power spectrum from the experiment very closely approximated the Von Karman spectrum. Additionally, the power spectrum of the free-stream turbulence in the experiment closely approximates the Von Karman spectrum. In anticipation of the direct simulation of the flow about an airfoil, most of the computing resources allocated to the project were used to obtain a spectrum that is much closer to the Von Karman spectrum. The first figure shows the spectrum obtained earlier compared to the Von Karman spectrum, and the second figure shows the improved spectrum obtained through a better choice of inlet parameters. The recently obtained spectrum is in much better agreement with the Von Karman spectrum.

Significance
This computation represents a first-of-a-kind simulation of flow transition on an airfoil. The computation will yield a wealth of information that can be used to understand the transition process and develop turbulence models. The finite-difference methodology developed can be used for direct simulations of flow over other complex geometries.

Future Plans
A refined grid airfoil computation will be completed.

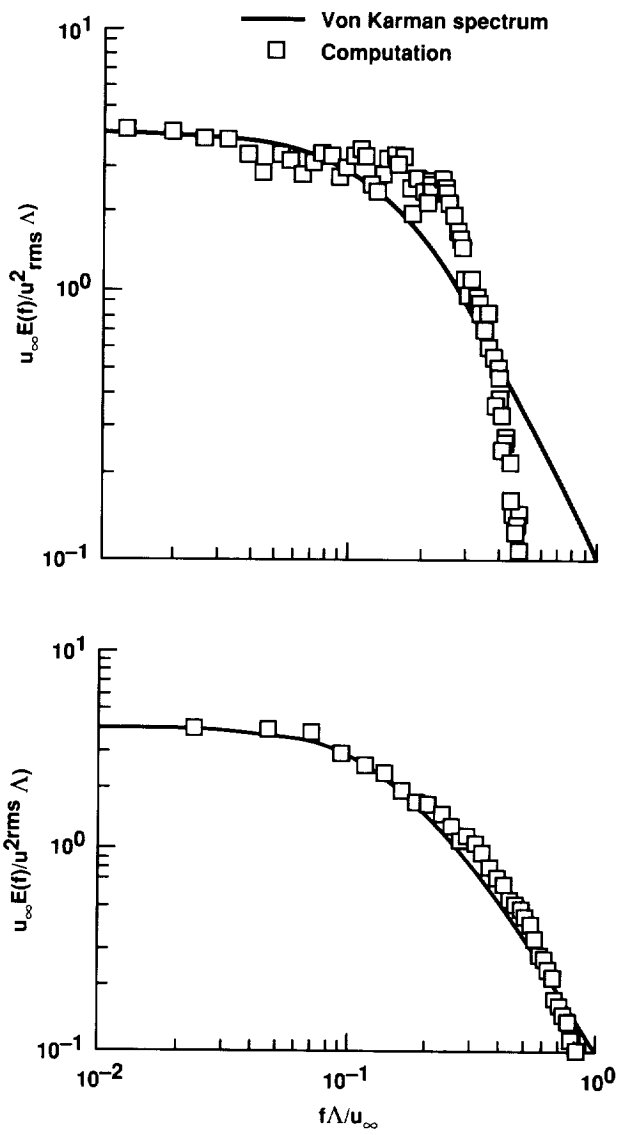

(Top) Computed power spectrum for the streamwise velocity component (used in a flat-plate simulation). (Bottom) Computed power spectrum for the streamwise velocity component (generated for the airfoil simulation).

Forced Plane Mixing Layers

Michael M. Rogers, Principal Investigator
Co-investigators: Robert D. Moser, S. Scott Collis, and Chris Rutland
NASA Ames Research Center/Stanford University/University of Wisconsin, Madison

Research Objective
To study the effects of two-dimensional (2-D) forcing on structures, statistics, and chemical reactions in incompressible fully turbulent plane mixing layers.

Approach
Direct numerical simulations of temporally evolving incompressible turbulent plane mixing layers with various levels of 2-D forcing were generated using previously simulated turbulent boundary layers to provide a realistic turbulent initial condition. Pseudospectral numerical methods were used to solve the fully three-dimensional Navier–Stokes equations.

Accomplishment Description
Three fully turbulent mixing layers with Reynolds numbers up to 20,000 were simulated. A passive scalar quantity was solved to permit the study of "fast" chemical reactions. In one case, no 2-D forcing (beyond what is present in the initial boundary layers) was used. The second case included mild levels of 2-D forcing, and the third flow was strongly forced. The first two layers evolved self-similarly, with mean velocity and Reynolds stress profiles that collapsed when scaled by the linearly increasing layer thickness. The third case was approximately self-similar, although the collapse in scaled coordinates was not as good as the other two cases. The evolution of the strongly forced case was different from the other two. The flow was dominated by large spanwise 2-D rollers with pronounced braid regions separating them in the streamwise direction (see figure). These rollers undergo a classical "pairing" process, and the large incursions of free-stream fluid engulfed in the layer result in mixed fluid with a fairly uniform scalar concentration across the layer. In contrast, the unforced and mildly forced cases do not exhibit such organization in the self-similar period. There are no "clean" braid regions separating rollers, and the mixed fluid scalar concentration across the layer resembles the mean scalar profile. The eddies in the flows provided good turbulence statistics. The profiles of all the terms in the Reynolds stress balance equation were computed to provide data for further model development. The simulations required up to $512 \times 210 \times 192$ modes. The two forced simulations required approximately 900 CPU hours and used up to 80 megawords of memory on the Cray Y-MP.

Significance
These simulations were the first turbulent free-shear-flow direct numerical simulations to achieve self-similarity. The strong effect of forcing on the layer structure helps explain discrepancies in experimental observations by different investigators.

Future Plans
Similar simulations of turbulent plane wakes will be generated.

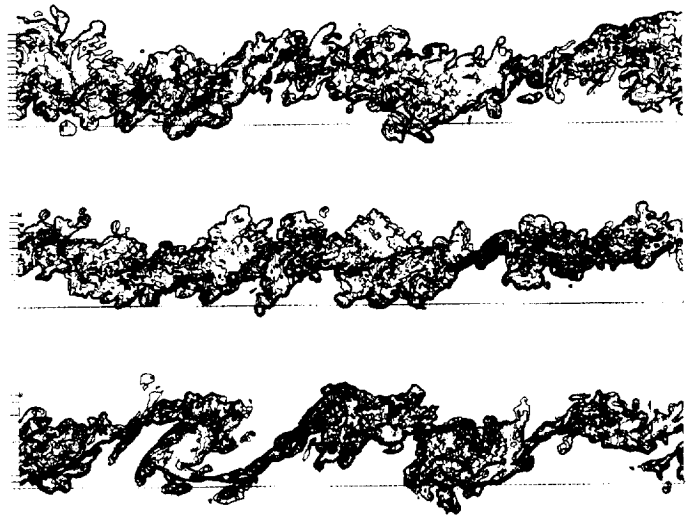

Concentration (red = high, blue = low) of passive scalar quantity in the self-similar period for the unforced layer (top), mildly forced layer (middle), and strongly forced layer (bottom). Views are at typical spanwise locations, with the streamwise direction horizontal.

Development of a Turbulent Spot

Bart A. Singer, Principal Investigator
Co-investigator: Ronald D. Joslin
High Technology Corporation/NASA Langley Research Center

Research Objective
To identify and understand the mechanisms involved in the formation and growth of a turbulent spot in a boundary layer.

Approach
Spatial direct numerical simulation (DNS) of the incompressible Navier–Stokes equations was used to generate the data for this study. Data visualization was performed using the Flow Analysis Software Tool.

Accomplishment Description
Previously, hairpin vortices were generated by a variety of different localized wall disturbances. In one case, the hairpin vortex grew, elongated, and spawned a secondary vortex head upstream of the primary vortex and a subsidiary vortex developed beneath the hairpin vortex legs. Work continued the DNS into the early stages of a turbulent spot. As the flow became more complicated and smaller scales developed, the resolution requirements rose from 5.8 to 8.9 million grid points, increasing the core memory requirements for the code from about 125 to 200 megawords. Approximately 500 Cray-2 hours were required in the computation. Multiple additional vortices developed in the flow. These vortices fell into three categories: (1) new hairpin vortex heads, (2) horseshoe vortices forming beneath other vortex legs, and (3) quasi-streamwise vortices. Examples of each can be seen in the first figure (low-pressure regions are used to mark the vortex cores). Beneath the hairpin vortex in the upstream portion of the flow is a small horseshoe vortex. The elongated structures in the figure consist largely of streamwise vorticity. The vortices seem to form the core region of a developing turbulent spot. In the second figure, a plan view of vertical vorticity contours reveals the arrowhead shape of a turbulent spot.

Significance
This work provides a better understanding of the way in which coherent flow structures evolve from a single localized disturbance to a group of structures that form the early stages of a turbulent spot. Clues are provided regarding the types of structures that dominate the flow and how these structures interact and regenerate, resulting in a more turbulent flow. These insights should result in more realistic models for predicting flows in the transition region.

Future Plans
The calculation will be continued until a fully developed turbulent spot is obtained. Data will be analyzed to understand how the various types of vortices form, interact, and regenerate. As new data become available, the role that the vortices play in engulfing new fluid into the turbulent region will be studied. Transition region modeling information will be obtained.

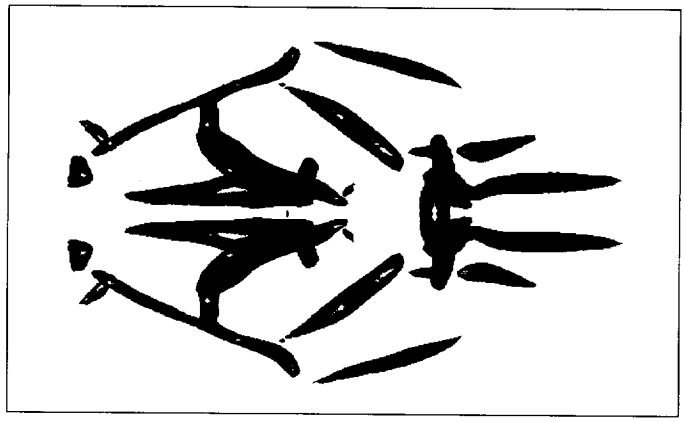

Plan view of low-pressure regions in flow. Flow goes from left to right.

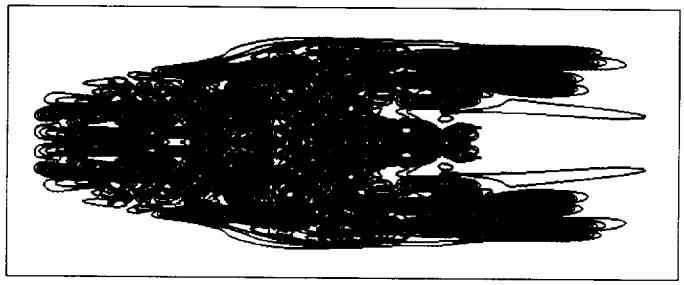

Plan view of vertical vorticity magnitude. Vorticity levels: red = high and blue = low.

Effect of Suction Holes

Philippe R. Spalart, Principal Investigator
Boeing Commercial Airplane Group

Research Objective
To understand and predict better the fluid dynamics associated with suction holes used in laminar flow control to prevent the transition of a boundary layer to turbulence.

Approach
Direct numerical simulations (DNS) were used to produce solutions to the full Navier–Stokes equations in boundary layers under conditions characteristic of the flow over a wing. The "swept Hiemenz flow," a classical exact solution of the Navier–Stokes equations, was considered with focus on stationary crossflow disturbances. The suction holes were represented by a prescribed nonzero, non-uniform normal velocity at the wall. Single rows and arrays of holes were treated. The Reynolds number, row location, hole diameter, hole spacing in each direction, and flow rate led to a large parameter space.

Accomplishment Description
About 20 converged solutions were obtained and grid-refinement studies were conducted. Linearity was checked when appropriate. In combination, these solutions allowed the calculation of the "receptivity coefficient," which gave the initial amplitude of the crossflow vortex created by the suction holes. The enhanced receptivity when the crossflow vortex was aligned with the holes was computed. The figure shows the streamwise direction and u' is the amplitude of the crossflow vortices, normalized by the average suction velocity. Pure crossflow vortex eigenmodes became unstable near $x = 250$. For x less than about 400, the response was dominated by the local disturbances identified with each row; their spacing was 10. Beyond $x = 400$ an unstable mode overshadowed the local disturbances and a fairly smooth growth curve was seen. The curve with square symbols had a low suction rate, which allowed rapid growth of the instability. The curve with diamonds had a much higher suction rate, which considerably reduced the rate of growth without completely suppressing it. The normalized amplitudes were very close around $x = 300$; thus the receptivity coefficient was not strongly affected by the suction level. The central processing unit time was several hundred hours for fully turbulent solutions and the central memory was up to 10 megawords.

Significance
Receptivity theories are making rapid progress, but it is essential to obtain quantitative results by other means in order to validate them. It is also necessary to find out when theories fail because of nonparallel, nonlinear, or similar effects. The conjunction of DNS and more theoretical approaches substantially improves the production of competitive designs for laminar flow control suction systems.

Future Plans
Related instability issues in three-dimensional boundary layers are being explored using a pressure distribution more realistic than in Hiemenz flow.

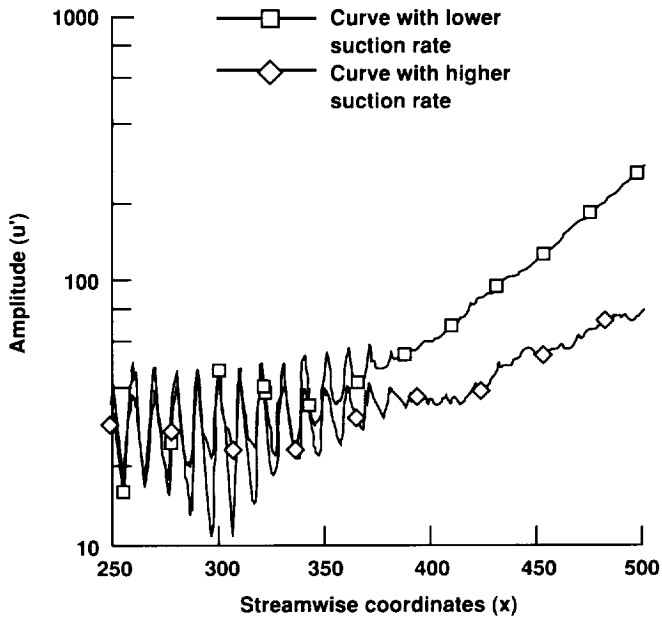

Crossflow vortices created by arrays of holes.

PAGE 116 INTENTIONALLY BLANK

General

Astronautics

Astronomy

Atmospheric Science

Chemistry

Computer Science

Electromagnetics

Fluid Mechanics

Hydrodynamics

Life Science

Reactive Flow

Space Science

Structural Mechanics

Space Station Flow Analysis

Paul McConnaughey, Principal Investigator
Co-investigators: Eric Stewart, Bruce Vu, and Lee Kania
NASA Marshall Space Flight Center/Sverdrup Technology, Inc.

Research Objective
To facilitate the design of the air distribution system aboard Space Station Freedom. By performing computational fluid dynamics (CFD) analyses of the internal ventilation flows, the ability of the air distribution system to satisfy performance requirements will be assessed and any shortcomings exposed. The results will be used by the environmental control and life support system (ECLSS) design team to devise any necessary system modifications.

Approach
The CFD analyses were performed with the INS3D code. The code was modified to permit the use of blocked grids, and it exhibited only a small increase in the characteristic time. The flow-field analyses were also conducted using an algebraic turbulence model specifically calibrated for internal ventilation flows. The model proved to be an acceptable compromise between computational efficiency and accuracy. A steady-state flow solution was obtained with volumetric flow rates specified at each of the ventilation registers.

Accomplishment Description
Grids were generated for a generic module and resource node and were comprised of 1.88 and 3.3 million points, respectively. The resource node contained eight supply registers and seven return registers. A converged, turbulent flow field was obtained in 11,000 iterations and required 160 Cray-2 hours and 57 megawords of memory.

Significance
The air distribution system produced average velocities in the range of 40 feet per minute, thus satisfying the ECLSS design requirement in limited portions of the node only. There were regions of low-speed flow and short-circuit ventilation that indicated the ventilation registers were not optimally located. These flow-field data will be used in conjunction with test data to devise modifications to increase system efficiency.

Future Plans
The node and module elements will be coupled via a berthing vestibule and the flow-field analysis will be repeated. Additionally, the flow fields will be used for performing contaminant tracking analyses in the design of the fire protection systems.

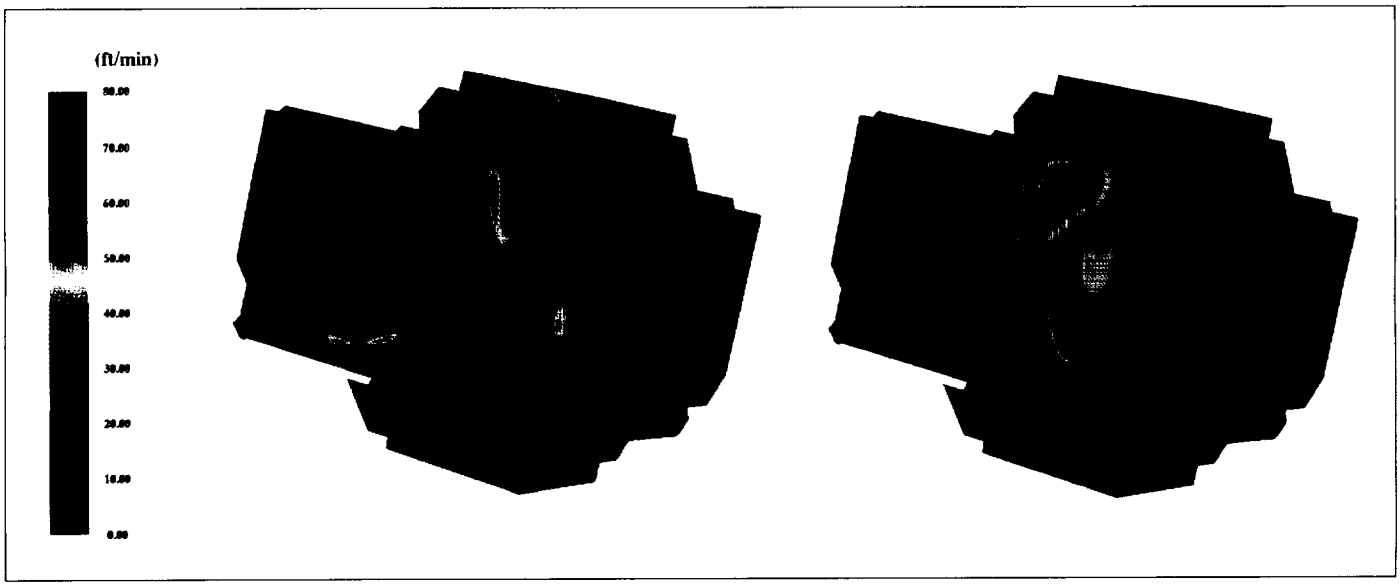

Resource node velocity magnitude contours; supply registers are green, return registers are red.

Parallel Integration of N-body Gravitational Systems

Jeffrey D. Scargle, Principal Investigator
Co-investigators: Jeffrey N. Cuzzi, Anthony Dobrovolskis, Luke Dones, Robert Hogan, Creon Levit, Mark Showalter, and Karl Young
NASA Ames Research Center

Research Objective
By simulating the long-term dynamical evolution of the satellites and ring particles of the planet Saturn, many questions were addressed: How did Saturn's ring structure originate? How stable is the configuration now observed? What is the connection between the shepherd satellites, Prometheus and Pandora, and the narrow, kinky F Ring that lies between them?

Approach
Direct numerical integrations were completed for the Newtonian equations of motion for a system with an oblate Saturn, its 18 most massive satellites, and a large number of massless particles. Accurate orbital trajectories and the largest local Lyapunov exponent of the system were computed to detect chaotic dynamics. Orbital integrations were carried out with a parallelized Bulirsch–Stoer integrator.

Accomplishment Description
A series of runs following the evolution of 8,000 moonlets uniformly distributed in the vicinity of the orbits of the shepherd satellites Prometheus and Pandora was completed. The moonlets underwent forced motions on short and long time scales and achieved orbital eccentricities on the same order as the F Ring. Their semimajor axes were redistributed much like the structure of the F Ring. Shepherd motion was not chaotic, but the local Lyapunov exponent was occasionally positive for some moonlets, indicating the presence of mildly chaotic, bounded excursions of these particles. A connection for observable chaotic variations in the orbital elements was established, allowing interpretation of relatively short integrations (thousands of years) in terms of long effects (millions to billions of years).

Significance
Orbits of the shepherding satellites are quite regular and will not evolve significantly over time equivalent to a large fraction of the age of the solar system. The motion of massless particles exhibits a mild form of chaos in which the orbits wander pseudo-randomly within a bounded region. Thus the system is chaotic, but also stable, against large-scale disruption over relatively long times.

Future Plans
Test particles will be distributed over the entire ring system. Estimates of the strengths of resonant and nonresonant interactions between satellites and test particles suggest that the structure of Saturn's main ring system is a result of dynamical effects. Computations will be done to learn more about the origin, evolution, and stability of the rings.

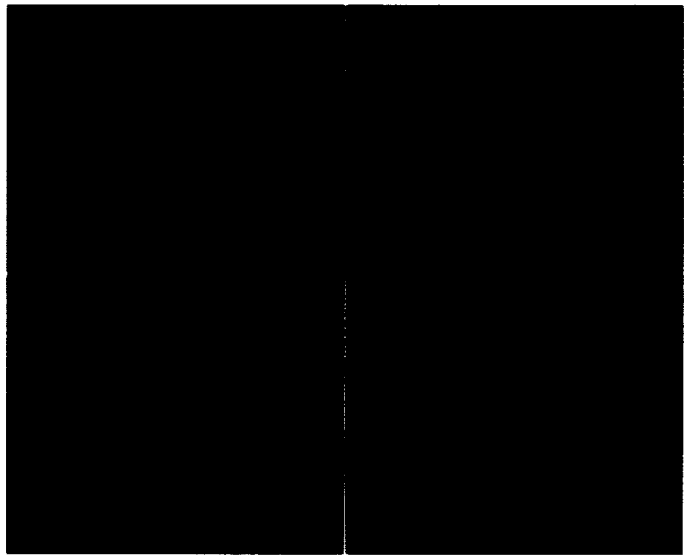

Evolution of orbital elements of an ensemble of 8,000 test particles surrounding Saturn's shepherd satellites Prometheus and Pandora. Upper panels based on the best estimates for the masses of Prometheus, and lower panels for masses twice as large. Left panels: initial semimajor axis of each particle plotted against its semimajor axis. Color indicates the eccentricity of the particle (red = circular orbit, blue = largest eccentricity). The X-shaped patterns are particles trapped in "horse-shoe" orbits. The reddish bar near the center is comprised of particles largely undisturbed by the shepherds. Right panels: semimajor axis of each particle plotted against its eccentricity; color indicates the inclination of the orbit relative to the main orbital plane of Saturn.

Numerical Experiments in the Formation and Evolution of Galaxies

Bruce F. Smith, Principal Investigator
Co-investigators: Richard H. Miller and Thomas Y. Steiman-Cameron
NASA Ames Research Center/University of Chicago/University of California, Santa Cruz

Research Objective
To develop numerical experiments to study the important dynamical processes at work in the formation and subsequent evolution of galaxies.

Approach
The numerical experiments were based on the time development of a fully three-dimensional, self-gravitational, and self-consistent particle system. The codes followed the motions of 10^5–10^6 particles that represent the stellar and gaseous components of galaxies. The gravitational potential and forces were calculated on a 256^3 grid.

Accomplishment Description
The particle codes were used on the Cray-2 and the Cray Y-MP to investigate several important problems in galactic dynamics. Observations and numerical experiments indicated that significant noncircular motions are present in disk galaxies. Global galactic oscillations were identified in galaxy models. The experiments suggested that normal-mode oscillations may be present in nearly all galaxies, including the Milky Way, at considerably higher amplitude than previously thought. The effects of these oscillations may be most prominent in disk galaxies. Recently, experiments were conducted on the dynamics of spiral galaxies embedded in oscillating, dark-matter halos. The results indicated the development of ring structures that can become offset relative to their center and the development of bars that are often observed.

Significance
Observations of galaxies give us intriguing snapshots of complex, evolutionary sequences. The numerical experiments proved to be an effective approach to understanding the dynamic sequences in galactic evolution. This computational capability is necessary to understand the wealth of new astronomical data becoming available from the Hubble space telescope and other new observational platforms. The results on the nature of non-steady-state motions in galaxies have a profound effect on our understanding of the morphology and dynamics of galaxies.

Future Plans
Additional physics will be incorporated into the codes used for the numerical experiments. The gas dynamics representing the gaseous component in galaxies was developed, and preliminary runs are under way. High-resolution studies of the interplay between stellar and gas dynamics are now possible, allowing galaxy formation studies and studies of galaxy interactions with highly stimulated star formation.

Various views of the warping of a disk galaxy after it has been captured by a larger nearby galaxy.

Numerical Simulations of Baroclinic Instability

Jeffrey R. Barnes, Principal Investigator
Oregon State University

Research Objective
To investigate nonlinear baroclinic instability and transient baroclinic eddies in the atmospheres of Mars and Earth through numerical simulation.

Approach
A three-dimensional, spectral, primitive-equation model of atmospheric circulation was employed to simulate the nonlinear evolution of transient baroclinic eddies. This model offered computational efficiency via a semi-implicit time scheme, high spatial resolution, flexibility in configuration, and on-line energy diagnostics.

Accomplishment Description
Synthetic basic states were developed for use in the nonlinear Mars simulations. Several states were fully global, but they proved to be computationally troublesome. A large set of single-wave experiments were performed using a hemispheric basic state (representing the winter flow). The simulations yielded several interesting results. There was great variation in structure between the longer (waves 1 and 2) eddies and the relatively short eddies (wave 4). The long eddies were extremely deep and latitudinally broad and exhibited maximum amplitudes at very high levels (above 20–30 kilometers altitude), while the short eddies were much shallower and more latitudinally confined. Wave 3 was an intermediate case, and it tended to reach the largest amplitudes in the simulations. Wave 4 had a close balance between energy conversions producing growth and decay, and thus the wave amplitude (and structure) stayed nearly constant. The longer eddies tended to have a "life cycle" behavior—the waves grew to large amplitudes and then decayed to relatively small amplitudes.

Significance
Transient baroclinic eddies are of great importance for the Earth's atmospheric circulation in middle latitudes. Cyclonic weather systems are manifestations of these eddies, which transport large amounts of heat poleward. Major NASA programs are directed at an enhanced understanding of the atmospheric heat balance and the global climate system. Spacecraft observations show that transient baroclinic eddies are present in the atmosphere of Mars, and observations and modeling demonstrate that they are of considerable importance for the atmospheric circulation and the climate system. The terrestrial and Martian atmospheres are similar in many ways; thus they constitute two "laboratories" where the basic dynamics of transient baroclinic eddies can be investigated.

Future Plans
Mars Observer data should soon yield a great deal of information on the structure of the transient eddies and the structure of atmospheric basic states. Mars Observer will also obtain very accurate topographic measurements. These new data should make it possible to launch a much more detailed modeling study of the dynamics of the transient eddies, with extensive examination of their seasonal, hemispheric, and interannual variations.

Publication
Barnes, J. R.; and Young, R. E.: Nonlinear Baroclinic Instability on the Sphere: Multiple Life Cycles with Surface Drag and Thermal Damping. J. Atmos. Sci., vol. 49, 1992, pp. 861–878.

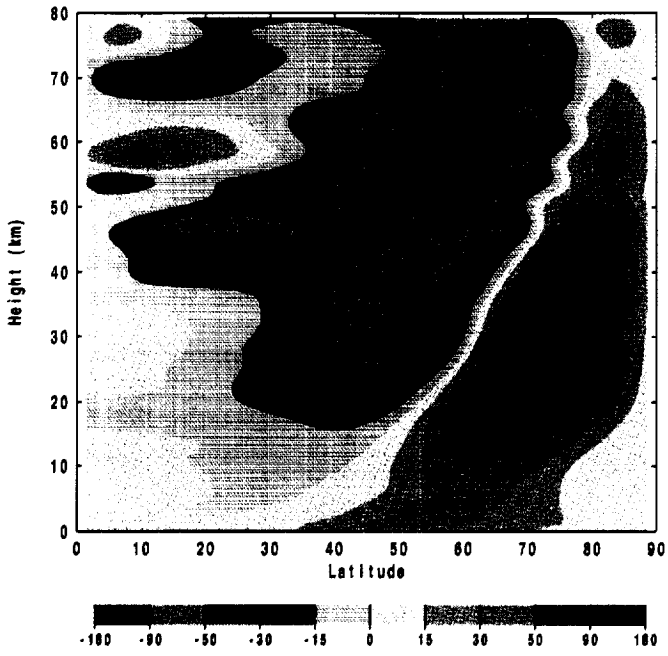

Latitude-height cross section of the north–south heat flux by a zonal wave 1 disturbance in a nonlinear simulation of baroclinic instability in the Mars atmosphere.

Orographically Forced Oscillations in the Martian Atmosphere

Christian L. Keppenne, Principal Investigator
Jet Propulsion Laboratory

Research Objective
The intraseasonal time scales of the terrestrial atmosphere's variability are dominated by oscillations induced by barotropic instability over orography. Since the irregularities of Earth's and Mars' surface reliefs compare similarly to their respective scale heights, orographically forced modes should also be expected in the Martian atmosphere. A model is used to search for such oscillations.

Approach
A high-resolution barotropic model with realistic Martian topography was run in several 6,000-sol (1 sol = 1 Martian day) integrations. The model was based on the same set of dynamical equations as terrestrial general circulation models, but its formulation did not account for thermodynamic processes such as the cycles of water on Earth or of carbon dioxide on Mars. As a result, barotropic instability over orography is the main cause of variability. The atmospheric angular momentum (AAM) of the last 5,000 sols of each run were submitted to maximum entropy spectral analysis. Extended empirical orthogonal function analysis was applied to the model's pressure field in order to analyze the spatial structure of the variability identified in the AAM time series.

Accomplishment Description
The code was multitasked on the Cray Y-MP. The prognostic equations were integrated in spherical harmonic space using a semi-implicit scheme, but the nonlinear terms were computed on a latitude–longitude grid. At high resolution, performance came close to 1 GFLOP using all 8 processors. At more modest resolution, performance decreased to 500 MFLOP (0.2 second/sol) and memory use was about 8 megawords. A robust oscillation with a mean period near 85 sols was identified. Two other, shorter period oscillations with mean periods near 3 and 6 sols were also present. The power spectra of local-pressure time series correspond well to those of the Viking Lander I and II data. This data suggests that orographically forced instability can play a significant role in triggering the Martian atmosphere's observed variability.

Significance
The oscillations identified are of sufficient amplitude to dominate the Martian atmosphere's intraseasonal variability. Not only does the study lead to advancements in Martian climatology, but an improved understanding of the mechanisms involved should have repercussions in the meteorology of Earth and other planets.

Future Plans
The model will be used to develop a sophisticated data assimilation scheme for Mars Observer data. This will result in near-optimal weights to combine observations and model data in order to obtain a better picture of the Martian atmosphere than could be provided by either the observations or model alone.

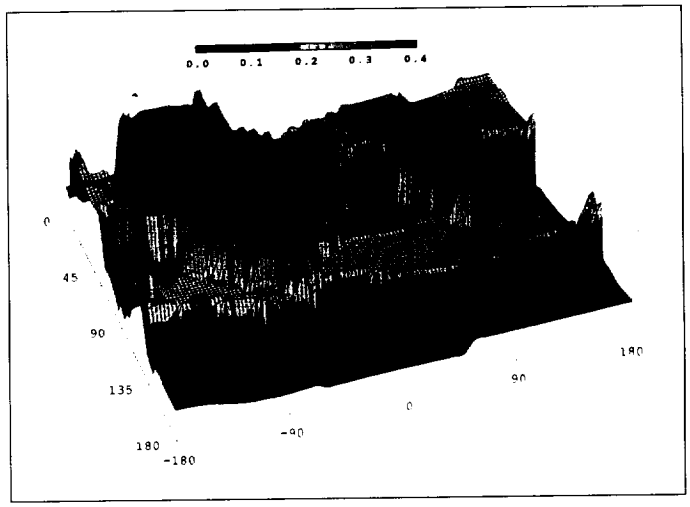

Geographical distribution of the frequency corresponding to the highest spectral density in the model's local-pressure time series. The latitude and longitude axes are labeled in degrees and frequencies are expressed in cycles/sol.

Dynamics of the Martian Atmosphere

James B. Pollack, Principal Investigator
Co-investigator: Robert Haberle
NASA Ames Research Center

Research Objectives

To simulate the present and past climate regimes on Mars. The tool used to do these simulations was a general circulation model (GCM) that predicted the time-evolving three-dimensional wind and temperature fields and surface pressure, temperature, and carbon dioxide ice abundance.

Approach

The Mars GCM was based on the primitive equations of meteorology used for terrestrial weather prediction. Uniquely Martian physics, such as the condensation and sublimation of carbon dioxide in the polar region, were incorporated into the Mars GCM. The Mars GCM was interfaced with an aerosol physics model to simulate the transport of dust by winds and the impact of absorption of sunlight by dust on temperatures and winds.

Accomplishment Description

Analyses of GCM simulations at different seasonal dates and dust loadings were carried out to define the properties of several major components of the atmospheric circulation. Eastward propagating high- and low-pressure systems develop at middle latitudes of the winter hemisphere. Their simulated properties compare favorably with meteorological measurements. Simulations required 250 Cray-2 hours, with a typical job using 5 megawords of memory.

Significance

From an atmospheric dynamical perspective, the Martian atmosphere represents the closest analogue to the Earth's atmosphere. By testing climate models extensively used for the Earth in other planetary atmospheres, we can assess the validity of these models and our understanding of basic dynamical processes. The traveling high- and low-pressure systems of the Martian atmosphere are produced by the same basic mechanism as the baroclinic instability that causes middle latitude weather on Earth. The Mars GCM predicts that the traveling lows and highs on Mars are more periodic than the ones on Earth, and it is in agreement with spacecraft data.

Future Plans

Improved simulations of the general circulation of the Martian atmosphere will be carried out using higher spatial resolution and introducing a parameterization for drag due to vertically propagating gravity waves.

Publication

Pollack, J. B.; Haberle, R. M.; Murphy, J. R.; Schaeffer, J.; and Lee, H: Simulations of the General Circulation of the Martian Atmosphere. Two Seasonal Pressure Variations. J. Geoph. Res., vol. 98, 1993, pp. 3,149–3,181.

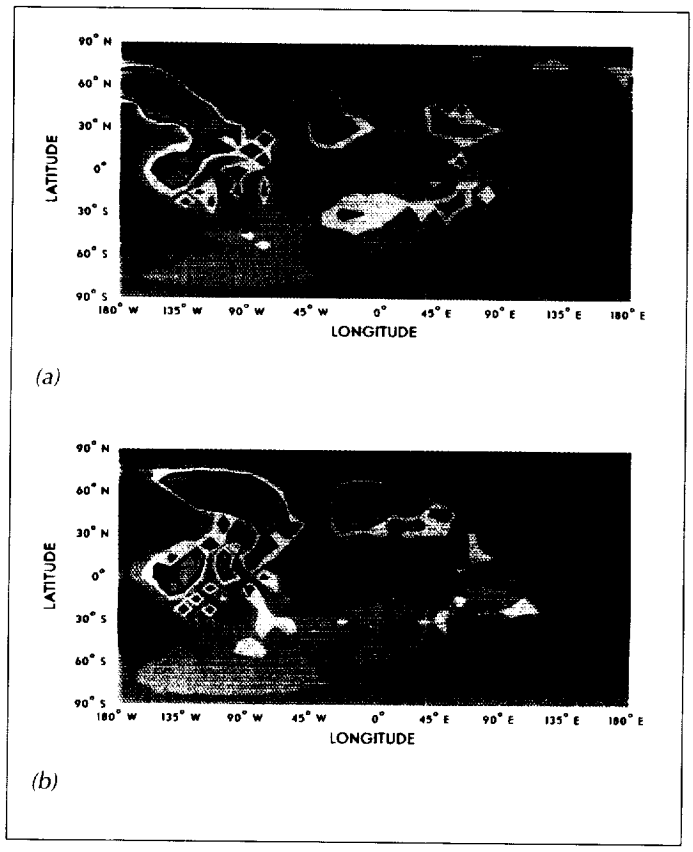

Surface pressure maps corrected for topography. The dark red and dark blue regions have pressures of –7.0 millibar and +0.45 millibar, respectively, relative to the zonal average. (a) Time = 984 hours; (b) time = 1,008 hours. Note the eastward displacement of highs and lows in (b), which is one Martian day later than (a).

Simulation of Volcanic Aerosol Clouds

Richard E. Young, Principal Investigator
Co-investigators: O. B. Toon and J. B. Pollack
NASA Ames Research Center

Research Objective

To numerically simulate the behavior of the El Chichon and Mt. Pinatubo volcanic aerosol clouds in the stratosphere in order to better understand stratospheric transport and aerosol microphysical processes. An associated goal is to assess the climatic impact of such large volcanic eruptions on stratospheric wind and temperature fields.

Approach

A three-dimensional (3-D), spectral, primitive equation model was used to compute wind and temperature fields in the stratosphere. The model was coupled to a 3-D aerosol transport and microphysical model, which computed the dispersion of the volcanic aerosol cloud using the computed winds from the circulation model.

Accomplishment Description

Both noninteractive and interactive tracer simulations for the Mt. Pinatubo (eruption latitude 15° north) volcanic aerosol cloud have been conducted for the first 3 months following the eruption. Each 3 month simulation required about 6 Cray Y-MP hours and 16 megawords of memory. The results were compared to the satellite, airborne, and ground-based data sets that exist for the aerosol cloud. Most of the aerosol mass resided in the stratosphere above 20 kilometers (km) altitude. The simulated Mt. Pinatubo cloud spread rapidly southward as observed only when interactive heating of the aerosol cloud was accounted for, reaching 20° south latitude within weeks after the eruption. The interactive model simulations reproduced these characteristics. The figure compares the simulated Mt. Pinatubo volcanic gas and aerosol cloud after it had circumnavigated the globe once with and without interactive heating. The noninteractive cloud (top) basically stays north of the equator; the interactive simulation (bottom) produces a cloud that spreads rapidly southward. Initially the cloud was a column 20–25 km over the Philippine Islands, but eventually it spread out because of wind shear.

Significance

Unique opportunities to better understand stratospheric transport and aerosol microphysical processes occurred when the El Chichon and Mt. Pinatubo erupted—the two largest volcanic eruptions this century in terms of aerosol material injected into the stratosphere. A comprehensive climatology of the subsequent dispersal of the volcanic clouds, gathered from aircraft, satellite, and ground-based observations, has been compiled for the years immediately following the eruptions. By simulating the behavior of the volcanic clouds, theoretical understanding of transport and aerosol processes in the stratosphere can be assessed and improved.

Future Plans

Multiyear simulations of both the Mt. Pinatubo and El Chichon volcanic aerosol clouds will be conducted in passive-tracer and interactive mode. Climatic feedback on the stratosphere will be assessed.

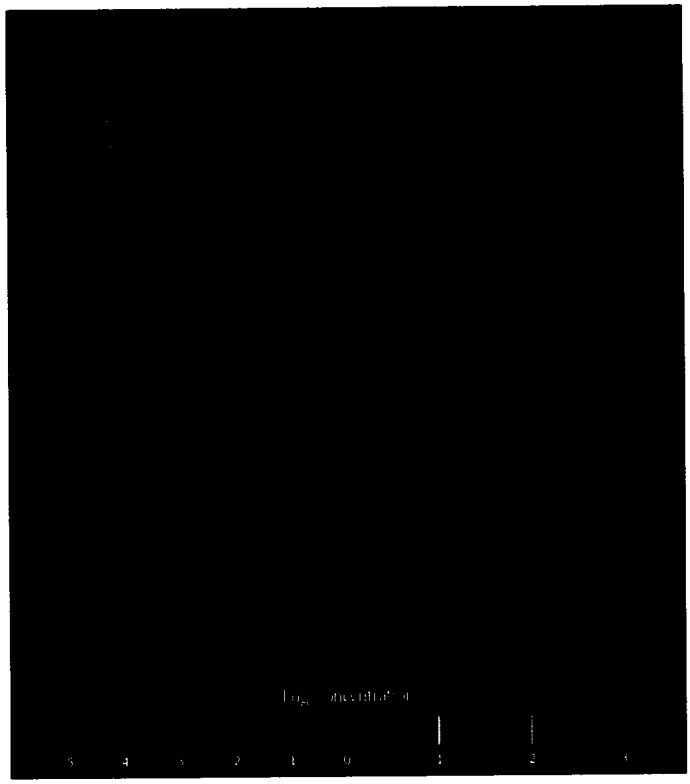

Comparison of noninteractive simulation (top) with interactive simulation (bottom) where heating of the volcanic cloud due to infrared radiation from the troposphere is accounted for. Solar heating is much smaller. Dotted lines represent 15° of latitude.

Propane–Air Combustion Mechanism

Richard L. Jaffe, Principal Investigator
Co-investigators: Charles W. Bauschlicher, Harry Partridge, David Schwenke, Christopher Dateo, and Stephen P. Walch
NASA Ames Research Center/Eloret Institute

Research Objective

To support the development of a detailed propane–air combustion model, which is being used to optimize the design of the propulsion system for the High-Speed Civil Transport (HSCT) under the High-Speed Research Program (HSRP), by calculating thermodynamic properties, transport coefficients, and reaction-rate coefficients for intermediate species formed during the combustion process.

Approach

Ab initio quantum chemistry methods were used to compute potential energy surfaces for individual molecular species or pairs of species. Collision cross sections and reaction-rate coefficients were computed for binary collisions with intermolecular forces determined from the gradients of the potential energy surface.

Accomplishment Description

There were four major accomplishments: (1) the accurate heat of formation of hydroperoxy radical (HO_2), universally the most important combustion intermediate, was computed to reduce the uncertainty in experimental determinations; (2) the thermodynamic properties of benzyl alcohol were computed to resolve a factor of 20 discrepancy in conflicting thermodynamic property data bases; (3) the potential energy surfaces were computed for methanol decomposition (CH_3OH) and for the prompt NOX initiation reaction $CH + N_2 \rightarrow N + HCN$; and (4) the high-temperature rate constants for the important chain branching reaction $H + O_2 \rightarrow OH + O$ (see figure) were computed. The calculations used 1,000 Cray-2 hours and required 15–24 megawords of memory and at least 300 megawords of temporary disk space. The HO_2 calculations required more than 1 gigaword of disk space.

Significance

These calculations provide input to detailed combustion models used for predictions of engine performance. Particular emphasis is placed on predicting the amount of NOX pollutants that would be formed during engine operation. One of the major goals of the HSRP is to design a nonpolluting supersonic aircraft engine.

Future Plans

Work will continue on individual aspects of the combustion mechanism for propane–air and propane–toluene–air systems.

Publications

1. Bauschlicher, C. W.; and Partridge, H.: Accurate Determination of the Heat of Formation of HO_2. Chem. Phys. Letters, vol. 208, 1993, p. 241.
2. Walch, S. P.: Theoretical Characterization of the Reaction $CH_3 + OH \rightarrow CH_3OH \rightarrow$ Products: The $CH_2 + H_2O$, $H_2 + HCOH$, and $H_2 + H_2CO$ Channels. J. Chem. Phys., vol. 98, 1993, p. 3,163.

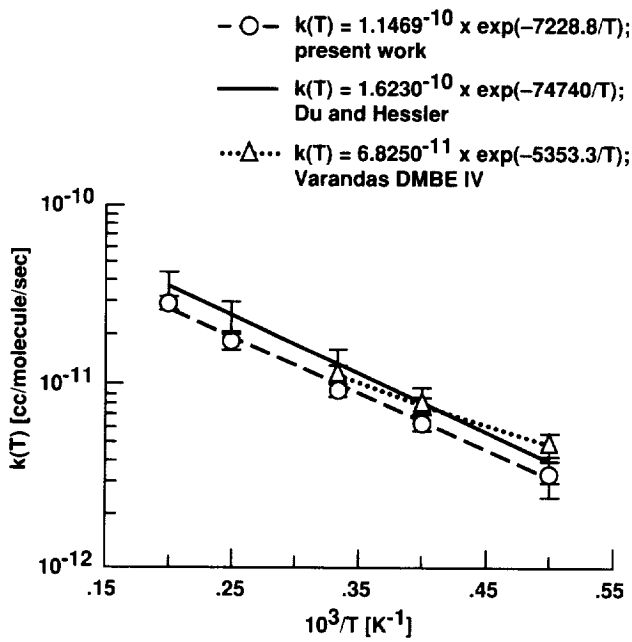

$H + O_2 \rightarrow O + OH$ rate coefficients.

Boost Phase Detection Studies

Stephen Langhoff, Principal Investigator
Co-investigators: Charles Bauschlicher, Richard Jaffe, Timothy Lee, and Harry Partridge
NASA Ames Research Center

Research Objective
To determine the radiation signature from the hard-body missile bow shock layer during the assent phase of the trajectory. Also studied was the chemistry occurring in the plume of the rocket because radiation from the plume constitutes a large part of the optical signature.

Approach
Computational chemistry methods were used to determine radiative intensity factors, transport properties, electron impact excitation cross sections, and reaction rate constants for air species under thermal nonequilibrium conditions. These methods were also used to determine the electronic structures and vibrational frequencies of polyatomic molecules in the plume.

Accomplishment Description
Electronic transitions in the nitrogen–oxygen (NO) molecule constituted an important source of radiation in the bow shock layer of hard bodies. Extensive theoretical calculations were done to determine the band strengths of the Ogawa band system of NO. To determine accurate electronic transition probabilities required 4 Cray hours and about 20 megawords of memory at each internuclear distance. Calculations were also carried out to characterize the quintet states of carbon–oxygen (CO). These states have not been characterized experimentally and they are potential precursor states for populating the upper state of the Cameron band system, which is prominently observed in plumes. Calculations showed that the quintet pi state was significantly bound. Furthermore, transitions between this state and the low-lying triplet states explained perfectly the emission spectrum between about 360–520 nanometers observed in a matrix. The calculations showed, however, that this could not be a mechanism for explaining the long-lived chemiluminescence from the Cameron band system. The relevant potential energy curves are shown in the figure.

Significance
Accurate transition probabilities are required to characterize the radiation from the bow shock in front of hard bodies and from the plume. The theoretical band strengths from this study are very accurate and remove one source of error in modeling the radiation. Calculations on the quintet states of CO have clarified their role in the spectroscopy of this molecule.

Future Plans
The study of selected band systems will continue. The goal is to characterize band systems that contribute to the radiation signature at wavelengths less than 2,000 angstroms.

Publication
Bauschlicher, C. W.; Langhoff, S. R.; and Partridge, H.: Theoretical Study of the Lowest Quintet Pi and Sigma States of CO. J. Chem. Phys., vol. 98, 1993, p. 8,785.

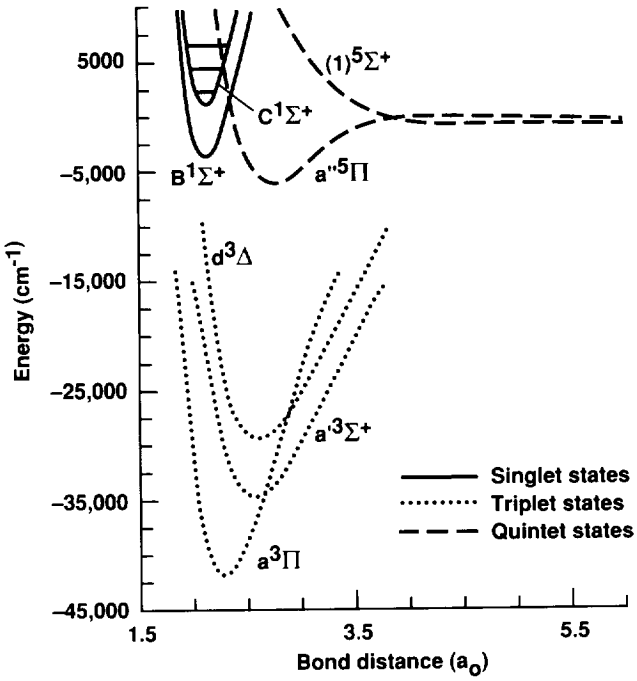

Computed potential energy curves for the lowest quintet pi and sigma states and the Klein Dunham curves for selected singlet and triplet states of CO. Horizontal lines denote the positions of the first three vibrational levels.

Computer Simulation of Astrophysical Ices

Michael A. Wilson, Principal Investigator
Co-investigator: Andrew Pohorille
NASA Ames Research Center

Research Objective
To create a computer simulation of water ices formed under astrophysical conditions.

Approach
A direct molecular dynamics (MD) computer simulation of deposition events was completed. A low-density amorphous (LDA) ice substrate was prepared by annealing a system of 343 water molecules from 300 K at a density of 0.94 grams per cubic centimeter. This substrate was then used for deposition of water and guest molecules from vapor.

Accomplishment Description
Computer simulations of hot (300 K) and cold (77 K) deposition of water molecules onto a cold LDA ice substrate were performed. The structure of the emerging ice retained much of the tetrahedral structure of the LDA ice, but the deposition experiments at 77 K were characterized by large void regions, whereas the 300 K simulations yielded a more compact structure. This compact structure occurred because of the larger net energy of the 300 K molecules, which allowed greater surface reconstruction after deposition. Computer simulations of co-deposition experiments of water with argon, krypton, and methane (in a ratio of 20:1) were carried out at 77 K. The ices formed in the co-deposition experiments were similar to the pure ices. The guest species were found to stick with probabilities of nearly one. Deposition simulations were also tried with neon, but it did not bind to the water substrate at 77 K. Preliminary studies showed that the microporous structure became denser upon warming and some outgassing occurred. Individual runs required about 15 Cray Y-MP hours and less than 8 megawords of memory.

Significance
Laboratory experiments on water ices involve depositing hot water molecules onto cold substrates. These conditions differ from astrophysical conditions, where the impinging molecules are at about the same temperature as the substrate. Consequently, the morphology of ices created in the laboratory might be quite different from those formed in the outer solar system.

Future Plans
We will investigate the structural changes and outgassing that occur upon heating and will calculate the thermal conductivity of amorphous ices.

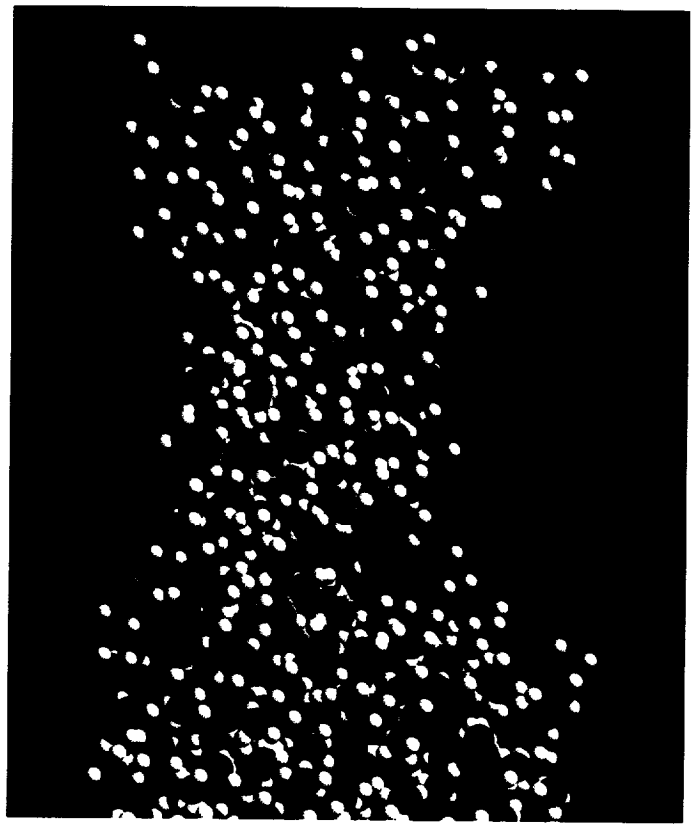

Surface of the system of water and krypton co-deposition experiment after 400 depositions. Ratio of argon to water = 1:20. Temperature of the impinging molecules and the substrate = 77 K. Neither the water nor the krypton atoms are particularly mobile on the surface of the substrate after they have been deposited. Periodic boundary conditions were used in the x (horizontal, points out of the page) and y (vertical) directions.

Radiation Effects in Intermetallic Compounds

James P. Wolfe, Principal Investigator
Co-investigators: Robert Averback and Huilong Zhu
University of Illinois, Urbana/Champaign

Research Objective

To investigate the atomistic processes that occur in intermetallic compounds during irradiation with heavy ions and to determine the number of defects produced and the amount of atomic disordering that takes place in displacement cascades.

Approach

Molecular dynamics simulations were employed to follow the atom trajectories in energetic displacement cascades initiated by assigning one target atom an initial kinetic energy of 10 kilo-electron volts (keV). Embedded atom method potentials are employed to represent the intermetallic compound, nickel–aluminum (NiAl).

Accomplishment Description

Molecular dynamics computer simulations were used to investigate the collision dynamics of energetic displacement cascades in a B2 crystal structure, NiAl, for the first time. The 10 keV event was the highest energy cascade in an intermetallic compound ever simulated by molecular dynamics. Careful analysis of the degree of chemical and structural order throughout the history of the cascade event was performed. As shown in the series of snapshots of atomic positions (see figure), crystal structure is temporarily lost in a well-defined region of space, giving the appearance of a local amorphous zone. Chemical order is also seen to be lowered in this region. These simulations made possible the determination of the number of atomic defects, Frenkel pairs, and anti-site defects produced in the cascade event. Each cascade event required 15 Cray-2 hours.

Significance

Stability of intermetallic compounds in a radiation environment is important in the design of structural components to be used in reactors or in space. The present molecular dynamics simulations provide understanding of the damage process in these materials on an atomic level. This investigation is easily generalized to other systems. The results are useful in understanding the point defects in crystalline matter and the stability of ordered phases.

Future Plans

New simulations of cascades at metal surfaces and interfaces are planned. The former is important for surface damage like roughening and sputtering; the latter is important for radiation effects involving second phase precipitates and artificially structured materials.

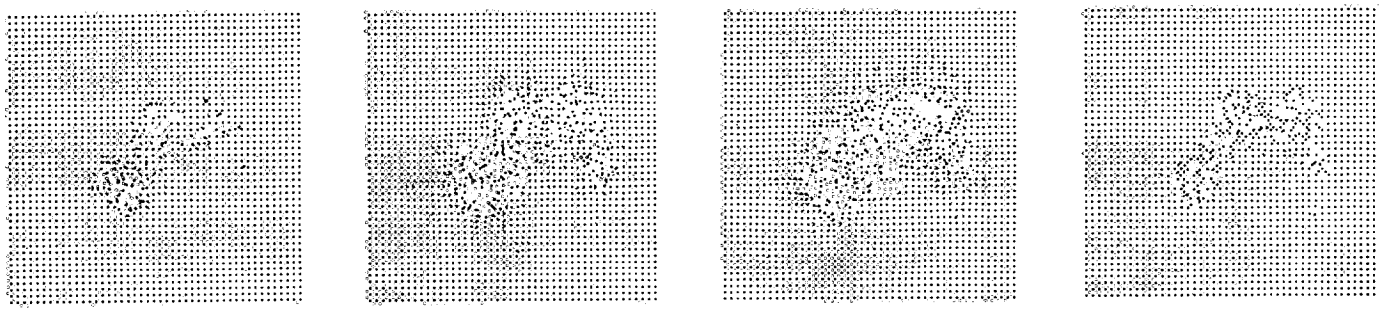

Cross-sectional slabs, two atomic layers thick, in a 10 keV cascade in NiAl alloy. (a) 0.1 picoseconds, (b) 0.3 picoseconds, (c) 0.5 picoseconds, and (d) 6.0 picoseconds. Open dots = aluminum and solid dots = nickel.

Performance and Scalability of Parallel Graphics Libraries

Thomas W. Crockett, Principal Investigator
ICASE

Research Objective
To develop a three-dimensional (3-D) parallel graphics library for message-passing architectures and to assess its performance and scalability as a function of scene complexity and machine size.

Approach
In previous work, a parallel polygon rendering algorithm suitable for multiple-instruction/multiple-data message-passing architectures was developed. That work was extended by incorporating an improved version of the algorithm in a parallel 3-D graphics library with significant improvements in functionality and performance. The parallel library was designed specifically for inclusion in parallel application programs that employ a single program multiple data programming style. Images generated were compressed and transmitted across the network to the user's workstation, where they were decompressed and displayed.

Accomplishment Description
A 3-D parallel graphics library (PGL) was developed to support a standard graphics pipeline, including modeling transformations, lighting computations, 3-D clipping, perspective viewing, Gouraud-interpolated rasterization, and z-buffered hidden surface elimination. The library incorporated an improved, span-based version of the Crockett/Orloff parallel rendering algorithm. Preliminary results indicated that the new algorithm was approximately twice as fast as the original on a standard test scene. Parallel efficiency was doubled, reaching 60 percent on the 128-processor iPSC/860 at NASA Ames. The compressed image transmission scheme incorporated within PGL appeared to be practical. Experiments using the Ames iPSC/860 from NASA Langley demonstrated transmission times of about three seconds per frame.

Significance
Applications that run on massively parallel supercomputers produce massive output datasets that are often cumbersome to move across the network for post-processing. Using the power of the parallel machines to perform graphics and visualization operations in place reduced the output to a manageable size. Embedding graphics calls within parallel applications allows users to take advantage of visual data representations for debugging, execution monitoring, and interactive steering.

Future Plans
Performance evaluation of the span-based rendering algorithm is under way. Of particular interest is the behavior as the number of processors approaches or exceeds the number of scanlines in the image. Additional work is needed to develop parallel visualization algorithms.

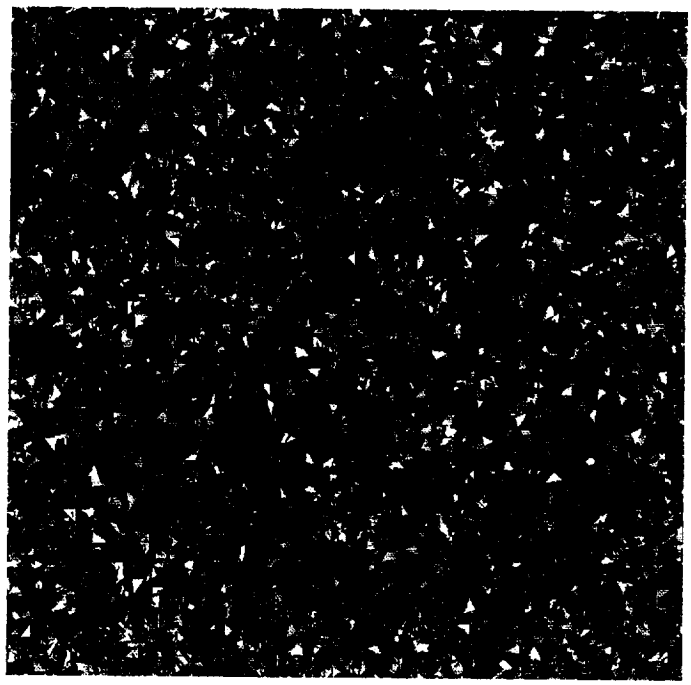

Test scene composed of 100,000 random triangles. The statistical properties approximate the assumptions of the analytical performance models.

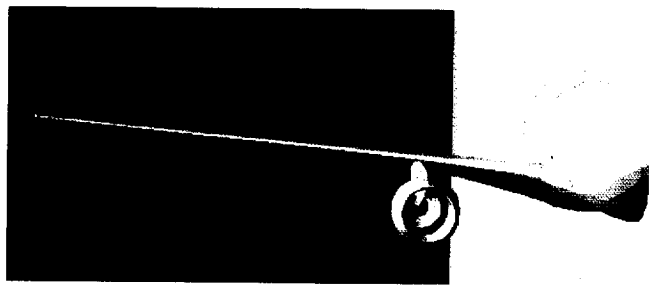

A more typical image. Load balancing becomes an issue because the geometric complexity varies within the scene.

Performance Monitoring of Parallel Programs

Jerry C. Yan, Principal Investigator
Co-investigators: Philip J. Hontalas, Catherine H. Schulbach, Pankaj Mehra, Sekhar R. Sarukkai, Melisa A. Schmidt, and Tarek S. Elaydi
Recom Technologies/NASA Ames Research Center/Lawrence Berkeley Laboratory

Research Objective
To develop tools and methodologies for performance evaluation of multiprocessors.

Approach
The Automated Instrumentation and Monitoring System (AIMS) is a software tool set that automatically instruments parallel FORTRAN and C programs, monitors their execution on multiple-instruction/multiple-data architectures, and analyzes their performance. Dynamic variation of system parameters and overall performance are automatically captured during execution and displayed on a color screen.

Accomplishment Description
AIMS was deployed and extended. AIMS has three major software components: the source-code instrumenter, the run-time monitoring library, and the visualization tool set. The source-code instrumenter inserted software probes directly into the application with little or no intervention by the user. The run-time monitoring library traced program execution. The visualization tool set processed the execution data gathered and displayed it using graphical representations. AIMS also provided source-code click-back—one click on an animated view will bring up a window with the program text. Major enhancements to AIMS included: (1) self-identifying trace files, (2) an "instrument enabling profile" to turn on/off instrumentation without recompiling the application software, (3) development of an alpha version of AIMS for the CM-5.

Significance
The development of tools and methodologies for High Performance Computing and Communication Program applications.

Future Plans
AIMS will be available to the public by the end of August 1993.

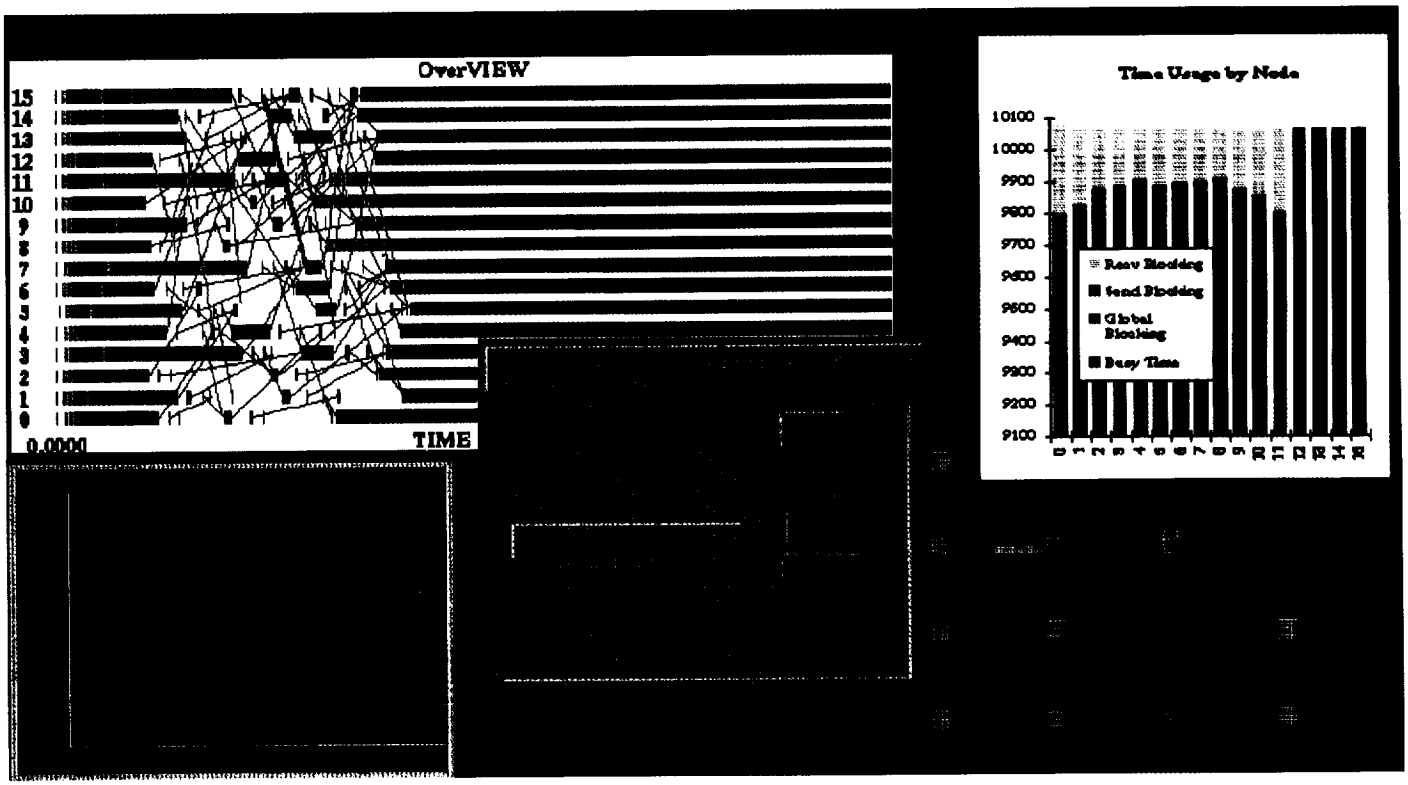

Example of graphical interface for trace control, performance data animation, statistical data visualization, and source-code click-back.

Computational Electromagnetics for Massively Parallel Processors

Michael J. Schuh, Principal Investigator
Co-investigators: Alex C. Woo and John D'Angelo
NASA Ames Research Center/General Electric Corporation

Research Objective
To develop electromagnetic scattering prediction codes for modeling large scatterers that cannot be accurately modeled by optical approximations or by low-frequency methods. The algorithms used, finite-volume time domain (FVTD), finite-difference time domain, and nodal-based finite-element method (FE), must be scalable because of the intense computational requirements of this resonant scattering problem.

Approach
The three-dimensional (3-D) FVTD code, ARCCEM, was implemented using FORTRAN 90. It used a multiblock structured grid to model complex geometries. A 3-D FE code, RF3D, for the radar cross-section prediction of complex objects was implemented on the Intel i860 Hypercube. This FE code used a completely unstructured mesh, high-order isoparametric elements, and a quasi-minimal residual complex matrix solver. The code used various finite-element types including hexahedral, tetrahedral, prism, and pyramid elements.

Accomplishment Description
ARCCEM was upgraded from a two-dimensional code to a 3-D code. A significant effort was devoted to obtaining Cray C-90 performance from the CM-5. Early indications show that Cray C-90 performance levels will only be obtainable for larger problems. Currently, small problems require 5–16 times more processing time on 32 nodes of the CM-5 compared to the Cray C-90. For implementation of the FE code on the Hypercube, a recursive, binary domain decomposition was used. The domain decomposition of the finite-element mesh was performed on a host computer. The Hypercube implementation showed increased speed corresponding to the number of processors. However, the speed improvement dropped significantly when the number of unknowns per processor dropped to less than 1,000 per node. A large problem consisting of approximately 240,000 complex unknowns required 208 seconds of computation.

Significance
Computational methods from serial and vector machines will be adapted to massively parallel machines for production problems larger than can currently be solved.

Future Plans
Further efforts will be made to get a higher level of performance from the CM-5 with the ARCCEM code. The code will be enhanced by adding materials and mismatched grid capabilities. Currently, a version of RF3D using the parallel virtual machine communication software is being examined.

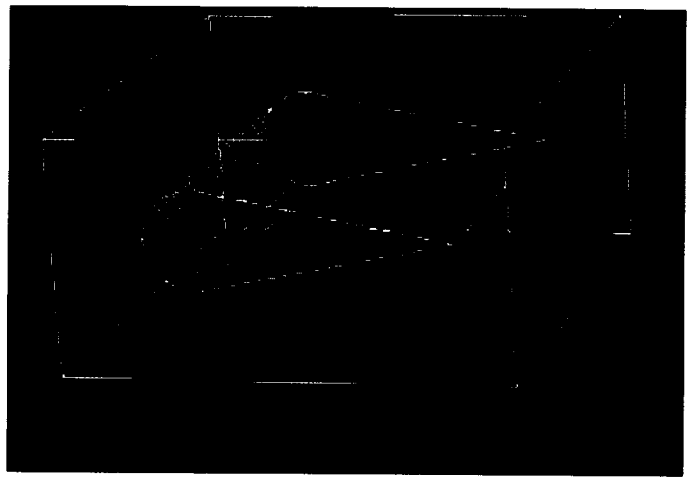

Outline of finite-element model of a perfect electrical conducting wedge cylinder; X = 3.5 wavelengths, Y = 1.0 wavelengths, and Z = 4.0 wavelengths.

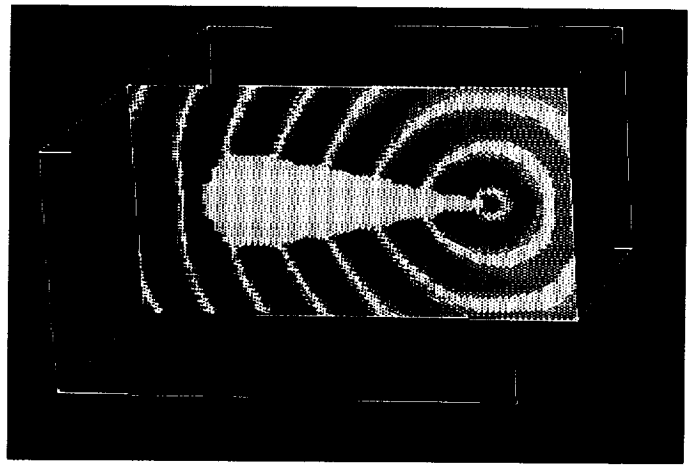

Finite-element method solution showing the scattered Y component of the H field. The incident field was a plane wave traveling in the X direction and polarized in the Y direction. The scale of the contours are 0.942 (red) to –1.10 (blue) with the incident field having a magnitude of 1.0. The mesh contained 3,808 second-order elements with 16,607 nodes.

Time-Domain Computational Electromagnetics

Vijaya Shankar, Principal Investigator
Co-investigators: William F. Hall, Alireza Mohammadian, Chris Rowell, and Michael Schuh
Rockwell International Science Center/NASA Ames Research Center

Research Objective
To advance the state of the art in electromagnetic computations, especially the prediction of radar cross section (RSC) of low observable targets, by solving the time-domain Maxwell's equations accounting for all types of material properties.

Approach
The time-domain Maxwell's equations cast in differential-conservation form were solved using an upwind-based finite-volume scheme. The interface fluxes were computed using an appropriate Riemann solver taking into account material property variations from cell to cell. A structured-grid multiblock procedure was employed to model arbitrarily shaped scattering targets. The transient near-field solution was processed through a fast-Fourier transform algorithm to obtain the RSC information as a function of frequency.

Accomplishment Description
The time-domain Maxwell's solver RSC3D runs efficiently in a vector/parallel architecture such as the Cray C-90. On a 16 processor C-90, it performs in excess of 10 GFLOPS. The code was successfully tested for RSC prediction on several two- and three-dimensional targets specified by the Electromagnetic Code Consortium. A typical scattering computation for a complete fighter geometry is shown in the figure. The many applications of this electromagnetic code include modeling antenna problems and printed microstrip circuits and biomedical simulations.

Significance
Accurate prediction of RSC for low observable targets in the frequency range 100 megahertz–20 gigahertz is a technology that is critically needed for many defense projects. This electromagnetic code development activity, by employing advanced algorithms and supercomputer architectures, is truly advancing the state of the art in computational simulation.

Future Plans
Work is progressing to adapt this technology to massively parallel computing architectures with a goal to provide teraflop performance in the near future.

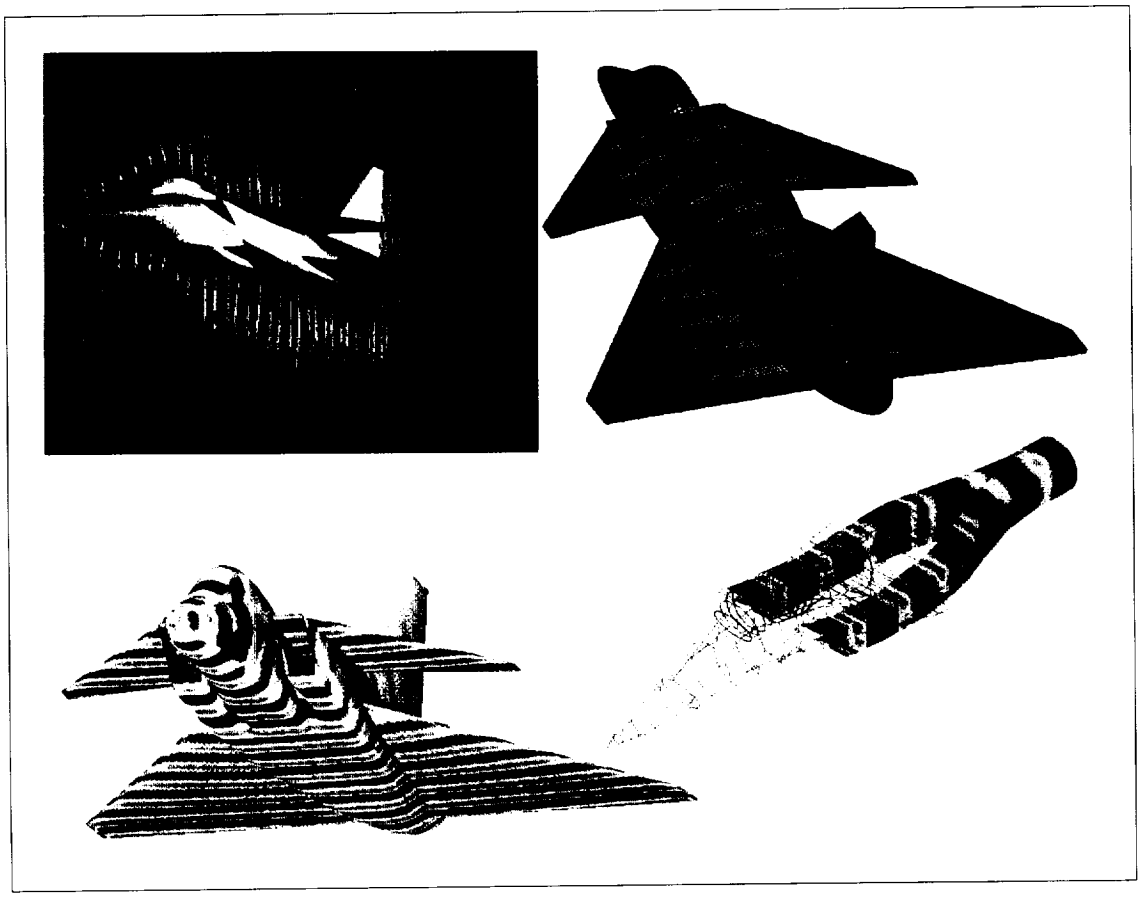

Radar cross-section studies and scattered field contours for a VFY218 fighter aircraft at 250 MHz.

Vortex-Ring/Free-Surface Interaction

Samuel Ohring, Principal Investigator
Co-investigator: Hans J. Lugt
Naval Surface Warfare Center

Research Objective
To understand vortex-ring interaction with a free surface (the deformation and connection of a vortex ring during encounter with a free surface), which is subject to deformation. This problem will help in the interpretation of surface signatures of wake flows.

Approach
The three-dimensional Navier–Stokes equations for a viscous, incompressible fluid with full-nonlinear free-surface conditions were solved with boundary-fitted coordinates, adaptive gridding, and artificial compressibility applied at each physical time step. This technique solves seven field equations for the three velocity components, pressure, and three spatial coordinates. The number of grid points is of the order of one million.

Accomplishment Description
Numerical computations for various Froude, Reynolds, and Weber numbers were made with a thick vortex ring that formed an inclination angle of 45 degrees with respect to the free surface. When the vortex ring approached the free surface, an upwelling above the ring's center and a half-moon-shaped ridge developed, with a deep trough in between. Near the outer part of the trough a circular dimple, signaling the connection of the vortex ring with the free surface, was expected. The computations, however, revealed a new connection process that deformed the vortex ring to a cylindrical vortex sheet. This connection process was first explained for a flat, free surface and then analyzed for a deformed, free surface, which generated vorticity tangential to the free surface. This additional vorticity formed secondary vortex rings of signs opposite to the primary vortex. The procedure is a combination of vortex stretching, helical vortex filaments generation, surface deformation, and secondary vorticity production. The average case took 70 Cray Y-MP hours and used up to 32 megawords of memory.

Significance
These findings contribute to the physical understanding of vortex-ring/free-surface interaction—particularly the intricate recollection process—and may help to obtain a complete picture of wave signatures.

Future Plans
Vortex rings of thinner cores and larger Reynolds numbers will be computed to find the transition process from circular filament reconnection to cylindrical sheet reconnection. A trial simulation is planned for the reflection of vortex rings at a free surface for inclination angles smaller than 23 degrees.

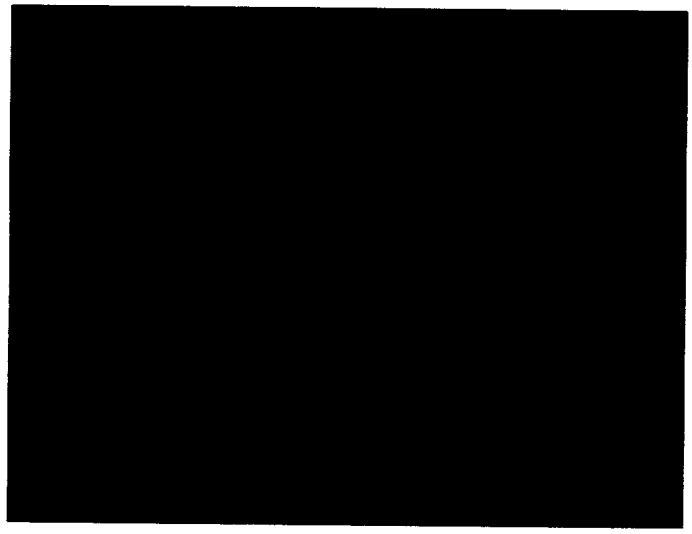

Vorticity lines for a vortex ring in orthographic projection. The color spectrum for the vorticity line magnitudes ranges from blue (2×10^{-5}) to red (10.0) and the symmetry plane spectrum ranges from blue (3×10^{-5}) to red (5.0).

Computational Hydrodynamic Performance Evaluation

Donald W. Davis, Principal Investigator
Co-investigator: Keith C. Kaufman
General Dynamics, Electric Boat Division

Research Objective
To investigate and quantify the effects of Reynolds number scaling on crossflow separation over unappended bodies of revolution at nonzero yaw angles using a Reynolds-averaged Navier–Stokes (RANS) solver.

Approach
The three-dimensional (3-D), steady-state, incompressible RANS solver NFC3D was used to solve for the turbulent flow over a body of revolution. Four Reynolds numbers were considered (4,900,000, 13,000,000, 100,000,000, and 1,100,000,000). Results from the two lower Reynolds number computations were compared to experimental data. Results from the higher Reynolds number computations were compared to predictions from semi-empirical and singularity based techniques.

Accomplishment Description
Turbulent flow computations were completed for a 9.5 lift-to-drag ratio body of revolution at a 15-degree angle of yaw. Half the symmetric physical domain was modeled. Computations were performed on two eight-block computational grids (lower Reynolds numbers = 814,200 grid points; higher Reynolds numbers = 854,910 grid points). The second figure shows crossflow perturbation velocities and streamlines at four body stations. Preliminary comparisons with experimental results show good correlation with body separation patterns and with the size and extent of the leeside crossflow vortex.

Significance
Geometry input simulators that reliably and efficiently predict maneuvering performance under all operating conditions are needed to achieve optimal designs. Accurate hydrodynamic representations for forces and moments in terms of geometry are required. For bodies of revolution at nonzero angles of yaw, vorticity shed from the body accumulates in the downstream direction and can cause large nonlinear forces and moments on the body. The inflow to the stern control appendages is also affected by shed vorticity. Shed vorticity can be ingested by stern propulsion systems. Because only limited full-scale data exist, independent studies of these effects using 3-D RANS techniques are necessary.

Future Plans
Current efforts will be expanded to include the effects of steady turns on bodies of revolution with and without appendages. Investigated parameters will be: rotation rate, rotation radius, angle of attack, angle of yaw, and the effects of fins mounted at the midbody and stern. More sophisticated turbulence models will be used to better account for rotation effects on the turbulent stresses.

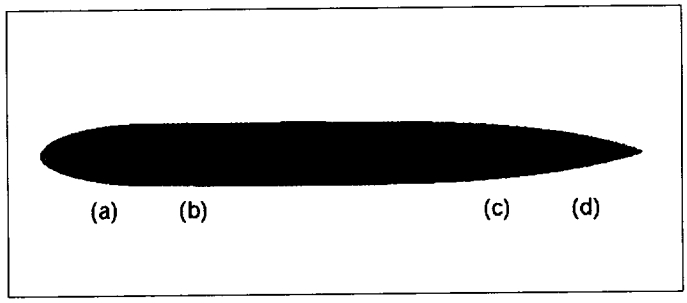

Body stations: (a) 0.10, (b) 0.25, (c) 0.75, and (d) 0.90.

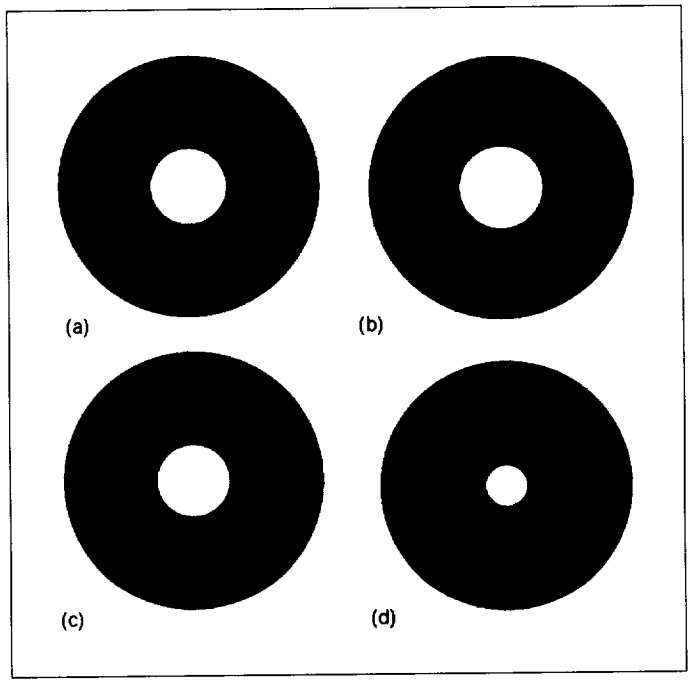

Crossflow perturbation velocities and streamlines for Reynolds numbers 13,000,000 ((a) and (c)) and 1,100,000,000 ((b) and (d)). Axial locations: (a) 0.10, (b) 0.25, (c) 0.75, and (d) 0.90.

Small Airway Fluid Dynamics

Jeffrey R. Hammersley, Principal Investigator
Co-investigators: Rama Reddy, Dan E. Olson, Boyd Gatlin, and Joe F. Thompson
University of Arkansas/Medical College of Ohio/Mississippi State University

Research Objective
To study the airflow mechanics within deep-seated and experimentally inaccessible small respiratory bronchioles. Confined bifurcating flows were examined within single two-dimensional (2-D) and three-dimensional (3-D) bifurcation models to determine the effects of variations in local geometry and grid design.

Approach
Multiblocked 2-D and 3-D structured grids, which accurately mimic the anatomic features of small airway bifurcations, were developed using the EAGLE grid system. The computational representations of the airways were studied over a biologically realistic range of Reynolds numbers using the multiblocked INS3D and the Taylor–Whitfield ABRAINS flow solvers.

Accomplishment Description
All 2-D computational models failed to reproduce accurately the experimental analyses done in expanded-scale 3-D physical models of similar design. The models appeared unable to handle a confined channel flow with secondary vortex development. The 3-D computational grid development was made difficult by the complex, multiply curved carinal (flow-splitting) surfaces at branch points. These surfaces required extensive grid manipulation to maintain smoothly curved branching and controlled cross-sectional expansion. A series of 3-D grids were constructed, and early grid design results closely followed experimental measurements. Wall-shear analyses indicated outer wall-flow separation and zones of increased wall shear downstream of the carina.

Significance
Medical scientists contemplate the localized delivery of aerosolized viral vectors for replacement gene therapy. They hope to quantify particulate deposition during environmental exposures by linking the minor changes in airway geometry that produce major disabilities such as asthma and emphysema. This work provided realistic biologic flow simulations of fluidic mixing, particle transport, and shear forces on airway walls. Three-dimensional models of biologic structures are needed to achieve reasonable simulations and specifically designed flow solvers are needed for biologic flow regimes.

Future Plans
Investigation of symmetrically bifurcating flows will be extended to asymmetrical bifurcations and serially branching 3-D cascades. These efforts will set the stage for the incorporation of wall elasticity and particle-flow interactions.

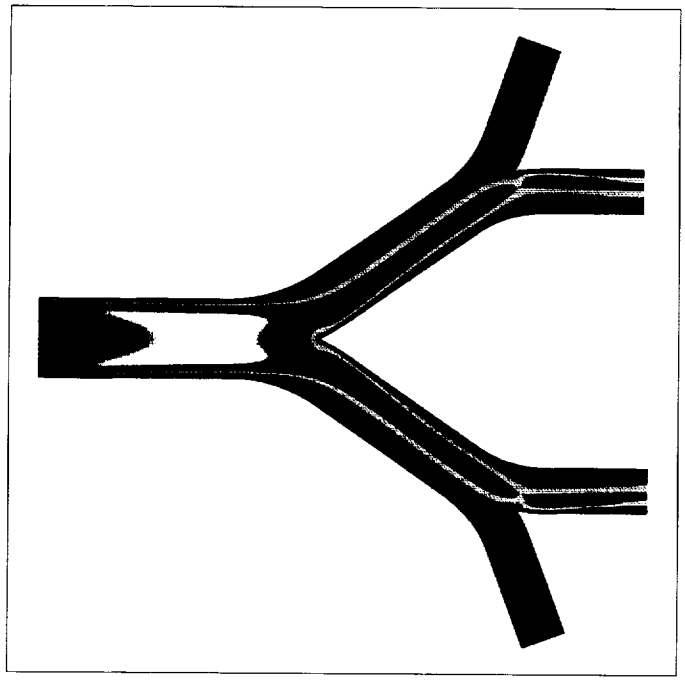

Two-dimensional flow simulation through a planar symmetrical double bifurcation model with non-dimensional velocities displayed from 0.0 (black) to 1.0 (white). Inspiratory directed flow Re = 500.

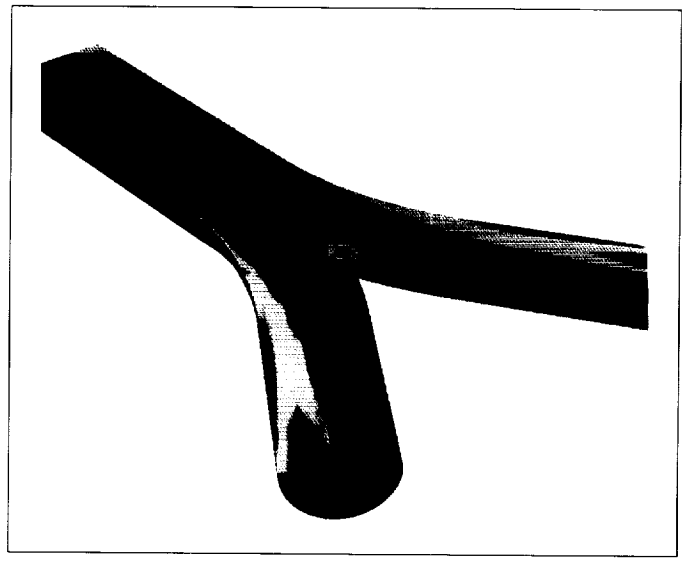

Pressure development in a single small airway bifurcation. Three-dimensional flow simulation with inspiratory directed flow Re = 500. Nondimensional pressures displayed from 0.0 (blue) to 1.0 (red).

Computer Simulation of the Structure and Function of Membranes

Robert D. MacElroy, Principal Investigator
Co-investigators: Andrew Pohorille and Michael Wilson
NASA Ames Research Center

Research Objective

To provide a molecular level description of the structure and function of the earliest living cells (protocells). It is generally assumed that protocells were closed spheroidal structures immersed in water, with walls composed of simple membranes. The study goal is to explain how interfaces between protocellular membranes and water could have promoted the development of two essential cell functions: energy and catalysis of chemical reactions.

Approach

Small solute molecule behavior that could have occurred in primitive catalysis and energy storage was simulated at the interface between a simple membrane and water using molecular dynamics methods. In this approach, Newton's equations of motion for all atoms in the system were integrated numerically. Results included statistical and dynamical properties of the system, which could be directly compared with experimental results and a detailed microscopic description of the system.

Accomplishment Description

Surface fluctuations in simple, fluid membranes were analyzed. These fluctuations obeyed the capillary wave model—a fundamental model describing liquid interfaces. As a consequence, deep thinning defects were occasionally formed in the membrane. Unassisted transport of ions (sodium and chloride) across membranes proceeded through the thinning defects and were associated with considerable water penetration into the membrane. As a result, ion penetration across fluid membranes was markedly increased compared to rigid membranes. This allowed the formation of ion gradients which can be used to store energy for chemical reactions. Many small molecules had free energy minima at water–membrane interfaces. The barriers to conformational changes of these molecules could be substantially lowered at the interfaces. This effect was characteristic of catalyzed reactions.

Significance

This work provides critical benchmark information needed for understanding the origins of cellular life. It demonstrates (1) the mechanism of charge (ion) transport across membranes in the absence of specialized proteins present in contemporary cells, and (2) the role of water–membrane interfaces as primitive catalysts.

Future Plans

Protocell structure and function studies will be continued by (1) assessing the feasibility of proton transport across membranes via the "proton wire" mechanism, (2) investigating a model electron transfer reaction at the water–membrane interface, and (3) studying simple peptides at interfaces for likely candidates of the earliest enzymes.

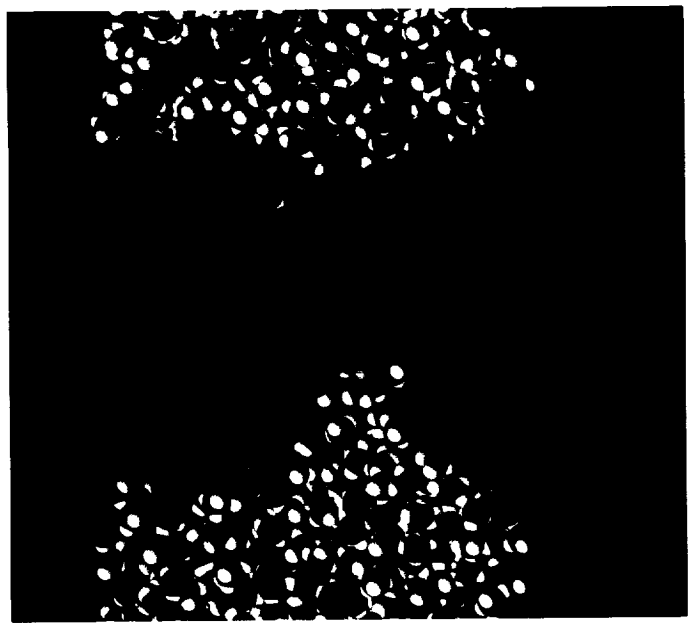

Ray-traced image of a sodium (Na+) ion perpetrating a water/glycerol-1-monooleate membrane. The Na+ is yellow, the oxygens and hydrogens of water are red and white, respectively; the membrane polar head groups are magenta and the hydrocarbon tail groups are blue.

Visualizing Neurons in Three Dimensions

Muriel D. Ross, Principal Investigator
Co-investigator: Kevin Montgomery
NASA Ames Research Center/Sterling Software Systems

Research Objective
To automate fully three-dimensional (3-D) reconstruction of biological neuronal networks from serial sections digitized directly from a transmission electron microscope (TEM).

Approach
A video camera and a personal computer captured and digitized images from a TEM and then automatically sent the images to a workstation. A mosaic of the images was created using a connection machine to reproduce the original sections. The mosaics were then viewed, enhanced, and enlarged on the workstation. Contour extraction was a manual process and was conducted by tracing objects displayed on the monitor. Algorithms were developed for contour registration, tesselation, 3-D reconstruction, and smoothing by computer.

Accomplishment Description
This is the first demonstration of a computerized method for complex object reconstruction directly from a TEM. Computerized reconstruction methods reduce time requirements by approximately 75 percent and have improved registration compared to manual approaches. Eliminating conventional photography results in a savings up to $5,000 per reconstruction. Benefits have already included revision of previously held theories of gravity sensor architecture, uncovering the fundamental organization of the sensors, and production of the first two-dimensional simulations of neuronal endings in the sensors. To create the mosaics, 90 hours of connection machine time were used.

Significance
Computerized reconstruction of neurons and thorough simulations based on true architecture have been goals of neuroscientists since advanced computers appeared. If this goal is achieved, the software designed in this study will greatly advance the fields of neuroscience and neurocomputation. At NASA, this tool enhances research into the effects of altered gravity on gravity sensors.

Future Plans
Software development will be improved until the method is fully automated and simulations of activity are transparent to the reconstruction process.

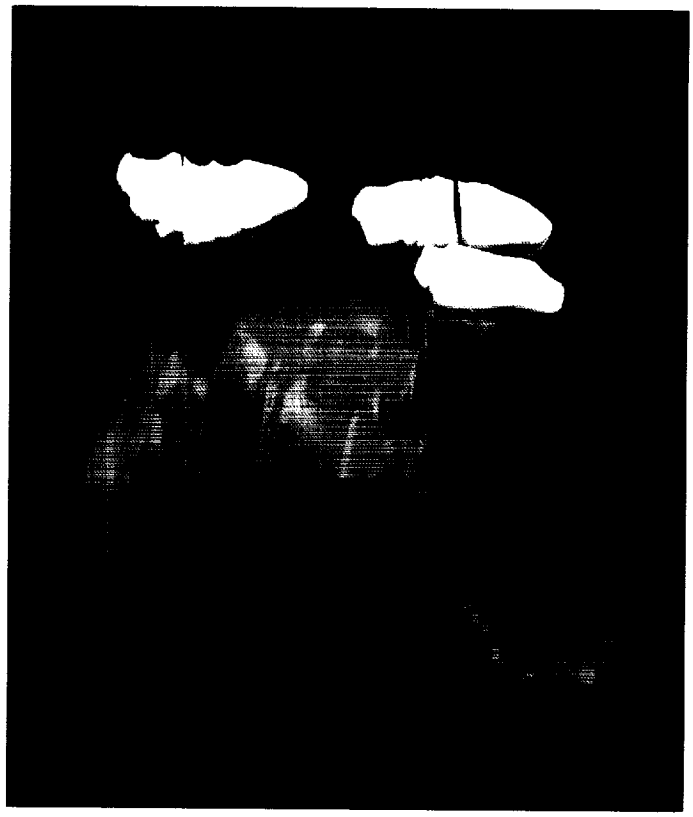

Computer generated reconstruction of a nerve ending (yellow) in a rat gravity sensor with enclosed gravity detecting neurons (type I hair cells are gray).

Large-Scale Numerical Simulations of Human Motion

Robert T. Whalen, Principal Investigator
Co-investigators: Marcus G. Pandy and Frank C. Anderson
NASA Ames Research Center/University of Texas at Austin

Research Objective
To assess the feasibility of computing large-scale optimal control solutions for human movement using massively parallel and vector-processing supercomputers. An optimal control problem for walking was developed for musculoskeletal loading during movement.

Approach
A detailed three-dimensional model of the human body was developed to simulate human motion on Earth and in space. The skeleton was represented as an 8-segment, 19-degree-of-freedom linkage, actuated by 46 muscles (first figure). Each muscle was represented as a 3-element, lumped-parameter entity in series with tendons.

Accomplishment Description
The computational expense of solving the optimal control problem was evaluated using a conventional serial machine, a parallel-vector-processing machine, and a multiple-instruction/multiple-data (MIMD) parallel machine. Computing the optimal control solution on serial machines was impractical since convergence required approximately three months of dedicated processing time. Using either a parallel-vector-processing machine or a Cray, a solution can be found with about 80 processing hours. The MIMD parallel machine performed best in the calculation of the derivatives. This performance was due to the fact that calculation of the derivatives scaled almost linearly with the number of processors used (second figure). In contrast, the Cray performed best during parameter optimization of the controls, executing the parameter optimization routine 37 times faster than the serial machine. The ideal computer architecture for solving very-large-scale optimal control problems appears to be a hybrid system in which a vector-processing machine is integrated into the communication network of a MIMD parallel machine. About 12 megabytes of memory are needed to compute the optimal control solution for walking.

Significance
The ability to simulate human movement and accurately compute musculoskeletal load histories is important where exposure to different load environments or gravitational fields can alter the functional properties of muscle and bone tissue. The combination of musculoskeletal modeling and optimal control theory has emerged as a powerful tool for determining musculoskeletal forces during movement. Unfortunately, accurate simulation of human motion and convergence to an optimal control solution is computationally expensive. It is now possible to use highly dimensioned musculoskeletal models to simulate human movement and specify musculoskeletal load histories.

Future Plans
A fully parallel computational algorithm for solving large-scale optimal control problems on MIMD supercomputers will be developed.

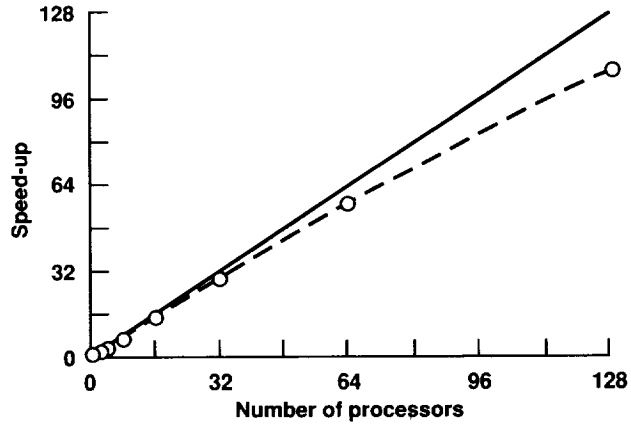

Speed-up factor for computing derivatives for the walking problem (dashed line) compared to ideal scaling (solid line) as the number of processors increases.

Multidimensional Burner-Stabilized Flames

K. Kailasanath, Principal Investigator
Co-investigator: G. Patnaik
Naval Research Laboratory/Berkeley Research Associates

Research Objective
To develop a better understanding of the effects of a burner on the structure and stability of premixed flames.

Approach
A detailed, time-dependent, multidimensional, multispecies, numerical model was used to simulate flames stabilized on a burner. The model included finite-rate, detailed chemical kinetics coupled with algorithms for convection, thermal conduction, viscosity, molecular diffusion, and external forces such as gravity. Boundary conditions were incorporated to account for the heat lost to the burner.

Accomplishment Description
The effects of systematically changing the inflow velocity on the structure and stability of multidimensional flames above a burner were investigated. For large inflow velocities, the flame structure was similar to that of a freely propagating flame. However, as the inflow velocity was decreased, heat loss to the burner increased and the cellular structure of the flame disappeared. For very low inflow velocities, nearly flat flames were obtained. The impact of different boundary conditions (isothermal or Hirschfelder) were also studied. The figure shows the structure of an 11 percent hydrogen–air flame on an isothermal burner for 4 different inflow velocities. A typical calculation required 30 Cray Y-MP hours.

Significance
This is the first multidimensional, detailed numerical simulation of burner-stabilized flames. The simulations indicate that obtaining a flat flame by adjusting the inflow velocity (as is often done in experiments) might distort the true structure of the flame.

Future Plans
The code will be used to simulate and understand a number of other interesting flame phenomena observed on Earth and in microgravity.

Publication
Patnaik, G.; and Kailasanath, K.: Simulations of Multidimensional Burner-Stabilized Flames. AIAA Aerospace Sciences Meeting, Reno, Nev., AIAA Paper 93-0241, Jan. 1993.

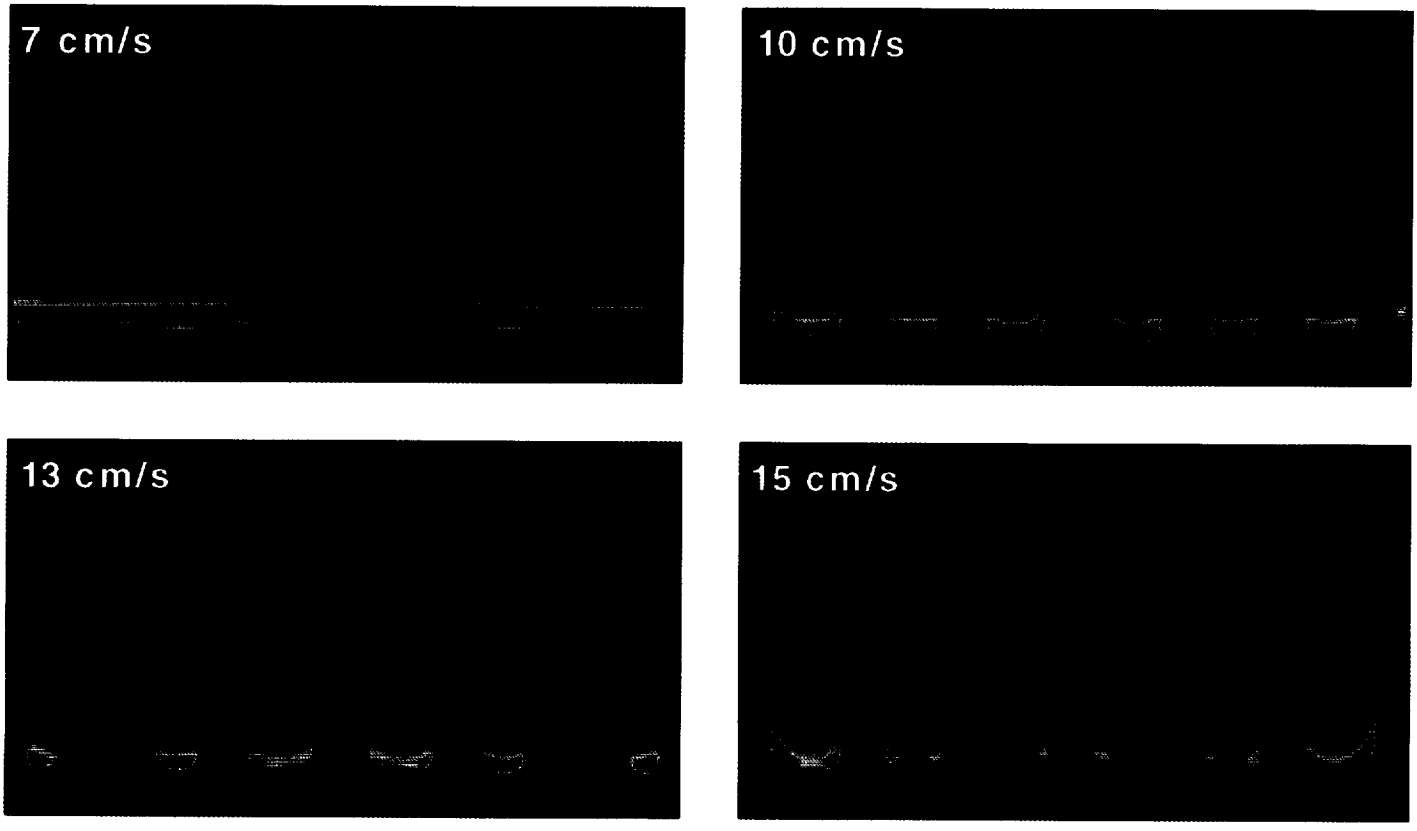

Effect of inflow velocity on an 11 percent hydrogen–air flame stabilized on an isothermal burner.

Protoplanetary Particle-Gas Dynamics

Jeffrey N. Cuzzi, Principal Investigator
Co-investigators: Anthony R. Dobrovolskis, Joelle M. Champney, and Robert C. Hogan
NASA Ames Research Center/University of California, Santa Cruz/Synernet, Inc.

Research Objective
To understand the turbulent two-phase fluid dynamical environment in which the first solid aggregates were formed in the protoplanetary nebula.

Approach
Vertical structure was modeled at various radii in a disk-shaped gaseous nebula at a stage when particles of centimeters to meters in size have accumulated and settled into a concentrated layer very near the nebula's midplane. Using a Prandtl approach, gas turbulence was modeled in the shear flows induced by orbital velocity differences between the particles and the pressure-supported gas. Using a spatial-spectral direct numerical simulation code, particles of various Stokes numbers were introduced into three-dimensional turbulence. Objective sampling and visualization techniques were developed, allowing us to follow the details of the particle clustering structure.

Accomplishment Description
There were substantial mean radial flows of gas and particles, which help explain planetesimal growth and mixing of high-temperature and lower-temperature mineralogical phases. Models were implemented with an array of particle sizes evolving simultaneously. Each run required several Cray-2 hours to reach convergence and 5 megawords of central memory. The structure and evolution of particle clumps that evolve in turbulence were determined. Particles evolved into small, Kolmogorov-scale clumps, and then stretched out in one or more dimensions (see figure). The clumps were persistent on a time scale longer than an eddy turnover time. The runs shown in the figure required 1.5 Cray-2 hours and 16–40 megawords of central memory.

Significance
These are the only models in existence of realistic two-phase fluid dynamics in the environment of the very earliest planetesimal and protoplanetary accretion.

Future Plans
Multiple-particle-size codes for different size distributions and nebula environments will be run. Clumping calculations will be pushed to higher Reynolds numbers. Correlations of particle clump evolution with various particle Stokes numbers, and velocity, pressure, and vorticity regimes in the turbulence will be studied.

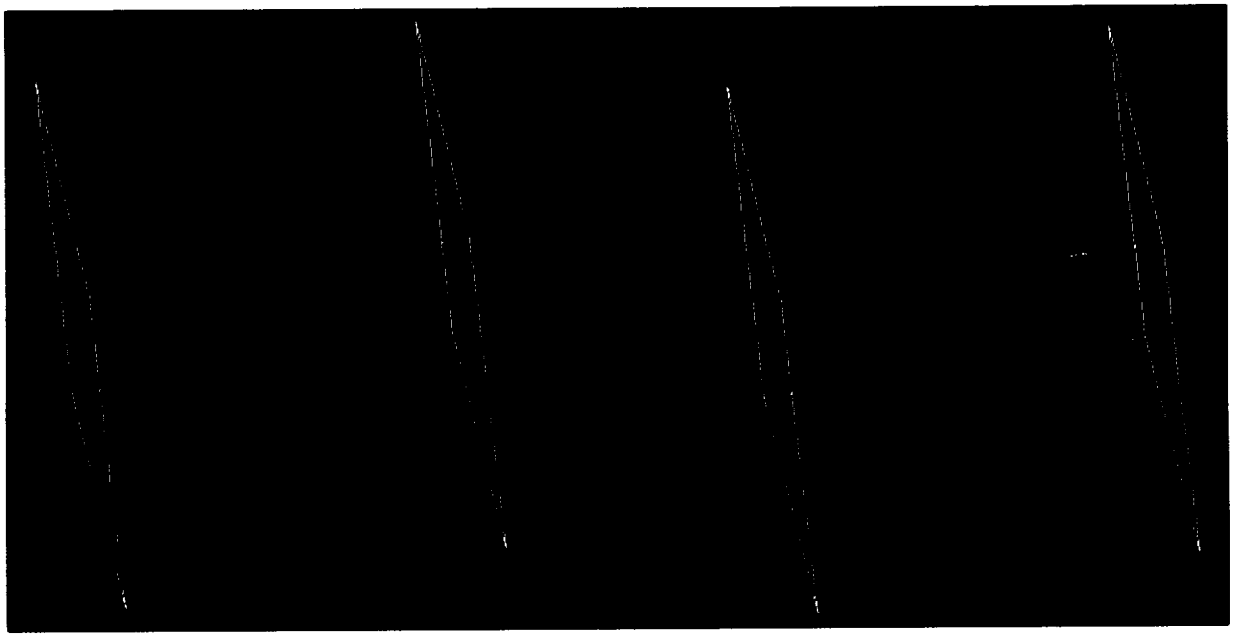

Five particle clumps at the beginning (left) and end (right) of a sequence lasting six eddy turnover periods. Particles are colored to indicate the clump they belong to.

Magnetoelectrohydrodynamics of Microgravity Crystal Growth

George S. Dulikravich, Principal Investigator
Co-investigator: Vineet Ahuja
Pennsylvania State University

Research Objective
To develop analytical models and software for simulation of solidification under the influence of separately applied magnetic and electric fields.

Approach
Both electrohydrodynamic and magnetohydrodynamic models incorporated Lorentz force, joule heating, latent heat using enthalpy methods, and thermally induced buoyancy via an extended Boussinesq approximation allowing for separate temperature-dependent physical properties in the melt and in the solid. Explicit central differencing on boundary-conforming non-orthogonal computational grids was used with four-step Runge–Kutta time integration.

Accomplishment Description
Depending on the mutual orientation of the gravity, electric, magnetic, and thermal gradient fields it was possible to significantly alter the solid/liquid interface shape, the amount of solid accrued, thermal gradients in the solid, and the charged particle deposition pattern in the solid.

Significance
This research indicates a possibility for using relatively weak magnetic and electric fields to actively control the distribution pattern of impurities and dopants and magnitudes of residual thermal stresses in crystals.

Future Plans
All codes will be converted to time-accurate versions capable of analyzing g-jitter and rotation.

Publications
1. Dulikravich, G. S.; Ahuja, V.; and Lee, S.: Three-Dimensional Control of Crystal Growth Using Magnetic Fields. SPIE Paper 1916-07, Feb. 1993.
2. Dulikravich, G. S.; Ahuja, V.; and Lee, S.: Three-Dimensional Solidification with Magnetic Fields and Reduced Gravity. AIAA Paper 93-0912, Jan. 1993.

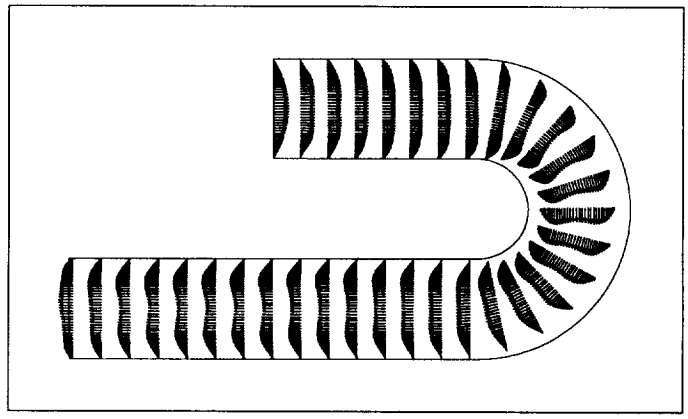

Solid accrued on the walls and the velocity profiles in a turn-around channel with a magnetic field applied in the elbow region.

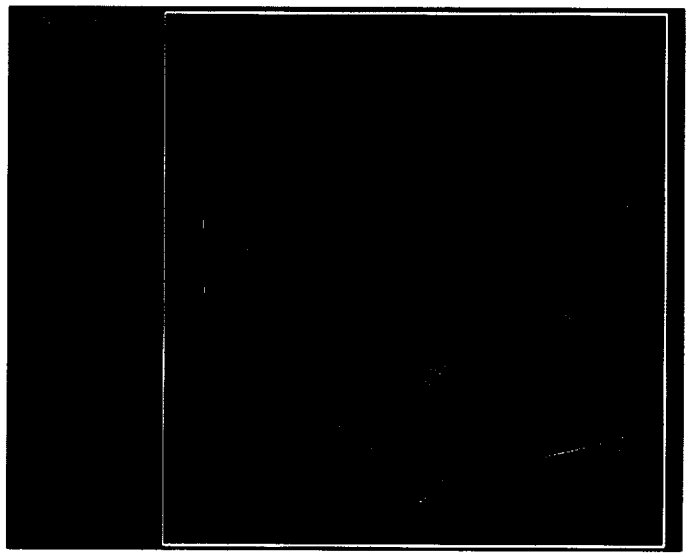

A deformed thoroidal melt motion in a container with solid accruing from the top wall. There is a downward centrally located jet and upward corner jets.

Computational Structural Mechanics Applications

Susan W. Bostic, Principal Investigator
NASA Langley Research Center

Research Objective
To develop an efficient algorithm for nonlinear design sensitivity analysis (DSA) on shared-memory, high-performance computers.

Approach
Nonlinear finite-element analysis was performed before computing DSA. Parallel-vector versions of Newton Raphson (N–R), Modified Newton Raphson (M N–R), and Broyden–Fletcher–Goldfarb–Shann (BFGS) algorithms were developed and compared for the nonlinear analysis applications. The adjoint variable method was used for the design sensitivity analysis. These nonlinear analyses and the DSA algorithms were optimized for parallel-vector supercomputers. In the adjoint variable method, each design variable is assigned to a processor that computes the partial derivatives of the internal loads with respect to the design variable in parallel and with no synchronization. Each violated displacement constraint is assigned to a processor that performs a back substitution to obtain the adjoint vector. Then, each processor multiplies the adjoining vector by the computed partial derivative. To complete the DSA, each processor computes the derivative of the constraints with respect to the design variable.

Accomplishment Description
Three parallel-vector algorithms (N–R, M N–R, and BFGS) are compared in the first figure. The N–R method outperforms the M N–R and BFGS methods. The N–R method requires forming a new stiffness matrix and a complete solution of the system of equations at each iteration. A previously developed parallel-vector algorithm, PVSOLVE, and the nodal algorithm for generation and assembly of the stiffness matrix were incorporated into all three methods. The N–R method gained the most from the previous algorithms and outperformed the other two methods (first figure). Since little synchronization is required in DSA, the computation time is reduced as the number of processors increases (second figure). The nonlinear analysis using the N–R method shows an efficiency of 86 percent, the DSA shows an efficiency of 98 percent, and the total solution efficiency is 96 percent.

Significance
The N–R method on parallel-vector supercomputers reduces the analysis time significantly, although the operation count is higher than those of other methods (first figure). A DSA algorithm resulted in a scalable reduction of time. Total analysis and DSA time is reduced as the number of processors used increases. This increase reduces the design cycle time.

Future Plans
The DSA algorithm will be implemented on a massively parallel computer.

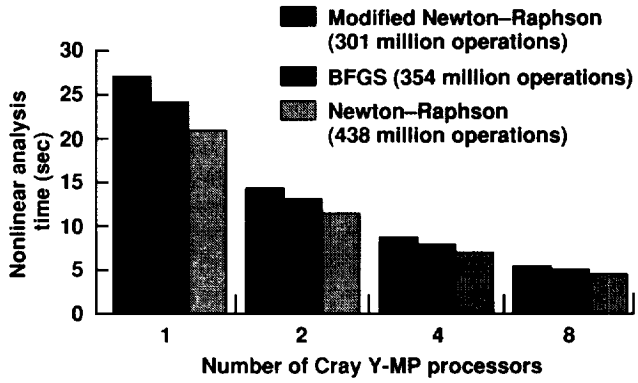

Central processing unit time for nonlinear analysis methods on the Cray Y-MP.

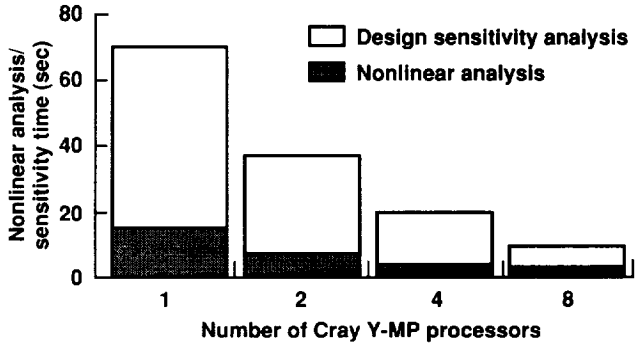

Central processing unit time for design sensitivity analysis on the Cray Y-MP.

Simulation of Vertical Tail Buffet

Osama A. Kandil, Principal Investigator
Old Dominion University

Research Objective
To simulate the buffet problem of fighter aircraft vertical tails using simple models. The basic concept is to generate an unsteady, vortex-breakdown flow and to place a cantilevered vertical tail downstream of the vortex-breakdown flow. This way, the buffet problem is isolated from the aircraft and the computational resources are focused on a small region for high resolution.

Approach
The multidisciplinary problem was solved successively at each time step using three sets of equations for the unsteady vortex-breakdown flow, aerodynamic loads, aeroelastic deflections, and grid displacements. For the unsteady aerodynamic loads, the full Navier–Stokes equations were solved using an implicit, upwind, flux-difference splitting, finite-volume scheme. For the aeroelastic deflections, the aeroelastic equations for bending and torsional vibrations were solved using the Galerkin method and a four-stage Runge–Kutta scheme. For the grid displacements, interpolation equations were solved to update the grid coordinates due to the tail aeroelastic deflections.

Accomplishment Description
Two models simulated the tail buffet problem. The first model had a configured duct in which an inlet, supersonic, swirling flow was forced to break down through a generated shock wave at the inlet region. Downstream of the break-down flow, a vertical cantilevered tail was placed and allowed to deform in a bending mode. The second model had a delta-wing/vertical-tail configuration. Flow conditions were selected so that the wing primary-vortex core experienced vortex break down before reaching the tail location. The first figure shows a delta-wing/vertical-tail configuration. The wing and the rectangular vertical tail each have an aspect ratio 1. The wing angle of attack is 35 degrees, the free-stream Mach number is 0.4, and the Reynolds number is 10,000; the tail thickness is 0.01 and its width is 0.5. An O–H grid of 1 × 258 × 584 points in the wraparound, normal, and axial directions was used to obtain the solution. The spiral saddle points of vortex break down and the surface pressure and the total-pressure surfaces at time step (t) 17,100 (Δt = 0.003) are shown.

Significance
Numerical simulation of fighter aircraft vertical-tail buffet problems was accomplished for the first time using simple models. The models enabled researchers to investigate the buffet problem, identify the critically dominant parameters, and find methods to control buffet efficiently.

Future Plans
The combined bending and torsional modes response of the vertical tails for both models will also be investigated.

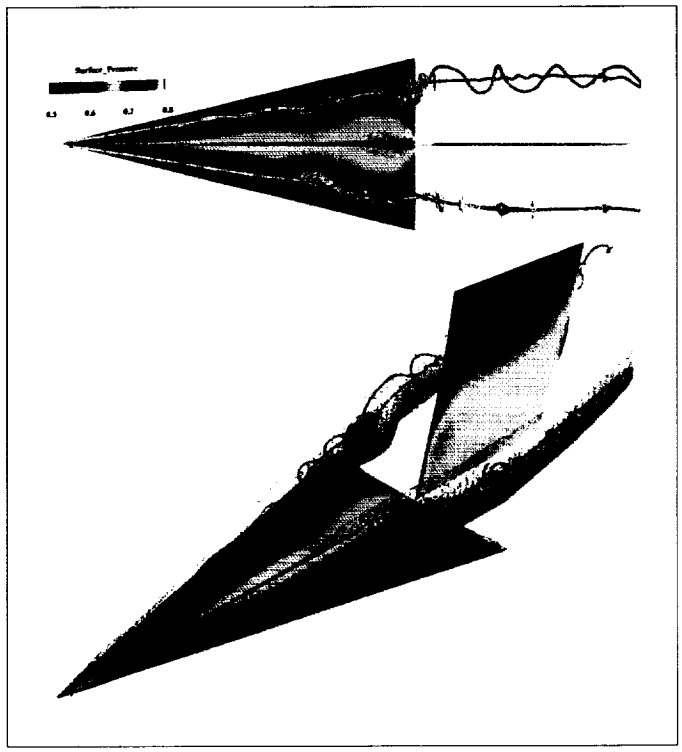

Top view and three-dimensional view of the delta-wing/vertical-tail configuration showing critical points of vortex breakdown, surface pressure, and total-pressure surfaces (0.65).

Buckling and Post-Buckling of Multilayered Composite Panels with Cutouts

Ahmed K. Noor, Principal Investigator
Co-investigator: Jeanne M. Peters
NASA Langley Research Center/University of Virginia

Research Objective

To study the buckling and post-buckling responses of multilayered composite panels with cutouts subjected to combined mechanical and thermal loads.

Approach

The computational model of the composite panels was based on the geometrically nonlinear shallow-shell theory, with the effects of both transverse shear deformations and anisotropic material behavior included. Analytic sensitivity coefficients were evaluated, measuring the sensitivity of the post-buckling response to variations in material and lamination parameters. The panels were subjected to combined applied-edge shear and either edge compressive loading or edge displacement. An efficient reduced-basis computational procedure was used for determining the stability boundary, generating the post-buckling response, and evaluating the sensitivity derivatives. The procedure allowed a significant reduction in the number of degrees of freedom used in the initial discretization.

Accomplishment Description

Extensive numerical studies were performed to understand the effects of lamination parameters and the size of the cutout on the stability boundary and post-buckling response of flat, unstiffened panels. The figure shows the effect of hole size on the stability boundary for a 16-layer quasi-isotropic panel. Also shown are the sensitivity coefficients of the total strain energy with respect to material parameters and fiber angles in the post-buckling range for a panel subjected to combined edge shear and uniform temperature change.

Significance

Future high-speed and high-performance aircraft will be subjected to combined mechanical and thermal loadings. This study will help in the lamination selection and identify the material systems required.

Future Plans

Panel response to combined thermal and mechanical loadings will be studied. The effect of temperature dependence of material properties will also be studied. Stiffened panels with cutouts will be considered. The numerical simulations will be coupled with laboratory experiments to identify failure mechanisms and develop panel failure criteria.

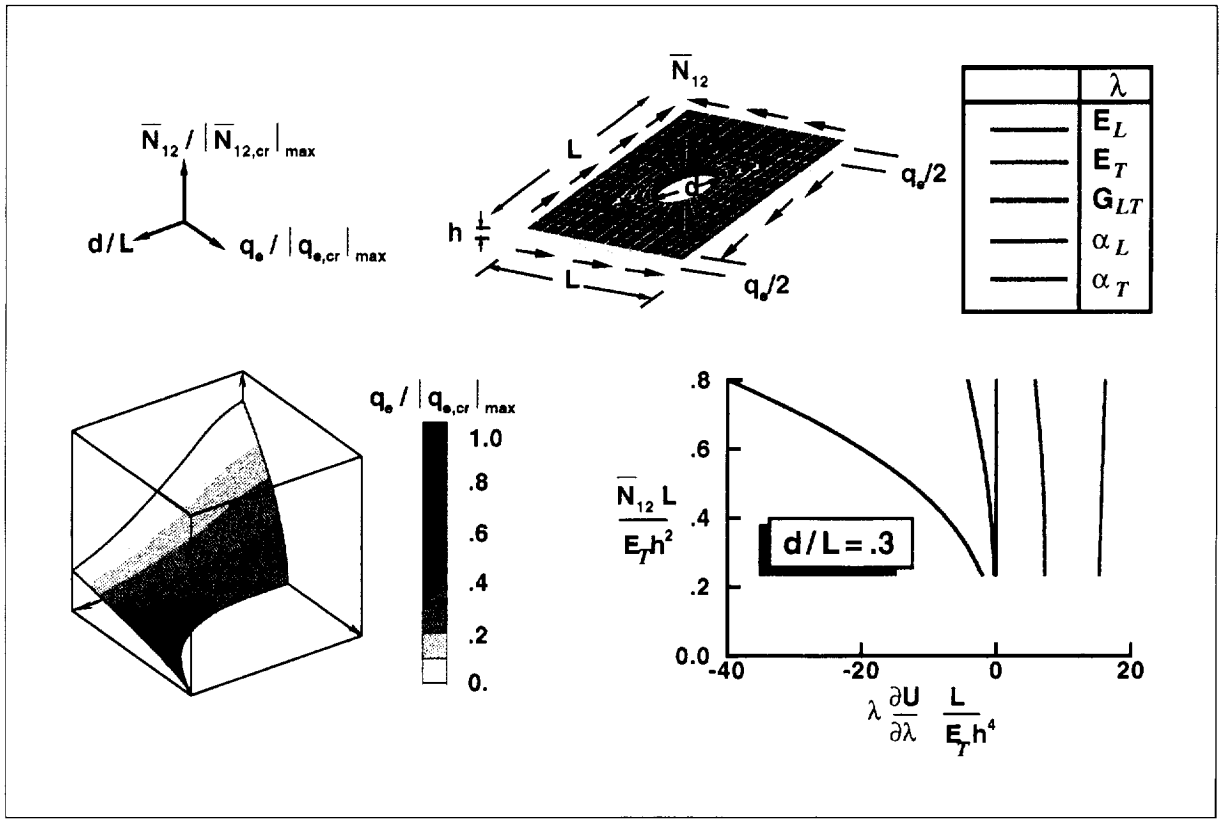

The effect of hole size on the stability boundary for a 16-layer quasi-isotropic panel.

Nonlinear Analysis of Damaged Stiffened-Fuselage Structure

James H. Starnes, Jr., Principal Investigator
Co-investigator: Vicki O. Britt
NASA Langley Research Center

Research Objective

Many commercial aircraft are operated beyond their designed service life because it is more economical to maintain long-service aircraft than to replace them. The possibility of damage to long-service aircraft makes important the structural integrity and the safety issues associated with maintaining an aging fleet. Reliable structural analysis is needed to determine the residual strength of aircraft with cracks in the fuselage skin and other structural elements.

Approach

A nonlinear shell analysis capability for stiffened shells with propagating cracks was developed and implemented using the STAGS (structural analysis of general shells) analysis code., Hierarchical stiffened-shell models of a fuselage shell skin were developed to predict accurate local stress and deflection gradients caused by frames, stringers, joints, and local cracks.

Accomplishment Description

The hierarchical scheme had three levels of finite-element models, beginning with the nonlinear analysis of a large stiffened-fuselage section subjected to internal pressure and a mechanical bending load. Structural details such as frames, stringers, tear straps, shear clips, floor beams, and stanchions were included. Damage was represented in the model by a longitudinal skin crack and a broken tear strap. Deflection gradients were shown as deformed structural geometry plots, and the hoop stress gradients were represented by the color contours (see figures). Global model analysis displacements at varying crack lengths were applied as boundary conditions to the second level of modeling (a 6-bay by 6-bay stiffened-fuselage crown panel). The local model had higher mesh refinement and modeling detail to characterize more accurately the local structural response. Displacements from the 6-bay by 6-bay stiffened-panel model were applied as boundary conditions to a more refined 2-bay by 2-bay local stiffened-panel model centered around the crack. The finer mesh better represented the local stress and deflection gradients in the crack region. Stress intensity factors from this local model helped determine the residual strength of the aircraft. A typical nonlinear analysis used 4 megawords of memory and 30–60 minutes central processing unit time.

Significance

This method makes possible in-depth analysis of the behavior of a fuselage shell with a crack. Properties such as stress intensity factors at the crack tip are determined and are used to assess residual strength and determine how long an aircraft can be flown before its residual strength becomes a concern.

Future Plans

This method will be expanded to include mechanical loads such as vertical shear and torsion loads. Adaptive mesh refinement capabilities will be added to STAGS to allow for curved crack growth. Algorithms will be added to STAGS to determine when and in what direction a crack will grow.

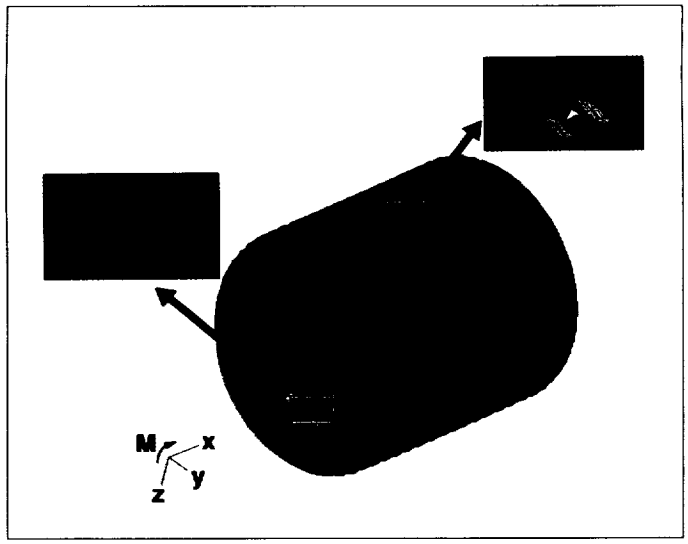

Hoop stresses in a global stiffened-fuselage shell model with a skin crack and subjected to internal pressure and a mechanical bending load. Blue = minimum stress; green, yellow, and red = maximum stresses.

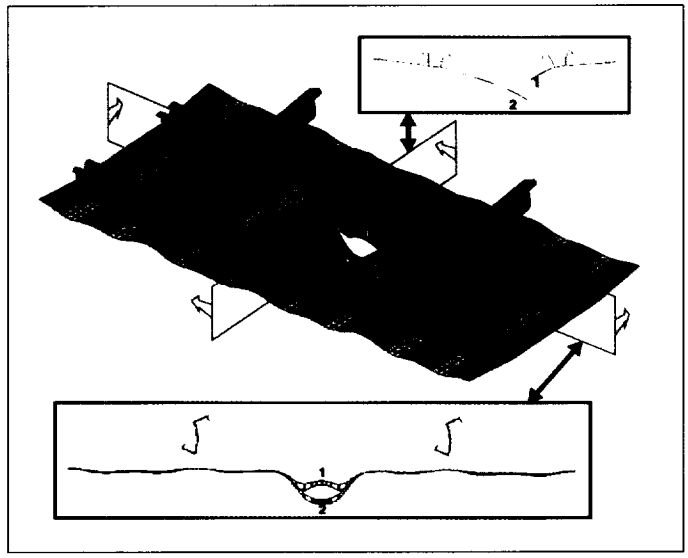

Hoop stresses in a local 2-bay by 2-bay stiffened-panel model with a skin crack and subjected to internal pressure and a mechanical bending load. Blue = minimum stress; green, yellow, and red = maximum stresses.

Index

NASA Lewis Research Center

REPORT DOCUMENTATION PAGE

Form Approved
OMB No. 0704-0188

1. AGENCY USE ONLY *(Leave blank)*	2. REPORT DATE	3. REPORT TYPE AND DATES COVERED
	March 1994	Reference Publication

4. TITLE AND SUBTITLE

NAS Technical Summaries, March 1992–February 1993

5. FUNDING NUMBERS

536-01-11

6. AUTHOR(S)

Numerical Aerodynamic Simulation Program

7. PERFORMING ORGANIZATION NAME(S) AND ADDRESS(ES)

Ames Research Center
Moffett Field, CA 94035-1000

8. PERFORMING ORGANIZATION REPORT NUMBER

A-94015

9. SPONSORING/MONITORING AGENCY NAME(S) AND ADDRESS(ES)

National Aeronautics and Space Administration
Washington, DC 20546-0001

10. SPONSORING/MONITORING AGENCY REPORT NUMBER

NASA RP-1321

11. SUPPLEMENTARY NOTES

Point of Contact: Pat Elson, Ames Research Center, MS 258-5, Moffett Field, CA 94035-1000; (415) 604-4463

12a. DISTRIBUTION/AVAILABILITY STATEMENT

Unclassified — Unlimited
Subject Category 99

Available from the NASA Center for AeroSpace Information, 800 Elkridge Landing Road, Linthicum Heights, MD 21090; (301) 621-0390

12b. DISTRIBUTION CODE

13. ABSTRACT ***(Maximum 200 words)***

NASA created the Numerical Aerodynamic Simulation (NAS) Program in 1987 to focus resources on solving critical problems in aeroscience and related disciplines by utilizing the power of the most advanced supercomputers available. The NAS Program provides scientists with the necessary computing power to solve today's most demanding computational fluid dynamics problems and serves as a pathfinder in integrating leading-edge supercomputing technologies, thus benefiting other supercomputer centers in government and industry. The 1992–93 Operational Year concluded with 399 high-speed processor projects and 91 parallel projects representing NASA, the Department of Defense, other government agencies, private industry, and universities. This document provides a glimpse at some of the significant scientific results for the year.

14. SUBJECT TERMS

Computational fluid dynamics, Supercomputing technology, Cray-2, Cray Y-MP, High-speed processing, Parallel processing

15. NUMBER OF PAGES

176

16. PRICE CODE

A08

17. SECURITY CLASSIFICATION OF REPORT	18. SECURITY CLASSIFICATION OF THIS PAGE	19. SECURITY CLASSIFICATION OF ABSTRACT	20. LIMITATION OF ABSTRACT
Unclassified	Unclassified		

☆U.S. GOVERNMENT PRINTING OFFICE: 1994-584-277

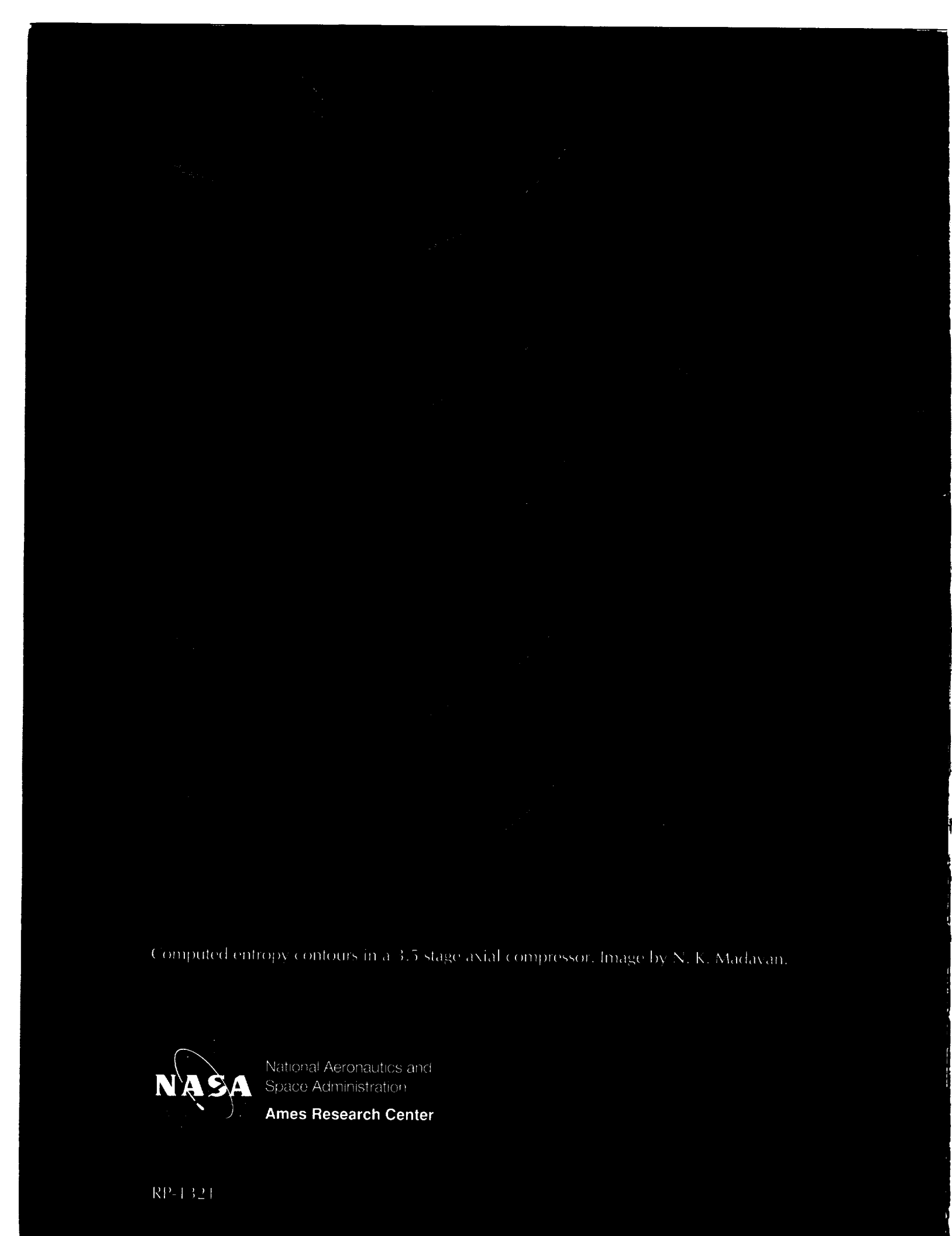

Computed entropy contours in a 3.5 stage axial compressor. Image by N. K. Madavan.

NASA
National Aeronautics and
Space Administration
Ames Research Center

RP-1321